LIÈGE université
Gembloux
Agro-Bio Tech

Influence of combined environmental constraints on photochemical capacity and CO_2 fluxes in a temperate managed grassland

Anthony Digrado

COMMUNAUTÉ FRANÇAISE DE BELGIQUE
UNIVERSITÉ DE LIÈGE - GEMBLOUX AGRO-BIO TECH

INFLUENCE OF COMBINED ENVIRONMENTAL CONSTRAINTS ON PHOTOCHEMICAL CAPACITY AND CO_2 FLUXES IN A TEMPERATE MANAGED GRASSLAND

Ir Anthony Digrado

Dissertation originale présentée en vue de l'obtention du grade de docteur en

Sciences agronomiques et ingénierie biologique

Promoteurs: Pierre Delaplace - Patrick du Jardin
Année civile: 2017

"An experiment is a question which science poses to Nature,
and a measurement is the recording of Nature's answer."
Max Planck (1858 - 1947)

Cette oeuvre est sous licence Creative Commons. Vous êtes libre de reproduire, de modifier, de distribuer et de communiquer cette création au public selon les conditions suivantes :

- paternité (BY) : vous devez citer le nom de l'auteur original de la manière indiquée par l'auteur de l'oeuvre ou le titulaire des droits qui vous confère cette autorisation (mais pas d'une manière qui suggérerait qu'ils vous soutiennent ou approuvent votre utilisation de l'oeuvre) ;
- pas d'utilisation commerciale (NC) : vous n'avez pas le droit d'utiliser cette création à des fins commerciales ;
- partage des conditions initiales à l'identique (SA) : si vous modifiez, transformez ou adaptez cette création, vous n'avez le droit de distribuer la création qui en résulte que sous un contrat identique à celui-ci.

À chaque réutilisation ou distribution de cette création, vous devez faire apparaître clairement au public les conditions contractuelles de sa mise à disposition. Chacune de ces conditions peut être levée si vous obtenez l'autorisation du titulaire des droits sur cette oeuvre. Rien dans ce contrat ne diminue ou ne restreint le droit moral de l'auteur.
`http://creativecommons.org/licences/by-nc-sa/4.0/deed.fr`

Résumé

Digrado Anthony (2018). Influence des contraintes environmentales combinées sur la capacité photochimique et les flux de CO_2 dans une prairie tempérée. (PhD Thesis) Gembloux, Belgique, University of Liège, Gembloux Agro-Bio Tech, 270 p., 8 tabl., 31 fig.

L'augmentation des productions agricoles afin de répondre aux besoins alimentaires et bioénergétiques en 2050 risque d'entrainer une augmentation des émissions en gas à effet de serre (GES) du secteur agricole. Cependant, les prairies offrent une opportunité de mitiger une partie des GES en stockant du carbone dans les sols via la photosynthèse. Cette dernière, cependant, est sensible aux conditions environnementales. En particulier, la capacité d'une plante à collecter et à utiliser l'énergie lumineuse peut être altérée par des stress abiotiques. Bien que beaucoup d'études se sont focalisées sur l'impact des stress environmentaux sur les flux de CO_2, peu se sont intéressées à leur influence sur la capacité photochimique des écosystèmes. L'objectif de cette thèse est d'étudier l'impact de contraintes environnementales sur la capacité photochimique d'une prairie et d'évaluer comment des variations des processus impliqués dans la phase claire de la photosynthèse influencent les flux de CO_2.

Des mesures de fluorescence chlorophyllienne ont été réalisées durant deux ans sur trois espèces prairiales (*Lolium perenne* L., *Taraxacum* sp., and *Trifolium repens* L.). La capacité photochimique de la prairie a été estimée sur base de ces mesures. Les flux de CO_2 ont été mesurés par eddy covariance. Les résultats ont montré une variation journalière et saisonnière de la capacité photochimique des trois espèces. La monocotylée *L. perenne* et les dicotylées (*Taraxacum* et *T. repens*) montraient des stratégies d'acclimation différentes. Toutes présentaient une dissipatation d'énergie au sein du photosystème II mais des réponses contrastées quant à l'efficience du photosystème I. En conséquence, l'écosystème prairial montrait également une variation dans sa capacité à collecter et à utiliser l'énergie lumineuse. La plus faible capacité photochimique a été mesurée en été quand les stress abiotiques tels que la haute luminosité et les hautes température étaient combinés. Cependant, la diminution de capacité photochimique n'a pas entrainé de diminution de fixation du carbone. Cette résilience de l'assimilation du carbone malgré les processus de dissipation d'énergie peut s'expliquer par la haute irradiance dans ces conditions.

Dans la dernière partie de cette thèse, nous discutons comment d'autres études peuvent contribuer à améliorer nos connaissance en écologie afin de clarifier le lien existant entre capacité photochimique et fixation du carbone par les ecosystèmes. Nous discutons également comment ces résultats peuvent servir dans les stratégies visant à mitiger les émissions de GES et comment les plantes influencent les flux de GES par d'autres processus que la photosynthèse.

Mots clés: Eddy covariance, fluorescence chlorophyllienne, flux de carbon, GPP, gaz à effet de serre, test JIP, prairie, respiration

Summary

Digrado Anthony (2018). Influence of combined environmental constraints on photochemical capacity and CO_2 fluxes in a temperate managed grassland. (PhD Thesis) Gembloux, Belgium, University of Liège, Gembloux Agro-Bio Tech, 270 p., 8 tabl., 31 fig.

Increase in agricultural production to insure food security and energy demand by 2050 might result in higher greenhouse gas emissions (GHG) from the agricultural sector. Managed grasslands, however, offer the opportunity to offset some of the GHG emission through the storage of carbon in terrestrial systems by photosynthesis. Photosynthesis, however, is highly sensitive to environmental conditions. Especially, plant ability to harvest and use light energy for photochemistry can be impaired by abiotic stresses. While numerous studies have focused on the impact of environmental constraints on ecosystem carbon fluxes, the influence on ecosystem photochemical capacity is understudied. The main goals of this thesis was to evaluate how environmental constraints impacted the grassland photochemical capacity and how variations in processes involved in light reactions of photosynthesis influenced ecosystem carbon fluxes.

Frequent chlorophyll fluorescence measurements were conducted over a two-year period, on three grassland species (*Lolium perenne* L., *Taraxacum* sp., and *Trifolium repens* L.). The ecosystem photochemical capacity was estimated from measurements performed on the three grassland species. In addition, monitoring CO_2 fluxes was performed by eddy covariance. Our results showed that photochemical capacity of the primary grasslands species exhibited diurnal and seasonal variations. The monocot *L. perenne* and the dicots (*Taraxacum* and *T. repens*) exhibited different acclimation strategies. All species exhibited the onset of energy dissipation mechanisms within the photosystem II but expressed contrasted response in the photosystem I efficiency. As a result, the ecosystem also exhibited variations in its ability to harvest and use photon energy. The strongest declines in photochemical capacity were observed in summer when abiotic stresses such as high light and high air temperature were combined. However, decrease in photochemical capacity did not result in a decreased ability to fix carbon in the grassland. The maintenance of carbon assimilation despite the onset of energy dissipation mechanisms can be explained by the higher availability

of light energy under these conditions.

In the final section of this PhD thesis, we discuss how future experiments can improve our knowledge in plants functional ecology and in the relationship between the photochemical capacity and ecosystem carbon fluxes. We also discuss how these results can benefit GHG mitigation strategies and how plants influence GHG balance through other routes than photosynthesis.

Key words: Carbon fluxes, chlorophyll fluorescence, eddy covariance, greenhouse gas, grassland, GPP, JIP-test, respiration

Acknowledgments

It all started with an interest in educational television programs such as 'C'est pas sorcier' and 'Il était une fois la vie' at the age of 8. Then it continued by the encounter of brillant and passionate professors who gave me the love of Science. There are many people who have contributed to this thesis in many ways. Here, I would like to express my deepest gratitude.

First of all, I want to express my gratitude to my two promotors and advisors. My deepest thanks to Dr Pierre Delaplace for the quality of its supervision during this thesis. This thesis have benefited a lot from his precious advices as a great scientist but also from his cheering during hard times. I cannot forget your unfailing devotion and how you helped me to give the best of myself these past years. Thank you for you guidance but also for all these extra-scientific moments and delightful unconventional sense of humour that made the time fly so fast. Thank you Dr Pr Patrick du Jardin for introducing me to the beauty of Plant Science through your amazing lectures. You made me discover a wonderful world full of mysteries still waiting to be explored and full of tremendous challenges yet to be overcome. You were also the first with which I discussed my will to realize a PhD thesis. Thank you for your advisements all along this PhD, you are a great inspirational figure on both scientific and human aspect.

I am also thankful to Dr Bernard Heinesch, coordinator of the CROSTVOC project within which the present thesis lies, for the management and the conception of this ambitious project of high interest for the scientific community and society. I want to express my gratitude as it offers me the opportunity to realize this thesis and develop my research on photosynthesis in a serendipitous way. I also want to thanks Dr Pr Marc Aubinet for his scientific input to this thesis and the great quality of his lectures during my academic years as he was among my favorite professors. I also thanks Henri Chopin and Frederic Wilmus from the Biosystems Dynamics staff which help was precious. Special thanks to Alain Debacq. You are so talented!

I also thank Dr Crist Amelynck and Dr Niels Schoon from the BIRA team. You were great partners and I learned a lot by working with you. I hope I will have the opportunity to work with amazing scientists like you in the future.

I am also grateful to Dr Pr Filippo Bussotti from the university of Florence for our constructive discussions and his scientific input. Your help in the interpretation of fluorescence emissions was precious. Thank you for the time and advices you gave to

this unknown young scientist.

Thank you to Dr Pr Marie-Laure Fauconnier for the useful discussions around the fascinating and challenging world of volatile organic compounds. You were always available to help a volatile like me.

I also want to express my gratitude to my fellow PhD students on this project, Mozaffar Ahsan and Aurélie Bachy for all the (non-)scientific discussions and their good spirit. It was good working with you. You are great people and I wish you all the best in your future career.

Thanks to the farmer Adrien Paquet who allowed us to conduct great research in his pasture. He also gave us a lot of his time during the setting of scientific equipment. Special thanks to the cows in the pasture who trampled and drooled on a lot of my precious leaf clamps. You were a real pain in the ass. But since you were -sometimes- funny to watch I still love you.

I also want to thank my fantastic colleagues. Thank you Caroline Baudson for all the good times, the laughter, the cheering and everything that helped me pursue this thesis. I've never ceased to be impressed by you. You are amazing. Thank you Laurence Galhaut for your constant good mood and shining smiles that contributed to brighten up our days. You are the sweetest and I really enjoyed these past years with you. Thank you Claudia Colot for all these passionate glances that brighten up my days in an other way. Thank you Florence Paquet for taking care of the team through good lab assistance and chocolates. Thank you Twilight Sparkles for your colorful mood. You are brilliant. We cannot dream of a better team. I wish you all the best life can offer because you deserve it. I also want to thank Magdalena de Cazenave. You were a great colleague and I miss the fun we had together.

I cannot forget to thank Dr Benjamin Delory who was my supervisor during my master thesis and he was a great one. You definitely contributed to this thesis as you gave me the taste for research. I was fortunate enough to have you, a scientist of great value, for my first steps in the world of research. From now I'll try my best to be at least as good as you.

I also thank people from the Organic Chemistry lab such as the fabulous Thomas Bertrand, Nathalie le Maire, Marie Davin, Gaëtan Richard, Matthew Saive, Tierry Kenne, Bastien Durenne, Simon Lebecque and also Pierre-Patrick Eloundou who contributed to make the time spent at the chemistry lab more pleasant. Special thanks to Franck Michels (alias Frank Michels) and Danny Trisman (alias Dany Trisman) who

considerably helped me with GC-MS analysis. It took me 4 years to spell your name correctly.

I also want to thanks Dr Pr Muriel Eyeletters for her introduction to chlorophyll fluorescence and Dr Frederic Collinet for computational resources.

There are also many friends that I want to thanks who helped keeping my sanity of mind during this thesis by spending terrific time together. Thank you Thomas Pongo, Pierre Lafontaine, Fanny Ramirez, Marine Hennaut, Anne-Sophie Voisin, Benjamin Willems, Elodie Denys and Guillaume Colla from the Climbing Unicorn Club. Maybe I am wrong about the 'sanity of mind' part but we sure spend great time together. I also thank Alexandre lawniczak, Glenn, Alexis Pedergnana, Marie Fosséprés and Jérôme Demoulin for the good times spend together. I cannot forget a dear friend of mine, Aurore Courcelle, who was always present for cheers and laugh. Thank you Aurore for being this awkward.

I will finish by expressing my deepest gratitude to my family for their unfailing thrust in me even when I doubted myself. Thank you dad for everything. Hundreds of pages won't be enough to say how you help me through your life lessons, the education you gave me and the inspirational figure you are. Thank you mum. You are definitely the one who gave me my strength of character and perseverance needed for this thesis. Thank you grandma for your devotion and unconditional love. Your caring nature was of great help during this thesis. Thank you grandpa. There is no doubt you were a great example for me since I was a child. I wish you were still here to see me.

Thanks again to everyone. I was so fortunate to have you by my side.

Anthony Digrado.

CONTENTS

List of Figures

State of the art

Objectives and methodology

Results

General discussion and perspectives

Supplementary materials

List of Tables

State of the art

Results

Supplementary materials

LIST OF ABBREVIATIONS

3-PGA: 3-phosphoglycerate

$\mathbf{A_{CO_2}}$: Carbon assimilation rate

ATP: adenosine triphosphate

BVOC: biogenic volatile organic compounds

BNI: biological nitrification inhibition

BNIs: biological nitrification inhibitors

CAM: crassulacean acid metabolism

CCA: canonical correlation analysis

CEF: cyclic electron flow

Chl: chlorophyll

ChlF: chlorophyll fluorescence

CP24, CP26, CP29, CP43, CP47: complex protein in the thylakoid membrane

Cyt: cytochrome

DCMU: 3-(3',4'-dichlorophenyl)-1,1-dimethylurea

DTO: Dorinne Terrestrial Observatory

E: transpiration rate

ETC: electron transport chain

ETR: electron transport rate

FeS: Rieske iron-sulfur protein

FNR: ferredoxin-$NADP^+$ reductase

G3P: glyceraldehyde-3-phosphate

GC-MS: gas chromatography-mass spectrometry

GHG: greenhouse gas

GLM: general linear model

GLVs: green leaf volatiles

$\mathbf{g_m}$: mesophyll conductance

GPP: gross primary productivity

$\mathbf{g_s}$: stomatal conductance

J: energy flux

LHC: light harvesting complex

LHCI: light harvesting complex of the photosystem I

LHCII: light harvesting complex of the photosystem II

NADPH: nicotinamide adenine dinucleotide phosphate

NEE: net ecosystem (CO_2) exchange

NPP: net primary productivity

NPQ: non-photochemical quenching

P680: Reaction centre pigments of photosystem II formed by two Chl *a* molecules

P700: Reaction centre pigments of photosystem I formed by two Chl *a* molecules

PAM: pulse amplitude modulated

PC: plastocyanin

PCA: principal component analysis

PEA: plant efficiency analyzer

PCR: photosynthetic carbon reduction

PEP: phosphoenol pyruvate

PEPcase: phosphoenol pyruvate carboxylase

PI: performance indice/index

PQ: plastoquinone

PPFD: photosynthetic photon flux density

PQH_2: plastoquinol

PSI: photosystem I

PSII: photosystem II

PTR-MS: proton-transfer-reaction mass spectrometry

Q_A: quinone A

Q_B: quinone B

RC: reaction centre

R_{eco}: Ecosystem respiration

RH: relative air humidity

ROS: reactive oxygen species

Rubisco: ribulose-1,5-biphosphate carboxylase-oxygenase

Ru5P: ribulose-5-phosphate

RuBP: ribulose-1,5-biphosphate

VPD: vapor pressure deficit

WUE: water-use efficiency

Yz : tyrosine-161 of the photosystem II D1

LIST OF SYMBOLS AND VARIABLES

$\Delta \mathbf{V_{IP}}$: the I-P phase. The efficiency/probability that a photon trapped by the PSII RC moves an electron into the electron transport chain beyond PSI to reduce the final acceptors of the electron transport chain (i.e., ferredoxin and NADP). [-]

$\mathbf{F_t}$: fluorescence intensity at the time t. [-]

$\mathbf{F_J}$: fluorescence intensity at 2 ms (J-step). [-]

$\mathbf{F_I}$: fluorescence intensity at 30 ms (I-step). [-]

$\mathbf{F_M}$: maximum fluorescence intensity (P-step). [-]

$\mathbf{F_V}$: maximum variable fluorescence. [-]

$\mathbf{F_V/F_M}$: maximum quantum yield of PSII of a dark-adapted leaf. Expresses the probability that an absorbed photon will be trapped by the PSII reaction centre. [-]

GPP: gross primary productivity. [μmol CO_2 m^{-2} s^{-1}]

$\mathbf{GPP_{1500}}$: gross primary productivity at light saturation. [μmol CO_2 m^{-2} s^{-1}]

$\mathbf{M_0}$: approximated initial slope of the fluorescence transient. [-]

NEE: net ecosystem (CO_2) exchange. [μmol CO_2 m^{-2} s^{-1}]

$\mathbf{O_3}$: ozone concentration. [ppb]

$\mathbf{PI_{ABS}}$: performance index (potential) on absorption basis for energy conservation from photons absorbed by PSII to the reduction of intersystem electron acceptors. [-]

PPFD: photosynthetic photon flux density. [μmol m^{-2} s^{-1}]

$\Psi_{\mathbf{E0}}$: the J phase. The efficiency/probability that a photon trapped by the PSII RC moves an electron into the electron transport chain beyond Q_A. [-]

RC/ABS: Q_A-reducing reaction centres (RC) per PSII antenna Chl. [-]

R_{10}: total ecosystem respiration normalized at 10°C. [μmol CO_2 m^{-2} s^{-1}]

R_{eco}: total ecosystem respiration. [μmol CO_2 m^{-2} s^{-1}]

RH: relative air humidity. [% v/v]

SM: soil moisture. [% v/v]

T_{air}: air temperature. [°C]

V_t: relative variable fluorescence at the time t. [-]

VPD: vapor pressure deficit. [kPa]

I

Background

With the forecasted increase of world population from 7.6 billion to 9.8 billion by 2050 (United Nations (UN) 2017), the agricultural sector is facing the challenge to roughly double its production in order to meet the demand of agricultural products for food and bioenergy (Foley et al. 2011). Increasing production through an augmentation of agricultural land might not constitute a feasible solution (or only partially) as the increase in population size might generate a competition in land use. Therefore, it is likely that the required increase in agricultural product need to be achieved through an improvement of the current production rate per hectare (Murchie et al. 2009). In the latter half of the 20th century, during the "green revolution", agronomical sector managed to achieve important yields increase, with a rise of the harvest index of the major grain crops around 0.6 (Flügge et al. 2016). This improvement was reached essentially by maintaining optimal plant growth conditions through water and nutrients inputs (Murchie et al. 2009). Adequate and timely control of weed and disease also contributed to optimise growth conditions and increase agronomic yield (de Bossoreille de Ribou et al. 2013).

These improvements in agronomic production, however, had detrimental repercussion on natural habitats, biodiversity and soil conditions (Foley et al. 2011). Agriculture also had an impact on air quality as it constitutes an important source of CH_4 and N_2O emission. It was estimated in 2010 to 5.0-5.8 $GtCO_2$ eq/yr the rate of greenhouse gas (GHG) emission from agriculture, representing 10-12% of total anthropogenic emissions (Smith et al. 2014). Moreover, with the growth of population, emissions from the agricultural sector are expected to triple if current diet preferences and food consumption were to continue with the same trends as 1995 (Popp et al. 2010). It is therefore essential to reduce the environmental footprint of agriculture while meeting the agronomical production requirements.

Managed grasslands are an important agro-ecosystem to consider when talking about food security and environmental footprint. Permanent pastures are estimated to cover 3.48 billion ha (Steinfeld et al. 2006) and represent around 80% of the world agricultural land (Boval and Dixon 2012). In Europe (i.e., EU-28), permanent grasslands are estimated to cover 59.3 million ha, representing 33.2% of the European agricultural surface (Eurostat 2016). By 2050, the world demand for livestock products is expected to grow by 70% (Gerber et al. 2013) meaning that agronomic activities related to grasslands such as livestock and forage production will have to increase consequently. This suggests a potential increase in GHG emissions related to pastures

activites, as they are an important source of methane (CH_4) emission by grazing ruminants and of nitrous oxide (N_2O) emission due to nitrogen fertilization in field (Chang et al. 2015). Grasslands, however, offer the opportunity to offset some of the GHG emission through the storage of carbon in terrestrial systems (Chadwick et al. 2011, Jones et al. 2017). Lugato et al. (2014) have estimated to 5.5 Gt the amount of carbon stored in the top 30 cm soil of European agricultural grasslands[1]. Carbon uptake by plants through photosynthesis is the key process in the storage of carbon in agricultural soil.

Environmental constraints, however, imposed by future climate constitute an important threat in the sequestration of carbon by grasslands as it can alter the process of photosynthesis and carbon fixation by the ecosystem (Hüner et al. 2016). Understanding photosynthesis in a changing climate is therefore crucial as carbon uptake by plants constitutes one of the major CO_2 fluxes on land (Pulles 2017). If the impact of environmental constraints on gas exchange at leaf and ecosystem-scale have been well-studied by the scientific community, less is known about the response of the photon use efficiency of an ecosystem to its environment and its impact on CO_2 fluxes. Still, plant photochemical capacity, which can be defined as the ability for plants to harvest and use photon energy to trigger the light reactions of photosynthesis, is crucial to generate photochemical energy and fix carbon (Arend et al. 2013).

A better comprehension of the grassland photochemical capacity response to its environment and the influence on CO_2 uptake is therefore essential. This was the aim of the present PhD thesis as part of a F.R.S.-FNRS research project (PDR, no. 14614874). The first step was to develop a protocol allowing the assessment in field condition of the photochemical capacity of this complex ecosystem characterized by a diversity in plant species. By simultaneously monitoring the micro-meteorological conditions on-site, we then identified how combined environmental constraints impacted the different steps involved in the light reactions of photosynthesis for the studied grassland species. Based on CO_2 fluxes measurements performed using the eddy-covariance technique, we were then able to assess the influence of seasonal variation in the ecosystem photochemical capacity on carbon uptake. Based on our results, we discuss perspectives for additional trials that could improve our understanding of

[1]Carbon storage of an grassland ecosystem is commonly estimated by the amount of carbon in soil since carbon accumulated in the aboveground part of plant biomass can be exported through harvest and grazing.

the existing relationship between the photosynthetic performance and ecosystem CO_2 fluxes. We also discuss how plants can be involved in mitigation strategies for GHG emissions in grasslands.

II

State of the art

1 GREENHOUSE GAS EMISSIONS IN MANAGED GRASSLANDS

1.1 Grassland management

Despite covering around 13% of the EU-28 area (Eurostat 2016), grassland is not a natural climax vegetation in most part of Europe (Chang et al. 2015). Since most of grasslands in Europe are maintained through grazing or cutting they are defined as semi-natural ecosystems (Soussana and Duru 2007). Managed grasslands can be divided into three main categories depending on their management practice: (i) pastures, which are devoted to the production of introduced or indigenous forage and usually managed by grazing, (ii) meadows, which are natural or semi-natural ecosystem devoted to the production of hay or sillage and managed by cutting, and (iii) grazed meadows, which are cut in spring and can be grazed later in the season (Allen et al. 2011, Hejcman et al. 2013). Grasslands production systems can be either extensive or intensive. The former is commonly found in dry regions of tropical area while the latter is common in Europe and North America (Boval and Dixon 2012).

Different management strategies are performed in order to increase the productivity. The application of nitrogen fertilizer is a common method used to increase livestock production as gain in animal production is observed with the increase in available forage (Boval et al. 2002). Depending on the soil and weather conditions, soil renovation through ploughing and harrowing are sometimes realized to improve soil structure. This mechanical manipulation generally improves soil condition which enhance grass productivity on grasslands (Drewer et al. 2017). System manager can also adjusts the frequency of grazing (rotational stocking) in order to adapt to herbage growth condition. In rotational stocking system, animals are periodically removed to allow plants to regrow in condition of low herbage production. This prevents a decrease in the efficiency of herbage harvesting (Lemaire et al. 2009). The stocking rate, defined as the number of animals per area on a certain period of time, is another variable the system manager can adjust to optimize the animal productivity. The optimal stocking rate is proper to each forage-livestock system and depend on the forage production and the animal production goal (Inyang et al. 2010, Boval and Dixon 2012). Nutritional quality of the forage can also have a crucial role in animal production. For instance, a deficiency in Cu, Zn and Mn elements can affect the reproductive efficiency

of livestock (Prasad and Gowda 2005). Supplementation with additional mineral or the introduction of legumes in pasture systems can be performed in order to increase the nutritive value of the diet (Boval and Dixon 2012).

1.2 Sources and factors influencing greenhouse gas fluxes in managed grasslands

Meteorological conditions as well as management practices can influence GHG fluxes in grasslands either by promoting the emission or the sink strength of the ecosystem for these gases (Table 1.1). In the present section, we present the influence of varied factors on CH_4, N_2 and CO_2 fluxes in managed grasslands.

Table 1.1 – Summary table of factors influencing greenhouse gas (GHG) fluxes in managed grassland ecosystems. An arrow indicates for each factor whether it promotes the emission (↑, positive feedback) or the sink strength (↓, negative feedback) of the ecosystem for the concerned GHG.

GHG	Factor	Feedback	Description
CH_4	Fertilizer	↓↑	Nitrogen (N) fertilization promotes CH_4 emission in natural grassland by inhibiting methanotrophic bacteria CH_4 oxidation but this inhibition is not observed in managed grasslands used to frequent N application. N-input can also promotes O_2 diffusion induced by N-stimulated root growth.
	Manure	↑	Manure application can lead to higher CH_4 emission due to the inoculation of methanogenic bacteria. However, the induced burst in CH_4 emission decline quickly after application because the contact with atmospheric O_2 inhibits methanogenic bacteria activity.
	Tillage	↓	Tillage was shown to reduce CH_4 oxidation by methanotrophic bacteria.
	Ruminant	↑	Enteric fermentation by ruminants is a source of CH_4 emission estimated at 176-202 g $animal_{-1}$ day_{-1} for cattle. Grazing was also shown to increase soil wetness leading to a reduced CH_4 oxidation.
N_2O	Temperature	↑	Since increase in temperature promotes the stimulation in microbiological activity and gas diffusion, studies generally report an exponential increase in N_2O emissions with increasing soil temperatures.

Continued on next page

Table 1.1 – continued from previous page

GHG	Factor	Feedback	Description
	Fertilizer	↑↓	Impact of fertilization on N_2O depends on the C/N ratio. A >75 C/N ratio (e.g., straw, farmyard manure) lead to an inhibition of nitrifying activity and N immobilization while synthetic fertilizers (low C/N ratio) increase the amount of available mineral N.
	Tillage	↑↓	Tillage tend to promote a more rapid mineralization of organic matter by improving O_2 diffusion, leading to high N_2O emission in the short-term. However, lower N_2O emission are observed in the long-term.
	Rainfall	↑	Rainfall creates anoxic environment which promotes denitrification activity. The latter are the main contributor to N_2O fluxes at >70% water-filled pore space while nitrification is an important contributor at 30-70% water-filled pore space.
	Ruminant	↑	Trampling improve soil compaction, which promotes zn anoxic environment for denitrification activity.
CO_2	Temperature	↑	High temperature promotes organic matter mineralization by bacteria and plant respiration.
	Fertilizer	↓	Fertilization promotes plants growth and hence carbon fixation. It also promotes root growth and hence carbon sequestration in soil. However, after a threshold, increase in fertilization does not promote further carbon assimilation.

Continued on next page

Table 1.1 – continued from previous page

GHG	Factor	Feedback	Description
	Tillage	↑	Tillage promotes the mineralization of residues and therefore CO_2 release into the atmosphere. Following tillage intervention, reduced CO_2 assimilation by the ecosystem can be observed for several days.
	Ruminant	↑↓	Ruminants constitutes a source of CO_2 emission through respiration. However soil compaction by ruminants reduces microbial biomass and thus soil respiration. Grazing was shown to reduce both the ecosystem CO_2 respiration and CO_2 assimilation but overall resulted in a stronger net CO_2 sink. Exportation in the form of milk and body mass represent a loss of carbon for the ecosystem. Manure and excreta application, however, can provide an additional C source even though manure application can stimulate microbial activity and microbial respiration.

1.2.1 Methane fluxes in managed grasslands

In most case, natural grasslands act as CH_4 sink because of CH_4 oxidation by methanotrophic bacteria (Mosier et al. 1991, Mori 2016). Application of nitrogen fertilizer in natural grasslands, however, was shown to reduce grasslands CH_4 sink capacity by inhibiting CH_4 oxidation (Mosier et al. 1991). Such inhibition, however, is not always observed in managed grasslands used to frequent application of nitrogen input (Shimizu et al. 2013) probably due to an increase in ammonium-oxidizing bacteria able to oxidise CH_4 or by an improvement in soil O_2 circulation promoted by N-stimulated roots development (Bodelier and Laanbroek 2004). Soil disturbance induced by tillage, however, was shown to reduce CH_4 oxidation (Hütsch 2001, Ding et al. 2004). CH_4 peak emissions are also observed directly after manure application (Jones et al. 2005) and are assumed to be induced by the inoculation of methanogenic bacteria (Jarecki et al. 2008). These emissions occur in a short period of time and CH_4 formation into manure is usually quickly inhibited by the O_2 diffusion (Chadwick et al. 2011). Decrease in soil pH might promote CH_4 emission in managed grassland as it is known in forest soil that acidic conditions can result in a decrease in methanotrophic activity (Hütsch 2001).

Enteric fermentation of ruminants is a significant source of CH_4 emission with cattle emissions ranging between 176-202 g animal^{-1} day^{-1} (McGinn et al. 2014, Richmond et al. 2015). Floristic composition of grasslands was shown to significantly affect CH_4 emission by cattle. In a grassland characterized by a low nutritive quality herbage, higher CH_4 emission per cattle was observed due to a higher dry mass intake by individuals (Richmond et al. 2015). Digestibility of forage, however, was not shown to have a significant impact on CH_4 emissions (Degola et al. 2016).

1.2.2 Nitrous oxide fluxes in managed grasslands

Depositions of N-compounds are usually observed in natural grassland even if weak N_2O emissions in the range of 69-74 g N ha^{-1} can be observed depending on soil moisture and temperature conditions (Chapuis-lardy et al. 2007, Kugler et al. 2008, Machon et al. 2010, Signor and Cerri 2013). N_2O emissions in grasslands are mainly determined by soil microbial activity through nitrification and denitrification of soil mineral N (NH_4^+ and NO_3^-) (Conrad 1996, Chang et al. 2015). Nitrification consists in the biological oxidation of ammonium to NO_2^- and NO_3^- with N_2O as a by-product

(Wrage et al. 2004). Denitrification, in contrast, consists in the reduction of NO_3^- or NO_2^- to NO, N_2O and N_2 (Bremner 1997).

Application of nitrogen fertilizer or manure in managed grasslands considerably enhances N_2O emissions as it increases the amount of available mineral N (Shimizu et al. 2013). Excreta from grazing animal (i.e., urine and dung) also constitute a source of N_2O emission (Novak and Fiorelli 2010). The C/N ratio of used fertilizer is determinant in N_2O fluxes as lower N_2O emissions are observed for product with a C/N ratio above 75. Residues with a high C/N ratio such as straw lead to an inhibition of nitrifying activity and an N immobilization. In these conditions, the low NO_3^- availibity associated with a surplus of electron lead to a more efficient reduction of N_2O to N_2 by denitrifiers (Benckiser et al. 2015). Therefore, synthetic fertilizers often induce more N_2O emissions than farmyard manure or equivalent (Mori 2016).

Tillage, however, can induce a more rapid mineralization of organic matter by improving soil O_2 diffusion. As a consequence, such soil restructuration was shown to induce significant N_2O emissions in grassland (Vellinga et al. 2004, Drewer et al. 2017). Lognoul et al. (2017), however, have shown in a 7 yr study that reduced tillage in agricultural crop resulted in higher N_2O soil emissions than conventional tillage, probably due to a better soil distribution of crop residues. This suggests that tillage practices might be responsible for higher short-term N_2O emission but result in lower total N_2O emission when considering the whole season. However, more experiments should be conducted to elucidate the influence of incorporated C/N ratio residues, soil texture and properties on long-term tillage-induced N_2O emissions.

Rainfall events following the application of fertilizer were also reported to enhance N_2O emissions in several studies (Chen et al. 2016, Lognoul et al. 2017). Because high precipitation creates anoxic conditions favoring denitrifiers, increase in denitrification activity has often been advanced as an explanation for high flux following rainfall (Mori 2016). However, other studies have also considered nitrification activity as the main contributor to burst of N_2O emissions following a rainfall (Barton et al. 2008, Chen et al. 2016). It appears that the relative contribution of nitrification and denitrification pathways in the amount of N_2O emitted to the atmosphere depends on the fraction of water-filled pore space. Nitrification process seems to be dominant at water-filled pore space within the 30-70% range while denitrification is reported to be the main source above ca. 70% (Chen et al. 2016, Smith et al. 2003). Grazing,

through soil compaction by trampling, can also contribute to enhance N_2O emissions by promoting anoxic environment favouring denitrification (Jones et al. 2017).

1.2.3 Carbon dioxide fluxes in managed grasslands

Grazing animals, soil heterotrophs (e.g., fungi and bacteria) and autotrophs (roots and plant shoots) respiration all contribute to CO_2 emission. Belowground respiration is often described as the most important contributor to the total ecosystem respiration (R_{eco}) and was shown to account for more than 70% in an alpine grassland study (Ganjurjav et al. 2014). Main sources of soil CO_2 production are organic matter decomposition by bacteria and root respiration (Savage et al. 2014). Temperature was shown to be the main controlling factor for CO_2 emission with the higher emission peaks being observed above 20°C in a managed grassland under a humid continental climate (Li et al. 2015). However, because photosynthetic activity by plants generally exceeds R_{eco}, grassland ecosystems commonly act as a carbon sink (Boval and Dixon 2012).

Agricultural activities, however, can alter CO_2 emissions and the soil carbon storage. Tillage, for instance, can increase residues mineralization with consequent CO_2 release in the atmosphere. Such enhanced CO_2 emissions following ploughing are characterized by a reduced ecosystem carbon uptake at daytime which can last ca. 40 days in temperate grasslands (Drewer et al. 2017). High grazing intensity can also reduce soil respiration (Cao et al. 2004) by promoting soil compaction and the reduction of microbial biomass (Andriuzzi and Wall 2017, He et al. 2017b). High stocking rate, however, can increase the loss of carbon from the ecosystem by animal respiration and by the reduction of leaf area index and the amount of carbon that can accumulate in the ecosystem (Soussana and Duru 2007, Chang et al. 2015). Reduction in LAI by grazing, however, can contribute to remove litter and standing dead biomass limiting light availability for photosynthesis (Gomez-Casanovas et al. 2017). Overall, higher carbon sink was reported in grazed pasture compared to ungrazed pasture, due to a stronger reduction in R_{eco} than in carbon assimilation (Gomez-Casanovas et al. 2017). Carbon can also be exported in the form of milk production and animal body mass (Chang et al. 2016). Still, exported carbon can partly be returned to the ecosystem through manure application and excreta (Chang et al. 2015). Manure application, however, can lead to a 1.6 times increase in soil respiration by stimulating microbial activity due to the presence of labile carbon (Jones et al. 2005).

Carbon sequestration by the ecosystem can be promoted by improving biomass production, as up to 50% of carbon assimilated by plants can be transferred to soil through root construction, maintenance, respiration, exudation and turn over (Rees et al. 2005). Addition of nitrogen fertilizer in situation of N limitation was shown to promote the carbon sink capacity of the ecosystem by increasing plant biomass and therefore net primary productivity (NPP) of the ecosystem (Chang et al. 2015). However, after a threshold, NPP of the ecosystem is less sensitive to fertilization and additional N input tends to stimulate CH_4 and N_2O emissions more than it improves the sink strength of the ecosystem for GHG (Gomez-Casanovas et al. 2016). This N saturation threshold for sink strength varies between sites as CH_4 uptake response to nitrogen fertilization can be affected differently among managed grasslands (Bodelier and Laanbroek 2004, Ding et al. 2004, Jarecki et al. 2008). Floristic composition can also influence NPP in grasslands with aboveground biomass increasing with plant diversity (Hector et al. 1999, Loreau et al. 2001). Higher productivity under higher species richness was partly explained by the functional diversity and complementary among species of different traits such as those associated with light-acquisition and nitrogen acquisition strategies (Roscher et al. 2013). High biodiversity was also shown to stabilize ecosystem productivity by increasing its resilience to climate events (Isbell et al. 2015).

Photosynthetic activity is determinant in the carbon uptake by ecosystems (Pulles 2017), meaning that events altering photosynthetic processes can affect the carbon sink strength of the ecosystem. Photosynthesis strongly depends on environmental conditions and important variations in ecosystem carbon uptake are observed along the season (Hirata et al. 2007, Takagi et al. 2015). Baldocchi et al. (2018) also showed that an important part of the yearly variability observed in CO_2 fluxes was attributed to biophysical factors affecting photosynthesis (Fig. 1.1). In the next chapter, we will discuss how the environment influences photosynthetic processes and which mechanisms are triggered in response to environmental perturbations.

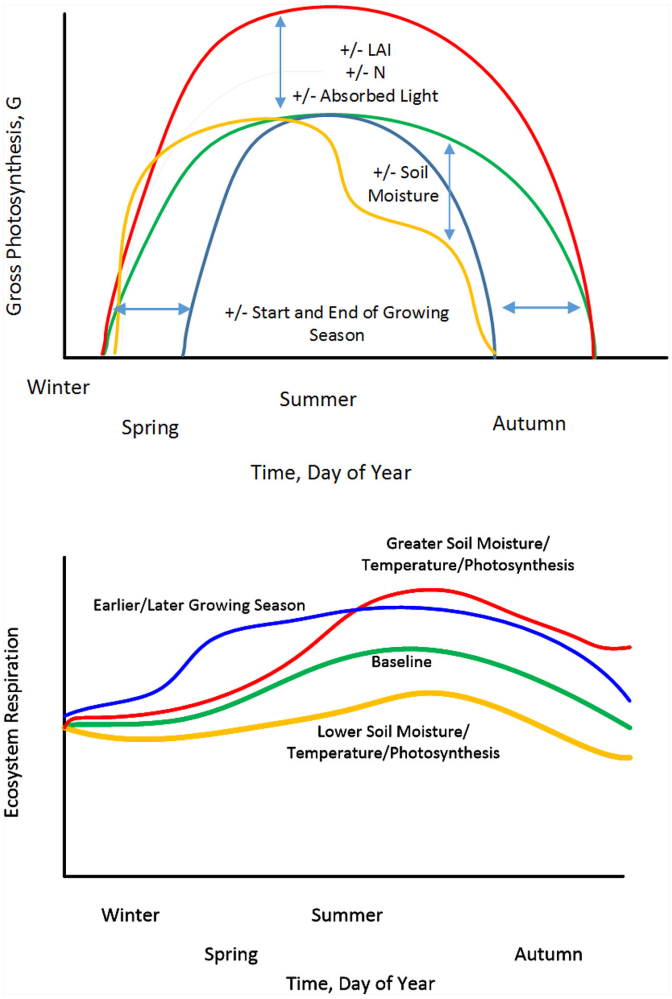

Figure 1.1 – Representation of the yearly variation of gross primary production (GPP) and ecosystem respiration depending biophysical forcings. The upper panel shows GPP, or the ecosystem photosynthesis, variations among different contrasted years. Indeed, GPP of a reference year (green) can vary depending on the soil moisture (orange), the amount of absorbed light by leaves (red), and the length of the growing season (blue). The lower panel shows variations in the ecosystem respiration between years. The ecosystem respiration of a reference year (green) can be affected by the length of the growing season (blue). Higher respiratory activity are observed in periods of high in soil moisture, high temperature and/or high photosynthesis activity (red) while lower ecosystem respiration are measured in periods of drought event, low temperature and/or low photosynthetic activity activity (orange). Figure from Baldocchi et al. (2018).

2 PHOTOSYNTHESIS UNDER ENVIRONMENTAL CONSTRAINTS

2.1 Photosynthesis, the basics

Photosynthesis in higher plants is a process by which light energy is mainly harvested for its conversion into chemical energy. This conversion is achieved by two key events taking place in chloroplasts which are the light reactions and the dark reactions.

During the light reactions, light energy is collected and converted into ATP and NADPH. This conversion of light energy takes place in the thylakoid membrane of chloroplast through successive electron transfers, the so-called 'Z-scheme' (Fig. 2.1). In this model, the sun energy absorbed by the antenna of the PSII is transferred to the reaction centre (RC) located in the dimeric core of the photosystem II (PSII). One of the most important constituent of the PSII antenna is the major peripheral light harvesting complex of the photosystem II (LHCII), a trimer multiprotein complex bounded to the PSII (Fig. 2.2). Two strongly bound trimers (S-LHCII) and 2 moderately bound trimers (M-LHCII) can be found in grana per PSII. A LHCII monomer is usually constituted of about 7 Chl *a*, 5 Chl *b* and 2 lutein. Neoxanthin and violaxanthin are also present in variable amounts. In light fluctuating environment, two more loosely bound trimers (L-LHCII) which approximately contain 100 Chl (*a*+*b*) can also be found found in the PSII-LHCII supercomplexes (Pan et al. 2013). The connection between the major LHCII and the PSII core complex is made by the protein complex CP24, CP26 and CP29 (Fig. 2.2) which contain approximatly 8-10 Chl (*a*+*b*) in addition to several xanthohylls. They form the PSII minor antenna. Their role in light harvest is less pronounced than that of the major LHCII as they contain only 15% of the total Chl content of the PSII. However, because of their strategic position, they can significantly contribute to regulatory mechanisms. The PSII core (Fig. 2.2) is formed by the proteins D1 (PsbA gene) and D2 (PsbD gene) which both bind 3 Chl *a*, the inner antenna complex proteins CP43 (PsbC gene) and CP47 (PsbB gene) containing both 13 Chl *a* and other Psb-genes related proteins. The photoactive RC (also called the primary electron donor of PSII or the P680) is formed by 2 Chl *a* coming from the D1 and D2 proteins. Depending on the connection between the PSII core and the different constituent of the PSII antenna, the PSII antenna varies in size and can be subdivided in three groups (α, β and γ). The antenna of the PSIIα contains about 230

Chl (*a*+*b*) while the antenna of the PSIIβ and γ contain respectively 130 and 50 Chl (*a*+*b*) (Whitmarsh and Govindjee 2001, Papageorgiou and Govindjee (Eds.) 2004).

Upon excitation, the P680 enables the transfer of an electron to the primary electron acceptor of the PSII, the pheophytin (Fig. 2.1). After charge separation, the $P680^+$ recovers an electron from the tyrosine-161 of the PSII D1 (Yz). The latter transfers its positive charge to the oxygen evolving complex (OEC) which extracts four electrons from two water molecules once four positive charges have been accumulated. Oxygen is released during the electron extraction from the water molecule. The electron is then transferred from the pheophytin to the Q_A, the primary quinone acceptor. Once the Q_A is reduced, the PSII RC is considered 'closed', meaning that it is not able to use further light excitation energy to send an additional electron into the electron transport chain (ETC). During the next step, the electron moves from the Q_A to the Q_B-site at the acceptor side of the PSII where it will reduce a plastoquinone (PQ) from the PQ pool. After two turnover of the P680, PQ is reduced into plastoquinol (PQH_2). A bicarbonate ion (HCO_3^-) located in this region is assumed to participate to the protonation. Despite being photochemically active, some PSII are not able to transfer an electron from Q_A to the Q_B-site. These are therefore termed as Q_B-non-reducing PSII (Mathur et al. 2011a). Electrons which have successfully reached the Q_B-site are then transferred to the cytochrome (cyt) b_6f complex by a mobile PQH_2. The cyt complex is formed by the Rieske iron-sulfur protein (FeS), the cyt f and the cyt b_6 containing the two subunits b_L and b_H. One electron is sent to the Rieske iron-sulfur protein (FeS) which delivers its electron to the cyt *f*. The second electron is sent to the cyt b_H via the cyt b_L (Fig. 2.1). After two PQ oxidation events, the cyt b_H transfers two electrons to an oxidized PQ during the so-called Q-cycle. The resulting PQH_2 can then transfer its electrons to the cyt b_6f complex. Electron from the cyt f is passed to the plastocyanin (PC) which diffuses in the membrane till the donor side of the photosystem I (PSI). Once at the donor side of the PSI the electron is delivered to the primary electron donor of the PSI (i.e. the P700 formed by two Chl *a* molecules). Since the core complexe of the PSI contains about 100 Chl *a* and its peripheral light harvesting complex (LHCI) about 14 Chl (*a*+*b*), it is photochemically competent. Under light excitation, the electron is sent to successive electron acceptors in the PSI till the acceptor side of the PSI where the ferredoxin eventually reduces $NADP^+$, the end acceptors of electrons, via the ferredoxin-$NADP^+$ reductase. During the whole process, a proton gradient is built across the thylakoid membrane, which enables the proton-dependent ATP synthase

to generate ATP from ADP and a phosphate ion (Papageorgiou and Govindjee (Eds.) 2004).

The dark reactions use products from the light phase to fix CO_2 into carbohydrates. Three different mechanisms of CO_2 assimilation exist among plants. The most widely spread, which is used by about 95% of plants, is referred as the photosynthetic carbon reduction (PCR) (Fig. 2.3) or the Calvin cycle in honor of Melvin Calvin who directed the research leading to the discrovery of this cycle, along with Andrew Benson and James Bassham. In the PCR, CO_2 is introduced into the cycle as a 3-carbon acid, the 3-phosphoglycerate (3-PGA), by reacting with the ribulose-1,5-biphosphate (RuBP) during a first step called the carboxylation. This process is catalyzed by the ribulose-1,5-biphosphate carboxylase-oxygenase (Rubisco) enzyme, a key enzyme in photosynthesis. As the RuBP is a 5-carbon keto sugar, two 3-PGA are derived from the reaction with the CO_2 molecule. Because of the CO_2 'conversion' into a 3-carbon molecule, the PCR is also referred as the C3 cycle and plants using this mechanisms of CO_2 assimilation are called the C3 plants.

The second step of the PCR is the reduction of the two 3-PGA produced at the end of the carboxylation. During this process, one ATP and one NADPH are used to reduce one 3-PGA molecule during a two-steps reaction. The result is a triose sugar-phosphate, the glyceraldehyde-3-phosphate (G3P), which can be used for different purposes.

One of the most important pathway of use of this constituted 'pool' of triose sugar-phosphate is the regeneration of the RuBP acceptor molecule, which is a necessity to keep the cycle in function and assimilate new CO_2 molecule. Two G3P can lead to the formation of a 6-carbon fructose phosphate which can then react with another 3-PGA to form a 5-carbon sugar and a 4-carbon sugar. The latter can react with another 3-PGA to form a 7-carbon sugar which can give two 5-carbon sugars by reacting with a 3-PGA. All the 5-carbon sugars deriving from the triose pool can be isomerized into a ribulose-5-phosphate (Ru5P). RuBP can be obtain by the phosphorylation of a Ru5P by using one ATP molecule. As illustrated in the figure 2.3, five 3-PGA are needed to regenerate three RuBP molecules. Since the uptake of one CO_2 leads to the formation of two 3-PGA, three CO_2 molecules generate an extra 3-PGA which can be used for the formation of carbohydrate.

In the presence of oxygen, oxygenase reaction of the rubisco competes with carboxylation. Indeed, the rubisco enzyme presents a natural affinity for the O_2 substrate.

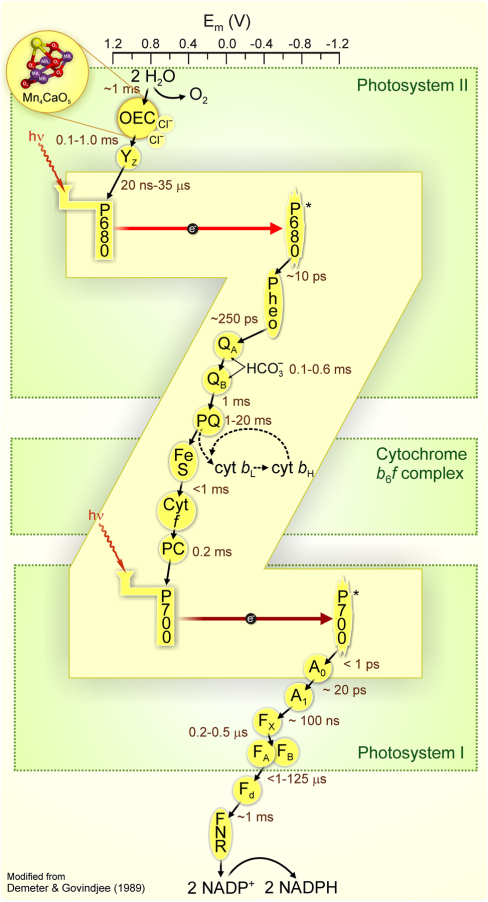

Figure 2.1 – Z-scheme representation of electron transport in photosynthesis. Upon light excitation, P680, the photosystem II (PSII) reaction centre (RC) goes into a singlet excited states (P680*) and reaches a higher redox potential. The P680* then transfers its electron to the pheophytin (Pheo) through the primary charge separation, i.e., the formation of the $P680^+$ and the $Pheo^-$. The P680* recovers the lost electron from the tyrosine-161 of the PSII D1 (Yz). The $Pheo^-$ then passes its electron to the primary quinone acceptor Q_A which then transfers its electron to the Q_B-site. There electrons enter the electron transport chain and reach the cytochrome b_6f complex. Electrons are then passed to the plastocyanin (PC) and delivered to the P700, the photosystem I (PSI) RC. Upon light exclitation, the P700* delivers its electron to intermediary phylloquinone ($A_{0,1}$) and iron sulfer culsters ($F_{X,A,B}$) acceptors till it reduces the end electron acceptor ($NADP^+$) through the ferredoxin (Fd) via the ferredoxin-$NADP^+$ reductase (FNR). Figure from Govindjee et al. (2017).

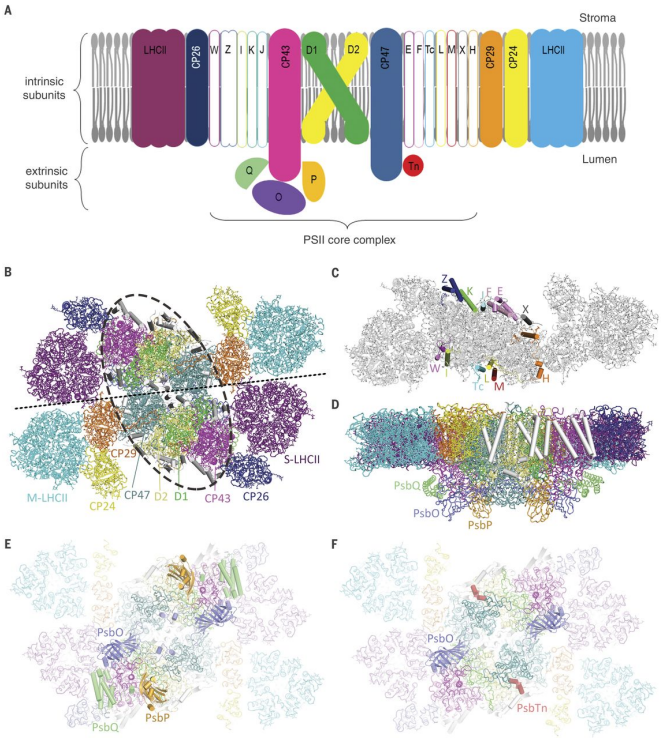

Figure 2.2 – Structures of the PSII-LHCII supercomplexes. (A) Representation of the major light harvesting complex of the PSII (LHCII) strongly (S-LHCII) or moderately (M-LHCII) bounded to the PSII core complex through the minor antenna (CP24, CP26, CP29). The PSII core is constituted by the reaction centre subunits (D1 and D2 proteins), the inner antennae complex proteins(CP43 and CP47) as well as Psb-genes related proteins including the cytochrome b559 (composed of PsbE and PsbF proteins referred as E and F in the upper figure A) and extrinsic subunits such as the oxygen evolving complex proteins (PsbO, PsbP and PsbQ proteins referred as O, P and Q in the upper figure A) and PsbTn (referred as Tn in the upper figure A). The PSII-LHCII is represented either in a stacked (B,C,D,E) or unstacked (F) state depending the sample was obtained and purified at pH 5.7 or 7.5 respectively. (B) PSII-LHCII supercomplex viewed from the stromal side. The black-dotted line separates the two PSII-LHCII monomers. A black-dashed circle highlights the dimeric PSII core. The color code is consistent with the representation in (A). (C) PSII-LHCII supercomplex viewed from the stromal side. (D) Side view of the PSII-LHCII supercomplex. (E) PSII-LHCII supercomplex viewed from the luminal side. (F) PSII-LHCII supercomplex viewed from the luminal side. Figure from Su et al. (2017).

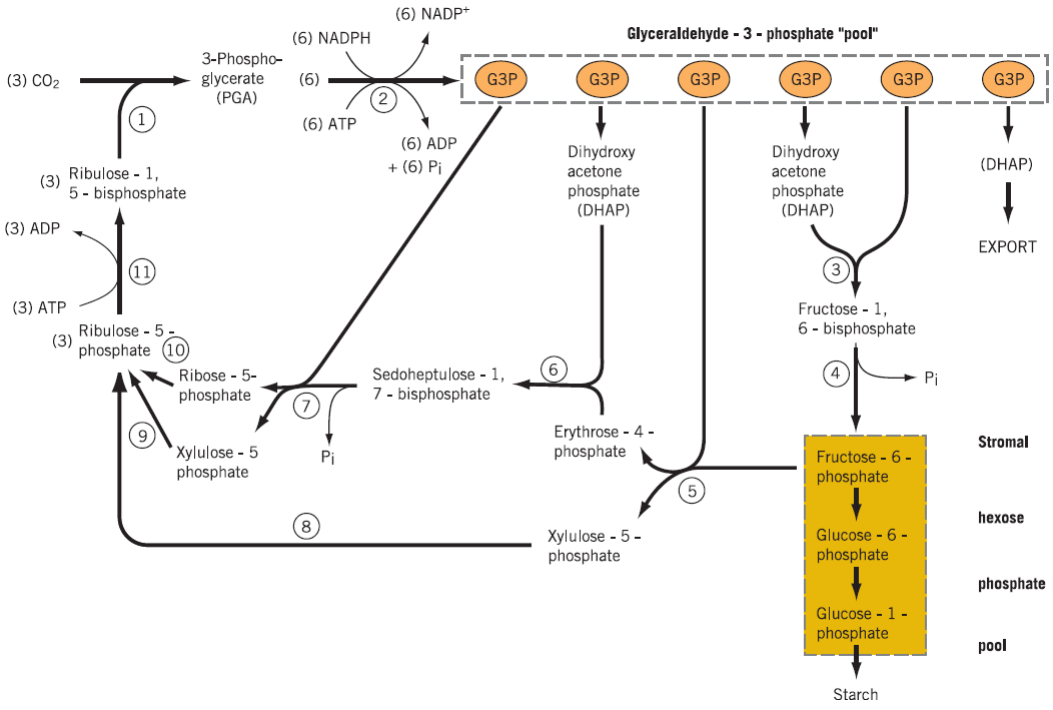

Figure 2.3 – The photosynthetic carbon reduction (PCR) cycle. Numbers in brackets indicate the stoichiometry for three CO_2 molecules. Circled numbers indicate enzymes catalyzing the concerned reaction. They are: (1)ribulose-1,5-bisphosphate carboxylase/oxygenase (Rubisco); (2) 3-phosphoglycerate kinase and glyceraldehyde-3-phosphate dehydrogenase; (3) aldolase; (4) fructose-1,6-bisphosphatase; (5) transketolase; (6) aldolase; (7) sedoheptulose-1,7- bisphosphatase; (8, 9) ribulose-5-phosphate epimerase; (10) ribose-5-phosphate isomerase; (11) ribulose-5-phosphate kinase. Figure from Hopkins and Hüner (2008).

This light-dependent consumption of O_2 by rubisco coupled with the release of CO_2 is termed photorespiration. The photorespiration pathway also refers to the mechanism which allows the regeneration of RuBP after its consumption during the RuBP oxygenase reaction (Hagemann and Bauwe 2016). Under cool and wet climate, carbon assimilation through the PCR pathway is well adapted. However, photorespiration activity increases more than photosynthesis under warmer climate as the rubisco affinity for O_2 increases with temperature. Plants which have evolved under warmer climate, such as tropical and subtropical conditions, have developed specific mechanisms for carbon assimilation and anatomical characteristics.

One of these adaptive mechanisms for carbon assimilation is the C4 metabolism which distinguishes itself from the C3 photosynthesis pathway as it concentrates CO_2 where the PCR cycle takes place. As a consequence, oxygenase activity of the rubisco enzyme is drastically reduced in C4 plants, which are therefore more efficient in carbon assimilation than C3 plants, especially under warm environment. Leaf of plants using C4 photosynthesis for carbon fixation presents a distinct arrangement, referred as the Kranz anatomy, and characterized by a distinction between the mesophyll and a bundle sheath surrounding each vascular bundle. Cells constituting the bundle sheath present a high concentration of chloroplasts and are tightly fitted with each other while the mesophyll presents large air spaces. The C4 photosynthesis also distinguishes from C3 photosynthesis by intermediary steps before the carboxylation. Absorbed CO_2, before entering the PCR cycle, is first converted into a 4-carbon acid in the mesophyll cell. To this end, CO_2 is first converted into bicarbonate by carbonic anhydrase in the mesophyll cytosol, preventing CO_2 accumulation in the cytosol. The produced anion then reacts with the phosphoenol pyruvate (PEP) to form the oxaloacetate. This reaction is catalyzed by the enzyme phosphoenol pyruvate carboxylase (PEPcase), a key enzyme in C4 plants. Using a NADPH molecule, the oxaloacetate is then reduced by a NADP-malate dehydrogenase enzyme to form a 4-carbon acid, the malate. Oxaloacetate can also be transaminated to another 4-carbon acid, the aspartate. The proportion of malate and aspartate produced vary depending the C4 species. Both of them act as a transient CO_2 storage form.

The 4-carbon acid is then exported to the nearest bundle-sheath cell where the PCR cycle takes place. There, the 4-carbon acid is decarboxilated, releasing a CO_2 molecule available for the Calvin cycle. The resulting 3-carbon acid, either a pyruvate or a alanine depending on the type of 4-carbon acid storage form (either malate or aspartate

respectively), is transported back to the mesophyll. Using two ATP molecules, the 3-carbon acid is used to regenerate the PEP molecule (Hopkins and Hüner 2008).

The crassulacean acid metabolism (CAM), a second adaptive mechanism for carbon assimilation, is found in species living in extremely dry or xerophytic habitats. This CO_2 concentrating mechanism also enables a better water conservation due to an inverted stomatal cycle. Indeed, CAM plants usually open their stomata at night and usually close them during the day. As a consequence, CO_2 uptake is mainly realized during the night, while the light phase of photosynthesis is not operating. Just like in the C4 photosynthesis, CO_2 is first converted into bicarbonate by carbonic anhydrase and then into oxaloacetate by reacting with a PEP molecule. The 4-carbon acid is then reduced into malate by a NADPH-dependent malate-dehydrogenase. The malate is eventually stored into the vacuole during night-time, depleting the cytosol from CO_2 . During the day, under light, malate is retrieved from the vacuole where it is decarboxylated to produce one pyruvate and one CO_2 molecule. The CO_2 can then diffuse into the chloroplast where the PCR cycle takes place to be converted into carbohydrate (Hopkins and Hüner 2008).

2.2 Photosynthesis response to abiotic stress

The word 'stress' is widely used in literature by biologists and may have different meaning depending on the context. A good definition of this concept of environmental stress was provided by Bijlsma and Loeschcke (2005) in an editorial review. They emphasized that, from an evolutionary perspective, a stress should be defined based on the stressor and the stressed (i.e., based on its environmental component and its biological component respectively) as optimal environmental conditions for a species can be life threatening for another. Definitions incorporating these aspects describe a stress as environmental changes reducing the fitness of organisms with potentially injurious change in their biological system. Here, we define stress from a physiological perspective and describe stress as environmental changes leading to physiological responses of the individuals and affecting their performance. Especially, in this section, we will discuss stress events affecting the photosynthetic capacity, i.e., the performance of photosynthesis determined by the light and the dark phase.

Plants are continuously exposed to environmental constraints that can negatively affect the process of photosynthesis. As a result, decline in photosynthetic rate can

be observed under unfavorable conditions such as high temperature, drought, flood, excess of light and high ozone concentration (Bussotti et al. 2007b, Bertolde et al. 2012, Goh et al. 2012). Mechanisms by which photosynthesis is hampered depend on the constraints and their intensity (Ashraf and Harris 2013). For instance, reduction of photosynthetic rate induced by drought is generally attributed to stomatal limitation while decline of photosynthesis observed during high temperature is explained by an impairment of the thylakoid membrane functionality in the chloroplast (Ashraf and Harris 2013).

Plants, however, can proceed to photosynthetic adjustments in order to acclimate to stressful conditions and alleviate the detrimental impacts on the photosynthetic apparatus. In this section, we describe how the different processes of photosynthesis are affected by the aforementioned stresses and which mechanisms are triggered in order to acclimate to these unfavourable conditions. We also highlight the importance of stress intensity, duration and interactions among stressors when assessing their impact on the photosynthesis process. Studies presented here assessed the response of the photosynthetic apparatus to abiotic stress through multiple methods such as fluorescence techniques, gas exchanges measurements and the dosage of leaf pigments, proteins, oxidation products and gene expressions.

2.2.1 High temperature

Whereas a moderate increase in air temperature can be favorable to the net photosynthesis (Arend et al. 2013), negative impacts are reported for temperature higher than the optimum temperature (Crafts-Brandner and Salvucci 2002). Different studies have indeed reported a reduction in Chl content under high-temperature stress (Balouchi 2010, Bouchemal et al. 2017). In wheat plants subjected to heat treatement, the higher abundance of pheophorbide *a* oxygenase, an enzyme involved in Chl degradation (Chung et al. 2006, Mishra et al. 2017), suggests a faster Chl degradation under these conditions. Inhibition of Chl biosynthesis might also be involved in the reduction in Chl content as a decrease in activity for enzymes involved in Chl biosynthesis was reported for heat-treated plants (Mohanty et al. 2006, Dutta et al. 2009).

Decline of photosynthesis due to a decrease in Rubisco activity is also a common feature observed under moderate heat stress (Salvucci et al. 2001). Loss of Rubisco activity in these conditions is explained by the thermal inactivation of Rubisco activase (Salvucci et al. 2001), a key enzyme involved in the ATP-dependent removal of

RuBP from the catalytic site of decarbamylated Rubisco (Salvucci and Ogren 1996). Increase in the oxygenation rate of Rubisco (i.e., photorespiration) due to the increased specificity of Rubisco for O_2 is also commonly observed at moderate elevation of air temperature (Sage 2013). Oxygenetation of Rubisco at increasing temperature is also promoted by the increase in O_2/CO_2 ratio in solution, as the two gases are characterized by different temperature responses of solubility (Cavanagh and Kubien 2014).

Heat stress can also induce the inhibition of the OEC component of the PSII (Luo et al. 2011, Mathur et al. 2011b, Brestic et al. 2012, Kalaji et al. 2016) due to an alteration of its manganese cluster functionality (Tóth et al. 2007a, Oukarroum et al. 2009). Hence, the PSII is reported as the most heat-sensitive component of the photosynthetic apparatus (Yan et al. 2013). Reduction in electron transport beyond the PSII can also be observed, leading to an accumulation of Q_A^- (Yan et al. 2011). Damage to the PSII, however, are generally not reported for temperature lower than 40-45°C (Crafts-Brandner and Salvucci 2002, Nellaepalli et al. 2011, Janka et al. 2013).

Change in the heterogeneity of the PSII antenna size and PSII reducing side, however, are reported at high temperature. Increase of temperature from 25 to 45°C was shown in wheat to lead to the conversion of PSIIα antenna to PSIIβ and γ antennae (Mathur et al. 2011a). It is likely that modification in the relative amounts of PSIIα, β and γ antennae results from the separation of the LHCII from the PSII complex (Mathur et al. 2011b, Brestic et al. 2012). Increase in the number of Q_B-non-reducing PSII has also been observed following heat stress with more than 50% of Q_B-reducing PSII being converted at 45°C (Mathur et al. 2011a). Complete recovery of modifications in the PSII heterogeneity (antenna size and reducing side) was observed at 35°C, suggesting these structural changes might be involved in plant acclimation. However, modifications in PSII heterogeneity were partly irreversible at 45°C.

Other perturbations of the photosynthetic process functioning without impairment of the PSII are also reported at moderate temperature (35-40°C) such as the stimulation of cyclic electron transport and the alteration of thylakoid membrane (Sharkey 2005). Temperature-induced leakiness of thylakoid membrane can result in proton leaks through transient pores. Increase in cyclic electron transport around the PSI at temperature up to 40°C might contributes in the maintenance of an energy gradient across the thylakoid membrane and the prevention of irreversible damages. Higher temperatures, however, may result in irreversible damages to the thylakoid membrane (Sharkey and Zhang 2010). The partial conversion of violaxanthin to zeaxanthin by

plant, however, may improve the thermostability of the membrane (Havaux et al. 1996).

2.2.2 Water stress

Main cause of reduced leaf photosynthesis under water stress conditions is attributed to the reduction of CO_2 diffusion from the atmosphere to the site of carboxylation, namely the Rubisco (Flexas et al. 2006). Stomatal conductance (g_s) which regulates the intercellular CO_2 concentration and mesophyll conductance (g_m) which control the chloroplastic CO_2 concentration are two key components involved in leaf CO_2 diffusion. Grassi and Magnani (2005) have shown in ash and oak trees that the decline in carbon assimilation at light saturation under moderate water stress (e.g., a g_s still higher than 0.1 mol H_2O m^{-2} s^{-1}) was fully explained by decline in these two components. About two-third of photosynthesis decline was attributed to g_s reduction while one-third was explained by g_m reduction.

More severe water stress, however, can induce structural damages and enzymes inhibition resulting in biochemical limitations of photosynthesis (Grassi and Magnani 2005, Yuan et al. 2016). Based on a litterature review, Flexas et al. (2006) define a severe water stress as an event leading to a maximum daily g_s below 0.05-0.1 H_2O m^{-2} s^{-1} rather than on the water status of leaf tissues. This threshold sets the limit for photochemical and biochemical impairement of components of photosynthesis and coincide with the decrease in leaf ATP content.

Several examples of photosynthesis decline under water stress conditions not related to CO_2 diffusion are reported in the literature. For instance, a study performed on transgenic tabacco plants with antisense Rubisco concluded that limitation in RuBP regeneration was involved in photosynthetic inhibition under water stress (Gunasekera and Berkowitz 1993) due to ATP restriction (Tezara et al. 1999). Degradation of photosynthetic pigments has also been reported (Ashraf and Harris 2013) with a change in the Chl *a*/*b* ratio resulting from a different decline in Chl *a* and Chl *b* pigments (Efeoğlu et al. 2009, Jaleel et al. 2009, Yuan et al. 2016). Decrease in Chl *a* and Chl *b* might either suggest the photooxidation of pigments or an adaptive mechanism aimed at reducing the amount of light absorbed energy. Some studies, however, report an increase in Chl content in water-deficit condition (Pirzad et al. 2011, Sengupta et al. 2013), suggesting the variation in Chl content in response to drought stress may vary depending on the cultivar and its drought resistance. A reduction in the density of

active RCs per PSII Chl antenna can also be observed following a drought stress and might be explained by a degradation of chlorophyll (Boureima et al. 2012) or a partial inactivation of PSII RC aimed at increasing energy dissipation by heat (Campos et al. 2014).

The PSII is usually reputed resistant to low leaf water potential (Manes et al. 2001). However, it is possible to observe a decline in the efficiency of the primary photochemical events of PSII under severe drought events (Lauriano et al. 2006, Goltsev et al. 2012, Tozzi et al. 2013, Ghotbi-Ravandi et al. 2014). Dissociation of the OEC from the PSII complex has also been observed in these conditions (Oukarroum et al. 2007) but mainly for the most drought-sensitive genotypes (Oukarroum et al. 2007, Redillas et al. 2011, Sengupta et al. 2013). Several studies have also reported a decrease in the energy transfer from the LHCII to the PSII RC caused by the loss of connectivity in the tripartite system (core antenna-LHCII-RC) (Oukarroum et al. 2007, Campos et al. 2014). A reduction in energy transfer to the PSII RC can also be explained by a decrease in D1 content (Ghotbi-Ravandi et al. 2014).

Transport of electrons beyond the Q_A is also disturbed by stresses leading to a decrease in relative water content (Goltsev et al. 2012, Ghotbi-Ravandi et al. 2014, Silvestre et al. 2014). Possible explanation for a disturbed electron transportation beyond PSII is a reduction of available $NADP^+$ pool on the acceptor side of PSI due to a lower PCR cycle activity because of a lower carbon uptake (van Heerden et al. 2007). However this response to drought stress is not the rule and a higher PSI activity has also been observed (Campos et al. 2014). A higher PSI/PSII ratio could be interpreted as an increase of the photochemical pathway for de-excitation to avoid ROS formation due to unmanaged electrons. This strategy is similar to that adopted by plants in situations of high light (Desotgiu et al. 2012a).

Excess of water in soil can also be detrimental to plants as it reduces O_2 availability for roots respiration. Flooding was shown to lead to a decline in carbon assimilation (A_{CO_2}) due to the reduction of g_s possibly promoted by a decrease in root hydraulic conductivity (Bertolde et al. 2012). However the decline in photosynthetic activity can also be explained by the inhibition of photosynthetic processes rather than by stomatal limitations. Reduction of photosynthetic pigments content observed in flooded plants and increase in ROS production also contributed to the decline in photosynthetic capacity (Arbona et al. 2009, Verma et al. 2014). However different genotypes can express different photosynthetic responses to flooding stress and moderate water-

logging was even shown to promote A_{CO_2} in a resistant *Salix integra* Thunb. cultivar (Zhao et al. 2014).

2.2.3 Excess of light

Excess of light absorption or prolonged exposition can result in the photoinhibition of the PSII and a reduction of the photosynthetic rate. Photoinhibition refers to a light-induced decline in the PSII efficiency or its inactivation caused by multiple chemical reactions affecting different components of the PSII unit (Goh et al. 2012). Photodamage of the manganese cluster in the OEC under both visible and UV light is suggested to be one of the primary events in the photoinhibition of PSII (Tyystjärvi 2008). In these conditions, the OEC becomes inactive and can no longer transfer an electron to the Yz, an intermediary between the OEC and the P680, leading to long-lived $P680^+$. This oxidized form of P680 can eventually oxidize a wrong component of the PSII RC. Light-induced degradation of D1 proteins has also been associated with PSII photoinhibition. With a half-life of 2.4 h, D1 proteins are continuously degraded and replaced by newly synthesized D1 protein during the PSII repair cycle (Goh et al. 2012, Järvi et al. 2015). It is possible that the turnover of D1 acts as a protective mechanism against oxidative stress by giving an 'information' about the light intensity, allowing the adaptation of the translational machinery (Adir et al. 2003). However, since the rate of degradation of the D1 protein is proportional to the intensity of light, net loss of D1 protein can be observed at high light intensity when damages exceed the rate of D1 repair, leading to the inhibition of PSII (Aro et al. 1994). Even though better recovery of the PSII efficiency are observed at low light (Aro et al. 1994), the PSII repair cycle cannot operate in dark condition (Järvi et al. 2015).

Over-reduction of the electron transport chain caused by an excess of light absorption can also result in the production of ROS, leading to irreversible damages to the photosynthetic apparatus structure. Indeed, in case of over-excitation of the PSII, electron flow might exceed the electron-accepting capacity at the PSI acceptor side. Thus, unmanaged high-energy electrons can react with dioxygen to eventually form ROS (Gururani et al. 2015). ROS can also result from the reaction between triplet excited Chl and dioxygen to form singlet oxygen. This occurs in situation of over-reduced PQ pool which is no longer able to act as an electron acceptor (Goh et al. 2012). Produced ROS can damage the photosynthetic apparatus and induce the aggregations between damaged D1 proteins and nearby polypeptides such as D2 or CP43 (Yamamoto et al.

2008). Under severe light stress, however, photodamaged D1 proteins show an irreversible aggregation with the PSII antenna and cannot be released from the PSII core for degradation and replacement (Yamamoto et al. 2014).

Different protective mechanisms are induced to preserve the photosynthetic apparatus from photooxidation under excess of light (Ashraf and Harris 2013). Decrease in the PSII efficiency has been identified as a photoprotective mechanism aimed at the dissipation the excess of light energy (Werner et al. 2001, 2002). Photoinhibition of the PSII also contribute to regulate the electron transport chain and is able to protect the PSI from permanent photodamage (Tikkanen et al. 2014). Another mechanism consists in the dissipation of the excess of energy within the LHCII to reduce the PSII excitation (Goh et al. 2012). The activation of this photoprotective mechanism requires the onset of a trans-thylakoid pH gradient (ΔpH) which serves as a signal for the onset of zeaxanthin-facilitated thermal dissipation and reorganization of the PSII antenna triggered by the PsbS (Photosystem II Subunit S) protein (Ruban et al. 2012, Derks et al. 2015). Under conditions of severe light stress, however, a ΔpH-independent sustained dissipation can occur along with the degradation of PSII core (Demmig-Adams and Adams 2006).

Promotion of the cyclic electron flow (CEF) around the PSI under high light was shown to play a role in the prevention of PSII photodamage (Takahashi et al. 2009). CEF enables the build up of a ΔpH which facilitates the activation of zeaxanthin-facilitated thermal dissipation. Plants submitted to high light can also drain faster the ETC by increasing the activity of the PSI. This quicker reduction of the end electron acceptor chain suggests a photochemical pathway for de-excitation (Pollastrini et al. 2011, 2016b, Desotgiu et al. 2012a).

2.2.4 Ozone

Exposition to elevated ozone concentration is known to induce foliar symptoms due to H_2O_2 accumulation (Desotgiu et al. 2010), especially in sensitive species which display a hypersensitive response characterized by the programmed death of palisade mesophyll cells (Bussotti et al. 2005). However, ozone can impact photosynthesis before visible symptoms appear. The reduction of A_{CO_2} has been reported as one of the early response to ozone stress (Soja et al. 1998) and might result from different physiological processes such as the alteration of chloroplasts and stomatal response (Bussotti et al. 2007b).

Exposure to ozone induces a decline in g_s within 10 min, followed by the reopening of stomata during the following hour (Kollist et al. 2007). Within the cell, ozone can degrade into ROS and induce oxidative damages. A reduced activity of Rubisco due to accelerated proteolysis of this protein is commonly observed in the early stages of ozone exposure (Brendley and Pell 1998). As a consequence, the lower activity of the PCR cycle caused by a reduced Rubisco activity in ozone-fumigated plants can leads to a decrease in PSI activity (Cascio et al. 2010, Desotgiu et al. 2010) and an accumulation of reduced Q_A (Manes et al. 2001). Treated plants can also exhibit an increase in their electron transport per RC, suggesting an increase in alternative electron sinks via photorespiration and/or the Mehler reaction (Manes et al. 2001). Increase of electron transport during stress episodes has also been attributed to the production of new metabolites required for the acclimation process (Liska et al. 2004, Retuerto et al. 2004).

Upon prolonged exposition to ozone concentration above 70 ppb, stomatal response becomes 'sluggish' due to a perturbation of Ca^{2+}-mediated mechanisms involved in guard cells opening and closure (McAinsh et al. 2002). With the apparition of visible symptoms, a decrease in the density of active RC and in the conservation of the absorbed photon energy along the ETC is observed (Bussotti et al. 2005, 2007a). The reduction of PSII efficiency occurs along with the increase in the energy dissipation by heat (Bussotti et al. 2005). Altogether, these observations suggest the onset of down-regulation mechanisms to dissipate the excess of light energy in order to prevent photo-oxidative damage. Reduction in PSII efficiency is mostly reported in symptomatic leaves (Calatayud et al. 2007) and might be the consequence of important structural damages of the PSII and/or the activation of controlled dissipation process (Bussotti et al. 2011). Resistant varieties under ozone fumigation, however, can exhibit a decrease in thermal dissipation within the PSII antenna associated with an increase in photosynthetic pigment content (Calatayud and Barreno 2004). In such case, the decrease in energy dissipation process therefore allows the maintenance of photochemical activity under ozone stress.

2.3 Impact of combined stresses on photosynthesis

Plants in field condition are usually exposed to a combination of multiple stressors. Vile et al. (2012) have shown that some growth traits in Arabidopsis were specifically

impacted by heat or drought stress but these effects were generally additives when the two stresses were combined. If no trait has been affected only by the combination of the two stresses, the growth was more severely impacted in the combined treatment. Interactive effects between two stresses have also been observed in spring wheat with stronger prejudice for total dry weight, harvest index and spikelet fertility when heat and drought were combined (Prasad et al. 2011). Recent studies have shown that combined stresses can induce a specific gene expression scheme, suggesting that the combination was perceived by the plant as a different stress and cannot be directly extrapolated from the response to individual stressor (Rizhsky et al. 2002, 2004, Aprile et al. 2013, Johnson et al. 2014). Still, it appears that the molecular response to combined stresses is mainly determined by the more severe stress (Pandey et al. 2015).

Combination of stressors can also impact the photosynthetic processes differently (Masojidek et al. 1991, Jiang and Huang 2001, Ogaya et al. 2011). Consideration of the interaction between environmental constraints and its influence on photosynthesis is therefore crucial in the assessment of carbon uptake by ecosystems. In this section, we emphasize the importance of several factors that must be considered when studying the impact of combined stresses on photosynthesis such as the intensity of the stressors and the order in which they operate. The influence of physiological processes not directly involved in photosynthesis is also highlighted.

2.3.1 Heat and water stress combination

Among the different abiotic stress combinations, the interaction between heat and drought stress is among the most studied. The interest in this combination is justified since heat and drought usually co-occur in natural conditions during summer. These stresses were shown to trigger antagonistic responses of photosynthesis. For instance, plants under water limitation were shown to reduce their g_s to limit water loss by transpiration. As a consequence, a decline in photosynthesis due to a reduced CO_2 assimilation was measured in plants experiencing such stress (Rizhsky et al. 2004, Bollig and Feller 2014). In contrast, plants in conditions of elevated temperature were shown to increase g_s to improve leaf cooling by transpiration (Rizhsky et al. 2004). Analysis of transcriptomic response also revealed that the combination of both stress can induce new gene transcripts expression (Rizhsky et al. 2004, Aprile et al. 2013, Johnson et al. 2014).

Impact of combined heat and drought stress on photosynthesis has been reported

to increase prejudice on photosynthesis with a stronger reduction in $A_{CO_2}$and more important oxidative damages (Osório et al. 2011, Balla et al. 2014). Still, response to combined stress is reported to depend on the varieties (Osório et al. 2013, Estrada et al. 2015), the soil properties (Contran et al. 2013) or can even lead to no additional effect (Hoover et al. 2014). Impact on photosynthesis can also differ if the water stress is applied as a pretreatment (Jiang and Huang 2000). Numerous studies have reported a benefit of water stress pretreatment on the PSII resistance to high temperature (Havaux 1992, Ladjal et al. 2000). The enhanced resistance of the PSII complex was explained by the stabilization of the OEC (Lu and Zhang 1999, Oukarroum et al. 2009) due to the accumulated osmolyte compounds like glycine betaine and proline during the drought period (Oukarroum et al. 2012). Proline was also suggested to act as an alternative electron donor by feeding the PSII in situation where the OEC is dissociated from the PSII complex by heat stress (De Ronde et al. 2004). However, the hypothesis that other mechanisms than osmolytes could be involved in the protection of the PSII has been suggested since the improved PSII thermotolerance has been seen to last up to 60 days after rewatering (Ladjal et al. 2000). Yet, a study showed that proline content was not affected by rewatering and that its production was rather a consequence rather than a beneficial stress-induced response (Souza et al. 2004). In some cases, drought preconditioning did not prevent the decrease of PSII efficiency but helps the plant recovery from a heat stress. In an experiment realized by Jedmowski et al. (2015), drought-preconditioned *Hordeum spontaneum* K.Koch exhibited a better recuperation of photosynthesis than the non-preconditioned control. Still, the grain yield for these plants was still affected by the drought episode.

However, drought applied as a pretreatment can sometimes exacerbate adverse impact of heat stress without benefit to photosynthesis (Rizhsky et al. 2004, Xu and Zhou 2006). One explanation for these contrasting results can be the possible difference in the dehydration tolerance strategies among genotypes, even inside the same species. For instance, three lines of chickpea presented different proline and sugars accumulation when submitted to a drought stress and had different antioxidative abilities (Pouresmael et al. 2015). These differences resulted in different PSII response to drought stress for these genotypes. Leaf ontogeny was also shown to have an influence in the thermotolerance of the PSII as younger leaves had lower reduction in PSII efficiency and A_{CO_2}than mature leaves under the same level of stress (Chastain et al. 2016). The mechanisms responsible for the higher stress tolerance in young leaves

still remain to be elucidated. Another possible explanation is the severity of the water stress applied. While a moderate water stress induced the accumulation of proline and sugars compounds, severe dehydration induced stronger increase of sugars compounds such as sucrose (Hoekstra et al. 2001). Interestingly, sucrose accumulation was also shown to be specific to the combination of heat stress and drought stress in Arabidopsis (Rizhsky et al. 2004). The proline content of poplar submitted to the combination of heat and drought stress was also shown to decline 24 h after the treatment, after an initial increase (Li et al. 2014). It is still unknown however if a difference in the proline:sugars content can influence the stabilization of the PSII and its thermotolerance. Growing conditions and especially the light intensity have also to be considered. The time gap between the pretreatment and the subsequent stress could possibly influence the plant response. The light intensity used in controlled environment experiments can also influence the photosynthetic response as high PPFD can act as a supplementary stress driver and interact with drought and heat.

2.3.2 Interactions with high light

Combination of high light with water stress can lead to an over-excitation of the PSII in a situation of low CO_2 availability in the chloroplast due to stomatal limitation (Georgieva et al. 2010). Therefore, electrons sent by the OEC can be in excess compared with the availability of reductant power, leading to a stronger oxidative stress due to ROS formation (Contin et al. 2014) and photosynthesis inhibition (Masojidek et al. 1991). Accelerated leaf dehydration can be found in water-stressed plants exposed to moderate light but without additional damage to the PSII during the first stage of dehydration. Prolonged exposition to combined stress, however, can lead to a decrease in trapping efficiency of the PSII RC and a decrease in the exchange capacity at the Q_B-site (Li and Ma 2012). Measurement of the far-red light induced transmission changes at 820 nm also highlighted a decline in P700 and PC contents due to accelerated leaf dehydration under combined stresses (Li and Ma 2012). Reduction of the PSII recovery capacity from a drought event can also be observed compared to a situation where plants were exposed to a lower light intensity during dehydration (Georgieva et al. 2010). Plants, however, can alleviate the electron pressure on the PSII and oxidative damage by promoting down-regulation of photosynthesis (Massacci et al. 2008, Sofo et al. 2009), by increasing photorespiration and other alternative electron sinks (Bai et al. 2008, Massacci et al. 2008) and by increasing ROS scavenging activity

(Guidi et al. 2008). Plants resistant to water stress under high light are also able to considerably enhance controlled dissipation of excess energy compared to more sensitive individuals, suggesting this trait is discriminant between susceptible and tolerant cultivars (Sofo et al. 2009). Change in spatial orientation of leaves upon dehydration might also influence light interception, with a consequence on the rate of photosynthesis (Feller 2016). It is therefore possible that plants that reduce their light interception in the early stages of drought might be able to reduce the over-excitation of the PSII and present a better resistance to the combined stresses.

Flooding can also alter photochemistry of photosynthesis response to light (Maurenza et al. 2012). Stronger PSII photoinhibition (Mielke and Schaffer 2010) and A_{CO_2} decline likely due to a lower internal CO_2 concentration (Lavinsky et al. 2007) was observed in plants submitted to combined flood and high light. Loss of photosynthetic pigments in flooded plants was also shown to be stronger when subjected to high light (Mielke and Schaffer 2011).

Combination of high light intensity with high temperature was found to enhance the reduction in PSII efficiency in chrysanthemum due to a higher energy dissipation. Increase in alternative electron sinks such as photorespiration was also observed in these conditions, leading to stronger reduction in A_{CO_2} (Janka et al. 2015). However, light of 1000 μmol m^{-2} s^{-1} was found to have a protective role by enhancing OEC stability from heat stress in barley whereas an exposition to 100 μmol m^{-2} s^{-1} did not lead to an increased thermotolerance (Georgieva et al. 2003). The authors suggested that high light led to the accumulation of heat shock proteins (HSP), providing an improved stabilization of the PSII. The importance of the interaction between light and temperature in the generation of HSP and their implication on the stabilization of the PSII efficiency was later confirmed in another study (Barua and Heckathorn 2006). A recent study has also suggested that a light-induced signal from chloroplast to the nucleus, either the PQ redox state or H_2O_2, could be responsible for the higher expression of HSP and thermotolerance during the day (Dickinson et al. 2018). Another experiment performed on alpine plants demonstrated that heat shock applied in dark conditions led to a higher level of oxidative stress compared with treatment applied in ambient light (Buchner et al. 2015). The protective role of light was also explained by the higher activity of xanthophyll cycle which had contributed to the reduction of ROS formation induced by heat treatments. An increase in the linear electron transport rate (ETR) along with a decrease of A_{CO_2} was also observed in Norway spruce (*Picea abies*

[L.] Karst.) when submitted to combined high light and moderate heat (Štroch et al. 2010). This enhancement of electron transport might probably indicate an increase in alternative electron sinks such as photorespiration (Janka et al. 2015).

2.3.3 The triple combination (heat × drought × light)

The impact of the triple combination between heat stress, water stress and high light on photosynthesis has been tested under controlled laboratory conditions on two grapevine varieties as well as the impact of the individual stresses and their level-two interactions (Carvalho et al. 2016). The triple stress combination and treatments involving water stress were the treatments which imposed the strongest limitation on carbon fixation. However, the triple stress did not induce the strongest photoinhibition neither the strongest reduction of g_s, suggesting another origin to the carbon fixation inhibition. The triple stress treatment distinguished from the others by a higher activation of the ascorbate-glutathione cycle. This mechanism is involved in the scavenging of ROS and more specifically of the hydrogen peroxide (H_2O_2) (Carvalho et al. 2015) which is produced by the PSI upon stress such as high light (Asada 2006, Goh et al. 2012). The highest pigment concentration (i.e. Chl, carotenoid and anthocyanins) was also observed under the triple stress treatment (Carvalho et al. 2016). Pigments such as carotenoid and anthocyanins are known to protect the photosynthetic apparatus against photo-oxidative damage through their ROS scavenging function (Gould 2004, Carvalho et al. 2015). Whereas the level of H_2O_2 was not significantly different from the control (Carvalho et al. 2016), these observations suggest that the triple stress treatment induced an important oxidative pressure on the photosynthetic apparatus but an efficient metabolic response.

In most field studies, where light irradiance can reach values higher than 1500 μmol m^{-2} s^{-1}, combination of high temperature and drought period commonly led to a stronger decline in carbon assimilation rate (Faria et al. 1998, Zavalloni et al. 2009, Arend et al. 2013, Tozzi et al. 2013) as well as to a stronger reduction in PSII efficiency (Faria et al. 1998, Bussotti 2004, Gielen et al. 2007, Arend et al. 2013, Ciccarelli et al. 2016). This reversible decline in the efficiency of the photosynthetic process can be explained by a down-regulation of photosynthetic processes reflected by the reduction in the density of active RC (Bussotti 2004). This active process for the dissipation of excess energy might be assisted by an increase in xanthophyll cycle activity (Faria et al. 1998, Gielen et al. 2007). Although drought was reported to decrease the ther-

motolerance of the PSII in the aforementioned field studies, low soil moisture was not reported as an important stress driver in the absence of other abiotic stresses. As a general rule, the combination of drought with high temperature in field conditions, under ambient light, was shown to have detrimental effects on photosynthesis. One case of improved PSII thermotolerance under water stress in the field, however, has been reported by Snider et al. (2013) on *Gossypium hirsutum* L. cultivars. In future long-term field study, the evolution of the PSII thermotolerance after a drought event and acclimation processes should be further investigated.

2.3.4 Interactions with ozone

Ozone uptake by plants can be reduced in situation of water stress, because of a lower g_s. As a consequence, a lower impact on photosynthesis of ozone is excepted under drought condition (Iyer et al. 2013). However the impact on photosynthesis of combined drought and ozone stress depends on the timing of the drought episode occurrence. It has been highlighted that plants must experience drought stress from the beginning of the ozone treatment in order to benefit from a reduced ozone uptake and delayed oxidative stress (Pollastrini et al. 2014). Moreover, since both stresses induce ROS production and similar antioxidative responses, plants exposed to drought stress prior to ozone might also be more effective in ROS detoxification (Matyssek et al. 2006). This implies that an ozone peak occurring during a drought season would have different consequences on photosynthesis than a peak of ozone occurring during the wet season. Intensity of the water stress might also influence the degree of protection against ozone since moderate drought may not be sufficient to reduce ozone uptake and could even be more detrimental to growth due to the cumulative effect of oxidative stress and reduced carbon acquisition (Retzlaff et al. 2000, Grulke et al. 2002). During a drought event, ozone fumigated-plants can also exhibit a delayed stomatal closure (Manes et al. 2001) likely due to an alteration of the plasma membrane of guard cells caused by ozone (McAinsh et al. 2002). This perturbation of stomatal closure can predispose the plant to drought stress and induce an inefficiently controlled transpiration (Matyssek et al. 2006).

It is likely that this impaired stomatal response might increase the sensitivity to high temperature of ozone-stressed plants due to uncontrolled transpiration. Combination of ozone and high temperature was also shown to lead to a reduced capacity to dissipate the excess energy by heat throught zeaxanthin-facilitated mechanism. As

zeaxanthin can improve the stability of the thylakoid membrane against heat stress (Havaux et al. 1996) and act as an antioxidant (Havaux et al. 2007), the decline in energy dissipation ability is likely due to a high consumption of the zeaxanthin pool under combined stress (Villányi et al. 2014). Sun irradiance can also affect plant response to ozone stress, as shaded-leaves of ozone-fumigated *Fagus sylvatica* L. seedlings showed a stronger A_{CO_2} decline than leaves exposed to full sun irradiance (Cascio et al. 2010). The authors attributed the stronger resistance of sun leaves to the higher g_s observed in shaded leaves at the end of the season, leading to a higher ozone uptakes for the latter.

3 MEASURE OF CO_2 FLUXES USING EDDY COVARIANCE TECHNIQUE

Continuous measurements of CO_2 exchange between the vegetation and the free atmosphere at the ecosystem scale can be achieved by using micrometeorological methods such as eddy covariance. This technique is based on the sampling of eddies for their vertical velocity and their concentration in the scalar of interest (e.g., CO_2 gas) (Aubinet et al. 1999). First experiments using this methods were performed in the 1980s where only few days of CO_2 fluxes measurements were performed (Ohtaki 1980, Leuning et al. 1982). Today, there is a growing number of eddy covariance studies with time series of several years (Jaksic et al. 2006, Ma et al. 2007, 2016).

The eddy covariance method uses the conservation equation to determine the scalar density (e.g., CO_2 concentration) in the three direction components of the wind (Aubinet et al. 1999, Loescher et al. 2006, Foken et al. 2012). The equation is expressed as:

$$\frac{\partial \rho_s}{\partial t} + u\frac{\partial \rho_s}{\partial x} + v\frac{\partial \rho_s}{\partial y} + w\frac{\partial \rho_s}{\partial z} = S + D \tag{3.1}$$

where ρ_s is the scalar density and u, v, w are the wind velocity components in the directions of the wind, respectively, x, y, z. The cartesian coordinate system is defined such as the x, y and z coordinates are parallel, respectively, to the direction of the mean wind, to the lateral wind and to the normal to the surface. S and D represent, respectively, the source/sink term and the molecular diffusion. After the application of the Reynolds decomposition (i.e., decomposition of an instantaneous quantity a into its time-averaged $\overline{a}$ and fluctuating quantities a') to the equation (3.1) and by neglecting the density fluctuation, we have:

$$\frac{\partial \overline{\rho_s}}{\partial t} + \overline{u}\frac{\partial \overline{\rho_s}}{\partial x} + \overline{v}\frac{\partial \overline{\rho_s}}{\partial y} + \overline{w}\frac{\partial \overline{\rho_s}}{\partial z} + \frac{\overline{u'\rho_s'}}{\partial x} + \frac{\overline{v'\rho_s'}}{\partial y} + \frac{\overline{w'\rho_s'}}{\partial z} = S \tag{3.2}$$

After the integration along the z component over the eddy covariance height (h_m), the

equation (3.2) gives:

$$\int_0^{h_m} S dz = \underbrace{\int_0^{h_m} \frac{\partial \overline{\rho_s}}{\partial t} dz}_{\text{I}} + \underbrace{\int_0^{h_m} \overline{u} \frac{\partial \overline{\rho_s}}{\partial x} dz}_{\text{II}} + \underbrace{\int_0^{h_m} \overline{v} \frac{\partial \overline{\rho_s}}{\partial y} dz}_{\text{III}} + \underbrace{\int_0^{h_m} \overline{w} \frac{\partial \overline{\rho_s}}{\partial z} dz}_{\text{IV}} + \underbrace{\int_0^{h_m} \frac{\overline{u' \rho_s'}}{\partial x} dz}_{\text{V}} + \underbrace{\int_0^{h_m} \frac{\overline{v' \rho_s'}}{\partial y} dz}_{\text{VI}} + \underbrace{\int_0^{h_m} \frac{\overline{w' \rho_s'}}{\partial z} dz}_{\text{VII}} \tag{3.3}$$

The term I represents the storage of the scalar between the soil and the h_m height and can be considered equal to zero over a day. The terms II-IV represent the advection (i.e., the transport of a particle by a bulk flow) through the layer between the surface and the height of measurement. The terms V-VII represent the turbulent flux divergence (i.e., the change in density of a flowing fluid in a given region of space according to a vector field). After the assumptions of horizontal homogeneity (terms II-III equal zero), no horizontal eddy flux divergence (terms V-VI equal zero) and steady state conditions (i.e., time derivative nullifies), the equation (3.3) gives:

$$\int_0^{h_m} S dz = \int_0^{h_m} \frac{\partial \overline{\rho_s}}{\partial t} dz + \overline{w' \rho_s'} \tag{3.4}$$

where $\int Sdz$ represents the net ecosystem exchange (NEE) when the scalar is CO_2 and $\overline{w' \rho_s'}$ the eddy covariance flux measured at height h_m. NEE are usually estimated over a 30 min period. Estimated NEE values can then be integrated to estimate daily, seasonal or annual fluxes. Subsequent footprint analysis based on lagrangian analysis and vertical flux then allow to estimate the source location (Aubinet et al. 1999).

Depending on the landscape and micrometeorological conditions, some of the aforementioned approximations cannot be made (Aubinet et al. 1999). For instance, in situation where the landscape is not flat or homogeneous, the assumption of negligible horizontal gradients may not be valid and can lead to a significant value of the term II. Estimation of NEE fluxes at night is also challenging because of low air mixing (Aubinet et al. 2010), incorrect measurement of the storage term (Baldocchi 2003), intermittent turbulence and gravity flows (Aubinet 2008). Under tall vegetation or complex topography, vertical advection may also lead to significant values of the

term IV, especially at night during low turbulence. If the term I can be approximated to zero over a 24 h period, it is not true in the short term. Positive values of the storage term can be observed during calm nights where CO_2 accumulate between the ground and the h_m height. During the day, however, negative values can be measured when accumulated CO_2 is flushed by turbulence or assimilated by the ecosystem vegetation. Measurements realized in complex landscape and unfavorable conditions need to estimate the storage term as well as the flux divergence and advection to reduce bias in NEE measurement (Baldocchi 2003).

Quality tests were developed to check if the required conditions were met during the collection of data such as the stationarity, the presence of sufficient turbulence and the absence of vertical movement of the air (Rebmann et al. 2005). This procedure usually results in the presence of gaps in the dataset. The subsequent use of gap-filling algorithms enable the production of a continuous dataset, allowing the estimation of integrated carbon budgets (Baldocchi 2008). However, correction procedures are not perfect and still debated (Hayek et al. 2018) as they are also subject to residual uncertainties which depend for instance on the choice of correction parameters (Gourlez de la Motte et al. 2016).

Measured NEE can be partitioned into its components fluxes GPP and R_{eco} according to the equation $NEE = R_{eco} - GPP$. One method consists in the estimation of the ecosystem respiration from night-time data based on its temperature sensitivity and to further extrapolate the ecosystem respiration from night-time to day-time (Reichstein et al. 2005). Even though this algorithm constitutes an improvement compared with previous partitioning methods and contributes to the estimation of less biaised partitioned fluxes, it is still subjected to some uncertainties as it does not take into account the inhibition of mitochondrial respiration by light (Atkin et al. 1997) and the photorespiratory activity (Wohlfahrt and Gu 2015). As a result, R_{eco} tends to be overestimated at low light and underestimated at high light. This have consequences on the GPP estimation which, over a daily cycle, is closer from the 'true photosynthesis' than the 'apparent photosynthesis' it is meant to be (Wohlfahrt and Gu 2015).

4 USE OF CHLOROPHYLL FLUORESCENCE TO STUDY PHOTOSYNTHESIS

4.1 Principles of chlorophyll fluorescence

Photosynthetic activity and its response to the environment is usually assessed by measuring gas exchange (i.e., CO_2 and H_2O) at leaf scale using a small leaf cuvette or at the ecosystem scale using an eddy covariance system. However, gas exchange measurement only gives a partial picture of the process of photosynthesis as it does not provide information related to the performance of photosynthesis, i.e., the absorption efficiency of light energy by the LHC antenna and how efficiently the absorbed energy is used for photochemistry. Plant photochemical capacity (i.e., the efficiency by which a photon can be absorbed by the LHC antenna and used to produce photochemical energy) can be assessed through the measurement of fluorescence emitted by leaf. This method is based on the principle that a small portion of the absorbed light energy is naturally dissipated by the photosynthetic apparatus in the form of heat and fluorescence emission. Even though the energy dissipated in the form of fluorescence only accounts for 2-10% of the total light absorbed energy, study of the fluorescence emission provides information on the functioning and regulation of the complex antenna and the photosystems (Stirbet and Govindjee 2012). Moreover, perturbations of the electrons progression inside the ETC caused by any events affecting photosynthesis is reflected by a change in the fluorescence induction kinetic. Therefore, study of the fluorescence emitted by leaf provides an insight of the photosynthetic apparatus structure, functioning and regulation of the complex antenna and the photosystems (Maxwell and Johnson 2000).

The rise of fluorescence following illumination of a dark-adapted chlorophyll containing material such as leaves (Fig. 4.1), known as the Kautsky effect, was first detected and described in 1931 (Kautsky and Hirsch 1931). Most part of the induced fluorescence at room temperature is emitted by the Chl *a* molecules within the PSII light-harvesting antenna, especially by the inner antenna CP43 and CP47 (Buonasera et al. 2011). The fluorescence emission is characterized by a major peak measured at wavelength of 685 nm and a shoulder between 700-750 nm (Stirbet and Govindjee 2012). It has been widely accepted that the transient fluorescence rise from the basal level (= F_0) reflects the accumulation of Q_A in its reduced form and therefore

represents the progressive closure of PSII RC. The maximum of fluorescence (= F_M or F_P) is reached when all PSII RC of the studied sample are closed. The rise from the basal level to the maximum level of fluorescence is achieved within 1 s during the so called 'fast phase'. The amount of variable fluorescence (F_V=F_M−F_0) emitted after a saturating light pulse informs about the photosynthetic apparatus potential to use photon energy for photochemistry. The kinetic of emission during the fast phase is representative of the energy conservation inside the ETC (Strasser et al. 1995) and can be studied using a plant efficiency analyzer (PEA).

After reaching a maximum, the fluorescence level starts to fall during the 'slow phase', called PSMT (Fig. 4.1), which lasts for a few minutes. This phenomenon described as fluorescence quenching is explained by the onset of carbon metabolism and energy dissipation processes by heat, respectively termed the 'photochemical quenching' and the 'non-photochemical quenching' (NPQ). Pulse amplitude modulated (PAM) fluorimeters enable the study of quenching processes and photochemical capacity under light. This is made possible thanks to a modulated measuring light (i.e., which can be turned on and off) at a frequency synchronized with the detector which allows measurements in the presence of background measuring light. Most of the protocols used for the study of the slow fluorescence kinetics consist in the exposition of a dark-adapted sample to a saturated light followed by the exposition to repeated saturated light pulses in the presence of actinic light (Fig. 4.2). The amplitude of the fluorescence peak emitted after a saturating pulse under light condition informs about the redox state of Q_A and the plant capacity to use photon energy for photoschemistry in light-adapted state. The maximum of fluorescence reached in these conditions is usually lower than in dark-adapted condition due to the activation of NPQ. The difference between the maximum of fluorescence measured in dark-adapted condition and in light-adapted condition (F_M−F_M') is used to quantified NPQ. Study of NPQ by PAM fluorimeter is often used to assess zeaxanthin-facilitated dissipation mechanism as NPQ is linearly correlated to violaxanthin deepoxidation (Roháček et al. 2008) even though change in light-harvesting antenna size and PSII inactivation can also influence NPQ response (Brestic and Zivcak 2013, Murchie and Lawson 2013). A fixed time of ca. 5 min is usually applied between each saturation pulse to allow the fluorescence level to reach a steady state. This protocol enables to assess the ability of the plant to use the absorbed photon energy in photochemistry and its efficiency to dissipate the excess of energy through non-photochemical processes (Brestic and Zivcak 2013).

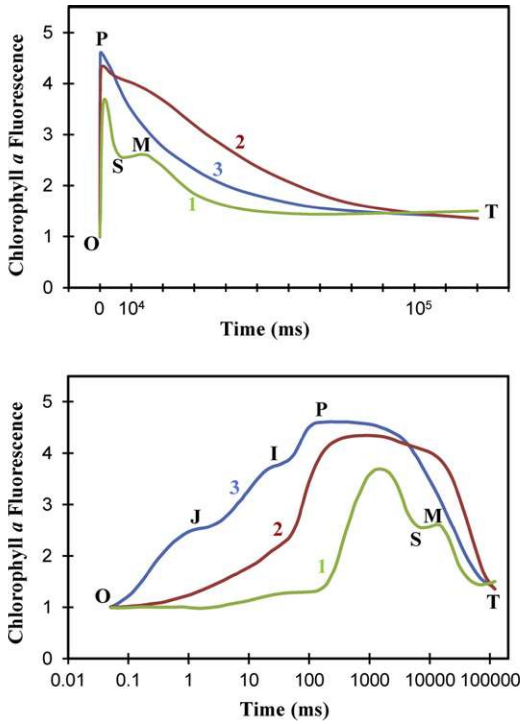

Figure 4.1 – Chlorophyll *a* fluorescence emission of a dark-adapted pea leaf. The top graph shows the fluorescence emission curve plotted on a linear time scale whereas the bottom graph shows the same fluorescence emission curves plotted on a logarithmic time scale. The fluorescence curves labeled 1, 2 and 3 were induced by a flash light of 32, 320, and 3200 μmol m^{-2} s^{-1} respectively. Fluorescence decrease during the slow phase, after illumination, is called PSMT for peak, semi-steady state, maximum and terminal steady state. The fluorescence rise during the fast phase is called OJIP for origin (the first measured minimal fluorescence level), J and I as intermediary steps, and peak. Depending on the light intensity, the shape of the curve can change, leading to missing steps. Fluorescence is given in arbitrary units. Figure from Stirbet and Govindjee (2011).

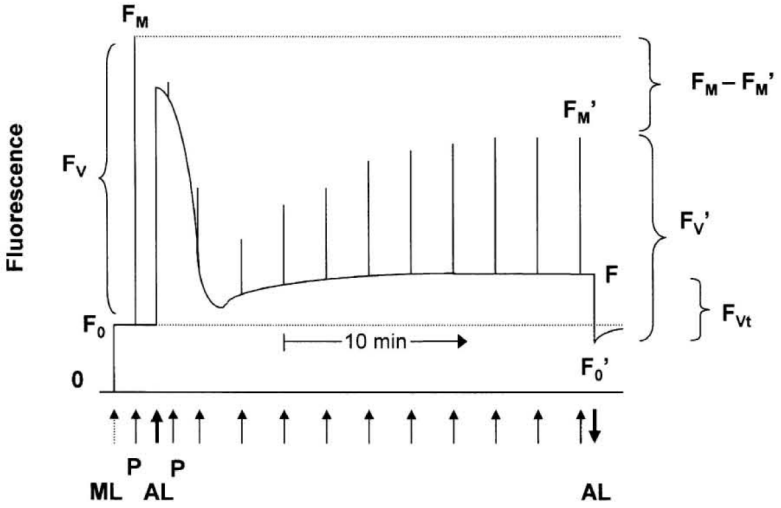

Figure 4.2 – Scheme of the fluorescence emission (arbitrary units) recorded during a typical measurement protocol using a pulse amplitude modulated fluorimeter. The minimum fluorescence in dark-adapted state (F_0) is determined under a modulated measuring light (ML) of ca. 0.01 μmol m^{-2} s^{-1}. After the application of a saturating light pulse (P), the maximum fluorescence yield in dark-adapted state (F_M) is measured. Frequent P are then applied in the presence of an actinic light (AL) of ca. 80-300 μmol m^{-2} s^{-1} to determine the maximum fluorescence yield in light-adapted state (F_M'). When the AL is turned off, F_0' and F_{Vt} can be measured and later used in the determination of the photochemical quenching. Figure from Krause and Jahns (2004).

4.2 Analysis of the OJIP curve using the JIP-test

4.2.1 Theory behind the JIP-test

When plotted on a logarithmic scale, the fast fluorescence transient exhibits a polyphasic rise (Fig. 4.3) called the OJIP curve (referring to the O, J, I, P steps at 50 us, 2 ms, 30 ms and maximum ChlF yield). The OJIP curve can be analyzed using the JIP-test which is based on the theory of energy fluxes in biomembranes to calculate several phenomenological and biophysical parameters that characterize the PSII behavior and therefore the photochemical capacity (Strasser et al. 1995, 2000, 2004). The method is based on several theoretical hypothesis including (i) that there is no energy transfer (i.e., connectivity) between the PSII units, (ii) that the PSII units are homogeneous, (iii) that the contribution of the PSI fluorescence can be neglected, (iv) that the Q_A molecules are reduced only once at the beginning of the fluorescence rise comprised between 0.01-0.25 ms, (v) that the reduction of Q_A is the main factor regulating the fluorescence intensity, and (vi) that all Q_A are reduced at the maximum fluorescence yield. These assumptions have been used to build simplified mathematical models even though some have a non-negligible impact on ChlF such as the PSI fluorescence, the heterogeneity of PSII units and the connectivity among PSII units. Those have been considered separately and can be estimated based on the OJIP curve using the JIP-test (Stirbet and Govindjee 2011).

Energy fluxes (J) characterized by the JIP-test represent the different steps of energy transfer from the PSII antenna till the reduction of the end electron acceptor at the PSI acceptor side:

- J_{ABS} represents the absorbed photon energy by the PSII antenna.
- J_{TR} is related to the energy trapped by the PSII RC.
- J_{DI} is indicative of the absorbed energy which has been dissipated as heat or fluorescence.
- J_{ET} describes the energy that enter the linear electron transport chain, beyond Q_B.
- J_{RE} is representative of the energy reaching the PSI acceptor side and reducing the end electron acceptor.

Since the different steps in the kinetics of fluorescence emission are representative

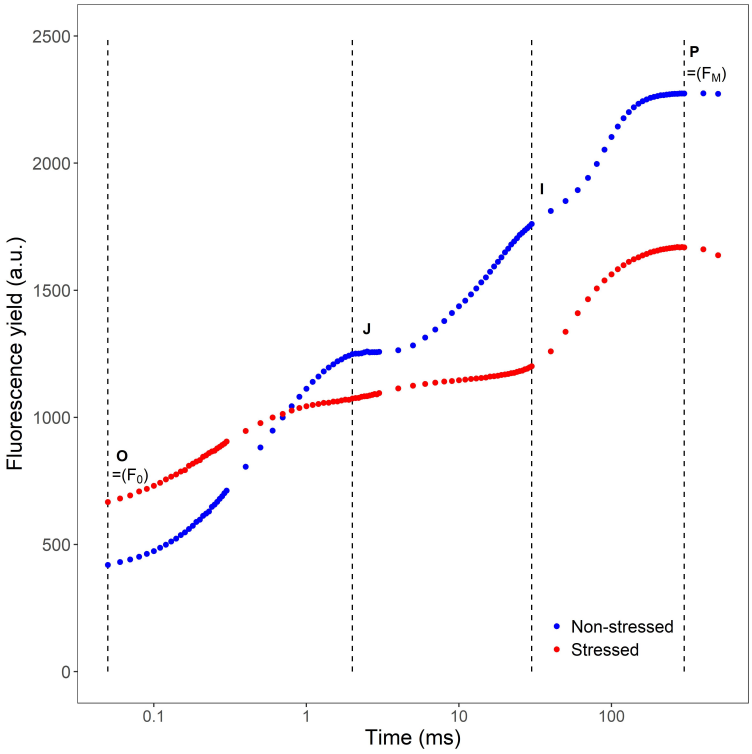

Figure 4.3 – Example of OJIP fluorescence induction curves plotted on a logarithmic time scale from 50 μs to 500 ms measured on a dandelion (*Taraxacum* sp.) in non-stressful (blue) and stressful (red) environmental conditions. Measurements were performed in field condition with a PEA fluorimeter on dark-adapted leaf sample by saturating red light at 3000 μmol m^{-2} s^{-1}. Dashed lines indicate the position of the O, J, I and P steps at 50 μs, 2 ms, 30 ms and maximum yield of fluorescence respectively. The dandelion chlorophyll fluorescence emission measured in stressful condition shows a clear alteration in its induction kinetic, including a higher fluorescence basal level (O step) and a lower maximum yield of fluorescence (P step).

of key phenomenons occurring during the transfer of excitation energy from the PSII antenna to electron acceptors, energy fluxes can be estimated based on the OJIP curve. The rise from O to J, also called the photochemical phase, is strongly dependent on the exciting light intensity (Buonasera et al. 2011). This phase is related to single turnover events (i.e., Q_A is reduced only once) of the primary reactions of photochemistry and represents the reduction of the acceptor side of PSII (Oukarroum et al. 2007). This interpretation is based on the similarity of the kinetic of fluorescence emission from leaf and chloroplast samples treated with DCMU (3-(3',4'-dichlorophenyl)-1,1-dimethylurea), an inhibitor of the PSII acceptor side (Strasser and Stirbet 2001). The fluorescence level at the J step was shown by Tóth et al. (2007b) to be dependent on the availability of oxidized PQ at the Q_B-site, giving an information about the redox state of the PQ pool. As 2 ms are required for the transfer of one pair of electrons to the PQ pool upon strong illumination, it is admitted that J-I phase of the curve is representative of the reduction/oxidation of the PQ pool (Petrouleas and Crofts 2005). Because of its sensitivity to temperature due to a temperature dependent kinetic of electron exchange at the Q_B-site and at the cytochrome complex, the J-I phase is also referred as the 'thermal phase' (Stirbet and Govindjee 2012). The last and slowest phase in the rise of ChlF emission, the I-P phase, was shown by Schansker et al. (2005) to be related to electron transfer through PSI. Experiments in dibromothymoquinone and methylviologen treated-leaves revealed that the electron transfer beyond both the cytochrome complex and the acceptor side of PSI were involved in the I-P fluorescence transient.

4.2.2 Assessment of electron transport using chlorophyll fluorescence parameters

One of the most used ChlF parameters is F_V/F_M which describes the maximum quantum yield of PSII of a dark-adapted leaf and can be expressed as:

$$F_V/F_M = \frac{F_M - F_0}{F_M} \tag{4.1}$$

Value of F_V/F_M measured in healthy leaves is usually around 0.8 for higher plants (Kasajima et al. 2011). This parameter is based on the assumption that all Q_A are fully oxidized at F_0 and all Q_A are fully reduced at F_M (Kalaji et al. 2017). Reduction of its value indicates a reduction in the efficiency of the whole PSII RC population. Decline in the PSII efficiency associated with a reduction in F_V/F_M may have different origins. The inactivation of PSII RC due to damage to the D1 protein has been identified as one

of the possible causes of photoinhibition of the PSII, leading to an increase in F_0 and thus a reduction in F_V/F_M (Adams et al. 2013). The physical separation of the PSII RC from the LHCII, resulting in a lower energy transfer from the antenna to the PSII RC, can also lead to an increase in F_0 and thus a decline in F_V/F_M (Mathur et al. 2011b, Kalaji et al. 2011, Janka et al. 2013). Sustained dissipation of excess radiation energy within the LHC associated with zeaxanthin retention, either in ΔpH-independent way or at low temperature, can also lead to a sustained depression in F_V/F_M (Demmig-Adams and Adams 2006, Jahns and Holzwarth 2012). Increase in the number of Q_B-non-reducing PSII RC, also referred as 'silent reaction centre', was also shown to be responsible for the decline in F_V/F_M as they dissipate all the excitation energy trapped (Strasser et al. 2004, Mathur et al. 2011a). Inactivation of the OEC can also lead to an inhibition of the PSII resulting in the decrease of the F_M value due to a lower capacity of the PSII donor side to provide electrons (Murata et al. 2007, Mathur et al. 2011b, Adams et al. 2013). Increase in energy transfer between the PSII and the PSI was also cited as a possible cause for the reduction of PSII efficiency and the associated decrease in F_V/F_M (Adams et al. 2013).

The Ψ_{E0} parameter is widely used to describe the J step and can be expressed as:

$$\Psi_{E0} = 1 - \frac{F_J - F_0}{F_M - F_0} \tag{4.2}$$

where F_J is the fluorescence level at the J step. The occupancy state at the Q_B-site was shown to influence the level of fluorescence at the J step (Tóth et al. 2007b). Limitation on the acceptor side of PSI may reduce the rate of oxidation of the PQ-pool and thus the electron flow beyond the Q_B-site, leading to an increase in F_J (Tóth et al. 2007b). Accumulation of Q_A in its reduced form was also shown to lead to an increase in fluorescence at the J-step due to a reduced efficiency in electron transport beyond the acceptor side of PSII (Strasser et al. 1995, Chen et al. 2015). Thus, Ψ_{E0} is used to assessed the efficiency of electron transport beyond the Q_B-site (Kalaji et al. 2014).

Changes in the amplitude of the I-P phase are assessed by the ΔV_{IP} parameter which is expressed as:

$$\Delta V_{IP} = \frac{F_M - F_I}{F_M - F_0} \tag{4.3}$$

where F_I is the fluorescence level at the I step. The physiological interpretation behind

the changes in the I-P phase is still controverted. Variations in the ΔV_{IP} were shown to correlate with leaf PSI content and confirmed by western blot analysis (Oukarroum et al. 2009, Ceppi et al. 2012). In addition, higher values of ΔV_{IP} are observed in sun leaves that characterized by a higher PSI/PSII ratio (Kalaji et al. 2017). This parameter was therefore proposed as a semi-quantitative indicator for relative changes in the leaf PSI content. However this interpretation is challenged by another study who did not observed changes in ΔV_{IP} after the photoinactivation of PSI (about 55%). Still, authors did not exclude that ΔV_{IP} may be indicative of the efficiency of electron transport around PSI if the amount of remaining active PSI in samples was not rate limiting for electron transport between the PSII and the PSI acceptor side. Using transmission change at 820 nm and real-time quantitative reverse transcription polymerase chain reaction, (Hamdani et al. 2015) showed that changes in the I-P phase can reflect a transient block in the electron transport at the PSI acceptor side, which may support the theory suggesting that ΔV_{IP} is indicative of the PSI efficiency.

Performance indices (PI) are multi-parametric indices derived from the OJIP curve combining information on the performance of PSII and efficiency of electron transport at specific steps within the thylakoid membrane. As they integrate different information related to the photochemical performance into one number, they are widely used to estimate the photosynthetic stress tolerance (Stirbet et al. 2018). Among them, the performance index on absorption basis, PI_{ABS}, is among the most widely used and is expressed as:

$$PI_{\text{ABS}} = RC/ABS \times \frac{F_{\text{V}}/F_{\text{M}}}{1 - F_{\text{V}}/F_{\text{M}}} \times \frac{\Psi_{\text{E0}}}{1 - \Psi_{\text{E0}}} \tag{4.4}$$

where RC/ABS represents the fraction of active RC per antenna Chl, expressed as:

$$RC/ABS = \frac{1 - F_0/F_{\text{M}}}{M_0/V_{\text{J}}} \tag{4.5}$$

where M_0 represents the initial slope of the fluorescent transient and V_J the relative variable fluorescence calculated as $(F_J\text{-}F_0)/(F_M\text{-}F_0)$. PI_{ABS} therefore integrates three keys parameters of photochemical efficiency : (1) the density of active RC, RC/ABS; (2) the PSII efficiency, F_V/F_M; and (3) the efficiency of electron transport beyond the Q_B-site, Ψ_{E0}. As a result, PI_{ABS} is sensible to any changes in these components (Tsimilli-Michael et al. 2000). Because of its sensitivity, it has been used in breeding

programs to rank variety according to their tolerance to abiotic stress (Živčák et al. 2008, Silvestre et al. 2014). Events affecting the electron flow around the PSI can be integrated to this indice by multiplying PI_{ABS} by $\Delta\ V_{IP}/(1-\Delta\ V_{IP})$, which gives $PI_{ABS,total}$ (Tsimilli-Michael and Strasser 2008). Alternative PI have also been developed to quantify plant tolerance to specific stress such as high temperature, drought and chilling temperature (Stirbet et al. 2018).

Parameters derived from the OIJP curve using the JIP-test therefore provide a very useful and powerful tool in the study of the photosynthetic apparatus functioning and structure (Maxwell and Johnson 2000, Strasser et al. 2000, Kalaji et al. 2016). Here, we detail how the JIP-test can be used to answer scientific question in plant research.

4.2.3 Stress assessment by the study of the OJIP curve

Heat stress was shown to alter the kinetic of ChlF emission, indicating perturbation in processes of photosynthesis in heat-treated plants. For instance, heat-induced damages to the OEC was detectable by a rise of fluorescence at 300 μs (called the K-band, Fig. 4.4) of the OJIP curve due to an imbalance between the electron transfer rate at the donor side and at the acceptor side of the PSII (Strasser 1997, Strasser et al. 2000, Oukarroum et al. 2016). Inactivation of OEC can also induce a decrease of F_M that indicates an alteration in the PSII donor side (Mathur et al. 2011a, Haque et al. 2014). A rise in the level of fluorescence at the J step is also observed during heat stress, suggesting an accumulation of Q_A in its reduced form (Luo et al. 2011, Yan et al. 2012) likely due to an impairment of events beyond Q_A. Separation of the LHCII from the PSII complex is also a common observed symptom after the exposition of plants to high temperature (Mathur et al. 2011b, Brestic et al. 2012). This dissociation is reflected by an increase in F_0 caused by the reduced transfer of harvested light energy to the PSII RC. Alteration of OEC can also lead to a rise of F_0 (Kalaji et al. 2016). As a result of the decrease in F_M and the increase in F_0, a decline in the variable fluorescence (F_V=F_M-F_0) is observed, leading to a reduction in F_V/F_M value (Georgieva et al. 2000). F_V/F_M is representative of the efficiency of the primary photochemical events of PSII. This parameter value is usually close to 0.8 in healthy plants for most species (Ashraf and Harris 2013). Damage to the PSII resulting in the decrease of F_V/F_M are generally not reported for temperature lower than 40°C (Crafts-Brandner and Salvucci 2002, Nellaepalli et al. 2011, Janka et al. 2013).

Impact on the photosynthetic apparatus by severe drought stress is also revealed

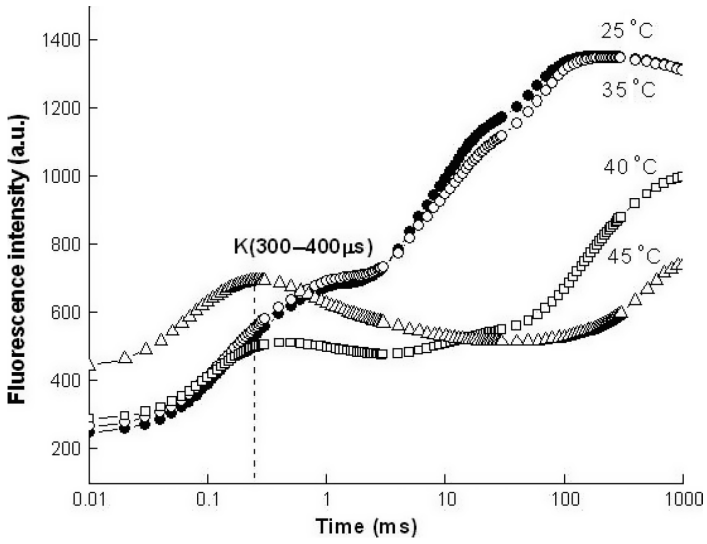

Figure 4.4 – Appearance of the K-band in the OJIP fluorescence induction curves. These fluorescence induction curves were measured on wheat (*Triticum aestivum* L.) leaves after 15 min immersion in a water for at temperatures of 25°C (filled circle), 35°C (empty circle), 40°C (square) or 45°C (triangle). Figure from Mathur et al. (2011b).

by change in the OJIP induction curve. A rise of fluorescence at 100-200 μs (called the L-band, Fig 4.5) can be observed in water-stressed plant (Oukarroum et al. 2007, Sengupta et al. 2013, Campos et al. 2014), indicating a decrease in energy transfer among active PSII units, a phenomenon also referred as 'grouping' or 'energetic connectivity' (Strasser and Stirbet 1998). Reduced PSII connectivity can be explained by an alteration of the structural organizations of the thylakoid membrane (Oukarroum et al. 2007). Severe water stress can also induce an increase in F_0, which was interpreted as an inactivation of PSII RC due to a decrease in D1 content (Ghotbi-Ravandi et al. 2014). Dissociation of the OEC from the PSII complex can also result in the appearance of the K-band under severe drougt stress or in sensitive species (Oukarroum et al. 2007, Redillas et al. 2011, Sengupta et al. 2013). Drought-induced perturbations in electron transport beyond Q_A (Goltsev et al. 2012, Silvestre et al. 2014) can also be assessed by modifications in the I-P phase of the fluorescence emission (Oukarroum et al. 2009, Sengupta et al. 2013). Since the PSII is reputed resistant to low leaf water potential (Manes et al. 2001), decrease in F_V/F_M are mostly observed in the case of severe drought stress (Lauriano et al. 2006, Goltsev et al. 2012, Tozzi et al. 2013, Ghotbi-Ravandi et al. 2014)

Photoinhibition of the PSII induced by light stress is reflected by a decrease in F_V/F_M (Pollastrini et al. 2011, Kalaji et al. 2012). High energy dissipation in the PSII antenna by the zeaxanthin-dependent mechanism can also contribute to the decline in F_V/F_M (Adams III et al. 2006). Increase in F_0 resulting from light stress has also been attributed to the detachment of the LHCII from the PSII or to the inactivation of PSII RC (Mathur and Jajoo 2015). The appearance of a higher L-band due to a loss in energetic connectivity among PSII units is also visible in light-stressed plants (Zivcak et al. 2014). High-light treatment also induce an increase in fluorescence in the region of the K-band due to the inactivation of OEC (Desotgiu et al. 2012a). Increased efficiency of the PSI due to a faster reduction of Fd can also affect the OJIP curve with an increase in the relative fluorescence contribution of the I-P region (Pollastrini et al. 2011, 2016b).

Change in the shape of the I-P phase of the fluorescence transient and increase of the J step in response to ozone stress were representative respectively of a decrease in the PSI efficiency (Desotgiu et al. 2010) and the accumulation of Q_A^- (Manes et al. 2001). Reduction of F_V/F_M is also observed in symptomatic leaves (Calatayud et al.

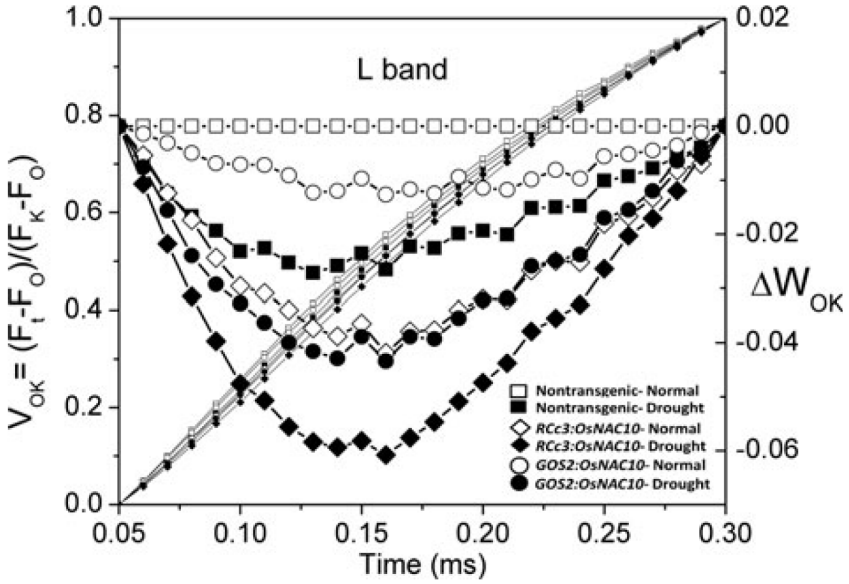

Figure 4.5 – Appearance of the L-band in the OJIP fluorescence induction curves. These fluorescence induction curves were measured on a wild-type rice and transgenic rice plants overexpressing OsNAC10 (a gene involved in drought tolerance) under drought and control conditions. The expression of the OsNAC10 gene in rice was under the control of the constitutive promoter GOS2 for GOS2-OsNAC10 and the root-specific promoter RCc3 fpr RCc3-OsNAC10. The figure shows the double normalization (V_{OK}) at F_O and F_K of the OJIP curves computed as $V_{OK} = (F_t - F_O)/(F_K - F_O)$; plotted at the left axis. The difference kinetics was computed as $\Delta W_{OK} = V_{OK,sample} - V_{OK,control}$ and reveals the appearance of the L-band at 150 μs; plotted at the right axis. Figure from Redillas et al. (2011).

2007), indicating structural damages of the PSII or high dissipation of energy depending on the behavior of F_0 and F_M (Bussotti et al. 2011).

Use of the JIP-test in stress assessment provide useful information in the study of the response and adaptive ability of the photosynthetic apparatus to a wide range of stressors. The table 4.1 summarizes the behavior of the most commonly used ChlF parameters derived from the OJIP curve in response to abiotic stresses. Interpretation in field study where multiple stressors co-occur can be challenging, as changes in one parameters can be induced by different stressors and their interactions. Still, the impact of two abiotic stresses on photosynthesis can be untangled when they have a different impact on the same region of the OJIP curve, such as light and ozone stress which have an opposite effect on the I-P region (Cascio et al. 2010). JIP-test derived parameters have also been used successfully to highlight interactions between abiotic stresses. For instance, fluorescence emitted by water-stressed plants exposed to heat stress exhibited a lower K-band than well-watered plants, indicating a better OEC thermotolerance for water-stressed plants due to the accumulation of osmolyte compounds during the drought period (Lu and Zhang 1999, Oukarroum et al. 2009). Georgieva et al. (2003) also highlighted the protective effect of light against heat stress on the PSII complex by measuring higher F_V/F_M values in light-acclimated plants after a heat treatment compared with plants grown in low light.

4.2.4 Ecology and adaptation strategy

In addition to the biochemical integrity of the photosynthetic apparatus, ChlF emission also informs on the mechanisms implemented by the apparatus to adapt to its environment. Different ecological studies have used ChlF to assess the diversity of adaptation strategies established by different functional groups (Ciccarelli et al. 2016) or plants under contrasted environmental conditions (Bussotti et al. 2010, Desotgiu et al. 2012a). By studying F_V/F_M evolution, Werner et al. (2002) have shown that sclerophylls species under a Mediterranean climate mainly related to a 'tolerance strategy' by promoting dissipation of the excess light energy to cope with summer stress (i.e., hot and dry conditions). In contrast, semi-deciduous species, which suffered more from photoinhibition, exhibited an 'avoidance strategy' by changing leaves orientation in order to reduce light interception. Pollastrini et al. (2016b) also revealed during a forest ecology survey that tree species living in Mediterranean conditions were char-

Table 4.1 – Examples of markers derived from the OJIP curve in the study of stress impact on the photosynthetic apparatus. Arrows indicate the sens of variation of the related ChlF marker.

Stress	Mechanisms	ChlF markers	
Heat stress	Loss of PSII efficiency	↓	F_V/F_M
	OEC alteration	↑	K-band
	LHCII-PSII dissociation	↑	F_0
	PSII alteration	↓	F_M
	Q_A^- accumulation	↑	J step
Drought stress	Loss of PSII efficiency	↓	F_V/F_M
	PSII units connectivity	↑	L-band
	OEC alteration	↑	K-band
	PSII RC inactivation	↑	F_0
	PSI alteration	↓	I-P phase
Excess of light	Loss of PSII efficiency	↓	F_V/F_M
	Adjustment of PSII structure	↑	L-band
	OEC alteration	↑	K-band
	LHCII-PSII dissociation	↑	F_0
	PSII RC inactivation	↑	F_0
	High PSI efficiency	↑	I-P phase
Ozone	Loss of PSII efficiency or damages	↓	F_V/F_M
	Q_A^- accumulation	↑	J step
	PSI alteration	↓	I-P phase

acterized by a stronger contribution of the I-P region to OJIP fluorescence rise, suggesting a good ability of leaves to manage high solar radiation (Desotgiu et al. 2012a).

5 CONCLUSIONS

Vegetation in managed grassland plays a key role in the sequestration of carbon by photosynthesis, allowing the mitigation of GHG emission by the ecosystem. The harvest and the conversion of photon into photochemical energy are crucial steps in the photosynthetic process and were shown to be highly sensitive to environmental conditions. Interactions between stressors were also shown to be determinant in the photosynthetic response as it could either alleviate or exacerbate the physiological stress perceived by the photosynthetic apparatus. Whether combinations could be beneficial or detrimental to photosynthesis depends on many factors including the nature of the stressors involved, their intensity and their order of occurrence. If the combination between environmental constraints are frequently encountered in fields, their impact on the different processes of photosynthesis remains understudied. In addition, uncertainties remains about how alteration in plant photochemical capacity in field condition could affect carbon uptake by the ecosystems. A better understanding of the photochemical capacity variation in field condition and acclimation strategy of primary plants in grasslands ecosystem can have a strategic importance in the management and the maintenance of a sufficient level of carbon uptake by this ecosystem.

III

Objectives and methodology

We have highlighted the importance of the primary light reactions in photosynthesis and its sensitivity to the environment. Under unfavorable conditions, plant ability to harvest and use photon energy can be altered, leading to an overall decline of the photochemical capacity. Variations of ecosystems carbon uptake have been reported in many studies that have assessed grassland CO_2 fluxes in response to environmental factors (Gilmanov et al. 2003, Ma et al. 2007, Mamadou et al. 2016, Gomez-Casanovas et al. 2017). However, they did not characterize the ecosystem photochemical capacity neither its potential impact on ecosystem CO_2 fluxes. Assessment of the photochemical capacity of an ecosystem is laborious as it required a great number of measurements in order to take into account the spatial and the temporal variation of this feature. The difficulty increases for ecosystems composed by different species such as grassland. Satellite images of sun-induced fluorescence can overcome most of these technical difficulties and can be successfully used to estimate the photosynthetic capacity of an ecosystem as well as the spatial variation (Walther et al. 2015, Liu et al. 2017). However they cannot be used to investigate photosystems functioning, energy conservation within the electron transport chain or acclimation strategy since fluorescence emission is measured under natural sunlight. Indeed, dark-adaptation of the photosynthetic material and application of a saturation light pulse are minimal requirements to investigate such processes. As a consequence, ecosystem photochemical capacity and its impact on ecosystem CO_2 fluxes remains understudied.

The overall objective of the present thesis was to study the relationship between the ecosystem photochemical capacity and CO_2 fluxes in a managed grassland. To this end, the study have been subdivided into three specific objectives:

- Assess the photochemical capacity of primary grasslands species and its evolution through the season.
- Identify how environmental constraints affect the different processes involved in the light reactions of photosynthesis.
- Determine if alteration in the ecosystem photochemical capacity affect ecosystem CO_2 fluxes.

The fourth part of this thesis will present the results of the research project. In the first chapter, we have assessed during two growing seasons the variation of the photochemical capacity of the perennial ryegrass *Lolium perenne* L., the most abundant species in the studied managed grassland (see Table S1 for floristic inventory). Its

ability to harvest and use photon energy was studied by the analysis of the OJIP curve using the JIP-test. Theory behind the JIP-test is explained in details in the section 4.2 page 49. Measurements of ChlF were performed using a PEA fluorimeter (Fig. 1). ChlF measurements were realized at four different time frames of the day in order to identify a potential diurnal pattern in the photochemical capacity. Variation in photochemical capacity was then analyzed along with meteorological data measured on-site in order to determine how environmental constraints affected the different processes of photosynthesis. In the second chapter, the photosynthetic response of the monocot *L. perenne* was compared with that of species of two other functional groups, *Taraxacum* sp. and *Trifolium repens* L., as representative of respectively the non-N-fixing and N-fixing dicots. In addition, we estimated the ecosystem photochemical capacity based on measurements realized on the three species which together covered >50% of the grassland surface. In order to determine if variation in the ecosystem photochemical capacity had an impact on ecosystem CO_2 fluxes, estimated ChlF parameters characterizing the ecosystem performance were analyzed along with CO_2 ecosystem gas-exchange measurements realized using eddy covariance technique (Fig. 2). In order to allow the association between CO_2 fluxes variations and changes in photochemical capacity, ChlF measurements were performed in 3 different blocs located within the eddy covariance footprint in the direction of the prevailing winds (Fig. 3).

In the last part of this thesis, we discuss the results obtained and formulate perspectives of future work on the understanding of plants influence on GHG exchanges through carbon assimilation. We also stress that plants can influence GHG balance through other mechanisms than photosynthesis.

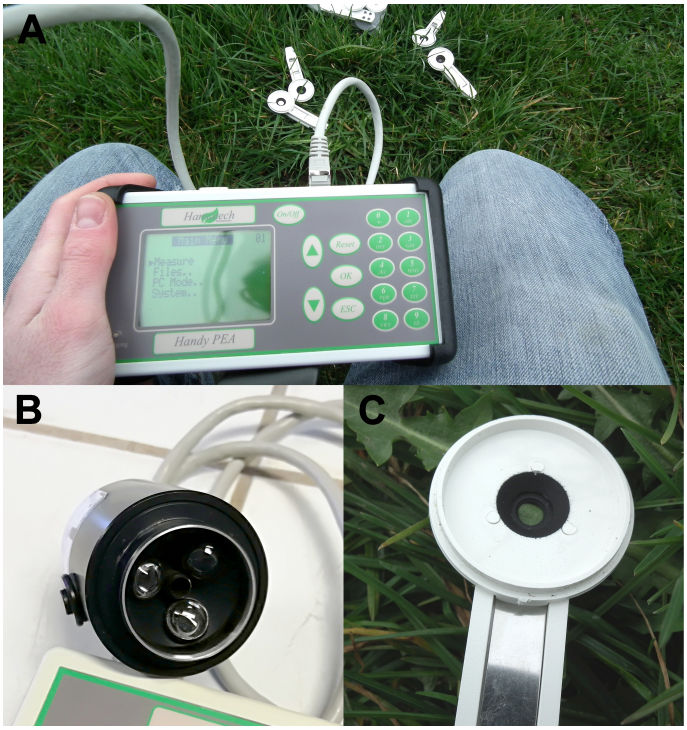

Figure 1 – Plant efficiency analyzer (PEA) fluorimeter. Photography of the (A) Handy PEA chlorophyll fluorimeter model (Hansatech Instruments, Pentney, Norfolk, UK) used in the study. The (B) sensor head is equipped with 3 ultra-bright red LED's optically filtered to a peak wavelength of 650 nm and a detector photodiode with RG9 long pass filter. (C) Leaf clamps have of a small shutter plate that can be closed to dark adapt the leaf area exposed by the 4 mm diameter hole. Leaf clamps were built to fit the sensor head in a way that external light can not penetrate inside the enclosed environment once the sensor head is plugged to the clamps.

Figure 2 – Eddy covariance system. (A) Eddy covariance system at the Dorinne Terrestrial Observatory equipped with (B) a three-dimensional sonic anemometer (CSAT3, Campbell Scientific Ltd., UK) and (C) a fast CO_2-H_2O non-dispersive infrared gas analyser (LI-7000, LICOR Inc., Lincoln, NE, USA) settled in a protective enclosure (white enclosures on the top figure).

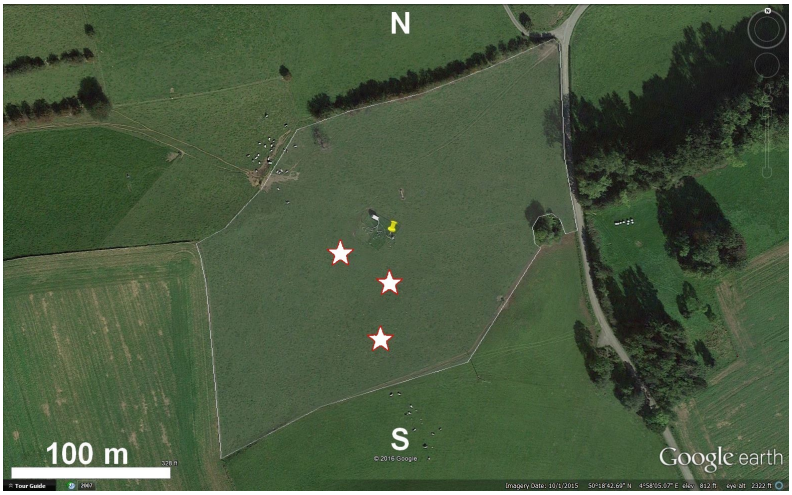

Figure 3 – Aerial photography taken on 10 January 2015 of the site of measurement (Dorinne Terrestrial Observatory, DTO) on Google earth imagery (Google^{TM} earth, version 7.1.5.1557). The yellow pin indicates the position of the meteorological station which GPS coordinates are 50.3119 N, 4.9680 E. The white stars indicate the approximate positions of the monitored areas.

IV

Results

1 VARIATION OF THE PERENNIAL RYEGRASS *Lolium perenne* L. PHOTOCHEMICAL CAPACITY AND THE INFLUENCE OF COMBINED ENVIRONMENTAL CONSTRAINTS

This chapter is adapted from the reference - Digrado A, Bachy A, Mozaffar A, Schoon N, Dalcq A-C, Amelynck C, Bussotti F, Fauconnier M-L, Aubinet M, Heinesch B, du Jardin P, Delaplace P. 2017. Long-term measurements of chlorophyll a fluorescence using the JIP-test show that combined abiotic stresses influence the photosynthetic performance of the perennial ryegrass (*Lolium perenne* L.) in a managed temperate grassland. Physiologia Plantarum, 161(3):355-371. doi: 10.1016/j.atmosenv.2016.12.041.

Abstract Several experiments have highlighted the complexity of stress interactions involved in plant response. The impact in field conditions of combined environmental constraints on the mechanisms involved in plant photosynthetic response, however, remains understudied. In a long-term field study performed in a managed grassland, we investigated the photosynthetic apparatus response of the perennial ryegrass (*Lolium perenne* L.) to environmental constraints and its ability to recover and acclimatize. Frequent field measurements of chlorophyll *a* fluorescence (ChlF) were made in order to determine the photosynthetic performance response of a population of *L. perenne*. Strong midday declines in the maximum quantum yield of primary photochemistry (F_V/F_M) were observed in summer, when a combination of heat and high light intensity increased photosynthetic inhibition. During this period, increase in photosystem I (PSI) activity efficiency was also recorded, suggesting an increase in the photochemical pathway for de-excitation in summer. Strong climatic events (e.g., heat waves) were shown to reduce electron transport between photosystem II (PSII) and PSI. This reduction might have preserved the PSI from photo-oxidation. Periods of low soil moisture and high levels of sun irradiance increased PSII sensitivity to heat stress, suggesting increased susceptibility to combined environmental constraints. Despite the multiple inhibitions of photosynthetic functionality in summer, the *L. perenne* population showed increased PSII tolerance to environmental stresses in August. This

might have been a response to earlier environmental constraints. It could also be linked to the selection and/or emergence of well-adapted individuals.

1.1 Introduction

Many studies have evaluated plant responses to environmental stresses and have reported effects on the photosynthetic process (Georgieva et al. 2000, Hassan 2006, Mathur et al. 2011b, Bussotti et al. 2014). For instance, high temperature have been shown to be particularly detrimental, with several studies reporting that photosynthesis is one of the most heat-sensitive processes in plants (Luo et al. 2011, Yan et al. 2012, Guidi and Calatayud 2014). High temperatures are also known to cause a loss of the manganese cluster functionality in photosystem II (PSII), which leads to the inhibition of the oxygen evolving complex (OEC) component (Nash et al. 1985, Tóth et al. 2007a, Oukarroum et al. 2009). This impairment of photosynthetic activity has been shown to affect CO_2 fixation (Guidi and Calatayud 2014). Under drought stress conditions, studies have also reported a decrease in the CO_2 assimilation rate due to a decrease in stomatal conductance (Cruz de Carvalho et al. 2010, Rahbarian et al. 2011). High ozone concentrations can also induce a depression in net photosynthesis (Bussotti et al. 2007b, Cascio et al. 2010) and the inactivation of the end acceptors of electrons by oxidative damage of the cellular content has been reported in numerous studies (Desotgiu et al. 2010, Bussotti et al. 2011).

The photosynthetic apparatus, however, is able to trigger protective mechanisms under stressful environments favouring acclimatization (for definition, see Wilson and Franklin (2002)). For instance, plants can promote an increase in energy dissipation within the light harvesting complex in order to reduce PSII excitation when submitted to high irradiance (Jahns and Holzwarth 2012, Goh et al. 2012) or to adjust the electron transport rate within the PSII reaction centre (RC) (Derks et al. 2015). Usually, however, plants encounter combined environmental stresses in natural conditions. Two stresses sometimes require antagonistic responses, such as drought and heat stress which lead to the opening or closure of stomata in Arabidopsis, respectively (Rizhsky et al. 2002, Mittler 2006). This makes it difficult to predict plant response to combined environmental constraints. Some studies have shown increased PSII thermotolerance under drought conditions (Oukarroum et al. 2009, Snider et al. 2013), whereas others have shown increased PSII sensitivity to heat (Jiang and Huang 2001, Tozzi et al. 2013). The combination of high temperatures with high levels of light has also been shown to promote PSII inhibition (Janka et al. 2015), whereas some studies have found that high levels of light could promote PSII thermotolerance (Georgieva et al. 2003). These examples highlight the complexity of stress interaction and the need for fur-

ther studies on the mechanisms involved in plant photosynthetic response to combined environmental constraints.

Analyses of chlorophyll *a* fluorescence (ChlF) have been used in several studies to investigate the physiological aspects of photosynthesis. Fast fluorescence transients measured by a plant efficiency analyser (PEA) and modulated fluorescence signals obtained from a pulse-amplitude modulated (PAM) fluorimeter both provide parameters that describe photosynthesis functionality and are widely used. Measurements conducted with a PAM fluorimeter use light-adapted leaves, whereas fast fluorescent transients are derived from dark-adapted leaves. This implies that measurements in dark-adapted conditions give information on the 'potential' photosynthetic performance rather than the actual photosynthetic efficiency. A PEA fluorimeter enables the acquisition of large amounts of data in a short period of time, making monitoring and large-scale surveys possible. The fast fluorescent transients can be analysed using the JIP-test, which provides useful information on the status and functioning of the photosynthetic apparatus (Maxwell and Johnson 2000, Kalaji et al. 2016). When plotted on a logarithmic scale, the fluorescence transients exhibit a polyphasic rise called the OJIP curve (referring to the O, J, I, P steps at 50 μs, 2 ms, 30 ms and maximum ChlF yield). The rise in ChlF emission from its basal level (= O step) reflects the gradual accumulation of Q_A^- in its reduced form. The O-J phase of the curve is related to single turnover events (i.e., Q_A is reduced only once) of the primary reactions of photochemistry and represents the reduction of the acceptor side of PSII (Oukarroum et al. 2007). The J phase is influenced by the rate limitation caused by the reduction of the plastoquinone (PQ) pool (Tóth et al. 2007b). The J-I phase of the curve is therefore representative of the reduction/oxidation of the PQ pool. The last and slowest phase in the rise in ChlF emission, the I-P phase, is related to electron transfer through PSI and is attributed to the reduction of the acceptor side of the PSI (Schansker et al. 2005). It has been demonstrated that the shape of the OIJP curve is related to the physiological status of plants (Strasser et al. 2000). The parameters determined with the JIP-test therefore provide a very useful tool for investigating the response and adaptive ability of the photosynthetic apparatus to a wide range of stressors (Bussotti et al. 2007b, 2010, Redillas et al. 2011, Brestic et al. 2012).

Among the various cultivated agro-systems, grasslands represent $\approx$ 26% of the terrestrial surface (Brunner et al. 2007, Boval and Dixon 2012) and about 80% of agricultural land (Boval and Dixon 2012). Grasslands play a significant role in carbon

sequestration (Boval and Dixon 2012, Chang et al. 2015) and water catchments, and are a reserve of biodiversity (Boval and Dixon 2012). A good understanding of the health status of these ecosystems is therefore a key issue if one wants to preserve or increase these ecosystem services under current and future climatic conditions. For these reasons, we decided to investigate the photosynthetic response to the naturally co-occurring environmental constraints of the perennial ryegrass (*Lolium perenne* L.), an important grassland species, over 2 successive years using the JIP-test. We sought to answer the following questions: (i) How does the photosynthetic apparatus respond to combined environmental constraints and which mechanisms of photosynthetic processes are involved? (ii) What is the recovery capacity of photosynthetic performance after repeated stressful events? (iii) Is there any evidence of photosynthetic acclimatization? We hypothesize that the greatest decline in photosynthetic performance will occur when environmental stresses are combined because of potential synergistic interactions. A succession of unfavourable events might also lead to the potential acclimatization in *L. perenne* population.

1.2 Materials and methods

1.2.1 Field site

The study was carried out within the framework of the CROSTVOC project (CROp STress Volatile Organic Compounds: http://hdl.handle.net/2268/178952). All measurements were performed at the Dorinne Terrestrial Observatory (DTO) in Belgium (50°18'44" N and 4°58'07" E). The climate at this site is temperate oceanic. The site area is a permanent grassland covering 4.22 ha, and the relief is dominated by a large colluvial depression oriented south-west/north-east. This depression lies on a loamy plateau with a calcareous and/or clay substrate. Altitudes range from 240 m (north-east) to 272 m (south). The paddock had been converted to permanent grassland at least 50 years before the start of this study and has been intensively grazed by cattle, with the application of cattle slurry and manure. The botanical diversity was evaluated on 24 quadrats (0.5 X 0.5 m) in September 2010 and June 2011. The plant communities were composed of 13 grass species (*Agrostis stolonifera* L., *Alopecurus geniculatus* L., *Bromus hordeaceus* L., *Cynosurus cristatus* L., *Dactylis glomerata* L., *Elymus repens* (L.) Gould, *Festuca pratensis* Huds., *Holcus lanatus* L., *Lolium multiflorum* Lam., *L. perenne*, *Poa annua* L., *Poa pratensis* L. and *Poa trivialis* L.), one nitrogen (N)-fixing

dicot (*Trifolium repens* L.) and seven non-N-fixing dicots (*Capsella bursa-pastoris* (L.) Medik., *Carduus* L., *Matricaria discoidea* DC., *Plantago major* L., *Ranunculus repens* L., *Stellaria media* (L.) Vill. and *Taraxacum* sp.). The perennial ryegrass *L. perenne* was the main and most representative species in the grassland, being present in every quadrat and in the greatest relative abundance (based on the surface occupation) in the quadrats.

1.2.2 Micro-meteorological data

Micro-meteorological data such as photosynthetic photon flux density (PPFD) (SKP215, Skye Instruments, Llandrindod Wells, UK), air temperature (T_{air}) and air relative humidity (RH) (RHT2nl, Delta-T Devices Ltd, Burwell, Cambridge, UK) at 2.62 m above soil level, as well as ozone concentration (O_3) (T400, Teledyne, San Diego, USA) at 1 m above soil level, and soil moisture (SM) (CS616, Campbell Scientific Inc., Logan, UT, USA) and soil temperature (TS) (PT 1000, Campbell Scientific Inc., Logan, UT, USA) at a depth of 5 cm were recorded every 30 min in the grassland during the measurement periods using the aforementioned equipment. The vapor pressure deficit (VPD) was calculated from the temperature and relative humidity measurements.

1.2.3 Analysis of the fluorescence transient using the JIP-test

Measurements of the ChlF emissions of *L. perenne* were conducted at the DTO on three plots (each 30 X 5 m) from June to October 2014 and from May to October 2015, using a HandyPEA fluorimeter (Hansatech Instruments, Pentney, Norfolk, UK). Cows were allowed to graze on days when no measurements were being taken. Measurements were performed in each monitored plot four times a day at 11:00, 13:00, 15:00 and 17:00 h (local time zone). The number of replicates for each plot and time period was 7 in 2014 and 8 in 2015. In addition, on 31 July 2015 and 13 August 2015, when there were contrasting micro-meteorological conditions, the full diurnal evolution of ChlF was investigated by taking measurements every 2 h from pre-dawn (5:00) till evening (19:00) on the three plots, giving eight sample time periods rather than four. Measurements were performed on non-senescent mature leaves. Prior to each measurement, leaves were dark-adapted with leaf clips for 30 min. The leaf clips were adapted to the width of the *L. perenne* leaves by reducing by half the measurement sur-

face with a black vinyl electrical tape, following the manufacturer's recommendations. The surfaces of the dark-adapted leaves were then exposed for 1 s to red light with a flux density of 3000 μmol m^{-2} s^{-1} provided by an array of three light-emitting diodes (peak wavelength at 650 nm). After irradiance of the sample, the induced subsequent fluorescence signals were recorded every 10 μs from 10 to 300 μs, then every 100 μs till 3 ms, then every 1 ms till 30 ms, then every 10 ms till 300 ms and finally every 100 ms till 1 s.

Fluorescence emissions measured at 50 μs (F_{50}, step O), 300 μs (F_{300}, step K), 2 ms (step J), 30 ms (step I) and maximum yield (F_M, step P) were used to determine several parameters describing photosynthesis activity according to the JIP test (Strasser et al. 2000, 2004, Tsimilli-Michael and Strasser 2008). These parameters are summarized in Table 1.1. When a ChlF parameter showed an aberrant value (i.e., infinite), all parameters derived from this specific measurement were discarded (0.06% of the dataset).

1.2.4 Statistical analysis

Three groups of comparable meteorological conditions were defined by clustering (Ward's method based on the Euclidian distance). Clustering was performed on coordinates of the two first principal components of a principal component analysis (PCA). All meteorological parameters were entered as variables in this PCA, apart from ozone concentration. In order to study the influence of monitored plots on ChlF response, a general linear model (GLM) type III was realized, with the meteorological group previously created and the monitored plots as factors. The monitored plots were considered as random factor. As its influence was not found to be significant, the values of ChlF parameters were averaged without consideration of the different plots. Three groups of comparable photosynthetic response based on ChlF measurements were then defined using the same methodological approach as that for the meteorological groups. The averaged ChlF parameter values were entered as variables in the PCA. The Tukey's Honest Significant Difference test (Tukey HSD) was used to classify the mean values of ChlF and the meteorological parameters between the meteorological and ChlF clusters created. When comparing days with contrasting meteorological conditions, the difference in ChlF parameter values between the 2 days was tested using a GLM for each of the eight sample time periods.

The correlations between ChlF and meteorological parameters were tested using

Table 1.1 – Summary of parameters and formulas used for the analysis of the fast fluorescence transient OJIP.

Parameters	Formulas	Description
Technical fluorescence parameters		
F_t		Fluorescence intensity at the time t.
F_{50}		Fluorescence intensity at 50 μs (O-step).
F_{300}		Fluorescence intensity at 300 μs (K-step).
F_J		Fluorescence intensity at 2 ms (J-step).
F_I		Fluorescence intensity at 30 ms (I-step).
F_M		Maximal fluorescence intensity (P-step).
F_V	F_M-F_{50}	Maximal variable fluorescence.
F_V/F_M (= φ_{P0})	$1-(F_{50}/F_M)$	Maximum quantum yield of PSII of a dark-adapted leaf. Expresses the probability that an absorbed photon will be trapped by the PSII reaction centre.
JIP-test derived parameters		
M_0	4 $[(F_{300}-F_{50})/(F_M-F_{50})]$	Approximated initial slope of the fluorescence transient.
V_t	$(F_t-F_{50})/(F_M-F_{50})$	Relative variable fluorescence at the time t.
V_J	$(F_J-F_{50})/(F_M-F_{50})$	Relative variable fluorescence at 2 ms (J-step).
V_I	$(F_I-F_{50})/(F_M-F_{50})$	Relative variable fluorescence at 30 ms (O-step).
RC/ABS	$\varphi_{P0}(V_J/M_0)$	Q_A-reducing reaction centres (RC) per PSII antenna Chl.
Ψ_{E0} (= J phase)	$1-V_J$	The efficiency/probability that a photon trapped by the PSII RC moves an electron into the electron transport chain beyond Q_A.
ΔV_{IP} (= I-P phase)	$1-V_I$	The efficiency/probability that a photon trapped by the PSII RC moves an electron into the electron transport chain beyond PSI to reduce the final acceptors of the electron transport chain (i.e., ferredoxin and NADP).
PI_{ABS}	(RC/ABS) $[\varphi_{P0}/(1-\varphi_{P0})]$ $[\Psi_{E0}/(1-\Psi_{E0})]$	Performance index (potential) on absorption basis for energy conservation from photons absorbed by PSII to the reduction of intersystem electron acceptors.

a Pearson correlation test. We decided to complement this approach with a canonical correlation analysis (CCA), a multivariate statistical test, to explore the relationship between photosynthetic responses and meteorological conditions and the interdependence within a set of variables. With this method, the first canonical axis is constructed as linear combinations of variables within the sets in order to maximize the correlation between the two datasets (i.e., ChlF and meteorological datasets).

A GLM was used to predict ChlF parameters based on meteorological variables and their second-order interactions. The minimum adequate model for each ChlF parameter was selected using a stepwise algorithm based on the Akaike's information criterion. Only significant interactions were conserved. The total variance explained by the models (R^2) was then decomposed in order to evaluate the relative variance explained by each predictor variable and the various interactions. Linear regression followed by an analysis of covariance (ANCOVA) was used to evaluate the potential modification in the relationship between the ChlF and meteorological parameters for different environments and months. All the operations were performed using Minitab software version 17.1.0 (State College, Pennsylvania, USA) and R software version 3.3.0 (R Development Core Team, 2012), with the following R package : 'FactoMineR' (Husson et al. 2016), 'Vegan' (Oksanen et al. 2012), 'CCP' (Menzel 2015), 'Car' (Fox et al. 2016) and 'Relaimpo' (Groemping and Matthias 2013). Square root-transformed values (unless stated otherwise) of the ChlF parameters were used to improve the normality and homogeneity of variances when required by the statistical test.

1.3 Results

1.3.1 Environmental conditions

The days of ChlF measurements and their dispersion were representative of the period studied, especially in the second year. Irradiance reached its highest values from May to August (referred to here as summer) for both years, with midday PPFD values above 1500 μmol m^{-2} s^{-1} on most of the measured days (Fig. 1.1A). From September to October (referred to here as autumn), the PPFD values were below that level. From June 30 to July 5 2015 a heat wave (as defined by D'Ippoliti et al. (2010)) hit Belgium and was recorded at the DTO. ChlF measurements during this period were limited to the first and third day of the heat wave, with maximum T_{air} of 28.9 and 33°C

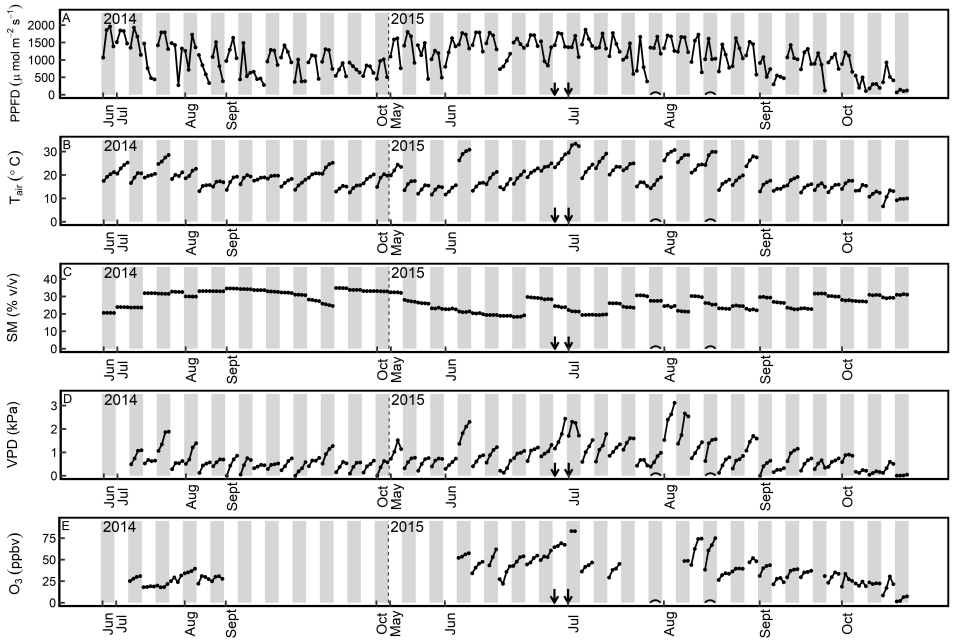

Figure 1.1 – Environmental conditions prevailing during chlorophyll fluorescence measurements in the 2014 and 2015 study periods. Values for (A) photosynthetic photon flux density (PPFD), (B) air temperature (T_{air}), (C) soil moisture (SM), (D) vapour pressure deficit (VPD) and (E) air ozone concentration (O_3) at 11:00, 13:00, 15:00 and 17:00 h for each day of chlorophyll fluorescence measurements are represented. Grey bars separate the different days of measurements for a better visualisation of the diurnal evolution of these parameters. The arrows indicate the first and third day of the heat wave recorded at the DTO. Brackets indicate 31 July 2015 and 13 August 2015

recorded during the ChlF measurement (Fig. 1.1B). In summer, the O_3 were above 60 ppbv, whereas it remained below this level in autumn (Fig. 1.1E). The second year of monitoring was characterized by two dry spells in summer. In June and August, the SM was ca. 20% for 2 weeks (Fig. 1.1C). The highest VPD values were measured from June to August, with values above 2.0 kPa, but in September and October they generally did not exceed 1.0 kPa (Fig. 1.1D).

1.3.2 Temporal evolution of ChlF induction

In both years of the study, a seasonal (Fig. 1.2) and diurnal (Fig. 1.3) evolution of ChlF parameters was observed in the grassland. The largest diurnal amplitudes of ChlF parameters were detected in summer with variations of 68, 99, 41 and 148% with respect to the initial morning value for the maximum quantum yield of PSII (F_V/F_M), the performance index (PI_{ABS}), the J phase (Ψ_{E0}) and the I-P phase (ΔV_{IP}) respectively. The ChlF parameters showed lower diurnal variation in autumn. The highest F_V/F_M values were measured in autumn, with average basal values of ca. 0.75, indicating high PSII efficiency. In contrast, values as low as 0.15 were measured in summer. The lowest PI_{ABS} values were also measured in summer, indicating a low photosynthetic performance of the *L. perenne* population. PI_{ABS} graphically exhibited an increasing trend at the end of the 2014 growing season. This increase also occurred in the following year, but was less pronounced. The Ψ_{E0} showed a less marked diurnal and seasonal pattern and fluctuated around 0.56, with occasional midday decreases below 0.40 observed in summer, reflecting a decrease in the efficiency of the electron transport beyond QA during these periods. The ΔV_{IP} presented stable values around 0.32 in autumn, but several midday peaks above 0.55 were observed in summer, indicating a rapid reduction of the end electron acceptor.

A diurnal decrease in F_V/F_M was observed simultaneously with a decrease in PI_{ABS} and an increase in ΔV_{IP} (Fig. 1.3). A less pronounced diurnal pattern was observed for Ψ_{E0} (Fig. 1.3C). The diurnal variation of ChlF parameters was stronger under environmental stress, as described in the next paragraph. There were few perceptible differences in Ψ_{E0} behaviour between the two contrasting days (Fig. 1.3C). Significant differences ($p \leq 0.001$) between these were observed in the morning for all ChlF parameters, with lower F_V/F_M, PI_{ABS} and Ψ_{E0} values and higher ΔV_{IP} values on 31 July 2015 than on 13 August 2015. These differences were not more significant ($p \geq 0.05$) 6 h after sunrise, except for PI_{ABS}. Even when strong diurnal variations of ChlF parameters were measured (e.g., 13 August 2015), the evening values (i.e., 14 h after sunrise) of ChlF parameters were comparable with those measured 6 h after sunrise (i.e., before the onset of strong diurnal variation) and did not differ ($p \geq 0.05$) from evening values measured on a day with lower diurnal variation (Fig. 1.3).

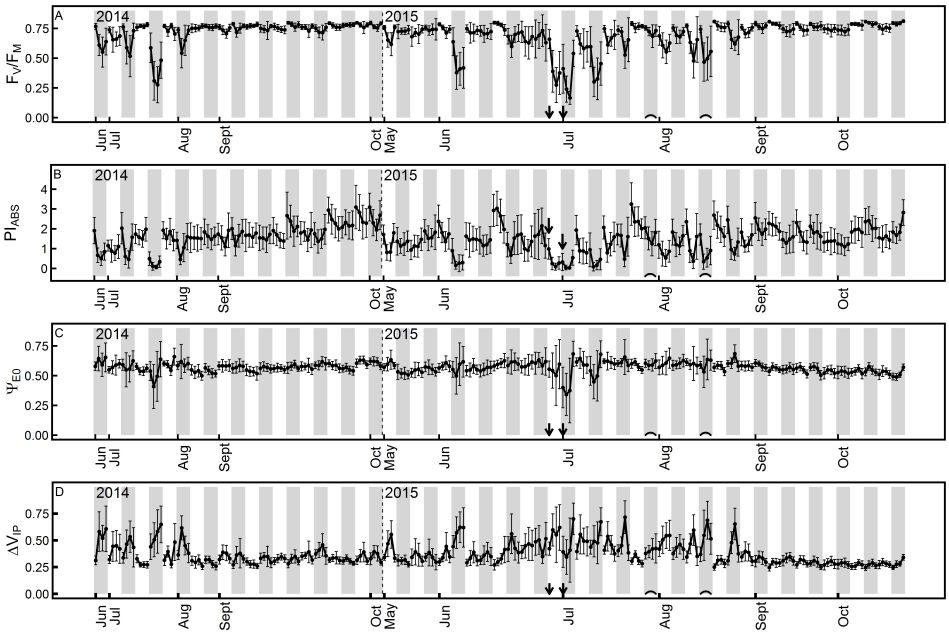

Figure 1.2 – Evolution of chlorophyll fluorescence (ChlF) parameters (F_V/F_M, PI_{ABS}, Ψ_{E0} and ΔV_{IP}) in the 2014 and 2015 study periods. The average value (n = 21-24) $\pm$ SD for each of the four measurement time periods (11:00, 13:00, 15:00 and 17:00 h) is represented for F_V/F_M, PI_{ABS}, Ψ_{E0} and ΔV_{IP} for each measured day. Grey bars separate the different days of measurements for a better visualisation of the diurnal evolution of these parameters. The arrows indicate the first and third day of the heat wave recorded at the DTO. Brackets indicate the 31 July 2015 and 13 August 2015.

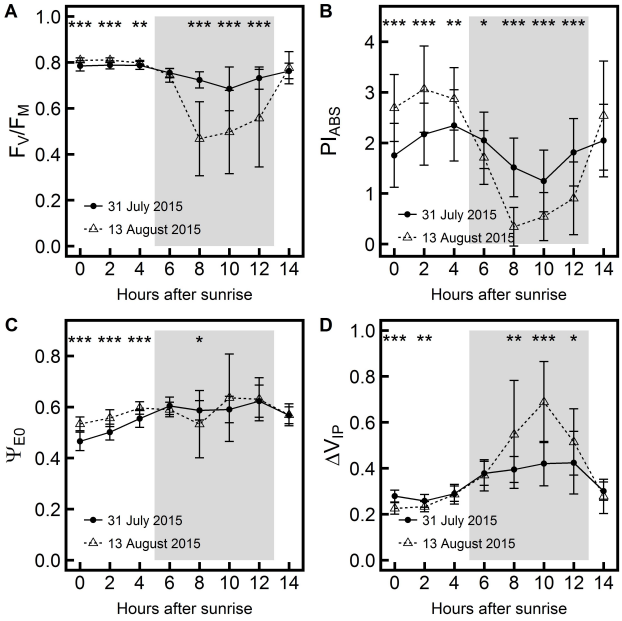

Figure 1.3 – Diurnal evolution of ChlF parameters over two contrasting days. The average values (n = 24) ± SD for each of the eight sampled time periods (0, 2, 4, 6, 8, 10, 12 and 14 h after sunrise) are represented for the (A) F_V/F_M, (B) PI_{ABS}, (C) Ψ_{E0} and (D) ΔV_{IP} on 31 July 2015 and 13 August 2015. Maximum air temperature was 18.9 and 29.9°C on 31 July 2015 and 13 August 2015, respectively. The photosynthetic photon flux density reached 1669 and 1612 μmol m^{-2} s^{-1} on 31 July 2015 and 13 August 2015, respectively. The maximum vapor pressure deficit was 0.98 and 1.56 kPa on 31 July 2015 and 13 August 2015, respectively. Soil moisture was 27.6±0.1 and 25.9±0.6% on 31 July 2015 and 13 August 2015, respectively. An asterisk indicates a significant difference in ChlF parameters average value between the 31 July 2015 and the 13 August 2015 at a specific sample time periods (GLM, $\alpha = 0.05$). Asterisks *, ** and *** indicate $p \leq 0.05$, $p \leq 0.01$ and $p \leq 0.001$ respectively. For the sake of presentation clarity, the three plots results were pooled because minor significant differences were observed at 0 h after sunrise for PI_{ABS} and Ψ_{E0} only. This did not qualitatively change the results. The grey zone identifies the period when ChlF measurement was routinely performed in the grassland.

1.3.3 Impact of environmental conditions on ChlF emissions

The Pearson correlations test (Table 1.2) showed that F_V/F_M and ΔV_{IP} were the ChlF parameters that were most affected by environmental conditions, correlations being higher than 0.52 in absolute value for six out of seven meteorological parameters. In contrast, Ψ_{E0} correlated poorly with meteorological parameters (all correlation coefficients were below 0.24 in absolute value). The relationship between environmental parameters and the ChlF parameters F_V/F_M and PI_{ABS} differed greatly from that between environmental parameters and the ChlF parameters Ψ_{E0} and ΔV_{IP}. PPFD, T_{air} and VDP were the meteorological parameters that had the strongest influence on ChlF parameters, the minimum correlation being above 0.55 in absolute value for F_V/F_M, PI_{ABS} and ΔV_{IP}. In contrast, SM was the meteorological parameter with the least influence on ChlF, with no correlation exceeding 0.35 in absolute value. The strong influence of PPFD, T_{air} and VDP on ChlF parameters was confirmed by the analysis of the relative contribution of meteorological parameters to ChlF variation (Fig. 1.4). The analysis also revealed the influence of synergistic interactions between meteorological parameters. Interactions between meteorological parameters had a non-negligible contribution to ChlF variation and explained 22.8, 12.3, 33.0 and 4.9% of the F_V/F_M, PI_{ABS}, Ψ_{E0} and ΔV_{IP} variance respectively. The Ψ_{E0} was the parameter most influenced by meteorological parameters interactions whereas ΔV_{IP} was the least influenced.

Three meteorological clusters were defined using PCA-clustering (Table 1.3). From the M1 to M3 clusters, environmental conditions were characterized by increasing PPFD, T_{air}, VPD and TS values and decreasing SM and RH values. Whereas M1 conditions were more frequently found in autumn, M3 conditions were more common in summer. Three ChlF clusters were also defined by PCA-clustering (Table 1.3). The C1 cluster was characterized by high F_V/F_M and PI_{ABS} values, indicating good functionality of the photosynthetic apparatus. A reduction of up to 60% and 93% in average values from the C1 to C3 cluster was observed for F_V/F_M and PI_{ABS}, respectively, indicating a decrease in photosynthetic performance in C3. Ψ_{E0} exhibited lower relative change between clusters and decreased by only 19% from C1 to C3. ΔV_{IP} exhibited a significant +50% increase from C1 to C2. The difference in ΔV_{IP} values between C2 and C3 was not significant. ChlF response characterized by the C3 response was common in summer, whereas the C1 response was common in autumn. CCA revealed that M1 conditions in the grassland could be associated with the ChlF response char-

Table 1.2 – Correlation values of meteorological parameters (PPFD, photosynthetic photon flux density; T_{air}, air temperature; SM, soil moisture; VPD, vapor pressure deficit; RH, relative air humidity; TS, temperature of soil; O_3, ozone) with ChlF parameters (F_V/F_M, PI_{ABS}, Ψ_{E0} and ΔV_{IP}). Asterisks *, ** and *** indicate $p \leq 0.05$, $p \leq 0.01$ and $p \leq 0.001$, respectively. ns, non-significant.

	Pearson correlation coefficients			
	F_V/F_M	PI_{ABS}	Ψ_{E0}	ΔV_{IP}
PPFD	-0.564 ***	-0.620 ***	0.164 *	0.622 ***
T_{air}	-0.715 ***	-0.632 ***	0.149 *	0.713 ***
SM	0.350 ***	0.327 ***	-0.052 ns	-0.333 ***
VPD	-0.700 ***	-0.676 ***	0.099 ns	0.682 ***
RH	0.515 ***	0.620 ***	-0.107 ns	-0.543 ***
TS	-0.564 ***	-0.442 ***	0.267 ***	0.609 ***
O_3	-0.581 ***	-0.488 ***	0.165 ns	0.553 ***

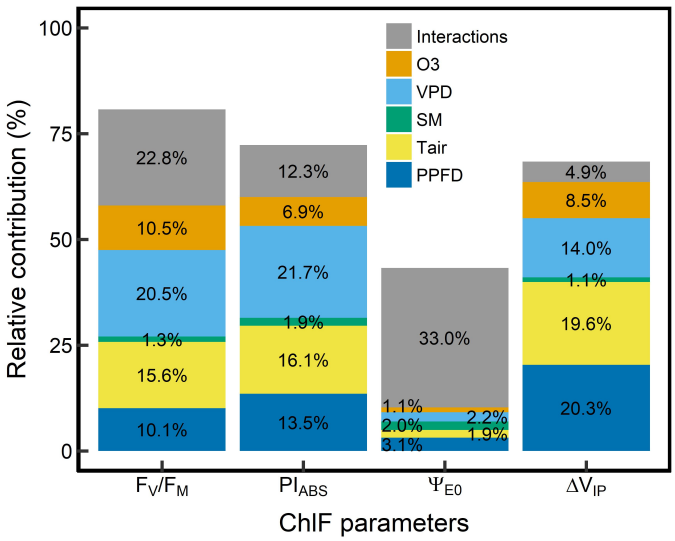

Figure 1.4 – Relative contribution of the meteorological parameters and their second-order interactions in the models explaining the variability in ChlF parameters. Predictor variables were the air temperature (T_{air}), soil moisture (SM), photosynthetic photon flux density (PPFD) and vapour pressure deficit (VPD). The models explained 80.8, 72.3, 43.3 and 68.4% of the variability in F_V/F_M, PI_{ABS}, Ψ_{E0} and ΔV_{IP}, respectively. Relative humidity and soil moisture were excluded from the model because of their high correlation with vapour pressure deficit (86.55%) and air temperature (84.06%) respectively.

acterized by the C1 cluster (Fig. 1.5) and could therefore be qualified as non-stressful conditions. The C3-cluster type of ChlF response was correlated with environmental conditions characterized by the M3 cluster that could therefore be qualified as conditions of strong environmental constraints. M2 conditions in the grassland could be associated to ChlF response characterized by either the C1 or C2 clusters (Fig. 1.3) and could therefore be qualified as conditions of moderate environmental constraints. Days usually began with meteorological conditions characterized by the M1 cluster and the ChlF response corresponding to the C1 cluster. At midday, meteorological conditions could change to the M2 or M3 clusters and the ChlF response to the C2 or C3 clusters.

Table 1.3 – Description of the ChlF (C1, C2, C3) and meteorological (M1, M2, M3) group clusters defined by principal component analysis (PCA)-clustering. Mean values ± SD are represented for each cluster. The relative change (Δ%) in the mean with respect to cluster 1 is indicated for each variable in clusters 2 and 3. PPFD, photosynthetic photon flux density (μmol m^{-2} s^{-1}); T_{air}, air temperature (°C); SM, soil moisture (% v/v); VPD, vapour pressure deficit (kPa); RH, relative air humidity (%); TS, temperature of soil (°C). Ozone was excluded from the PCA-clustering because of the low coverage of these measurements during the measurement period. Different letters indicate significant differences among the clusters (Tukey HSD, α = 0.05).

	Variables	Average (±SD) in the different clusters and the percentage change for the C1 or M1 clusters				
		C1 or M1	C2 or M2	Δ%	C3 or M3	Δ%
ChlF	F_V/F_M	0.764±0.023^a	0.660±0.088^b	−13	0.307±0.074^c	−60
	PI_{ABS}	1.881±0.467^a	1.207±0.514^b	−36	0.131±0.093^c	−93
	Ψ_{E0}	0.556±0.029^b	0.599±0.031^a	+8	0.451±0.066^c	−19
	ΔV_{IP}	0.303±0.028^b	0.456±0.092^a	+50	0.491±0.087^a	+62
Meteo.	PPFD	674±352^c	1242±325^b	+84	1432±311^a	+112
	T	15.38±3.01^c	18.48±3.01^b	+20	26.81±3.03^a	+74
	SM	30.90±3.42^a	25.91±4.34^b	−16	24.29±3.75^c	−21
	VPD	0.34±0.20^c	0.77±0.22^b	+126	1.68±0.48^a	+394
	RH	81.52±9.96^a	64.49±7.29^b	−21	53.28±8.41^c	−35
	TS	14.32±2.43^c	15.76±3.67^b	+10	21.01±2.18^a	+47

The F_V/F_M response to combined stresses received particular attention because it is one of the most studied ChlF parameters and in our study was one of the parameters the most influenced by the combination of meteorological parameters. The linear relationship between F_V/F_M and abiotic stresses varied with environmental conditions (Fig. 1.6). A stronger decrease in F_V/F_M in relation to air temperature was measured where soil moisture was below 20.5% ($p \leq 0.001$, Fig. 1.6A). Soil moisture conditions, however, did not have a significant influence on the F_V/F_M response to increasing PPFD ($p \geq 0.05$, Fig. 1.6B) and increasing VPD ($p \geq 0.05$, Fig. 1.6C). An altered linear relationship between F_V/F_M and abiotic stresses in the grassland was also observed at different sun irradiance levels. Stronger decreases in F_V/F_M in relation to increasing air temperatures were observed at higher sun irradiance levels ($p \leq 0.001$, Fig. 1.6D). The F_V/F_M response to VPD did not differ at moderate and high sun irradiance levels (Fig. 1.6F). The relationship between F_V/F_M and VPD at moderate and high sun irradiance levels, however, could not be compared with the relationship at low irradiance level because no observations at VPD > 2.0 kPa were performed for the latter. Sun irradiance levels in the grassland did not induce a stronger decrease in F_V/F_M in relation to increasing soil moisture (Fig. 1.6E).

1.3.4 Sensitivity of PSII throughout the season

Despite high irradiance and the occurrence of high temperatures and high VPD in the late summer, the diurnal decreases in F_V/F_M in August 2015 were less pronounced than in the earlier summer months (Fig. 1.2). The hypothesis of an increased PSII stability was tested by comparing the linear relationship of the F_V/F_M response to environmental constraints in August 2015 with those in other months that year. In August, we observed a less steep decline in F_V/F_M in relation to increasing T_{air} ($p \leq 0.001$, Fig. 1.7B), and VPD ($p \leq 0.001$, Fig. 1.7D) compared with the F_V/F_M response in the two previous months. In August, the linear relationship of F_V/F_M to these environmental constraints was similar to that observed in September and October. The F_V/F_M response to SM in August 2015 also exhibited a different linear relationship compared with July, with a stronger decrease in relation to decreasing soil moisture ($p \leq 0.001$, Fig. 1.7C). The response of F_V/F_M to increasing PPFD in August did not differ from the response observed in other months ($p \geq 0.05$, Fig. 1.7A).

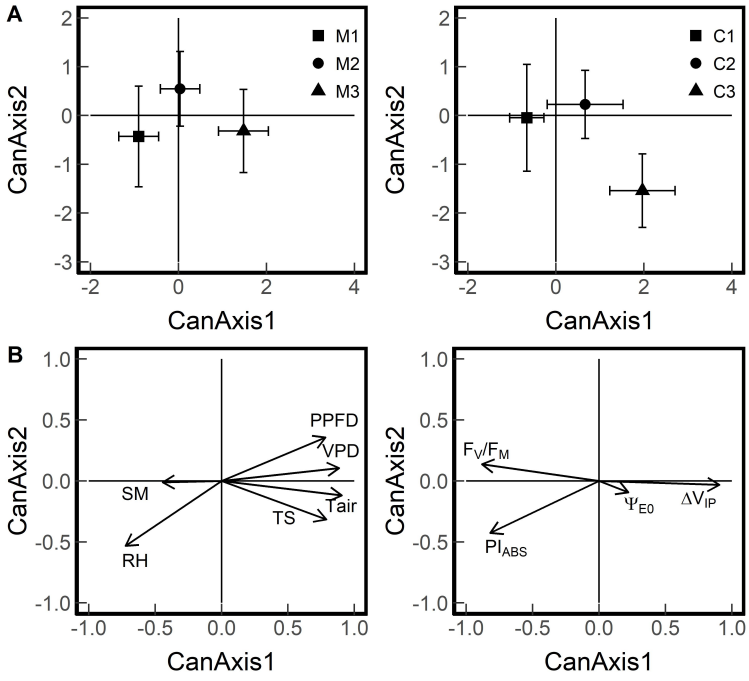

Figure 1.5 – (A) Canonical correlation analysis (CCA) plot of the distribution of meteorological parameters (left) and ChlF parameters (right) according to the canonical axis 1 (CanAxis1) and 2 (CanAxis). The correlations between the CanAxis1 of the two CCA plot and between the CanAxis2 of the two CCA plots were 86.8% (Wilks' Lambda = 0.158, $F_{24,761}$ = 22.11, p value $\leq$ 0.001) and 48.2% (Wilks' Lambda = 0.641, $F_{15,605}$ = 7.03, p value $\leq$ 0.001), respectively. Meteorological (M1, M2 and M3) and ChlF clusters (C1, C2 and C3) derived from the PCA-clustering were represented in the CCA space to enable the association between the different meteorological conditions and ChlF response groups. See Table 1.3 for a description of the different group clusters. (B) Correlation circle derived from CCA by combining meteorological parameters (left) and ChlF parameters (right). Meteorological parameters used for the CCA included: photosynthetic photon flux density (PPFD), air temperature (T), vapour pressure deficit (VPD), soil moisture (SM), relative air humidity (RH) and soil temperature (TS). Ozone was excluded from the CCA because of the low coverage of these measurements during the measurement period. ChlF parameters used for the CCA included: F_V/F_M, PI_{ABS}, Ψ_{E0} and ΔV_{IP}.

1.4 Discussion

Summer was characterized by episodes of low photosynthetic performance due to a combination of environmental constraints. In contrast, high and stable PSII efficiency values were measured in autumn. The discussion here focuses on how meteorological factors influenced the different photosynthetic processes and on which mechanisms were involved in the response of the photosynthetic apparatus in the *L. perenne* population.

1.4.1 The L. perenne *population showed a down-regulation of PSII photochemical activity in summer under combined stresses*

The *L. perenne* population suffered more from PSII photoinhibition in summer, as illustrated by the stronger diurnal F_V/F_M decreases measured in this period (Fig. 1.2A). Several field studies have reported stronger PSII inhibition in summer for various ecosystems (Fernández-Baco et al. 1998, Arend et al. 2013, Ciccarelli et al. 2016). Reversible diurnal decreases in F_V/F_M have been shown to be related to the cumulative light interception during the day and is described as dynamic photoinhibition (Werner et al. 2001, 2002, Guidi and Calatayud 2014). Photoinhibition is the inactivation of PSII, leading to reduced photosynthetic capacity (Goh et al. 2012), and is generally associated with D1 protein turnover (Aro et al. 1994). It is also described as a photoprotective mechanism that results in the preservation of PSII by diverting light energy from the photosynthetic process (Werner et al. 2001, 2002). The relationship of F_V/F_M with light was confirmed by their comparable diurnal behaviour (Fig. 1.1A,1.2) and its strong correlation with PPFD (Table 1.2). Lower F_V/F_M values in summer suggest reduced PSII photochemical efficiency and stronger energy dissipation during this period. The photochemical efficiency of PSII in the *L. perenne* population, however, did not suffer from multiple photoinhibition and was able to recover, as indicated by similar high F_V/F_M values measured in autumn in both years.

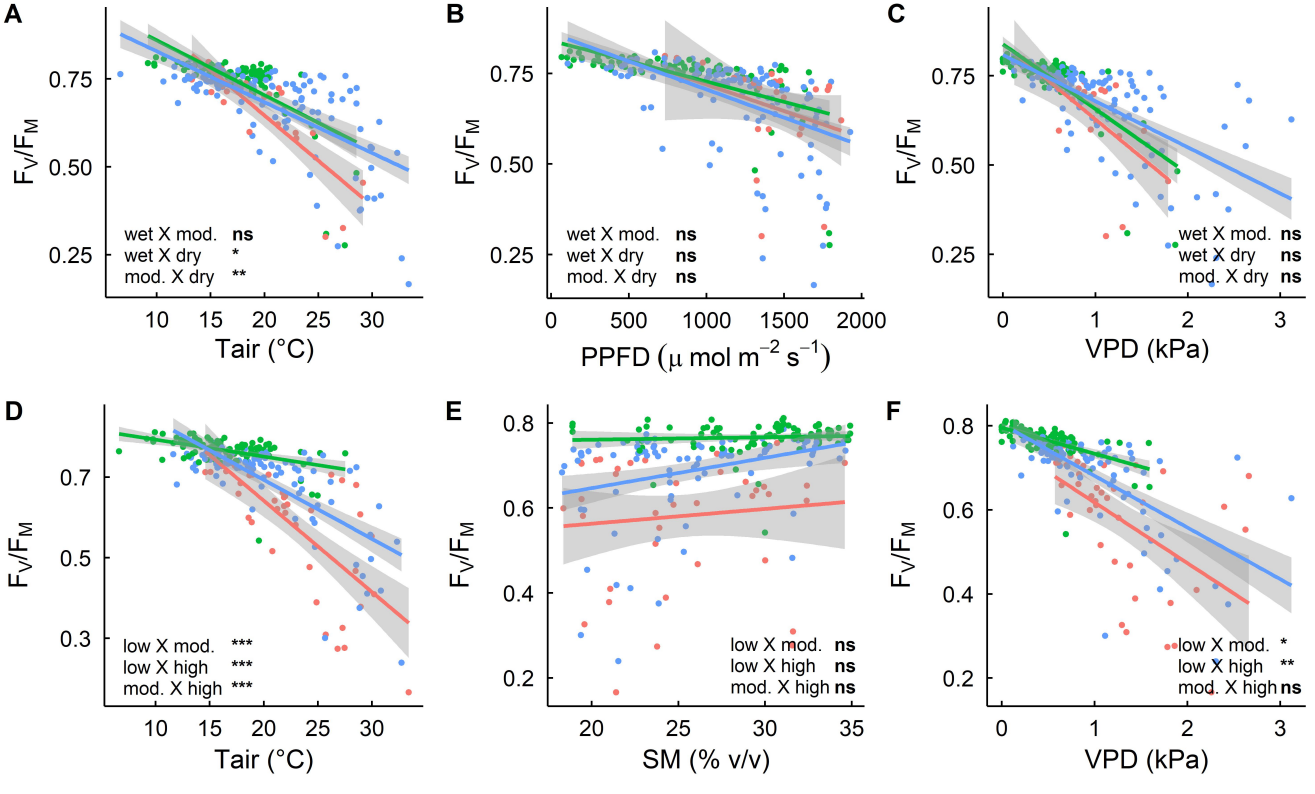

Figure 1.6 – (Continued on the following page.)

Figure 1.6 – Response of the maximum quantum yield of PSII (F_V/F_M) ($\pm$IC 0.95) to environmental constraints at different soil moisture and sun irradiance levels. Linear regressions of F_V/F_M to (A) increasing air temperature (T), (B) photosynthetic photon flux density (PPFD) and (C) vapour pressure deficit (VPD) for observations performed under three soil moisture conditions in the grassland: wet (SM > 30.5% v/v, green line), moderate (25% v/v $\leq$ SM $\leq$ 27% v/v, blue line) and dry (SM < 20.5% v/v, red line). Linear regressions of F_V/F_M response to increasing (D) T_{air}, (E) SM and (F) VPD for observations performed at three different sun irradiance levels in the grassland: low (PPFD < 1000 μmol m^{-2} s^{-1}, green line), moderate (1000 μmol m^{-2} s^{-1} $\leq$ PPFD $\leq$ 1500 μmol m^{-2} s^{-1}, blue line) and high (PPFD > 1500 μmol m^{-2} s^{-1}, red line). Equality of slopes between the different linear regressions was tested by a two-way ANCOVA. Asterisks *, ** and *** indicate $p \leq 0.05$, $p \leq 0.01$ and $p \leq 0.001$, respectively. Different slopes, suggesting a different F_V/F_M response to environmental constraints under different environmental conditions, are reflected by a significant interaction between linear regressions performed under two environmental conditions.

The combination of high PPFD in summer with other environmental constraints was associated with a reduction in the overall photosynthetic performance of the *L. perenne* population, shown by the decline in PI_{ABS} under increasingly unfavourable conditions (Table 1.3, Fig. 1.5). As indicated in Table 1.1, the performance index is a multiparametric expression that takes into consideration three important and independent steps regulating photosynthetic activity: the density of active RC per PSII antenna chlorophyll (RC/ABS); the maximal quantum yield of PSII (F_V/F_M); and the electron transport beyond Q_A (Ψ_{E0}) (Strasser et al. 2000). In our case, PI_{ABS} appeared to be influenced mainly by RC/ABS (data not shown) and F_V/F_M because they exhibited very similar behaviour. A reduction in PI_{ABS} could therefore be related to an increase in excitation energy dissipation as well as to an increase in inactive (i.e., non-Q_A reducing) PSII RC. These so-called 'silent RC' are considered a 'heat sink' involved in the down-regulation of the photosynthetic process because they participate in the controlled dissipation of excitation energy (Bussotti et al. 2007b, 2011). Large changes in PI_{ABS} have been interpreted in desert scrub species as an ability to down-regulate PSII photochemical activity in order to adapt to environmental changes (van Heerden et al. 2007). In our study, the effects of environmental constraints on photosynthetic activity were usually fully reversible, as illustrated by the recovery of PI_{ABS} in the evening (Fig. 1.3). This supports the viewpoint of decline in PI_{ABS} as a down-regulation pro-

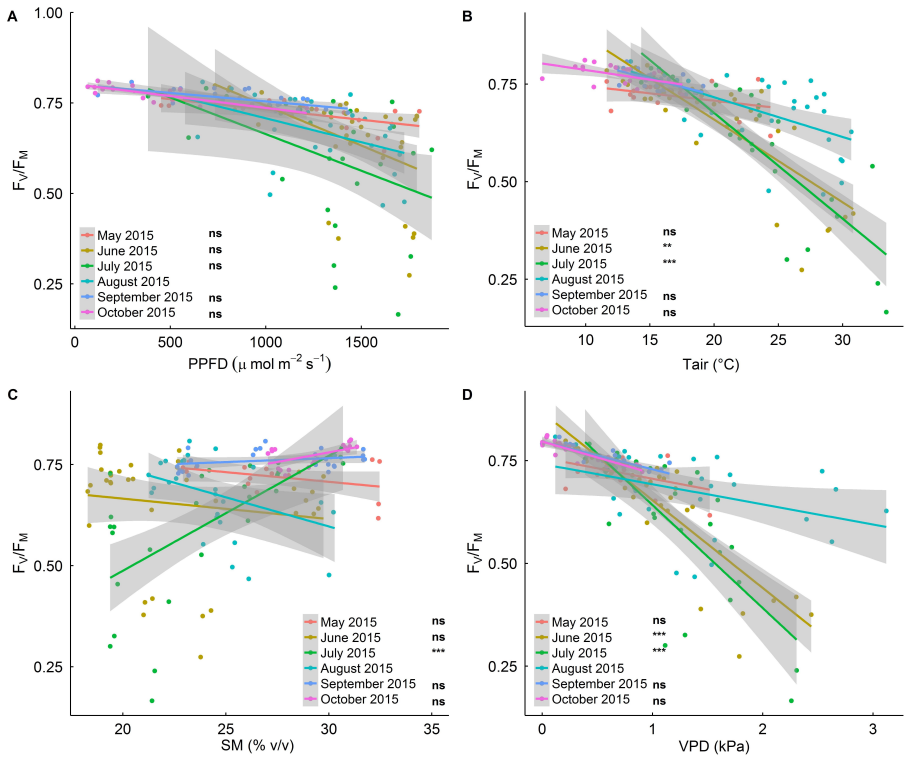

Figure 1.7 – Response of the maximum quantum yield of PSII (F_V/F_M) ($\pm$IC 0.95) to environmental constraints in different months in 2015. Linear regressions of F_V/F_M response to (A) photosynthetic photon flux density (PPFD), (B) increasing air temperature (T), (C) soil moisture (SM) and (D) vapour pressure deficit (VPD) for observations performed in different months in 2015. The hypothesis of an altered PSII response to environmental constraints in August 2015 compared with other months was tested by a two-way ANCOVA. Asterisks *, ** and *** indicate $p \geq 0.05$, $p \geq 0.01$ and $p \geq 0.001$, respectively. A significant p value indicates a different F_V/F_M response to environmental constraints between August 2015 (reference) and the month under consideration.

cess in response to environmental change and suggests good tolerance in the *L. perenne* population to combined environmental constraints.

1.4.2 Down-regulation of PSII activity is associated with increased efficiency in PSI activity under moderate environmental constraints

The *L. perenne* population demonstrated a higher capacity to reduce the end electron acceptor (i.e., ferredoxin and $NADP^+$) in summer, as indicated by the higher midday ΔV_{IP} values during this period (Fig. 1.2D). This suggets an up-regulation of the photochemical pathway for the de-excitation of the *L. perenne* population (Pollastrini et al. 2011, Desotgiu et al. 2012a). Rapid reduction of the end electron acceptor is typical of 'sun leaves' and expresses a high PSI/PSII ratio (Cascio et al. 2010). Similar photosynthetic behaviour was observed among southern European tree species, which exhibited a higher electron transport beyond PSI, as well as lower F_V/F_M and PI_{ABS} values than species from more northern regions (Pollastrini et al. 2016b,a). This behaviour was interpreted as acclimatization to higher solar radiation for these species and suggests a rapid delivery of electrons to the final acceptors and then on to the Calvin cycle (photochemical de-excitation). A higher IP phase in rice cultivars was also associated to lower $P700^+$ accumulation (Hamdani et al. 2015). The hypothesis of higher efficiency in electron transport beyond PSI is also supported by the moderate Ψ_{E0} increase, along with ΔV_{IP} increase in conditions of moderate environmental constraints (Table 1.3), indicating a stimulation in electron transport beyond Q_A.

1.4.3 Strong environmental constraints associated with high temperatures lead to decreased electron transport efficiency beyond Q_A

Stronger environmental constraints, however, could be detrimental to electron transport. Reduced electron transport efficiency (-19% in the Ψ_{E0}) was observed under conditions of strong environmental constraints, but no significant change in ΔV_{IP} was observed (Table 1.3, Fig. 1.5). The J phase has been associated with the redox state of the PQ pool (Tóth et al. 2007b). Decreased Ψ_{E0} values therefore suggest an accumulation of reduced Q_A and PQ pool (Bussotti 2004, Chen et al. 2015). The absence of a significant increase in PSI activity efficiency under conditions of stronger stimulation of the PSII may have been responsible for the slower regeneration of the oxidized form of Q_A and PQ pool. We assumed that reduced in electron transport efficiency

beyond Q_ASP– was caused by an imbalance between the electron flow through PSII and the availability of end electron acceptors on the PSI acceptor side. Similar observations have been reported in ozone-fumigated woody species in which events beyond PSI were affected, leading to a reduced ability to manage the electron flux (Cascio et al. 2010, Bussotti et al. 2011). In the case of imbalance between electrons leaving the PSII and those reaching the acceptors beyond PSI, unmanaged electrons (those that come from PSI, but do not reach the end acceptors) can lead to the formation of hydrogen peroxide through the Mehler reaction (Asada 2006) and eventually cause photo-oxidative damage of the cellular content.

A reduction in the efficiency of electron transport between PSII and PSI may play a protective role by limiting the possibility of 'free electrons' beyond the PSI acceptor side. Given that we did not observe a decline in ΔV_{IP}, we assumed that the PSI was not altered by environmental constraints. We therefore suggest that the decline in electron transport was a self-protection strategy because the PSI was not unable to manage the increase in electron flow under conditions of stronger constraints. Our results also revealed that electron transport was affected mainly by stress interactions (Fig. 1.4), particularly during periods of high temperatures such as heat waves (Fig. 1.2C). A reduction in electron transport efficiency between Q_A and PQ pool was shown to occur at 43°C without alteration of the PSI (Yan et al. 2013). It is possible that interaction between stresses may have reduced the heat threshold above which reduction in electron transport occurs. Taken together, these results indicate the good ability of PSI to manage electron flow except in conditions of strong climatic events when multiple abiotic stresses involving high temperature are combined.

1.4.4 PSII sensitivity to abiotic stress is influenced by sun irradiance and soil moisture

Stronger inhibitions of PSII by heat stress were observed during periods of low soil moisture in the grassland (Fig. 1.6 A). This contrasts with studies that have reported that drought pretreatment benefits PSII thermotolerance (Havaux 1992, Ladjal et al. 2000) due to the accumulation of osmolyte compounds (Oukarroum et al. 2012). These contrasting results might be explained by the potential need for a period of acclimation to drought conditions that is long enough to allow osmolyte accumulation. High levels of sun irradiance in field conditions might also have influenced plant response to combined water and heat stress. Our results, however, are in accordance with Tozzi

et al. (2013)) who observed a predisposition of PSII to heat stress during a period of drought for Fremont cottonwood grown outdoors.

Exposure to high solar irradiance was also shown to predispose PSII to heat stress (Fig. 1.6D). Stronger inactivation of PSII under combined stresses might suggest a greater alteration of the thylakoid membrane, as observed for wheat plants (Al-Khatib and Paulsen 1989). Other studies, however, have reported improved PSII stability to heat stress under light exposure due to the accumulation of heat shock proteins (Georgieva et al. 2003) and the activation of the xanthophyll cycle (Buchner et al. 2015). The reversibility in F_V/F_M diurnal declines observed in our study suggests that there was no irreversible damage to the photosynthetic structure. The stronger decline in F_V/F_M values in response to heat stress under high sun irradiance, however, might indicate increased susceptibility to photoinhibition under combined stresses.

In the case of low stomatal aperture (e.g., caused by high VPD or low soil moisture), increased PSII photoinhibition can result from the reduced CO_2 availability for plants continuously exposed to stimulation by high levels of light (Masojidek et al. 1991). Indeed, the limitation of end electron acceptors availability caused by a slow-down in the Calvin cycle can lead to the formation of reactive oxygen species (ROS) beyond the PSI acceptor side (Guidi and Calatayud 2014). A decrease in stomatal conductance might also reduce leaf transpiration, leading to an increase in leaf temperature (Duan et al. 2008, Gago et al. 2015). In our study, however, we did not found increased PSII sensitivity to high levels of light under conditions that promote stomatal closure (Fig. 1.6B,E,F), suggesting that internal CO_2 concentration was not limiting for photosynthesis. The absence of higher PSII sensitivity to increasing VPD under low soil moisture conditions (Fig. 1.6C) also suggests that *L. perenne* was still able to regulate leaf temperature by transpiration even under conditions of low soil moisture.

1.4.5 L. perenne *population showed an improved PSII tolerance in the late summer*

Improved PSII tolerance to abiotic stresses was measured at the end of the summer in 2015, suggesting the acclimatization of the *L. perenne* population in the grassland (Fig. 1.7). This enhanced PSII stability was evident through better tolerance to low soil moisture, heat stress and high VPD in August than in earlier months. Previous long-term studies conducted on grassland populations did not find any indications of PSII acclimatization after long-term exposure to unfavourable conditions. Gielen et al. (2007), who exposed grassland populations to high temperatures over 3 years, did not

observe improved PSII tolerance to midday stress compared with the control. In contrast, the midday depression of F_V/F_M was stronger for populations grown under high air temperature conditions. Different hypotheses might explain this improved PSII tolerance in the *L. perenne* population in August. It is possible that proline and other osmolyte compounds had accumulated in response to the two dry spells in June and July, improving the PSII stability in response to heat stress (De Ronde et al. 2004, Oukarroum et al. 2012). This assumption is supported by experiments showing that cedar seedlings could benefit from drought-induced PSII thermotolerance up to 60 days after re-watering (Ladjal et al. 2000). Improved PSII tolerance in response to VPD might result from the strong correlation between T_{air} and VPD (0.892, $p \leq 0.001$). The stronger decrease in F_V/F_M in response to decreasing soil moisture in July might be explained by the occurrence of a heat wave during this period. The apparent improved PSII tolerance could also result from the selection of genotypes better fitted to the environment (i.e., local adaption). The development of new leaves with different physiological backgrounds might also have contributed to the change in PSII response. These results suggest either the good ability of PSII in the *L. perenne* population to acclimatize and/or an adaptation to local conditions.

1.5 Conclusions

Photosynthetic performance of L. perenne exhibited a diurnal and seasonal evolution. The strongest photoinhibition of PSII was measured in the summer, when high solar irradiance was combined with other abiotic stresses. Given than the diurnal decreases in ChlF parameters were reversible, the depression of F_V/F_M during this period might indicate increased energy dissipation. The summer was also characterized by stronger PSI activity, reflecting an increased ability in photochemical de-excitation during this period. PSI was unable to increase its activity during strong environmental constraints, however. Strong climatic events led to a reduction in the efficiency in electron transport beyond Q_A. This reduction might, however, contribute to the protection of PSI from oxidative stress by reducing the probability of unmanaged electrons beyond the acceptor side. Low soil moisture had a negligible impact on PSII performance, but was shown to enhance the PSII sensitivity of the *L. perenne* population to heat stress. Increased PSII sensitivity to heat stress was also observed under high sun irradiance. These results illustrate the greater susceptibility of photosynthetic performance under combined stresses. Improved PSII tolerance of heat stress and high VPD was observed

in the late summer. Several hypotheses might explain this behaviour. Further studies are needed to determine whether or not the improved PSII tolerance measured at the end of the summer was due to improved PSII stability in the *L. perenne* population in response to earlier environmental constraints or the selection of better adapted individuals. In addition, we need to investigate whether or not the photosynthetic performance of different grassland species (e.g., dicots) would respond similarly to these combined climatic events and if an acclimatization of the photosynthetic apparatus is also possible for them. We also need to determine how adjustments in photosynthetic processes influence CO_2 fluxes at the ecosystem level. Experiments are under way to test these hypotheses.

1.6 Acknowledgments

We are very grateful to A. Genette and E. Hanon for their useful advice and constructive remarks. We also thank M. Eyletters for constructive discussions and H. Chopin, A. Debacq and F. Wilmus for their technical support. We are grateful to Frederic Collinet and the Calcul et Modélisation Informatique (CAMI) platform of the AGRO-BIO-CHEM department for providing computational resources. The comments by two anonymous reviewers are highly appreciated. This work was supported by the National Fund for Scientific Research of Belgium (PDR, no. 14614874).

1.7 Author contributions

B. Heinesch, M. Aubinet, P. Delaplace, P. du Jardin, C. Amelynck, N. Schoon and M-L. Fauconnier planned and designed the research. A. Digrado, A. Bachy, C. Amelynck, N. Schoon and A. Mozaffar performed experiments and conducted fieldwork. Meteorological data from the DTO were collected and corrected by the Biosystems Dynamics and Exchanges team. Ozone data were collected and corrected by A. Bachy. Chlorophyll fluorescence data were collected and interpreted by A. Digrado. F. Bussotti helped with the interpretation of ChlF data. A-C. Dalcq helped with the statistical analysis of data. A. Digrado wrote the paper. B. Heinesch, M. Aubinet, P. Delaplace, P. du Jardin, C. Amelynck, N. Schoon, A. Bachy, F. Bussotti and M-L. Fauconnier revised the paper.

2 INFLUENCE OF THE ECOSYSTEM PHOTOCHEMICAL CAPACITY ON CO_2 FLUXES

This chapter is adapted from the reference - Digrado A, Gourlez de la Motte L, Bachy A, Mozaffar A, Schoon N, Bussotti F, Amelynck C, Dalcq A-C, Fauconnier M-L, Aubinet M, Heinesch B, du Jardin P, Delaplace P. 2017. Decrease in the photosynthetic performance of temperate grassland species does not lead to a decline in the gross primary production of the ecosystem. Frontiers in Plants Science: accepted. doi: 10.3389/fpls.2018.00067

Abstract Plants, under stressful conditions, can proceed to photosynthetic adjustments in order to acclimatize and alleviate the detrimental impacts on the photosynthetic apparatus. However, it is currently unclear how adjustment of photosynthetic processes under environmental constraints by plants influences CO_2 gas exchange at the ecosystem-scale. Over a two-year period, photosynthetic performance of a temperate grassland ecosystem was characterized by conducting frequent chlorophyll fluorescence (ChlF) measurements on three primary grassland species (*Lolium perenne* L., *Taraxacum* sp., and *Trifolium repens* L.). Ecosystem photosynthetic performance was estimated from measurements performed on the three dominant grassland species weighed based on their relative abundance. In addition, monitoring CO_2 fluxes was performed by eddy covariance. The highest decrease in photosynthetic performance was detected in summer, when environmental constraints were combined. Dicot species (*Taraxacum* sp. and *T. repens*) presented the strongest capacity to up-regulate PSI and exhibited the highest electron transport efficiency under stressful environmental conditions compared with *L. perenne*. The decline in ecosystem photosynthetic performance did not lead to a reduction in gross primary productivity, likely because increased light energy was available under these conditions. The carbon amounts fixed at light saturation were not influenced by alterations in photosynthetic processes, suggesting photosynthesis was not impaired. Decreased photosynthetic performance was associated with high respiration flux, but both were influenced by temperature. Our study revealed variation in photosynthetic performance of a grassland ecosystem responded to environmental constraints, but alterations in photosynthetic processes appeared to exhibit a negligible influence on ecosystem CO_2 fluxes.

2.1 Introduction

Continuous exposure to environmental constraints can negatively affect plant growth and cause yield loss in agricultural crop plants. In particular, environment affects photosynthesis. Photosynthesis and the photosynthetic apparatus can be respectively altered and potentially damaged by elevated air temperatures, high light levels, and drought (Bussotti et al. 2007b, Bertolde et al. 2012, Goh et al. 2012, Ashraf and Harris 2013). Plants, however, can proceed to photosynthetic adjustments in order to acclimatize under stressful conditions and alleviate the detrimental impacts on the photosynthetic apparatus. For instance, under high light, plants promote the dissipation of excess energy within the light harvesting complex to decrease photosystem II (PSII) excitation (Jahns and Holzwarth 2012, Goh et al. 2012). Plants can also protect PSII by adjusting the electron transport rate within the PSII reaction centre (RC) or passing electrons to alternative electron acceptors (Derks et al. 2015). Cyclic electron flow around photosystem I (PSI) is also triggered to alleviate photoinhibition, as it contributes to the generation of an acidic lumen, which promotes energy dissipation via heat through the xanthophyll cycle (Takahashi et al. 2009). Oxidative stress also results from an imbalance between dark and light-phases of photosynthesis under stressful environmental conditions. In such cases, ATP and NADPH accumulate, but are not converted to ADP and $NADP^+$ to feed the primary reactions (e.g., light phase). Photorespiration, by using ATP and NADPH energy, enables acceptor regeneration for photosynthetic primary reactions and prevents reactive oxygen species (ROS) production (Voss et al. 2013).

Perturbation of photosynthetic processes can impact plant photosynthetic performance, which is defined here as the efficiency in which a photon can be absorbed and used to produce chemical energy. Chlorophyll *a* fluorescence (ChlF) analysis was employed in several studies to investigate the physiological aspects of photosynthesis and characterize plant photosynthetic performance (Murchie and Lawson 2013, Guidi and Calatayud 2014). Measure of the fast fluorescent transient (i.e., the OJIP curve) of dark-adapted leaves using a plant efficiency analyser gives information on the 'potential' plant photosynthetic performance, whereas a pulse-amplitude modulated fluorimeter provides measures of the actual plant photosynthetic efficiency (Kalaji et al. 2017). Analysis of the OJIP curve analysis derived from a plant efficiency analyser fluorimeter provides useful information related to the photosynthetic apparatus status and functioning (Maxwell and Johnson 2000). Studies reported ChlF transient analysis us-

ing the JIP-test a very useful tool to investigate the photosynthetic apparatus response and adaptive ability to a wide range of stressors (Bussotti et al. 2007b, 2010, Redillas et al. 2011, Brestic et al. 2012). Its utilisation in ecological studies also demonstrated its relevance in assessing different taxa for photosynthetic properties and characterising taxon adaptive photosynthetic strategies (Pollastrini et al. 2016a). The JIP-test applies energy fluxes in biomembrane theory to calculate several phenomenological and biophysical parameters that characterize PSII behaviour and therefore photosynthetic performance (Strasser et al. 2000). PSI activity was later described using new parameters (Tsimilli-Michael and Strasser 2008, Smit et al. 2009), which enabled the study of energy fluxes from the plastoquinone pool to the PSI acceptor side. Many studies have contributed to increase the empirical knowledge on the possible association between the shape of the fluorescence transient and the physiological status of the studied sample (Kalaji et al. 2016).

The relationship between the fast fluorescent transient and gas exchange, however, is not straightforward and is still largely debated (Kalaji et al. 2017). Whereas reduced PSII efficiency was sometimes associated with decreased carbon assimilation (van Heerden et al. 2003, Bertolde et al. 2012); and a reduction in net photosynthesis was typically related to stomatal limitations (Bollig and Feller 2014) and inactivation of the rubisco enzyme (Feller 2016). Indeed, a decline in photosynthetic activity can be observed during moderate heat stress without impairment of the PSII (Štroch et al. 2010, Pettigrew 2016) as the entire photosynthetic process is affected at lower temperature than its PSII component alone (Janka et al. 2013). Furthermore, Lee et al. (1999) reported PSII complexes were sometimes observed in excess in leaves and the photosynthetic apparatus is able to suffer considerable damages before a reduction in net photosynthesis occurs. Despite these observations, different photosynthetic responses among species under equal environmental constraints were reported, likely from variable abilities to efficiently use photon energy under stressful conditions (Gravano et al. 2004, Jedmowski et al. 2014, Kataria and Guruprasad 2015). Differences in photosynthetic component sensitivity to abiotic stress (Oukarroum et al. 2016) also explained varied photosynthetic response to environmental constraints. As a consequence, plants living under different climatic conditions expressed variation in their photosynthetic performance and sensitivity to environmental factors due to local adaptation (Ciccarelli et al. 2016, Pollastrini et al. 2016a,b). This emphasises the impor-

tance to better characterize the photosynthetic functionality of different ecosystems in varied climatic conditions to circumvent climate change impacts on photosynthesis.

Here, we addressed the following questions: (i) do different species and/or taxonomic groups display different response mechanisms; and (ii) do variations in the photosynthetic performance in a grassland ecosystem affect CO_2 fluxes at the ecosystem level. In a previous study, we detected important seasonal variation in the photosynthetic performance of the perennial ryegrass (*Lolium perenne* L.) in a temperate grassland due to the influence of combined environmental constraints (Digrado et al. 2017). However, we did not compare L. perenne response to those of other grassland species neither analyse if variations in photosynthetic performance were associated with changes in carbon assimilation by the ecosystem. Indeed, it is likely that grassland species differing in various anatomic aspect (leaf shape, root system, ...) might express contrasted photosynthetic responses. In such case, it is reasonable to assume that the photosynthetic performance at the ecosystem level must be influenced by its different components (i.e., photosynthetic response at leaf scale for the different species). Based on the current literature, we hypothesize that different species may be characterized by a different photosynthetic performance response explained either by a different acclimatization strategy, stress perception or metabolic response. We also hypothesize that increase in energy dissipation mechanisms at the ecosystem level may be associated with a decrease or a plateau in carbon assimilation as proportionally less photon energy is used for photochemistry. To test our hypothesis, we measured over two growing seasons in field by ChlF the photosynthetic performance response of *L. perenne* and two other important grassland species. ChlF parameters derived from the JIP-test were used to determine which mechanisms triggered the photosynthetic apparatus under stressful environmental conditions and if they differed among species. We also estimated ecosystem level photosynthetic performance by extrapolating leaf-scale measurements and addressed whether an alteration in ecosystem photosynthetic performance affected ecosystem CO_2 fluxes measured using the eddy covariance technique.

2.2 Material and methods

2.2.1 Field site

The study was conducted within the CROSTVOC project (CROp STress Volatile Organic Compounds: http://hdl.handle.net/2268/178952) framework. All measurements were performed at the Dorinne Terrestrial Observatory in Belgium (50°18'44" N 4°58'07" E). The climate at the site is temperate oceanic. The study area supports permanent grassland, which covers 4.22 ha, and the relief is dominated by a large colluvial depression oriented south-west/north-east. The depression lies on a loamy plateau with a calcareous and/or clay substrate. Altitudes range from 240 m (north-east) to 272 m (south). The paddock was converted to permanent grassland at least 50 years before the start of this study and was intensively grazed by cattle, with the application of cattle slurry and manure. Botanical diversity was evaluated on 24 quadrats (0.5 X 0.5 m) during the months of September 2010 and June 2011. Plant communities were composed of thirteen grass species (*Agrostis stolonifera* L., *Alopecurus geniculatus* L., *Bromus hordeaceus* L., *Cynosurus cristatus* L., *Dactylis glomerata* L., *Elymus repens* (L.) Gould, *Festuca pratensis* Huds., *Holcus lanatus* L., *Lolium multiflorum* Lam., *L. perenne*, *Poa annua* L., *Poa pratensis* L. and *Poa trivialis* L.), one N-fixing dicot (*Trifolium repens* L.), and seven non-N-fixing dicots (*Capsella bursa-pastoris* (L.) Medik., *Carduus* sp. L., *Matricaria discoidea* DC., *Plantago major* L., *Ranunculus repens* L., *Stellaria media* (L.) Vill., *Taraxacum* sp.). The dominant species were *L. perenne*, *Taraxacum* sp. and *T. repens*.

2.2.2 Micro-meteorological data

Grassland micro-meteorological data, including photosynthetic photon flux density (PPFD) (SKP215, Skye Instruments, Llandrindod Wells, UK), air temperature (T_{air}), air relative humidity (RH) (RHT2nl, Delta-T Devices Ltd, Burwell, Cambridge, UK) at 2.62 m above soil level, soil moisture (SM) (CS616, Campbell Scientific Inc., Logan, UT, USA), and soil temperature (T_{soil}) (PT 1000, Campbell Scientific Inc., Logan, UT, USA) at 2 cm depth were recorded every 30 min throughout the measurement period. Vapor pressure deficit (VPD) was calculated from T_{air} and RH measurements.

2.2.3 CO_2 flux measurements

CO_2 flux measurements and computation procedures were performed as described by Gourlez de la Motte et al. (2016). High frequency flux losses were corrected following Mamadou et al. (2016). CO_2 flux measures were conducted using the eddy covariance technique and a three-dimensional sonic anemometer (CSAT3, Campbell Scientific Ltd, UK) coupled with a fast CO_2-H_2O non-dispersive infrared gas analyser (IRGA) (LI-7000, LI-COR Inc., Lincoln, NE, USA) to measure CO_2 fluxes. Air was drawn into the IRGA through a tube (6.4 m long; inner diameter 4 mm) by a pump (NO22 AN18, KNF Neuberger, D) with a 12 l min^{-1} flow at a height of 2.6 m above ground. Data were sampled at a rate of 10 Hz. Zero and span calibrations were performed for CO_2 approximately once per month. Pure nitrogen (Alphagaz 1, Air Liquide, Liege, Belgium) was used for the zero and 350 μmol CO_2 mol^{-1} mixture (Chrystal mixture, Air Liquide, Liege, Belgium) for the span. Net ecosystem CO_2 exchange (NEE) from half-hourly eddy covariance measurements was partitioned into gross primary production (GPP) and total ecosystem respiration (R_{eco}) according to the method described by Reichstein et al. (2005).

The GPP response to photosynthetic photon flux density (PPFD) for days where ChlF measurements were performed was fit by a Mitscherlich equation (Dagnelie 2013) where the quantum light efficiency α (i.e., the initial slope of the curve) and GPPmax (i.e., the asymptotic value of GPP for PPFD $\rightarrow \infty$) were deduced using R software version 3.3.0 (R Development Core Team, 2012). Only measurements with PPFD values above 50 μmol m^{-2} s^{-1} were applied during the procedure. The equation was as follows:

$$GPP(PPFD) = GPP_{\max} \times \left[1 - \exp^{\left(-\frac{\alpha \times PPFD}{GPP_{\max}}\right)}\right] \quad (2.1)$$

This equation was used to calculate GPP_{1500} (i.e., GPP at PPFD = 1500 μmol m^{-2} s^{-1}) to estimate GPP at light saturation. This parameter was used in this study rather than GPP_{max} because the latter can lead to GPP overestimation at light saturation. Conclusions of this study were not dependent on this choice, as similar results were obtained applying both parameters. The response of R_{eco} to T_{soil} for days when ChlF measurements were conducted was fit based on the Lloyd and Taylor (1994) equation

where the activation energy E_0 (i.e., respiration sensitivity to temperature) and R_{10} (i.e., dark respiration normalized at 10°C) were deduced from R software version 3.3.0. The equation was as follows:

$$R_{\text{eco}}(T_{\text{soil}}) = R_{10} \times \exp\left[E_0 \times \left(\frac{1}{T_{\text{ref}} + 46.02} - \frac{1}{T_{\text{soil}} + 46.02}\right)\right] \quad (2.2)$$

The reference temperature (T_{ref}) was set at 10°C.

However, because respiratory activity is extrapolated from night measurements, CO_2 fluxes estimated at day may have been biased because of several mechanisms related to plant physiology that were not taken into account in this method. The omission of the inhibition of plant mitochondrial respiration by light (Atkin et al. 1997), for instance, may have led to an overestimation of R_{eco} at day (Heskel et al. 2013, Wehr et al. 2016). In contrast, the omission of photorespiratory activity may have led to an underestimation of R_{eco} (Wohlfahrt and Gu 2015), especially during hot days when photorespiration is high due to the increasing specificity of Rubisco with O_2 at high temperature (Sage 2013). This have consequences on GPP estimation since it is derived from NEE and R_{eco}. These issues are well known by the eddy covariance researcher community and it is difficult to quantify the contribution of each potential biases in our measurements. By using an adapted 'big-leaf photosynthesis model', a study was able to assess the bias in CO_2 fluxes measured by eddy covariance in response to light (Wohlfahrt and Gu 2015). They showed that Reco was overestimated at low light (ca. <800 μmol m^{-2} s^{-1}) because the mitochondrial inhibition bias overweighed photorespiration in these conditions. In contrast, R_{eco} was underestimated at high light (ca. >800 μmol m^{-2} s^{-1}) because photorespiration became stronger. They also showed that, over a daily cycle, GPP was more representative of the 'true photosynthesis' (i.e., gross photosynthesis, carboxylation) rather than the 'apparent photosynthesis' (i.e., true photosynthesis minus photorespiration) and only overestimated 'true photosynthesis' by 3% on average. This was acknowledged in the interpretations of our results.

2.2.4 Analysis of the fluorescence transient using the JIP test

Grassland ChlF emission measures were conducted on *L. perenne*, *Taraxacum* sp., and *T. repens* at three plots (each 30 X 5 m) from June to October 2014 and May to Oc-

tober 2015, using a HandyPEA fluorimeter (Hansatech Instruments, Pentney, Norfolk, UK). Cows were allowed to graze between measurement periods. Measurements were performed in each monitored plot 4x day^{-1} at 11:00, 13:00, 15:00, and 17:00 h (local time zone). The number of replicates for each plot and time period was seven in 2014 and eight in 2015. Measurements were performed on non-senescent mature leaves. Prior to each measurement, leaves were dark-adapted with leaf clips for 30 min. The leaf clips applied to *L. perenne* were modified to fit the width of leaves by reducing the measurement surface by half using black vinyl electrical tape, following the manufacturer4s recommendations. The dark-acclimated leaf surfaces were then exposed to red light with a flux density of 3000 μmol m^{-2} s^{-1} for 1 s, which was provided with an array of three light-emitting diodes (peak wavelength at 650 nm). After irradiance of the sample, the induced subsequent fluorescence signals were recorded every 10 μs from 10 to 300 μs, then every 100 μs till 3 ms, then every 1 ms till 30 ms, then every 10 ms till 300 ms and finally every 100 ms till 1 s.

Fluorescence emissions measured at 50 μs (F_{50}, step O), 300 μs (F_{300}, step K), 2 ms (step J), 30 ms (step I), and maximal (F_M, step P) were used to characterize fluorescence emission dynamics and determine several parameters describing photosynthetic activity based on the JIP test (Strasser et al. 2000, 2004). Table 1 summarizes the ChlF parameters used in this study. When a ChlF parameter showed an aberrant value (i.e., infinite), all parameters derived from this specific measurement were discarded. This represented < 0.16% of the dataset.

2.2.5 Statistical analyses

Three groups of comparable meteorological conditions were defined by clustering (Ward's method based on the Euclidian distance). Clustering was performed on the coordinates of the two first principal components of a principal component analysis (PCA). All meteorological parameters (PPFD, T_{air}, VPD, SM, RH and T_{soil}) were entered as variables in the PCA. The influence of monitored plots on ChlF response was examined using a General Linear Model (GLM) type III. The assigned cluster number previously identified for each time period of measurement were used as a meteorological factor in the GLM analysis. The monitored plots were used in the GLM as a block factor and was considered as random factor. Plot influence was not found significant; therefore ChlF parameter values were averaged for the three species without consideration of the different plots.

Ecosystem photosynthetic performance was approximated from measurements performed on the three dominant grassland species. In order to achieve this, ChlF parameters from the three species were weighed based on the relative abundance of their respective group (i.e., grass, N-fixing dicot, and non-N-fixing dicot) to extrapolate ChlF parameters for the entire pasture/grassland ecosystem. Relative abundance values from the last survey were used. Three groups of contrasting photosynthetic ecosystem performance based on ecosystem ChlF parameters were then defined using the same methodological approach employed in the meteorological groups. The three grassland species behaviour within groups was analysed. Ecosystem ChlF parameters (F_V/F_M, PI_{ABS}, Ψ_{E0} and ΔV_{IP}) were entered as variables in this second PCA followed by clustering, with the exception of the raw fluorescence values F_{50} and F_M which were used to calculate ChlF parameters. The behaviour of the three grassland species within these groups was analysed. A type III GLM and Tukey's Honest Significant Difference test (Tukey HSD) were used to classify mean ChlF parameter values at species and ecosystem levels, meteorological mean parameter values and CO_2 fluxes among ChlF clusters. Prior to statistical analyses, a correction factor based on the reduction ratio surface measurements of *L. perenne* leaf clips was applied to F_{50} and F_M values to enable the monocot comparisons with those measured on dicot species. ChlF parameters (except for PIABS due to the presence of negative values) and CO_2 fluxes were square root-transformed for type III GLM analyses to improve normality and homogeneity of variances. Photosynthetic processes influence on daily variation in ecosystem respiration and grassland capacity to fix carbon at light saturation were tested by simple linear regressions between the daily amplitude variability in ecosystem ChlF parameters and R_{10} and GPP_{1500}.

Relationships among ChlF-based photosynthetic responses, meteorological conditions, and CO_2 fluxes were explored using Canonical Correlation Analysis (CCA). This multivariate statistical test serves to identify linear combinations among random variables between two datasets (e.g., ChlF and meteorological data) in order to maximize their correlation. The two new sets of canonical variates, constructed based on the original datasets, determine a pair of canonical variates with a maximized simple correlation. Each set of constructed canonical variates has a variance = 1 and are uncorrelated with other constructed variates. The correlation relevance between the two groups of datasets is tested by the significance of the correlation between the pairs of canonical variates. Significance in at least one canonical pair means the two analysed

datasets are not independent and enable the associations among the different variables. Compared with the Pearson correlation test, CCA explores interdependence within a set of variables. Approach of the canonical correlation is very similar to PCA as axis are a linear combination of data. However, in contrast to PCA where linear combination maximizes the variance on the first axis, CCA maximizes the correlation between two datasets. Three CCA analysis were performed by combining ChlF and meteorological data; meteorological and CO2 fluxes data; and ChlF and CO2 fluxes data.

All analyses were performed using the software Minitab version 17.1.0 (State College, Pennsylvania, USA) and R software version 3.3.0 with the following R package: 'FactoMineR' (Husson et al. 2016), 'Vegan' (Oksanen et al. 2012), 'CCP' (Menzel 2015), 'Car' (Fox et al. 2016), and 'Relaimpo' (Groemping and Matthias 2013).

2.3 Results

2.3.1 Environmental conditions

The highest solar irradiance values were detected during summer (i.e., May to August) for both years, with midday PPFD values above 1500 μmol m^{-2} s^{-1} (Fig. 2.1A). This period was also characterized by the highest midday T_{air} and VPD values, which exceeded 30°C and 2.0 kPa, respectively (Fig. 1B,D). Autumn (i.e., September to October) was characterized by PPFD, T_{air}, and VPD values below 1500 μmol m^{-2} s^{-1}, 25°C and 1 kPa, respectively for most ChlF measurement days. Three specific meteorological events were observed in the grassland during the second year of the study. A heat wave from 30 June to 5 July 2015 (Fig. 2.1A) characterized by six consecutive days with maximum T_{air} between 28.9°C and 34°C, and two dry spells with 20% SM during the months of June and July 2015 (Fig. 2.1C).

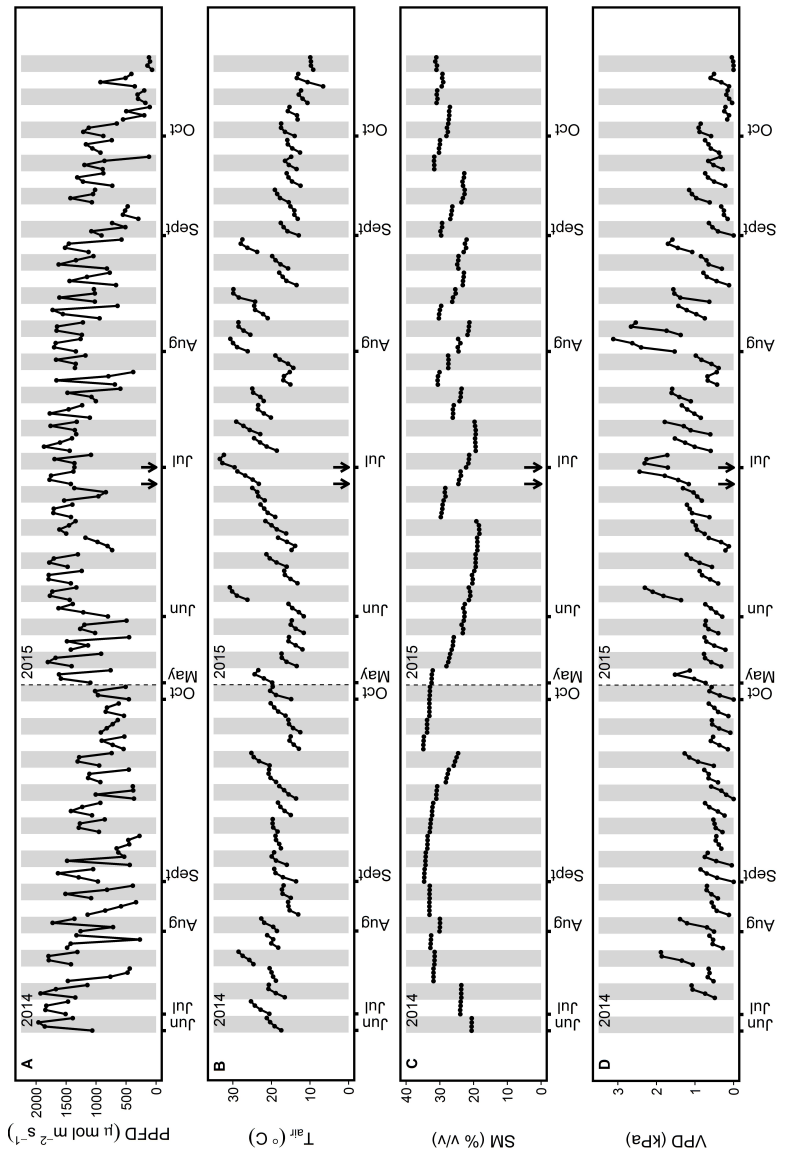

Figure 2.1 – Environmental conditions encountered during chlorophyll fluorescence measurements in the 2014 and 2015 study periods. Values at 11, 13, 15 and 17 h for each day of chlorophyll fluorescence measurements are represented for (A) PPFD, photosynthetic photon flux density; (B) T_{air}, air temperature; (C) SM, soil moisture at a depth of 5 cm; (D) VPD, vapor pressure deficit. Grey bars separate the different days of measurements. The arrows indicate the first and third day of the heat wave.

2.3.2 *Grassland ChlF parameters dynamics and influence of environmental conditions*

Grassland ChlF parameters exhibited diurnal variation and showed a pattern consistent with PPFD (Figures 2.1A,2.2). Indeed, while other environmental parameters such as T_{air} and VDP were still high at the end of the day, ChlF parameters usually went back to a value similar to that of the first measurement performed, following the diurnal pattern of PPFD. Variation in ChlF parameters for the three grassland species was highest in summer, where the greatest diurnal decreases were measured around midday, when high PPFD values were measured with high T_{air} and VPD. During the midday period, frequent declines in absorbed photon energy use efficiency, expressed as a strong decrease in maximum quantum yield of primary photochemistry (F_V/F_M) and performance index (PI_{ABS}) were observed for the three grassland species. These declines were characterized by decreased F_V/F_M and PI_{ABS} values as low as 0.12 and < 0.01, respectively. In contrast, a stable F_V/F_M value of ≈0.76 was measured in autumn for the three grassland species, indicating high PSII performance during this period. During the summer sampling period, decreased F_V/F_M was accompanied by strong midday increased energy flux reduction in end electron acceptors (ΔV_{IP}) for the three grassland species measured (Fig. 2.2E). More stable ΔV_{IP} values of 0.31 were observed in autumn. Reduced variation in electron transport efficiency beyond Q_A^- (Ψ_{E0}) (Fig. 2.2B) was observed, with stable values of ≈0.53 for Ψ_{E0}. Changes in Ψ_{E0} were only observed during episodes with high increased ΔV_{IP}. During these episodes, the three grassland species presented the following Ψ_{E0} response: strong augmentation in Ψ_{E0} were observed in *Taraxacum* sp. and *T. repens*, whereas *L. perenne* showed reduced variation or even decreased Ψ_{E0}.

Three groups of contrasted ecosystem photosynthetic performance were determined by PCA-clustering (Table 2.1). The first group (C1) was characterized by increased capacity to employ photon energy, illustrated by high F_V/F_M and PI_{ABS} values for the ecosystem and the three grassland species. C1 cluster response was characterized as dominant in autumn and as it was detected in 171 observed time periods (Fig. 2.2A). *L. perenne* and *Taraxacum* sp. exhibited the highest PI_{ABS} values in the C1 group. In contrast, the third group (C3) was characterized by the lowest F_V/F_M and PI_{ABS} values for the grassland ecosystem and the three species, demonstrating low photosynthetic performance. The photosynthetic response characterized by this group was detected in 11 observed time periods and the responses were only detected

in summer, particularly at midday (Fig. 2.2A). *Taraxacum* sp. presented the highest F_V/F_M values in this group, whereas the lowest values were observed in *T. repens*. The second group (C2) showed intermediate F_V/F_M and PI_{ABS} values, where *Taraxacum* sp. exhibited the highest F_V/F_M values in C2. Photosynthetic response characterized by this cluster was observed throughout the season in 54 observed time periods (Fig. 2.2A). These results indicated the grassland ecosystem was more efficient in photon energy use for photochemistry in autumn. Increased initial fluorescence (F_{50}) and decreased maximum fluorescence yield (F_M) were responsible for decreased F_V/F_M in clusters C2 and C3 (Table 2.1). Only moderate Ψ_{E0} changes were observed in the three species between the C1 and C2 clusters. However, results indicated differences in electron transport efficiency between dicot and monocot species beyond Q_A in the C3 cluster. Indeed, dicot species exhibited either a stable (non-significant Ψ_{E0} increase for *Taraxacum* sp. even though high values were recorded in July 2014 and July 2015) or an increased value (+86% Ψ_{E0} increase for *T. repens*) of Ψ_{E0} whereas a decrease in Ψ_{E0} was observed for *L. perenne* (-19%). F_V/F_M and PI_{ABS} decreased values were accompanied by increases in ΔV_{IP} for dicot species in clusters C2 and C3. *L. perenne*, however, did not exhibit a significant change in ΔV_{IP} between the cluster C2 and C3 despite changes in environmental conditions (Table 2.1). The photosynthetic ecosystem response based on ChlF parameters was similar to *L. perenne* as the contribution of grass species to the ecosystem response was estimated at 88.6%.

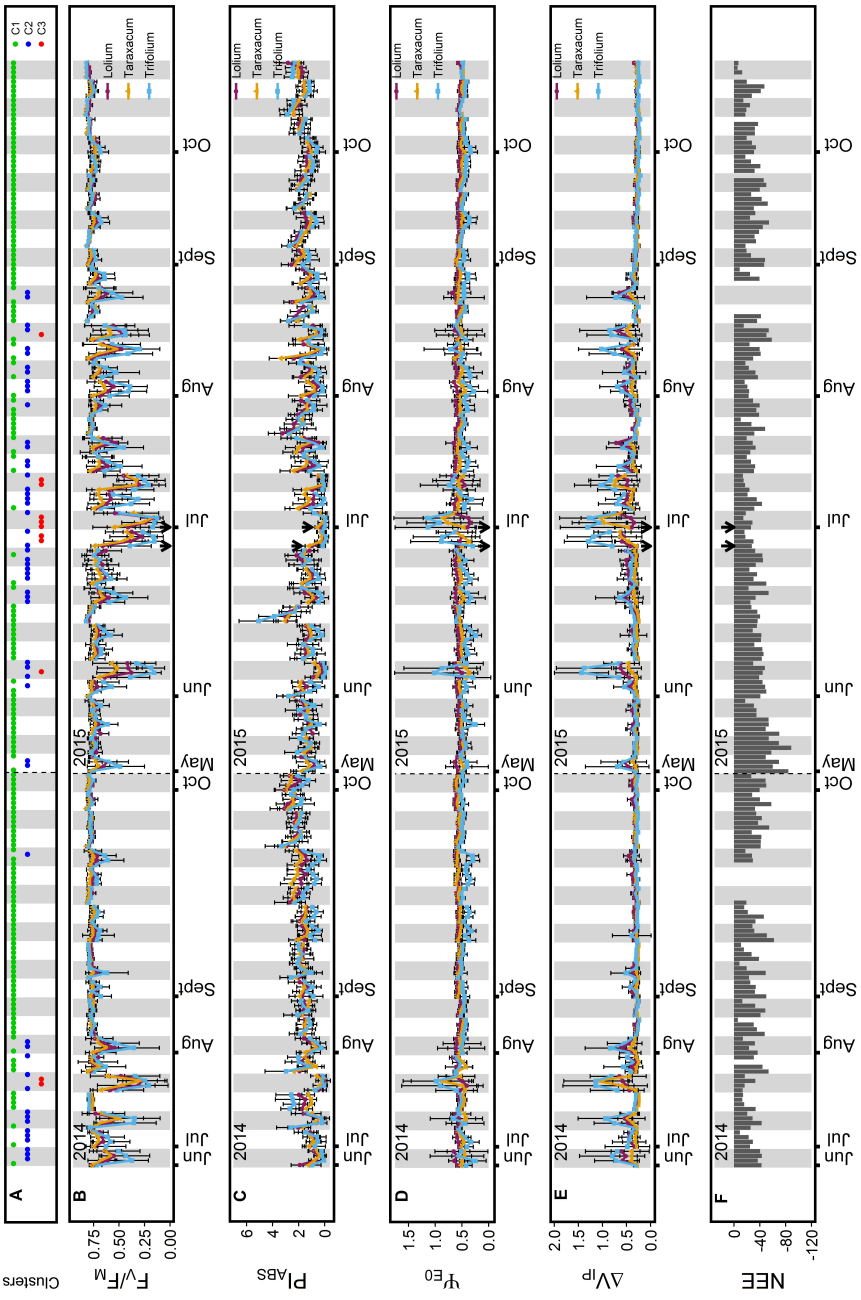

Figure 2.2 – (Continued on the following page.)

Figure 2.2 – Evolution of ChlF parameters (F_V/F_M, PI_{ABS}, Ψ_{E0} and ΔV_{IP}) for the three grassland species and net CO_2 exchange ecosystem (NEE, μmol CO_2 m^{-2} s^{-1}) during the two measurement campaign in the grassland. For each measured day, the ChlF parameter average value (n = 21 or 24) $\pm$ SD for each of the four measurement time periods (11:00, 13:00, 15:00, and 17:00 h) is represented for the three grassland species (purple, *L. perenne*; orange, *Taraxacum* sp.; light blue, *T. repens*). The top plot indicates the ChlF cluster (green, C1; dark blue, C2; red, C3) the group has been assigned during each time period by the Principal Component Analysis (PCA)-clustering. Grey bars separate the different days of measurements. The arrows indicate the first and third day of a heat wave.

CCA analysis revealed significant correlations between environmental factors and the photosynthetic performance of the studied grassland species and the ecosystem; correlation for the first and the second canonical pairs equaled to 88.6% ($p \leq 0.001$) and 60.5% ($p \leq 0.001$) respectively (Fig. 2.3A). ChlF parameters F_V/F_M, PI_{ABS}, and ΔV_{IP} showed similar relationships with environmental parameters for the three species. Decreased F_V/F_M and PI_{ABS} was associated with increased PPFD, VPD, T_{air}, and T_{soil}, and decreased RH and SM. These results suggested a decline in photosynthetic performance under these conditions, typically observed in summer, especially at midday. Compared with F_V/F_M and PI_{ABS}, ΔV_{IP} exhibited an opposite relationship with environmental parameters. The parameter representative of electron transport efficiency beyond Q_A, Ψ_{E0} was least influenced by meteorological parameters, particularly for *L. perenne*. SM exhibited the lowest influence on ChlF parameters. ChlF parameters which described the ecosystem photosynthetic performance exhibited a similar relationship with meteorological parameters than ChlF parameters describing *L. perenne* response.

2.3.3 Influence of environmental conditions and ChlF-based photosynthetic parameters on CO_2 fluxes

Significant correlations between environmental factors and CO_2 fluxes, with correlations for the first and the second canonical pairs equal to 78.8% ($p \leq 0.001$) and 54.7% ($p \leq 0.001$) respectively, were shown by the CCA (Fig. 2.3B). Elevated R_{eco} and GPP fluxes were associated with high PPFD, T_{air}, T_{soil}, and VPD, but low RH and SM values. R_{eco} was primarily correlated with temperature and VPD, whereas GPP was

mainly correlated with PPFD, suggesting an augmentation of photosynthetic activity with increased light energy availability.

The same approach was used to determine the influence of ecosystem photosynthetic performance on CO_2 fluxes (Fig. 2.3C). The correlation for the first canonical pair was 72.4% ($p \leq 0.001$) while the correlation for the second canonical pair was not significant (P = 0.155). The relationship between ChlF parameters and CO_2 fluxes was therefore defined by the correlation of variables on the first canonical pair. High CO_2 flux values were associated with high ΔV_{IP} values and low F_V/F_M and PI_{ABS} values. This was particularly noted in R_{eco}, where GPP was mainly represented on the second canonical axis and poorly correlated with ChlF parameter variation. The ChlF parameter Ψ_{E0} was least related with CO_2 flux changes, as it was poorly represented on the first canonical axis.

Linear regression detected the absence of significant relationships between variation in ChlF parameters with GPP_{1500} and R_{10} (Fig. 2.4), suggesting the influence of changes in photosynthetic processes were negligible. Average NEE decreased in absolute value with decreased ecosystem photosynthetic performance (Fig. 2.5A). However, reduction in net CO_2 uptake by the grassland was not significant. Ecosystem respiration exhibited an opposite trend and increased with decreased ecosystem photosynthetic performance (Fig. 2.5D), probably due to its strong correlation with temperature (Fig. 2.3B). Stable R_{10} values detected in the three photosynthetic performance clusters (Fig. 2.5E) supported this hypothesis. The lowest GPP values were observed during periods of high photosynthetic performance, while the highest GPP values were observed at lower ecosystem photosynthetic performance (i.e., C2 and C3 clusters) (Fig. 2.5B). Difference in GPP between the C2 and C3 ChlF clusters was not significant, despite reduced potential performance of photosynthesis in the C3 cluster. The three photosynthetic performance clusters showed the absence of differences in GPP_{1500} values (Fig. 2.5C), indicating GPP_{1500} was not affected by ecosystem photosynthetic performance.

2.4 Discussion

2.4.1 *Combined abiotic stresses in summer led to a decline in PSII photosynthetic performance.*

The three grassland species examined showed strong decreases in photosynthetic performance in summer (Fig. 2.2), when environmental constraints were combined (Fig. 2.1). Important F_V/F_M decreases in summer were reported in various ecosystems (Fernández-Baco et al. 1998, Bussotti 2004, Ciccarelli et al. 2016) and primarily attributed to an excess in solar radiation. A relationship between F_V/F_M and PPFD was confirmed in our study by a similar diurnal evolution and strong correlation between the parameters (Fig. 2.3A). Werner et al. (2001, 2002) interpreted the reduction in PSII photochemical efficiency as a protective mechanism, serving to preserve PSII by dissipating excess light energy as heat. The associated increase in F_{50} also suggests the dissociation of the antenna complex from the PSII which might contribute to the reduction of the transfer of excess energy to the RC (Mathur and Jajoo 2015). Such reorganisation within the thylakoid membrane has been observed in *Arabidopsis thaliana* (ecotype Col-0) after long-term acclimatization to high light and was characterized by the detachment of the moderately bound LHCII trimer from the PSII supercomplexes (Bielczynski et al. 2016). It is also possible that a (zeaxanthin-antheraxanthin)-dependent sustained non-photochemical quenching was operating during sunny days and contributed to the reduction of F_V/F_M. In such situation, some components of the non-photochemical quenching can still operate after dark-adaptation and lead to the measurement of not fully unquenched F_M values (i.e., not fully relaxed in darkness) (Adams and Demmig-Adams 2004). However, such sustained energy dissipation mechanism is usually observed at low temperature while warm condition (such as observed at midday) was observed to efficiently relax this photoprotection process (Demmig-Adams and Adams 2006).

Table 2.1 – (Continued on the following page.)

			Average in the different clusters and associated relative change				
			C1	C2	Δ%	C3	Δ%
Species PP	Lolium	F_V/F_M	0.755^{a}	0.610^{c}	−19	0.307^{f}	−57
		PI_{ABS}	1.807^{a}	0.894^{c}	−51	0.150^{d}	−92
		Ψ_{E0}	0.565^{c}	0.608^{b}	+8	0.458^{ef}	−19
		ΔV_{IP}	0.324^{e}	0.516^{c}	+59	0.497^{c}	+54
		F_{50}	459^{f}	558^{d}	+21	791^{b}	+72
		F_M	1895^{b}	1530^{d}	−19	1192^{e}	−37
	Taraxacum	F_V/F_M	0.768^{a}	0.662^{b}	−14	0.398^{e}	−48
		PI_{ABS}	1.736^{a}	0.662^{b}	−39	0.269^{d}	−85
		Ψ_{E0}	0.531^{d}	0.520^{de}	−2	0.568^{bcd}	+7
		ΔV_{IP}	0.294^{f}	0.384^{d}	+31	0.687^{b}	+134
		F_{50}	519^{e}	607^{c}	+17	856^{b}	+65
		F_M	2262^{a}	1940^{b}	−14	1517^{d}	−33
	Trifolium	F_V/F_M	0.746^{a}	0.503^{d}	−33	0.206^{g}	−72
		PI_{ABS}	1.592^{b}	0.541^{d}	−66	0.072^{d}	−95
		Ψ_{E0}	0.470^{f}	0.472^{f}	0	0.618^{a}	+89
		ΔV_{IP}	0.312^{ef}	0.618^{b}	+98	1.139^{a}	+264
		F_{50}	566^{d}	821^{b}	+45	1178^{a}	+108
		F_M	2277^{a}	1805^{c}	−21	1500^{d}	−34
Ecosystem PP		F_V/F_M	0.755^{a}	0.607^{b}	−20	0.320^{c}	−58
		PI_{ABS}	1.791^{a}	0.884^{b}	−51	0.153^{c}	−91
		Ψ_{E0}	0.558^{b}	0.595^{a}	+7	0.489^{c}	−12
		ΔV_{IP}	0.322^{b}	0.514^{a}	+60	0.544^{a}	+62
		F_{50}	469^{c}	575^{d}	+23	816^{a}	+74
		F_M	1938^{a}	1568^{d}	−19	1228^{c}	−37
Meteo.		PPFD	917^{b}	1463^{a}	+59	1639^{a}	+79
		T_{air}	17.06^{c}	23.84^{b}	+40	28.27^{a}	+66
		VPD	0.59^{b}	1.34^{a}	+129	1.67^{a}	+185
		SM	28.37^{a}	25.07^{b}	−12	23.86^{b}	−16
		RH	72.57^{a}	57.22^{b}	−21	57.29^{b}	−21
		T_{soil}	14.69^{b}	18.71^{a}	+27	20.21^{a}	+38

Table 2.1 – Description of the three clusters of photosynthetic performance (PP) based on ChlF measurements (C1, C2, and C3) for each grassland species and the ecosystem, and the prevailing micrometeorological conditions. Mean values are represented for each cluster. The relative change ($\Delta\%$) in the mean with respect to cluster 1 is indicated for clusters 2 and 3. PPFD, photosynthetic photon flux density (μmol m^{-2} s^{-1}); T_{air}, air temperature (°C); VPD, vapour pressure deficit (kPa); SM, soil moisture at a depth of 5 cm (% v/v); RH, relative air humidity (%); T_{soil}, temperature of soil at a depth of 2 cm (°C). Different letters indicate significant differences among the clusters (Tukey HSD, α = 0.05) within species, ecosystem, or micrometeorological data

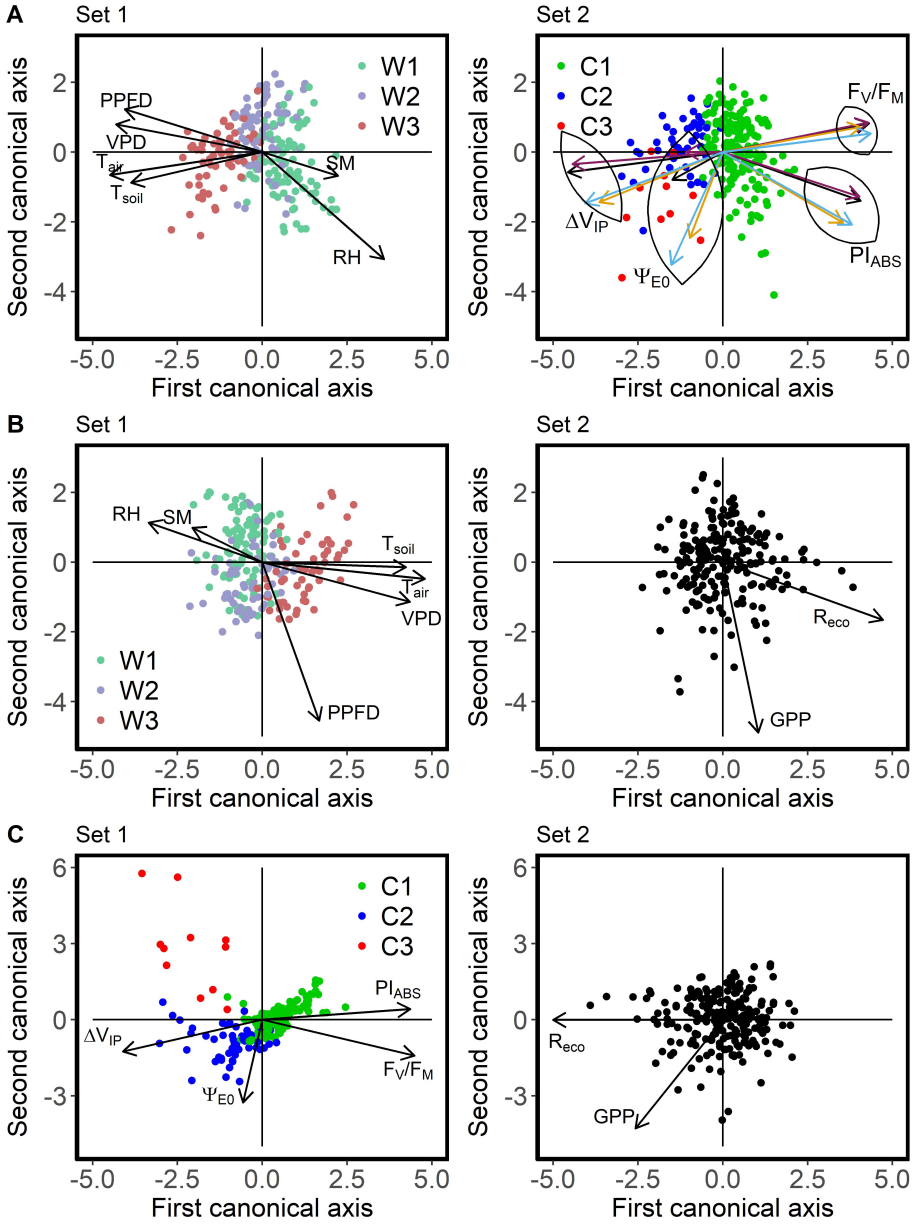

Figure 2.3 – (Continued on the following page.)

Figure 2.3 – Canonical Correlation Analysis (CCA) with variables performed by combining the (A) meteorological parameters and ChlF parameters (with distinction between purple, *L. perenne*; orange, *Taraxacum* sp.; blue, *T. repens*; black, ecosystem) data. This analysis establishes a multivariate relationship between parameters from the two datasets. Correlations between the first canonical axis of the two CCA plots and between the second canonical axis of the two CCA plots were 88.6% (Wilks' Lambda = 0.071, $F_{96,\,1173}$ = 7.26, $p \leq 0.001$) and 60.5% (Wilks' Lambda = 0.333, $F_{75,995}$ = 3.42, $p \leq 0.001$), respectively. The same approach was then used by combining (B) meteorological parameters and CO_2 flux data. Correlations between the first canonical axis of the two CCA plots and between the second canonical axis of the two CCA plots were 78.8% (Wilks' Lambda = 0.266, $F_{12,402}$ = 31.44, $p \leq 0.001$) and 54.7% (Wilks' Lambda = 0.701, $F_{5,\,202}$ = 17.26, $p \leq 0.001$), respectively. Finally, the same approach was used by combining (C) ecosystem ChlF parameters and CO_2 flux data. Correlations between the first canonical axis of the two CCA plot and between the second canonical axis of the two CCA plots were 72.4% (Wilks' Lambda = 0.468, $F_{8,422}$ = 24.4, $p \leq 0.001$) and 15.6% (Wilks' Lambda = 0.976, $F_{3,\,212}$ = 1.8, P = 0.155), respectively. Green, blue and red colors highlight ChlF response from the C1, C2 and C3 PCA clusters respectively. Light green, purple and brown colors highlight meteorological data from the W1, W2 and W3 PCA clusters respectively. PPFD, photosynthetic photon flux density (μmol m^{-2} s^{-1}); T_{air}, air temperature (°C); VPD, vapour pressure deficit (kPa); SM, soil moisture at a depth of 5 cm (% v/v); RH, relative air humidity (%); T_{soil}, temperature of soil at a depth of 2 cm (°C); Reco, respiration of the ecosystem (μmol CO_2 m^{-2} s^{-1}); GPP, gross primary productivity (μmol CO_2 m^{-2} s^{-1}).

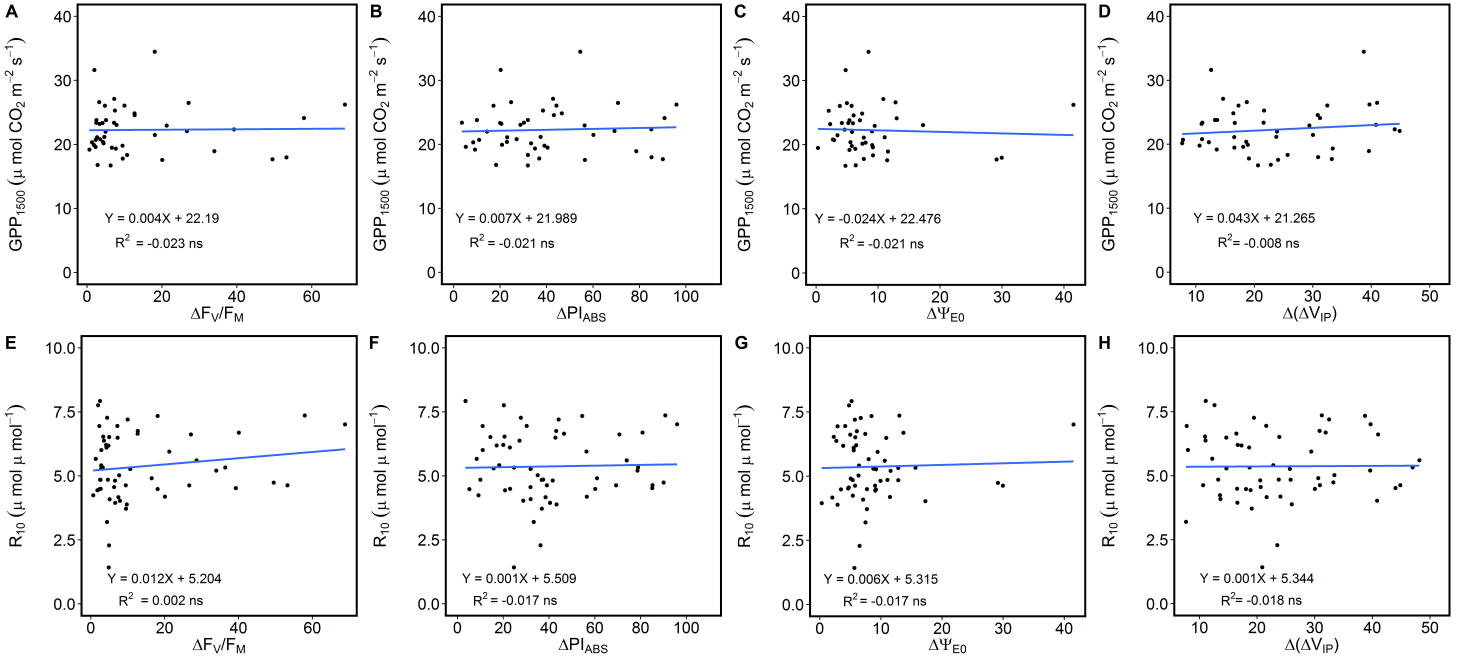

Figure 2.4 – Linear regression between (A) gross primary productivity at light saturation (GPP_{1500}) and the daily variation of ecosystem ChlF parameters (F_V/F_M, PI_{ABS}, Ψ_{E0} and ΔV_{IP}) and (B) dark respiration normalized at 10°C (R_{10}) and the daily variation of ecosystem ChlF parameters. Data were not root squared transformed for this test, but relationships were similar on transformed data and results are not dependent of this choice.

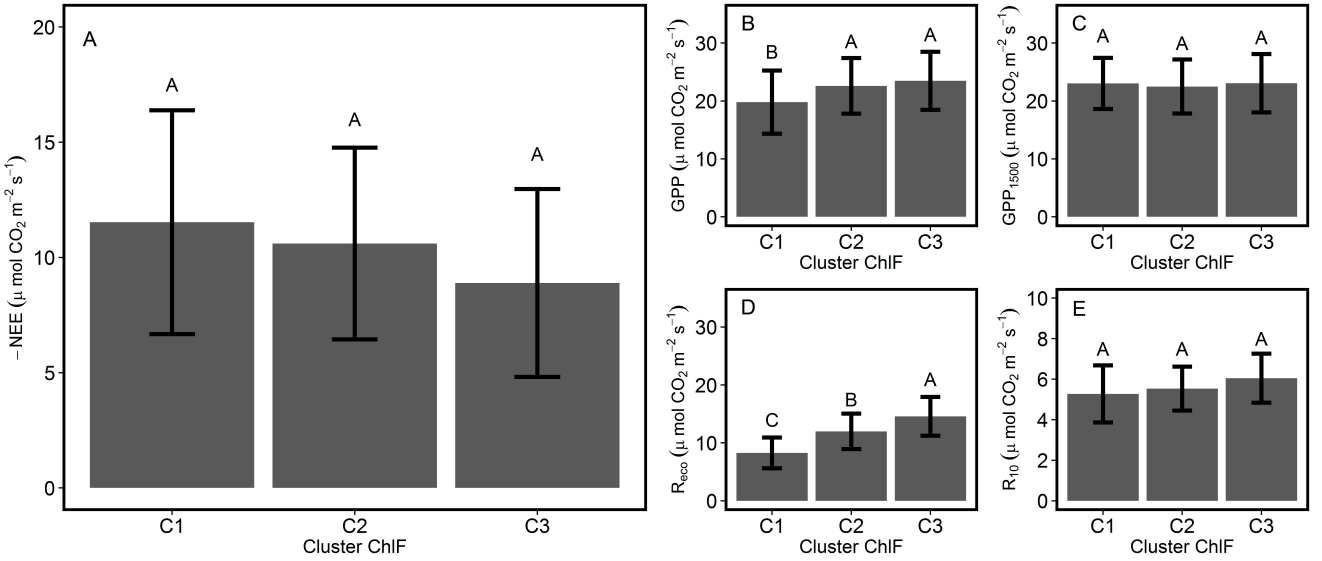

Figure 2.5 – Average CO_2 fluxes associated with the different ecosystem photosynthetic performance clusters. The average $\pm$ SD (A) NEE, net CO_2 exchange ecosystem; (B) GPP, gross primary productivity; (C) GPP_{1500}, GPP at light saturation (D) R_{eco}, respiration of the ecosystem and (E) R_{10}, dark respiration normalized at 10°C were compared for the different photosynthetic performance responses based on the ChlF clusters defined during the PCA-clustering analysis. Different letters indicate significant differences among the clusters (Tukey HSD, $\alpha = 0.05$).

High temperature can also lead to reversible conformational changes in some RC, which can no longer reduce Q_A. These 'silent RC' act as excitation energy traps, where the energy is subsequently dissipated (Strasser et al. 2004, Bussotti 2004). This reduction in the PSII donor side efficiency can lead to decreased F_M (Mathur et al. 2011b), which was observed in our study (Table 2.1). RC inactivation also caused F_V/F_M and RC/ABS reductions (data not shown), which exhibited strong diurnal decreases and were responsible for the low midday PI_{ABS} values in summer during hot sunny days (Fig. 2.2C). End of day increased PI_{ABS} along with reduced PPFD indicated PSII functionality was not irreversibly impaired, but rather down-regulated. PI_{ABS} reductions reaching 95% in the C3 cluster for the three grassland species (Table 2.1) suggest a high capacity to dissipate excess excitation energy within PSII under stressful environmental conditions.

The PSII is generally described as drought-resistant (Kalaji et al. 2016) although drought-induced damages to the PSII are observed in situation of severe drought stress (Goltsev et al. 2012) especially in sensitive variety (Ghotbi-Ravandi et al. 2014). It is difficult to assess the potential impact of the two dry spells periods observed in June and July 2015 on ChlF parameters because of the low amount of data and the implication of other environmental factors during this period, especially in July due to the heat wave. Regarding the June period, most of the ChlF measurements performed during this period belonged to the high photosynthetic performance cluster, which suggests a low/negligible impact of the relatively low soil moisture content on ChlF parameters. This is in accordance with the low influence of soil moisture observed on ChlF parameters (Fig. 2.3A). This does not exclude, however, the influence of soil moisture in combination with other environmental factors as low soil moisture was suggested to enhance PSII sensitivity to heat stress in cottonwood (Tozzi et al. 2013) and *L. perenne* at this site (Digrado et al. 2017).

2.4.2 Studied dicot species exhibited the highest capacity to increase PSI efficiency.

High midday ΔV_{IP} values measured in summer (Fig. 2.2E) suggested up-regulation of the photochemical pathway for de-excitation under stressful conditions (Pollastrini et al. 2011, Desotgiu et al. 2012a), particularly in dicot species (Table 2.1). Cascio et al. (2010) suggested rapid reduction of the end electron acceptor might play a role in protecting the photosynthetic structure by limiting formation of unmanaged electrons beyond the PSI acceptor side, which contributes to the formation of ROS in sunny

environments. Increased PSI efficiency was accompanied by increased electron flux efficiency beyond Q_A^- in the C3 cluster for dicots, especially in *T. repens* (Table 2.1). It is possible electron flow in the electron transport chain was stimulated by increased PSI efficiency. Interestingly, these changes in ΔV_{IP} and Ψ_{E0} in the C3 cluster were more related to an increase in air temperature than in light availability (Table 2.1) emphasizing the influence of temperature in these processes. This might suggest that PSI accepted almost all electrons as electron supply by the PSII was partly inhibited by high temperature (Brestic et al. 2012).

In contrast, *L. perenne* did not exhibit increased electron transport efficiency beyond PSI under stressful conditions and a decrease in Ψ_{E0} was observed (Table 2.1). This limitation in PSI efficiency could be attributed to PSI photoinhibition due to light-induced oxidation of the PSI iron-sulphur component commonly observed in condition of chilling temperature (Scheller and Haldrup 2005). However, it was shown in a recent study that such inactivation of PSI can be observed at high light and at room temperature (Tiwari et al. 2016). Inactivation of the PSI induced by light, however, would require a flux of electrons from the PSII higher than the PSI acceptor side could handle. Therefore, photoinhibition of PSI could be questioned in our case as a decrease in the efficiency of electron transport beyond Q_A was also observed. The decrease in Ψ_{E0} observed in our study can be interpreted as a mechanism to preserve PSI under imbalance between electrons leaving PSII and those reaching electron acceptors beyond PSI (Cascio et al. 2010, Bussotti et al. 2011). A high electron flux under sunny environments might lead to the formation of 'free electrons' if the availability of end electron acceptors is insufficient. The free electrons can subsequently activate oxygen and lead to hydrogen peroxide production (Asada 2006). Reduction in electron transport efficiency beyond Q_A might therefore contribute to the reduction of 'free electron' formation, and therefore, oxidative damage. Further experimentations such as the measurements of the actual electron flow through leaf gas exchange measurements and the monitoring of PSI RC oxidation by leaf transmission changes at the 820 nm wavelength band would be required to test and verify these hypotheses.

2.4.3 Decline in photosynthetic performance did not lead to a decrease in GPP.

GPP variation was well explained by environmental conditions, such as PPFD, compared with ecosystem photosynthetic performance (Fig. 2.3). Moreover, declined ecosystem photosynthetic performance did not result in reduced carbon uptakes (Fig.

2.5B). The absence of GPP decrease during episodes of high-energy dissipation can be explained by increased photons received during these periods. Stable GPP values in C2 and C3 clusters (Fig. 2.5B) also suggested the lack of stomatal limitations to carbon assimilation in the grassland during summer stress conditions.

The carbon amounts fixed by the ecosystem at light saturation were not affected by the ecosystem photosynthetic performance (Fig. 2.5C) or variation in the different photosynthetic processes (Fig. 2.4A). A close relationship between F_V/F_M and carbon uptake was found in studies on maize plants and fodder shrubs, particularly under severe stress, when non-stomatal components effected photosynthesis (Xu et al. 2008, Boughalleb et al. 2009). Our results suggested the absence of non-stomatal limitations during photosynthesis and high ecosystem tolerance to environmental stress during the study but for a particular period of time in which high VPD and T_{air} were recorded.

A previous study conducted at the Dorinne Terrestrial Observatory has shown that herbage height was subjected to small variation during the grazing season as the stocking density was adapted to plants (re)growth by the farmer (Gourlez de la Motte et al. 2016). Beginning of the grazing season in May 2015, however, was characterized by a higher herbage height which might have been responsible for the higher GPP and the stronger negative NEE fluxes observed at this period (Fig. 2.2F) as higher biomass has been associated to higher negative NEE in another grazed temperate grassland study (Zhu et al. 2015). Outside this period, we do not expect a significant influence of variation in biomass on CO_2 fluxes as herbage height only fluctuated by around 2 cm (data not shown).

2.4.4 Photosynthesis saturation was associated with PSI limitations to manage high electron flux.

Results indicated a lack of GPP increase between C2 and C3 clusters despite increasing temperature, suggesting optimal temperature conditions and/or photosynthetic saturation due to high PPFD recorded under these conditions. Subsequently, an associated absence of significant increased ΔV_{IP} was observed for the ecosystem whereas dicot species exhibited a significant ΔV_{IP} increase in these conditions (Table 2.1). The incapacity for additional carbon assimilation by the grassland ecosystem under these conditions might be attributed to an impairment of the PSI acceptor side to manage a higher electron flux. Indeed, a high correlation between net photosynthesis and I-P phase related parameters was found in ozone stress studies under high light (Cascio

et al. 2010, Desotgiu et al. 2012b), suggesting this OJIP curve region might be applied as a probe for the photosystem's capacity to feed the Calvin-Benson cycle. In our study, however, we detected a weak correlation ($r = 0.111$, $p \leq 0.001$, data not shown) between the I-P phase and photosynthetic activity (i.e., GPP) compared with r-values reported in the aforementioned studies ($r = 0.324$ and 0.425 for Cascio et al. (2010) and Desotgiu et al. (2012b), respectively). The lower coefficient we observed might be explained because gas-exchanges were not measured on specific leaf species, but resulted from a blend of different species.

It is also likely that photorespiration activity in the grassland have increased with increasing temperature (Sage 2013), competing with Rubisco carboxylation and thus reducing the apparent photosynthesis (i.e., 'true photosynthesis' plus photorespiration). Photorespiration serves a protective role in the photosynthetic apparatus, particularly under excess light conditions, by consuming excess photon energy and preserving PSII from photodamage (Massacci et al. 2008, Bai et al. 2008). Increased photorespiration can stimulate the apparent linear electron transport, which is not fully dedicated to carbon fixation (Rho et al. 2012, Osório et al. 2013). Increase in the efficiency of electron transport beyond PSI and Q_A was measured in dicot species in the absence of GPP increase in the C3 cluster and can be indicative of an increase in photorespiration activity. Dicot species, however, only represented 11.4% of the population, which questions dicots contribution to CO_2 fluxes. In addition, as explained in the material and methods section, GPP in high light condition is likely to more representative of 'true photosynthesis', which represents only carboxylation activity and would not reflect increase in Rubisco oxygenation. It is also possible that the observed increase in the electron transport efficiency for dicots results from enhanced cyclic electron transport, a mechanism involved in the protection of the photosynthetic apparatus under high light (Takahashi et al. 2009, Kalaji et al. 2012). This hypothesis is supported by the associated ΔV_{IP} increase which was also observed by Campos et al. (2014) in *Agave salmiana* Otto ex Salm-Dyck seedlings where the enhancement in cyclic electron flow had promoted PSI activity.

2.4.5 High respiration activity was associated with low photosynthetic performance.

Total ecosystem respiration increased with temperature in the grassland (Fig. 2.3B), most likely due to increased enzyme activity. Aboveground vegetation and soil might have contributed to increased R_{eco}. Indeed, several studies demonstrated soil respira-

tion (i.e., root and microbial components) responded positively to increasing temperature (Hill et al. 2015, Borchard et al. 2015, Chen et al. 2017). Belowground respiration might have been an important contributor to R_{eco}, as soil respiration represented more than 70% of ecosystem respiration in an alpine grassland study (Ganjurjav et al. 2014). However, Hoover et al. (2016) cautions comparisons of CO_2 soil fluxes among studies must be conducted carefully, as different plant communities were shown to influence soil respiration. The potential important soil respiration contribution to R_{eco} increase, however, does not exclude the potential for increased vegetation respiration. Atkin and Tjoelker (2003) reported plant respiration responded positively to increasing temperature. Chen et al. (2016) also showed the response of carbon flux to warming was dependent on plant functional types in meadow grasslands, emphasising the integral role of vegetation on aboveground fluxes. Our results did not determine the contribution of aboveground vegetation and soil to R_{eco} fluxes.

Increasing ecosystem respiration was also associated with decreasing photosynthetic performance (Fig. 2.3C,2.5D). This observation, however, might result from the common Reco and photosynthetic processes sensitivity to temperature, as decreased photosynthetic performance was associated with increased temperature (Fig. 2.3A). Moreover, the absence of a significant linear relationship between variation in ChlF parameters and R_{10} (Fig. 2.4) suggested the Reco response to temperature was not influenced by changes in photosynthetic processes measured by ChlF. Because photorespiratory activity was not taken into account in the partitioning, R_{eco} may have been underestimated, especially during hot and sunny days. Even though the absence of significant increase in the efficiency of electron transport beyond PSI and Q_A for the ecosystem suggests a negligible activity of alternative electron sink, this hypothesis need to be confirmed by gas-exchange measurements at leaf scale.

2.5 Conclusions

Results of this study revealed contrasted responses of the photosynthetic apparatus in three grassland species under combined environmental stresses in summer. Because stress drivers are multiple and untangled, it is probable that the observed photosynthetic response for the different species results from the combination of different events such as energy dissipation within the antenna, dissociation of LHCII from the PSII supercomplexes, PSII RC silencing, regulation of the electron flow and change in PSI

efficiency. The causes for the contrasted responses observed among measured species are yet to be identified and might also depend on plant/leaf anatomy as well as physiological factors such as the phloem loading capacity (Demmig-Adams and Adams 2006). In a grassland study, Gielen et al. (2007) also suggested that difference in plants height among species might lead to difference in shading and, therefore, different susceptibility to midday photoinhibition between species. Results also highlighted that a decrease in the ecosystem photosynthetic performance did not result in reduced carbon fixation. We wonder if an increase in abundance of the studied dicot species might improve carbon fixation during stress episodes, as the two dicots expressed an enhanced capacity to stimulate PSI efficiency under stressful conditions. However this response, which was associated with improved efficiency in electron transport, might also indicate increased alternative electron sinks, such as photorespiration. Further studies are needed to partition the relative contribution of these different electron sinks to PSI activity under stressful conditions. Better understanding of these mechanisms in response to environmental constraints and their impact on ecosystem CO_2 fluxes might be useful in elucidating ecosystem response to climate change and might help in selecting cultivated varieties favouring carbon fixation during stress episodes.

2.6 Acknowledgments

We are very grateful to A. Genette and E. Hanon for their useful advice and constructive remarks. We also thank M. Eyletters for constructive discussions. We also wish to thank H. Chopin, A. Debacq and F. Wilmus for their technical support. This work was supported by the National Fund for Scientific Research of Belgium (PDR, no. 14614874).

2.7 Author contributions

B. Heinesch, M. Aubinet, P. Delaplace, P. du Jardin, C. Amelynck, N. Schoon and M-L. Fauconnier planned and designed the research. A. Digrado, L. Gourlez de la Motte, A. Bachy, C. Amelynck, N. Schoon and A. Mozaffar performed experiments and conducted fieldwork. Meteorological data from the DTO were collected and corrected by the Biosystems Dynamics and Exchanges team. Carbon dioxide fluxes were collected and corrected by Louis Gourlez de la Motte who was also responsible for the partitioning of NEE into GPP and R_{eco}. Chlorophyll fluorescence data were collected

and interpreted by A. Digrado. F. Bussotti helped with the interpretation of ChlF data. A-C. Dalcq helped with the statistical analysis of data. A. Digrado wrote the paper. B. Heinesch, M. Aubinet, P. Delaplace, P. du Jardin, C. Amelynck, N. Schoon, A. Bachy, F. Bussotti and M-L. Fauconnier revised the paper.

V

General discussion and perspectives

1 GENERAL DISCUSSION

GHG emissions from agriculture was estimated to 5.2-5.8 $GtCO_2$ eq/yr in 2010 (Smith et al. 2014) and is expected to increase due to a rise in agricultural activity in order to meet the growing demand in food and bioenergy (Popp et al. 2010). Part of the GHG emissions can be offset by grassland ecosystems through the storage of carbon in soil via photosynthesis. However, as previously discussed in the 'State of the art' of this thesis, detrimental environmental conditions can lead to an impairment of photosynthesis by altering various process involved in carbon assimilation. While the impact of an individual stress on photosynthesis has been well characterized in laboratory conditions, the impact of combined stresses on the photosynthetic process appears to be more difficult to predict. Indeed, multiple factors such as the intensity of the different stressors, the timing of their occurrence and the involvement of physiological response not directly related to photosynthesis (e.g., osmolytes accumulation) contribute to determine the photosynthetic response. In addition, it is still unknown to which extend acclimation of photosynthetic process occurring at leaf scale can influence ecosystem CO_2 fluxes. This is particularly true in complex ecosystems such as grasslands as they are composed of different species which can potentially express contrasted photosynthetic response. As unfavorable climatic events such as heat wave and drought are expected to increase in future climatic conditions (IPCC 2014), a better understanding of photosynthetic response under combined environmental stressors in grasslands is therefore essential in the establishment of strategies aimed at the GHG mitigation. The objectives of this PhD thesis were to evaluate how processes involved in the light reactions were impacted by environmental constraints and if alterations in the photochemical capacity of grassland species had a detrimental impact on the carbon fixation by the ecosystem.

In this study, we showed through frequent chlorophyll fluorescence measurements that photochemical capacity of primary grasslands species exhibited diurnal and seasonal variations. The strongest declines in photochemical capacity were observed in summer when abiotic stresses such as high light and high air temperature were combined. Among the different photosynthetic process investigated, the efficiency in electron transport Ψ_{E0} appears to be the least influenced by the environmental conditions. The monocot *L. perenne* and the dicots (*Taraxacum* and *T. repens*) exhibited different acclimatization strategies. All species exhibited the onset of energy dissipation

mechanisms within the PSII but expressed contrasted response in the PSI efficiency. Important declines in the efficiency of electron transport beyond Q_A were observed in the monocot *L. perenne* only during strong climatic events such as heat waves. In contrast, dicot species exhibited an increase in the efficiency of electron transport along with PSI efficiency under comparable conditions. Variations in GPP fluxes and in ecosystem photochemical capacity estimated based on leaf-scale measurements were observed in the grassland. However, decreases in photochemical capacity were not associated with a decreased ability to fix carbon in the grassland. The maintenance of carbon assimilation despite the onset of energy dissipation mechanisms is probably explained by the higher availability of light energy under these conditions.

The use of a PEA fluorimeter instead of a PAM fluorimeter to assess the photochemical capacity was determined by practical reasons in addition to the physiological information provided by the analysis of the OJIP curves. Indeed, in order to correlate variations in ecosystem CO_2 fluxes to plants photochemical capacity, it was essential to perform an important number of measurements in order to take into account both the temporal and the spatial variation in photochemical capacity in the grassland for the three investigated species. Assessment of photochemical capacity using PAM fluorimeter was therefore not feasible since about 20 min are required for the assessment of the photochemical capacity of one leaf due to the application of successive saturating pulses of light. PEA analyzer, in contrast, offered us the possibility to collect a large number of data in a short amount of time since only 1 sec is needed to take one measurement. Still, measurements using a PEA analyzer are performed manually and does not enable data collection at high frequency such as performed for eddy covariance measurements. In addition, leaves have to be dark-adapted prior to measurements. However, the development of a new type of fluorimeter, the monitoring-PAM fluorimeter (Porcar-Castell et al. 2008), makes possible data collection at a higher frequency. This device can be left outdoor on a leaf for continuous automated measurements under ambient light (e.g. every 10 min), allowing long-term study and the study of the full diurnal dynamic of photochemical capacity. The presence of blue LED providing modulated fluorescence excitation light, actinic light and saturation flashes makes possible the measurement of parameters describing the PSII functioning in light condition such as the actual quantum yield of PSII (Φ_{PSII}) (García-Plazaola et al. 2012, Janka et al. 2015). Value of F_V/F_M can also be obtained if the first measurement is scheduled before sunset to obtain F_V/F_M at predawn. Evolution of predawn F_V/F_M provides

further information as decline of its value is indicative of chronic photoinhibition or sustained down-regulation of PSII (Maxwell and Johnson 2000, Murchie and Lawson 2013). However, monitoring-PAM cannot be used to estimate JIP-test derived parameters. Frequency of saturating flash application during automated measurements also have to be thought carefully as repeated saturating flash at high frequency can lead to a chronic photoinhibition (Porcar-Castell et al. 2008).

Whereas average ChlF parameters were characterized by a low standard deviation in periods of high photochemical capacity, strong variations around the mean were observed during stressful periods. In addition, we occasionally observed differences in average ChlF parameters between blocks for particular time period of measurement, especially during events characterized by strong variations (Fig. S1,S2,S3). Still, we did not find a spatial heterogeneity (i.e., a significant influence of the block factor) in the investigated ChlF parameters during our study (Table S2) and behavior of ChlF parameters among blocks was consistent. Spatial heterogeneity of ChlF parameters at leaf scale was shown to increase during stressful events (Guidi and Degl'Innocenti 2011, Bresson et al. 2015) and might explain the high standard deviation observed during period of low photochemical capacity. Grazing may also represent an additional source of variation in the leaf photochemical capacity as herbivory damages were also shown to increase spatial heterogeneity of ChlF at leaf scale due to water loss around the sites of damaged (Tang et al. 2006). Difference in background between plants may also have contributed to the variability in our measurements.

Spread in the pasture, there was patches of ungrazed vegetation characterized by leaves taller than the average. ChlF measurements were not performed on plants from these ungrazed areas because they were considered not representative of the pasture. These small areas of ungrazed vegetation were expected to be less exposed to environmental conditions due to self-shading and thus to present a photochemical efficiency response specific from this microcosm. Indeed, it was shown that plants exposed and acclimated to high irradiance prior to an exposition to high light were more resistant to photoinhibition and exhibited a faster recovery of photochemical capacity (Aro et al. 1994). Thus, measurements on leaves from ungrazed plots used to shading conditions would have lead to conclusions that could not be extrapolated to grazed leaves exposed to full sun which represented most of the vegetation area in the pasture. As a result, responses from these ungrazed regions were not integrated in our estimation of the ecosystem photochemical efficiency even though it certainty contributed to some

extent. Leaves showing visual symptoms of biotic stress were not measured either. Still, virus (Spoustová et al. 2013) and fungal infection (Rios et al. 2017, 2018) can be responsible for the decline of photochemical capacity by leading to increase energy dissipation within the LHC and the inactivation of RC. However, because the pasture did not experienced any episodes of high biotic stress pressure during the study, measurement on infected leaves was considered not representative of the overall pasture condition. Still, we cannot exclude that present infected leaves contributed to the overall ecosystem photochemical capacity. This inability to take into account these small variations in the photochemical capacity within the pasture and to integrate them into the estimation of the ecosystem constitute a weakness of the method used in our study. Only measurements at high density such as satellite data would have allowed to highlight this spatial variation. Considerable effort are made to export the study of photosynthesis at a larger spatial scale. For instance, a research team is currently working on a method to extract PAM-derived parameters from satellite data by the analysis of wavelength-specific fluorescence emission (Magney et al. 2017). A recent study has also shown the possibility to estimate the maximum carboxylation rate of Rubisco from satellite data (Landsat TM/ETM satellite, 30 m resolution) by estimating the leaf Chl content from the canopy-level reflectance (Croft et al. 2017). Such advances offer great perspectives for the study of photosynthesis at the ecosystem-scale.

Our results have shown that variations in ChlF parameters did not explain variations in GPP and that strong decrease in the ecosystem photochemical capacity did not result in an impairment of CO_2 assimilation by the ecosystem. Decline of ecosystem photochemical capacity was usually observed at midday in periods of light saturation. In environmental condition where light is a limiting factor, increase in light availability leads to an increase in the photosynthesis rate. However, after reaching the point of light saturation, increase in light intensity does not lead to a further increase in CO_2 fixation because light is no more a limiting factor for photosynthesis and other factors such as CO_2 concentration becomes limiting (Formighieri 2015). Light energy that is in excess compared to downstream biochemical reactions is then dissipated to limit the production of ROS. While the diurnal downregulation of PSII activity can play a photoprotective role to avoid irreversible damage, it eventually results in the deviation of light energy away from the photosynthetic energy conversion, leading to a reduction in the potential carbon gain (Werner et al. 2001). Such process is reflected by the reversible decrease in F_V/F_M and is often referred as a reversible photoinhibition.

If the amount of light energy were to overcome photoprotective mechanisms of the photosynthetic apparatus and the rate of the PSII repair cycle, ROS production would eventually lead to a photoinhibition of photosynthesis associated with net damage of the photosynthetic apparatus and a lower recovery (Goh et al. 2012). Photoinihibition increases with light intensity (Aro et al. 1994) and the duration of light exposure (Werner et al. 2001). Prolonged exposure to high light regime (5 days of 500 μmol m^{-2} s^{-1} from 6:00-18:00 with 2 hours at 1000 μmol m^{-2} s^{-1}) was shown to induce strong reduction in carbon assimilation partly attributed to an irreversible destruction of PSII RC reflected by the decline in F_V/F_M, leading to a reduction in energy conversion efficiency and electron transport between the PSII and PSI (Lu et al. 2017). Carvalho et al. (2016) have also shown that the oxidative pressure on the photosynthetic apparatus was higher under combined stresses compared to a situation where stressors are applied alone. Stronger declines in carbon assimilation, associated with declines in F_V/F_M, were also observed in treatments when stressors were combined compared with treatments when stressors were applied alone. Results in our study suggest that even in periods of strong combined environmental constraints, photoprotective mechanisms efficiently prevented oxidative damages to the photosynthetic apparatus, contributing to the maintenance of carbon assimilation by the ecosystem in periods of strong reduction of photochemical capacity (i.e., during periods associated to the C3 cluster).

There are other acclimation mechanisms of photosynthesis that could have been responsible for an impairment of CO_2 assimilation and that have not been assessed in our study. For instance, it was shown that energy dissipation by heat within the LHCII through the zeaxanthin-facilitated process can lead to lower carbon assimilation by reducing the quantum yield for CO_2 uptake (Φ_{CO_2}), especially under light fluctuating environment (Kromdijk et al. 2016). The measure of NPQ using modulated fluorimetry (i.e., PAM) can be used to estimate energy dissipation within the LHCII mediated by the xanthophyll activity (Krause and Jahns 2004, Brestic and Zivcak 2013). Assessment of the photosynthetic apparatus using PAM technique also enables the study of the PSII under light conditions. While the study of the OJIP curve is indicative of the 'potential' photochemical capacity, PAM-derived parameters give information on the actual photosynthetic efficiency such as Φ_{PSII} and the proportion of open PSII RC under illumination. It is likely that these parameters would have been more correlated with CO_2 fluxes as they characterize the photosystem in light condition in contrast

with OJIP-derived parameters. Indeed, Genty et al. (1989) found a strong linear correlation between Φ_{PSII} and Φ_{CO_2} at 1% O_2 for barley and 20% O_2 for maize. This good relationship, however, can be altered in stress condition when alternative pathways for electrons such as photorespiration increase (Baker 2008). Because quantum yield parameters in light-adapted leaves (e.g., Φ_{PSII}) tend to be more sensitive to stress events than the maximum quantum yield in dark-adapted leaves (F_V/F_M) (Calatayud et al. 2007) differences can be observed between PEA- and PAM-derived parameters (Nussbaum et al. 2001). Still, because parameters derived from PAM measurements are more representative of the photosynthetic apparatus activity under light condition, this does not impair the relevancy of our study nor the conclusions driven by our study of fast ChlF kinetics. The consistency existing between results derived from the two fluorescence techniques was illustrated in several studies using both PAM and PEA fluorimeters (Chen et al. 2014, Ajigboye et al. 2016) with changes in the efficiency of electron transport measured by a PEA fluorimeter supported by results derived from PAM fluorimeter measurements (Zivcak et al. 2014). As already mentioned, the two techniques provide complementary information and can be used together for a more exhaustive diagnosis of the photosynthetic apparatus.

We also found contrasted ability between *L. perenne* and dicots species to improve PSI efficiency (ΔV_{IP}) under stressful conditions. However, if the amplitude of the I-P phase can be used to characterize the efficiency of electron transport beyond the PSI, it does not represent the actual PSI activity or a change in PSI content (Zivcak et al. 2015). Leaf transmission changes at the 820 nm wavelength band, however, can be used to accurately monitor P700 oxidation (Harbinson and Woodward 1987, Strasser et al. 2004). The reasons for different PSI efficiency under stressful conditions are still uncertain. A possible explanation is the natural variation in the FNR enzyme activation/deactivation dynamics among the observed species, leading to a difference in electron transfer on the acceptor side of PSI after dark adaption (Hamdani et al. 2015). The difference among species in the dark relaxation of the FNR enzyme was made by Schansker et al. (2008) who observed the inactivation of FNR in the dark after 15 min for *Pea sativum* L. and more than 45 min for *Pinus brutia* Ten. trees. Since differences in ΔV_{IP} between monocot and dicots were essentially observed in stress conditions, it is possible that environmental conditions influenced the FNR enzyme activation/deactivation dynamics. Measurements of the fast fluorescence transient along with transmission changes at 820 nm under changing environmental conditions for the

three grassland species can provide a better understanding of the acclimation mechanisms of the PSI.

The absence of leaf-scale gas exchange measurements constitutes a missing link between plants photochemical capacity and ecosystem CO_2 exchange. Questions remain in our study regarding how disturbance in photosynthetic processes affected the carbon assimilation of individual plants. Measurement of photosynthesis using a portable infrared gas analyzer in addition to ChlF measurement could help in the identification of the most limiting process to carbon assimilation under stress condition and assess the impact of different photosynthetic acclimation strategies on carbon assimilation and respiration. Other photosynthetic traits such as the stomatal conductance, the carboxylation rate of Rubisco and the actual ETR can be derived from such leaf-scale gas measurements and provide further information related to the acclimation response. Light-response curve of photosynthesis using a portable infrared gas analyzer would also allow the determination of the quantum light efficiency (i.e., the photon use efficiency in low light represented by the initial slope of the curve) for the different species at the different time periods of the day. Photoinhibition is known to affect the quantum light efficiency and changes in F_V/F_M were shown to influence in the initial slope of the light-response curve of photosynthesis (Björkman and Demmig 1987, Genty et al. 1989, Werner et al. 2001). Thus, the reduction of CO_2 assimilation by moderate PSII inactivation is only visible at low light or during transient change in light intensity (Kornyeyev et al. 2006, Hubbart et al. 2012). Since photoinhibition usually occurs at high light, a reduction in the photon use efficiency is expected to have only a minor impact on carbon assimilation at light saturation unless limitation in PSII efficiency leads to an increase of the point of light saturation or affect photosynthesis at all light intensity (Long et al. 1994, Werner et al. 2001). Indeed, we did not observed in our study F_V/F_M values below 0.74 in low light condition (Fig S4) and variations in GPP were not explained by variations in F_V/F_M in high light environment (Fig S5). The impact of photoinhibition on light-saturated photosynthesis was also tentatively assessed in our study by investigating the influence of variations in the photochemical capacity on GPP_{1500}. Our results showed that GPP_{1500} was not depressed during days of strong decline in photochemical capacity suggesting no severe impairment of carbon assimilation at light saturation. However, since GPP_{1500} is derived from the Mitscherlich equation based on flux measurements during the whole day, this does not inform us on potential variations of light-saturated GPP occurring through the day. Explor-

ing the relationship between the photon use efficiency and JIP-test derived parameters would have provide further information on potential limitations of photosynthesis induced by the light reaction. Even though in our study we estimated the quantum light efficiency α of the ecosystem by using the Mitscherlich equation, we could not use the estimated α to explore its relationship with the different ChlF parameters for different reasons. First, the standard error associated with its estimation was too high because there were not enough reliable eddy covariance measurements of CO_2 fluxes at low light, making the estimation of α not robust enough for analysis (Fig. S6). Second, because α represents the quantum photon efficiency at low light, only comparison with ChlF measurements performed at predawn would have been pertinent. Light-response curve at the different time periods would also have allowed us to assess the evolution of light-saturated photosynthesis through the day along with the onset of photoinhibition.

Based on leaf-scale measurements of gas exchange, the contribution of the different plant species to ecosystem fluxes could also be determined. Heterotrophic respiration from soil, which is expected to be an important contributor to respiration flux (Ganjurjav et al. 2014), could also represent a valuable information in order to appreciate the relative contribution of plants to the total ecosystem respiration flux.

Leaf-scale gas exchange measurements combined to ChlF can also provide valuable information regarding alternative electron sinks. We highlighted in our study that R_{eco} and GPP did not account for photorespiratory activity in the grassland which is assumed to be high under hot and sunny conditions. We also hypothesized that the increase in PSI efficiency and in the efficiency of electron transport beyond Q_A (Ψ_{E0}) for dicot species could be indicative of an increase in alternative sinks for electrons, such as Mehler reaction and photorespiration. This hypothesis could be verified by measuring plant CO_2 assimilation and estimating the actual ETR through the PSII. One method consists in the comparison between ETR calculated through gas-exchange measurements (ETR_g, eq. 1.1) according to Harley et al. (1992):

$$ETR_g = 4\left(A_{CO_2} + R_L\right)\left(c_i + 2\Gamma^*\right)/\left(c_i - \Gamma^*\right) \tag{1.1}$$

and the ETR calculated based on ChlF measurements (ETR_{PSII}, eq. 1.2) as described by Genty et al. (1989) and Krall and Edwards (1992) :

$$ETR_{\text{PSII}} = \Phi_{\text{PSII}} \,.\, PAR \,.\, \alpha_{\text{II}} \,.\, f \tag{1.2}$$

Where A_{CO_2} represents the carbon assimilation rate, c_i represents intercellular content of CO_2, R_L represents mitochondrial respiration in light, and Γ^* represents CO_2 compensation point measured in the absence of respiration in eq. 1.1. The parameter PAR represents the photosynthetically active irradiance, α_{II} represents proportion of absorbed quanta used by PSII RC, and f represents the fractional light absorbance in eq. 1.2. A $ETR_{PSII} > ETR_g$ may therefore indicates the presence of alternative electron pathways, suggesting that the PSII releases more electrons than used for carboxylation (Zivcak et al. 2013). An alternative method is based on the assumption that 4 electrons are required to fix one CO_2 molecule. Therefore, the alternative electron pathways can be estimated by dividing ETR_{PSII} by four and subtracting the gross photosynthetic rate from this value (Long and Bernacchi 2003, Massacci et al. 2008, Yi et al. 2016).

The improvement in PSII thermotolerance of *L. perenne* highlighted during our study also constitutes an interesting observation and deserves further study. Different hypotheses were put forward as possible explanations for this improved resistance of the PSII. One of them was the possible accumulation of osmolyte compounds such as glycine betaine and proline after a water stress event. These compounds were shown by Oukarroum et al. (2012) to improve OEC stabilization during heat stress and are known to be produced by grass species (Hitz and Hanson 1980, Gargallo-Garriga et al. 2015, He et al. 2017a). Analysis of proline content in leaf along with the evaluation of the OEC activity by ChlF would allow to test this hypothesis. A second hypothesis was the selection of better adapted genotypes. This hypothesis could be tested by determining the genetic diversity in *L. perenne* population in the grassland with the use of microsatellite DNA markers (Evans et al. 2014). Change in *L. perenne* genetic diversity after stressful events would indicate the selection of potentially more adapted genotypes. Analysis of single nucleotide polymorphisms could open the way to the identification of favorable alleles (Dwivedi et al. 2017). Such experiments, along with a long-term monitoring of the floristic composition in the grassland, may offer a better insight of the long-term impact of repeated environmental constraints. They can also

help in the prediction of a potential shift in the grassland floristic composition and/or loss of biodiversity in the absence of farmer intervention (e.g. sowing) if sensitive species were to be determined. Alteration in plant diversity might have an impact on the resilience of grassland ecosystem and its ability to fix carbon under stressful conditions (Isbell et al. 2015).

2 PERSPECTIVES

2.1 The CROSTVOC project. Stress and emission of biogenic volatile organic compounds by plants.

How biogenic volatile organic compounds (BVOC) emissions in managed grasslands are influenced by abiotic environmental factors constituted an important question of the CROSTVOC project. BVOC are continuously produced and released by plants through their above- and belowground organs (Laothawornkitkul et al. 2009). These compounds are chemically diverse and most of them can be assigned to one of the following classes: isoprenoids (i.e., compounds derived from the deoxyxylulose-5-phosphate pathway in chloroplast or the mevalonate pathway in the cytoplasm such as isoprene and monoterpenes), fatty acid and derivatives including lipoxygenase pathway products, benzenoids and phenylpropanoids as well as various nitrogen and sulfur containing compounds (Dudareva et al. 2004). Once released into the atmosphere, BVOC are degraded and ultimately oxidized to CO_2 (Atkinson and Arey 2003), resulting in a carbon loss for the ecosystem and an indirect CO_2 emission (Kesselmeier et al. 2002). Depending on the degradation pathway, intermediary reactions can have various implications for air quality and climate. For instance, by reacting with hydroxyl (OH) radicals, BVOC can reduce the oxidation capacity of the atmosphere and indirectly increase the lifetime of CH_4, resulting in an increase in CH_4 air concentration (Peñuelas and Staudt 2010). BVOC degradation can also promote O_3 formation in the troposphere. Indeed, by reacting with OH radicals, BVOC can lead to the production of peroxide radicals. In presence of NO_x, produced peroxide radicals can react with nitric oxide to form NO_2. In light conditions, degradation of NO_2 can lead to the formation of O_3 (Calfapietra et al. 2009). As a result, BVOC emissions can have a significant influence on the atmospheric chemistry and GHG balance.

Emission profile of BVOC in grassland ecosystems were shown to be composed of more than 40 volatile compounds, which bouquet was mostly constituted of compounds such as methanol (Bamberger et al. 2010), aldehydes and monoterpenes (Fukui and Doskey 2000). By reacting with OH radicals, monoterpenes might decrease the oxidation capacity of the atmosphere, with a consequent increase in CH_4 lifetime. However, monoterpenes can also lead to OH radicals production by reacting with O_3, making difficult prevision on atmospheric OH radicals pool (Atkinson and Arey 2003).

Grassland ecosystems are not reported as important monoterpenes emitters compared to forest ecosystems (Hantson et al. 2017) and some studies even report monoterpenes deposition in mountain grasslands (Spielmann et al. 2017), especially when these compounds are present in the atmosphere at high volume mixing ratio (Bamberger et al. 2011). Management practices, however, can have a significant influence on the emission profile of BVOC. Over-grazing, for instance, can lead to an increase in the proportion of monoterpenes emitters as shown in Inner Mongolia grassland (He et al. 2005). Grazing can also be an important source of BVOC emission in pasture since important fluxes of methanol, acetaldehyde, acetone and GLV compounds were reported from manually cut grass (Davison et al. 2008). Increase in grazing stocking rate could therefore result in an increase in CH_4 lifetime due to a stronger depletion of atmospheric OH radicals by grazing-induced aldehydes compounds (Atkinson and Arey 2003). Increase in forage production may also result in higher methanol emissions, a compound related to plant growth (Bamberger et al. 2010), which can also react with OH radicals (Atkinson and Arey 2003). Environmental conditions also strongly influence BVOC emissions from plants (Peñuelas and Staudt 2010). Temperature for instance, by regulating chemical reaction rates and the BVOC vapor pressure, is one of the major driver of emission (Laothawornkitkul et al. 2009, Tiiva et al. 2017). It was estimated that a 2-3°C increase in mean air temperature could result in a 30-45% increase in BVOC global emission (Peñuelas and Llusià 2003). Drought events, however, negatively affect emissions essentially by reducing stomatal diffusion (Loreto and Schnitzler 2010). However, because of differences in solubility among BVOC, the increase in intercellular partial pressure induced by g_s reduction differently affects volatile compounds. As a consequence, the most highly volatile compounds such as isoprene and monoterpenes characterized by a lower solubility were shown not to be controlled by stomatal aperture in contrast to soluble compounds such as methanol (Niinemets and Reichstein 2003). Other factors such as UV-B radiation and ozone (at a certain threshold) can be responsible for cellular damages and lead to the emission of green leaf volatiles (GLVs) compounds (Holopainen and Gershenzon 2010). The GLVs are 6- or 9-carbon compounds derived from lipoxygenase activity acting on the fatty acids linolenic acid and linoleic acid found in the plasma membrane (Feussner and Wasternack 2002, Gigot et al. 2010) frequently observed after mechanical damages (Holopainen and Gershenzon 2010). As a result, stressful events can have a significant influence on BVOC emission profile. Whereas carbon emissions as iso-

prenoids are estimated to represent around 1% of fixed carbon in forest (Kesselmeier et al. 2002), stress events such as high temperature and water stress can increase this ratio to 20-67% (Sharkey and Loreto 1993, Staudt and Bertin 1998). Whereas it is well established that BVOC play a key role in air quality and GHG balance, considerable uncertainties remain regarding how combined abiotic environmental factors affect BVOC emissions in a managed grassland ecosystem.

To answer this question, BVOC were sampled using two different approaches. One method consisted of BVOC sampling using the eddy covariance method to estimate BVOC fluxes at the ecosystem scale. A second method consisted in realizing BVOC sampling using dynamic chambers installed in the grassland. In both methods, BVOC were identified by proton-transfer-reaction mass spectrometry (PTR-MS), allowing a real-time detection and analysis of sampled BVOC. ChlF measurements performed in this study can be usefully used to identify stressful events in the grassland, allowing to assess changes in BVOC emission profiles in relation with plants physiological stress. Modeling of ChlF response to meteorological conditions would further allow to extent the analysis to days where ChlF measurements were not performed. In the same way some empirical PI multiparametric indice are built to be sensitive to specific stress (Stirbet et al. 2018), the construction of a PI_{BVOC} indice dedicated to the identification of environmental conditions leading to altered BVOC emission could be performed.

Isoprene and monoterpenes are considered as side products of leaf photosynthesis and their production therefore depends on photosynthetic activity (Loreto et al. 1996, Hantson et al. 2017, Machado et al. 2017). In addition, light was shown to play an important role in the *de novo* emissions of some isoprenoid compounds (van Meeningen et al. 2017) and experiments using ^{13}C isotope have shown that around 80% of the carbon in the isoprene molecule originated from recently fixed carbon (Ferrieri et al. 2005, Brilli et al. 2007). Gas-exchange measurements in shoot enclosures have also demonstrated that the increase in monoterpenes emission from Scots pine in spring was closely related to the recovery of photosynthetic activity after winter (Aalto et al. 2015). Emissions of volatile terpenes, however, can be uncoupled from photosynthesis as these compounds can be emitted at night from storage structures (Ghirardo et al. 2010). Moreover, growth under elevated CO_2 concentration was shown to reduce isoprene emission despite an increase in photosynthetic activity (Scholefield et al. 2004), supposedly due to the reduction in cytosolic phosphoenolpyruvate enzyme involved in the production of precursor in isoprene biosynthesis (Rosenstiel et al. 2003, Ve-

likova et al. 2009). Still, because of the dependence of isoprene and terpenes on photosynthesis, events altering photosynthetic process and acclimation response of the photosynthetic apparatus can influence their emissions. Reduction in net photosynthesis induced by high temperature stress, for instance, was accompanied by a reduction in monoterpenes emissions, supposedly due to the substrate limitations coming from photosynthesis for monoterpenes biosynthesis (Staudt et al. 2011). Under water stress, isoprene emissions were also shown to decline with the reduction of photosynthetic activity at both a leaf (Beckett et al. 2012) and ecosystem scale during drought events (Zheng et al. 2017). It may therefore be expected that events altering leaf photochemical capacity may affect isoprene and monoterpenes emissions. However, it may be expected that only a strong reduction in photochemical capacity, resulting in a depressed carbon assimilation and photosynthate limitation, leads to reduced isoprene and monoterpenes emissions.

Whereas isoprenoids emissions are intrinsically linked to photosynthetic activity, alteration in the emission of other BVOC such as methanol and GLV during stressful events are related to structural damages. Increase in methanol emissions observed in hybrid poplar exposed to ultraviolet-A irradiation was attributed to damages to the cellular structure and was accompanied by a decline in carbon assimilation (Pallozzi et al. 2013). Heat treatment was also shown to induce high emission in GLV compounds in Mediterranean oaks which was attributed to membrane damages and oxidative stress (Staudt et al. 2011). In this study, the high emission in GVL compounds was also associated with a sustained depression of F_V/F_M and net photosynthesis, indicating irreversible damages of the photosynthetic apparatus. Association of BVOC emission profile with ChlF measurements could therefore provide a new insight into the study of stress perception and physiological response by plants.

In the PTR-MS techniques, BVOC are identify by their characteristic protonated parent ions or fragments. However, since the same ion can result from the protonation of different BVOC, it is difficult to determine the contribution of each BVOC in the yield of resulting protonated masses. It was therefore necessary to complement PTR-MS analysis with another technique: gas chromatography-mass spectrometry (GC-MS) which allows to formally identify and quantify BVOC compounds present in the sample. BVOC sampling for off-line GC-MS analysis required that BVOC are preconcentrate on an adsorbent trap such as the Tenax TA. Such samplings were realized in static and dynamic chambers within the CROSTVOC project. However, BVOC sam-

pling in field condition for off-line GC-MS analysis can be technically challenging. Indeed, the sampling condition must not disturb the sampled material (i.e., grassland vegetation) in order to be representative. BVOC also have to be sampled in a sufficient amount to allow their detection and identification by GC-MS, which depend on the rate of emission of the material and the volume sampled. Preliminary experiments performed on static chambers revealed that a 2L sampling was not enough to detect BVOC emitted by the grassland vegetation, even during favorable environmental conditions such as hot and sunny days. This suggested that the grassland vegetation was not a high emitter of compounds with a high molecular weight, as Tenax TA adsorbent only traps volatile compounds of >5 carbons meaning that very volatile compounds like methanol could not be sampled using this adsorbent. The sampling volume had to be increased up to 12L in order to sample sufficient BVOC for GC-MS analysis. However, increasing the sampling volume implied to increase the sampling flow from 100 mL min^{-1} to 200 mL min^{-1} and to extent the sampling duration for 10 min to 60 min. Such sampling conditions could not be performed in a static chamber because the long duration of sampling tended to increase the air temperature and the relative humidity inside the chamber. As a consequence, the rate of BVOC emission was altered and not representative of real conditions anymore. The increase in air relative humidity inside the cuvette caused by the vegetation transpiration also led to the partial solubilization of the most hydrophile BVOC compounds. BVOC sampling was therefore realized in an automated chamber by performing successive sampling every 10 min for 10 min on the same Tenax TA cartridge. Preliminary experiments have highlighted important emissions of GLV after grazing events whereas only few compounds were retrieved in low quantity in the absence of grazing (Fig. 2.1), which is in accordance with Davison et al. (2008) results. Alternative adsorbent trap such as Carbosieve SIII, Carboxen 569, Carboxen 1003 can be used in order to sample volatile compounds with lower molecular weight (i.e. as low as 2 carbons). However, these adsorbents possess a higher affinity for water, which can lead to serious problem during GC-MS analysis (Gawryś et al. 2001). This is problematic for sampling in field conditions where atmospheric humidity is high. Different methods exist in order to reduce the water-uptake by adsorbent traps by heating the trap during sampling (Gawryś et al. 2001) or by setting a drying agent in front of the cartridge (Dettmer and Engewald 2003). However, these techniques can induce some biases by altering BVOC sampling (Niinemets et al.

2011). Flowing a helium gas through the cartridge prior to analysis can also reduce the amount of water adsorbed but can also lead to a loss of some sampled compounds.

Further experiments are needed to determine how environmental conditions and grazing influence BVOC emission in pasture and their impact on GHG budget. The selection of grassland species based on their BVOC emissions may also provide a better control of the impact of agricultural activity on the atmospheric chemistry as grass species are known to be low methanol emitter (Galbally and Kirstine 2002, Brunner et al. 2007). Cultivar selections based on their BVOC emission profile, however, should not neglect the ecological role of these compounds as they play an important role in plant defense and communication with its environment (e.g., attraction of pollinators, interaction with others plants, etc.) (Maffei 2010). Some BVOC also promote a protection against herbivores by having a repellent role or by attracting natural enemies (Arimura et al. 2005, Heil 2008, Kos et al. 2009, Maffei 2010). In addition to their ecological role, BVOC can also exert a protective function against abiotic stress (Dudareva et al. 2006). For instance, monoterpenes was reported to enhance leaf thermotolerance by improving membrane stability (Loreto et al. 1998). Isoprene was also shown to be involved in the photosynthetic apparatus resistance to high temperature (Holopainen and Gershenzon 2010) by improving the photosynthetic membrane stabilization and electron transfer through PSII (Pollastri et al. 2014). Isoprene can also confer the photosynthetic apparatus a protection against ozone stress at the membrane level by quenching H_2O_2 formed in leaves (Loreto and Velikova 2001). Even though BVOC emissions constitute a loss of carbon by the ecosystem and may unfavorably alter GHG balance by reacting with other atmospheric compounds, their protective functions can contribute to the carbon sink resilience of the ecosystems. The carbon balance of BVOC emission is complex and require further studies. However, since most of the BVOC having a protective role are induced in response to a stress factor, it is possible that their emission benefit carbon storage by the ecosystem. Maybe improvement in the reduction of carbon loss could be achieved by tuning their emission both quantitatively and qualitatively.

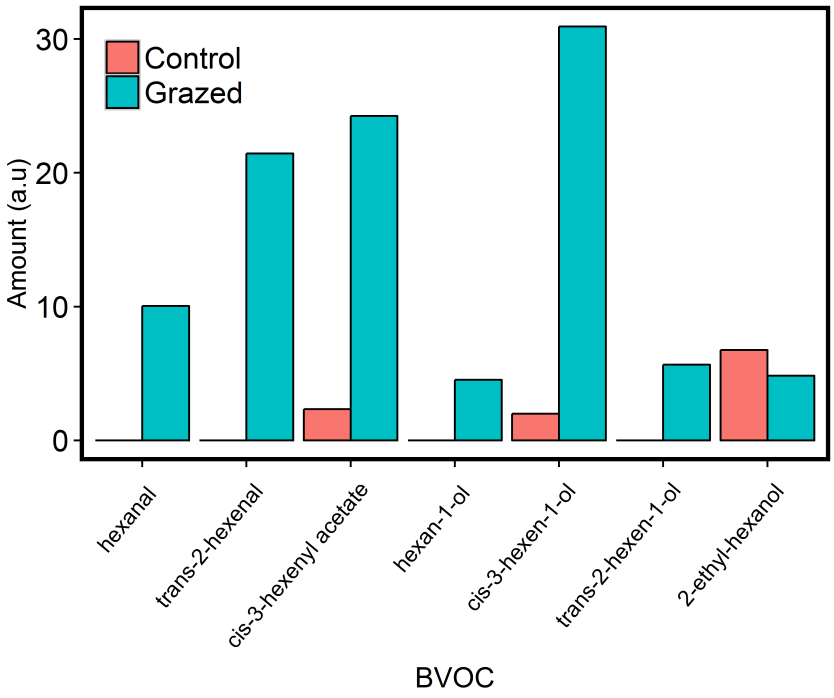

Figure 2.1 – Emission of biogenic volatile organic compounds (arbitrary units) after grazing. Compounds were collected on a Tenax TA cartridge 40 min after grazing by sampling air from a 5 L home-made Teflon cuvette. Cuvette air inlet was set at 2 L min^{-1} and was purified on an active charcoal filter. The sampling flow was set at 200 mL min^{-1}. A total volume of 12 L was sampled by performing 6 successive run of 10 min sampling and 10 min break (e.g., let the cuvette open to avoid an increase in air relative humidity and temperature inside the cuvette). Tenax TA cartridges were analyzed by gas chromatography-mass spectrometry. Our unpublished data.

2.2 How photosynthesis can help in the mitigation of greenhouse gas emission?

2.2.1 Exploitation of the diversity in plants photochemical capacity and acclimation response.

The maintenance of photosynthesis activity under unfavorable condition is a growing interest in the scientific community (Johnson et al. 2015) due to climate change (Abberton et al. 2016). Grasslands productivity was shown to be more resistant and resilient after unfavorable climatic events in ecosystems characterized by a high diversity in plant communities (Isbell et al. 2015). Shading induced by species presenting different plants height may also contribute to reduce photoinhibition in sunny day in multispecies ecosystems (Gielen et al. 2007). It is also possible that species exhibiting different photosynthetic acclimation strategies to environmental constraints, such as observed in our study, might contribute to the resilience of the ecosystem by expressing complementary response to environmental constraints. Intraspecific diversity is also advantageous as a genotype well-adapted to its environment may not be suited in altered environmental conditions. Systems characterized by high diversity may therefore be more resilient. The benefit of genotypic diversity to changing environmental conditions was highlighted in seagrass populations confronted to a shading treatment (Evans et al. 2017). It was shown that populations characterized by a high diversity were more likely to present individuals more adapted to altered conditions. In the mentioned study, high performing genotype were determined as individuals with F_V/F_M of 0.8 or greater. This enhanced resilience to stress events of ecosystems characterized by high diversity is well known of farmers who sometimes use seeds that are constituted by a mix of genotypes adapted to local conditions (i.e., landraces) (Blair et al. 2010). Experiments comparing the productivity resilience of grassland ecosystems characterized by different acclimation strategies, floristic composition and intraspecific variation can contribute to improve our understanding of the resilience of these ecosystems and be of strategic importance in the management of its diversity.

Diversity in photosynthetic traits among or within species constituting an ecosystem might contribute to the resilience of the ecosystem by expressing different response to environmental constraints. Significant variations in key catalytic parameters for the Rubisco enzyme was shown among plant taxa (Orr et al. 2016) as well as differences in Rubisco large subunit gene sequence and photosynthetic rate in wil-

low species (Andralojc et al. 2014). The exploitation of such diversity to select crops with improved stress resilience has been suggested in many studies (Silvestre et al. 2014, Thiry et al. 2016). The use of ChlF to assess photochemical capacity and stress tolerance among species was shown to be successful in many experiments (Mauromicale et al. 2006, Strauss et al. 2006, Brestic et al. 2012, Ghotbi-Ravandi et al. 2014, Pouresmael et al. 2015, Estrada et al. 2015). Recently, correlations between JIP-test parameters and quantitative trait loci (Czyczyło-Mysza et al. 2013, Yin et al. 2015) underlying the intrinsic features of the photosynthetic apparatus (Yin et al. 2010, 2011) and stress response (Šimić et al. 2014, Ripoll et al. 2016) were also reported, offering new opportunities in breeding programs. Screening of such photosynthetic traits might provide a new insight into the range of photochemical capacity present in nature which can later be used by breeders.

2.2.2 Plant engineering as a strategy to mitigate greenhouse gas emission by improving carbon uptake.

Plant breeding and engineering offer great opportunities to mitigate GHG emission by improving CO_2 uptake (Pulles 2017). Increasing photosynthesis capacity is often cited as one of the prime target to increase carbon assimilation by plants (Reynolds et al. 2009, Flügge et al. 2016). Indeed, the theoretical conversion efficiency of solar energy into biomass is about 4.6% and 6% for C3 and C4 photosynthesis respectively (Zhu et al. 2008) while the maximum conversion efficiency of solar energy to biomass currently observed is only 2% (de Bossoreille de Ribou et al. 2013).

Rubisco is a promising target for the enhancement of photosynthesis as improving its regeneration or increasing its content in leaves can considerably enhance carbon uptake by plants (Murchie et al. 2009). The transfer of a more efficient Rubisco from another species in an agricultural cultivar also offer promising perspectives (Furbank et al. 2015). Many research on photosynthesis and its improvement are also focused on the improvement of Rubisco carboxylase activity through engineering of the Rubisco. Genetic engineering of the entire Rubisco, however, is technically challenging due to the dual origin of the genome coding for its constitutive proteins: the large and the small subunits which are respectively encoded by the chloroplast and the nuclear genomes (Whitney et al. 2011). The difficulties to express a functional Rubisco in a bacterial host has also hampered genetic engineering for long (Parry et al. 2011). This challenge, however, has been recently overcome by Aigner et al. (2017) who

were the first to successfully assemble plant Rubisco in *E. coli* with five chloroplast chaperones. This offers great perspectives for Rubisco engineering in C3 plants aimed at the improvement of its catalytic properties.

Reduction of photorespiration activity by increasing CO_2 concentration around Rubisco and the conversion of C3 plants to C4 have also received considerable attention these last years (Murchie et al. 2009). Such manipulations have the potential to both improve carbon uptake and to reduce carbon emission from the oxygenase activity of Rubisco in ecosystems. This could be achieved by the introduction of carbon concentrating mechanisms from single celled photosynthetic organisms in C3 plants. Thylakoid-located CO_2 pumps found in cyanobacteria and microalgae constitute interesting candidates due to the small number of genes required for their introduction (Price et al. 2013, Hagemann and Bauwe 2016). Conversion of C3 grassland species to C4 is more challenging as it involves a more important number of genes due to the important number of traits. Indeed, C4 leaf is characterized by specialized enzymes and anatomical features referred as the Kranz anatomy. Reproduction of this anatomy in C3 plants would involve considerable modifications including the restructuring of the mesophyll, bundle sheath, veins order and photosynthetic enzymes compartmentalization (Schuler et al. 2016). However, it appears that some features such as veins spacing are not indispensable for C4 function (von Caemmerer et al. 2012). Considerable efforts have been made for the development of C4 rice with promising results of a C4 rice prototype (Furbank et al. 2015).

Improving the rapidity of photosynthesis recovery from photoprotection was also estimated to potentially increase crops yield by 20% (Kromdijk et al. 2016). Zeaxanthin-facilitated dissipation of the excess of energy within the LHC contributes to reduce the PSII excitation and potential photooxidation damages under high light (Goh et al. 2012). Under plant canopy, leaves are usually subjected to sharp fluctuations of sun irradiance. As a consequence, light conditions often switch between high to low light conditions where dissipation mechanisms are not fully required. Zeaxanthin-facilitated energy dissipation processes involved in NPQ, however, are not instantaneous and can therefore lag in response to changes in irradiance. Moreover, the rate of relaxation of energy-dissipation process is slower than the rate of induction. This results in an inefficient light exploitation and substantial loss of carbon assimilation. Improved relaxation in NPQ was achieved in tobacco plant by enhancing xanthophyll cycle kinetics and PsbS expression, resulting in a 15% increase in

dry matter (Kromdijk et al. 2016). The onset of photoprotective mechanisms was frequently observed in our study as reflected by the reversible diurnal decrease in F_V/F_M values. Improving the recovery from photoprotection might therefore allow consequent improvement in the exploitation of light energy and lead to potential increase in ecosystem carbon storage.

Manipulations of the photosynthetic light reactions were also shown to constitute a promising pathway for improved photon use efficiency by plants. For instance, Bressan et al. (2016) have recently shown in Arabidopsis (*Arabidopsis thaliana*) mutant lacking its LHCI antenna system that the energy transfer from LHCII to PSI was more efficient. However, due to a reduction in light harvesting, a reduction in growth was observed for these mutants. This limitation in light harvesting was explained by a decrease in the absorption cross-section due to the reduction in light harvesting system but also by a reduction in the absorption above 700 nm. It is likely that an increase in LHCII might partially contribute to offset this reduction in light harvesting efficiency. Another promising result in the improvement of photosynthetic efficiency was obtained by Jin et al. (2016) who optimized light-harvesting pigments by altering the *High Photosynthetic Efficiency1* (HPE1) gene in Arabidopsis. This mutation led to a reduction in the size of light-harvesting complexes but optimized light capture and energy conversion during the light reaction. As a result, mutants presented a faster electron transport and a higher biomass production. However, field experiments should be conducted to determine if the reduction in chlorophyll content does not lead to an increased sensitivity of *hep1* mutants to abiotic stress such as drought or salt stress which are known to lead to a reduction in photosynthetic pigment (Ashraf and Harris 2013). Another approach that has been recently considered in the improvement of photosynthesis is the broadening of the spectral range which can be harvested and used by plant. This could be achieved by the generation of transgenic plants able to synthetize and utilize Chl *d* and/or Chl *f*, expending the plants absorption spectra near infrared (700-750 nm) (Miyashita et al. 1996, Chen et al. 2010, Chen and Blankenship 2011). Marosvölgyi and van Gorkom (2010), however, cautioned against the increase of absorption spectrum due to the energy cost of the light harvesting system. According to the authors, it is possible that the energy cost required for molecular structure aimed at expansion of absorbed photon energy by the photosynthetic apparatus at other wavelength exceeds the benefit. As a consequence, mutant plants might not be able to properly grow.

The improvement of the ETR between the PSII and the PSI is another pathway considered for the increase of carbon assimilation by plants. Especially, manipulation of the cyt b_6f complex is a promising target for the increase of ETR as it catalyzes the most rate-limiting step of the linear electron transport (Schneider et al. 2007, Tikhonov 2014, Schöttler et al. 2015). A recent study performed on Arabidopsis observed both an increase in photosynthesis and biomass yield on transgenic plants overexpressing the Rieske FeS protein, a component of the cyt b_6f complex, along with an increase in ETR. However, this observation could not be solely attributed to an improvement in electron transport as transgenic plants also expressed an increase in proteins involved in both the PSII and the PSI complexes.

2.3 Plants' influence on greenhouse gas balance through other pathways than carbon uptake.

2.3.1 Stomatal conductance and transpiration

The amount of water in soil is known to have a significant influence on microbial activity and GHG fluxes (see Section 1 of the 'State of art'). Plant continuously harvests water from soil through its root system for its growth and tissue expansion. As plant biomass increase, water consumption increases as well, progressively depleting water resource in the root zone. Plants influence on soil water content can have a considerable impact on microbial activity by promoting oxygen diffusion in soil and therefore CH_4 oxidation (Feng et al. 2017) and N_2O emissions (Zhang et al. 2015). As a consequence, water consumption by plants should be taken into account when considering plant impact on GHG balance.

Projected increase in mean annual air temperature (IPCC 2014) within the next 50 years is susceptible to induce an increase in plant transpiration rate (E). Selection of plants characterized by an enhanced photosynthesis is also likely to promote E, as carbon assimilation and stomatal conductance are highly correlated (Farquhar and Sharkey 1982). Both phenomena tend to induce a faster plant-mediated depletion of the soil water content in the surrounding rhizosphere, which might benefit CH_4 oxidation and nitrification processes in the following years. Such situation might also impair plants growth due to a quicker water limitation, resulting in NEE decline and carbon storage by ecosystems.

Improvement in plant water-use efficiency (WUE), however, might counterbal-

ances this trend. More than 90% of the water taken by plant is not used in biochemical reactions and is subsequently emitted in the atmosphere through stomata. In a context where water availability is one of the major limiting factor in crop production, many efforts are underway to improve WUE in plants (Morison et al. 2008). The challenge in such improvement lies in the maintenance of high carbon uptake while reducing water loss. The most intuitive approach that has been adopted in many experiments was to manipulate stomatal aperture in order to save water. However, improved WUE by the reduction in g_s was often accompanied by a reduction in photosynthesis (Lawson and Blatt 2014) as g_s and carbon uptake are usually coupled. However, recent studies using antisense technology have shown that g_s and carbon assimilation could be uncoupled in situation of reduced Rubisco activity (von Caemmerer et al. 2004) or electron transport (Baroli et al. 2008). These results, by showing that g_s can be independent of carbon assimilation, therefore offer new perspectives in the amelioration of the WUE. Short-term variations in environmental condition such as light irradiance frequently encountered in field can also lead to transient situation where g_s and A_{CO_2} are not synchronized as shown by McAusland et al. (2016). The authors revealed that upon sudden increase in light, the slow stomatal response could lead to a 10% limitation in A_{net}. However, after reaching 95% of optimal A_{CO_2} in steady conditions, g_s continued to increase by 80% for only a 5% gain in photosynthesis. Improvement in the dynamic of stomatal response to its environment therefore constitutes an interesting alternative approach in the amelioration of WUE (Lawson et al. 2014). Manipulation of genes involved in stomatal development can also offer promising results as shown by the success story of Yoo et al. (2011). Alteration in the expression of GT-2 LIKE 1, a transcription factor involved in the regulation of stomatal density and transpiration, was shown by the authors to reduce by 25% transpiration in Arabidopsis without affecting net carbon assimilation. Regulation of photosynthesis gene expression and regulatory networks involved in the coordination response to the environment still need to be elucidated (Wang et al. 2017). There are also evidences that the redox state of the ETC acts as a signal regulating the opening of stomata, with a higher reduction of the ETC corresponding to a higher stomatal conductance (Busch 2014). In tobacco plants, the overexpression of the PsbS protein, which is involved in NPQ, resulted in a lower reduced state of Q_A and a lower stomatal conductance (Głowacka et al. 2018). Since no significant reduction of photosynthesis was observed in a steady-state, this manip-

ulation resulted in an improved WUE. Such results offer encouraging perspectives in the implication of single gene involved in the regulation of plant WUE.

2.3.2 Biological nitrification inhibition

Recent studies have highlighted the biological nitrification inhibition (BNI) ability of certain plants by releasing biological nitrification inhibitors (BNIs) through their root system (Subbarao et al. 2017). Such activity allows the immobilization of N-soil resource into the less mobile form NH_4^+ by suppressing microbial nitrification. BNI is particularly advantageous in environments where N-soil resources are limited and subjected to leaching in their NO_3^- form. The production and the release of BNIs by plants is triggered by the presence of NH_4^+ in the immediate environment of roots. As nitrifiers are especially found in NH_4^+-rich environment, the release of BNIs is essentially active in environment with potentially high nitrification activity (Subbarao et al. 2015).

Grass species expressing such ability have already been found in savanna (Lata et al. 2004) and tropical pasture (Subbarao et al. 2013) ecosystems. Transfer of BNI traits into highly productive cultivated grassland species offer the opportunity for considerable reduction in ecosystem N_2O emissions (Subbarao et al. 2012, Coskun et al. 2017). Their potential in the reduction of N_2O fluxes was illustrated in an experiment where plants characterized by a high BNI activity was able to reduce N_2O emission from soil treated with bovine urine by 60% compared with plants expressing a lower BNI capacity (Byrnes et al. 2017). A bioassay involving 18 species revealed that the pasture grass *Brachiaria humidicola* was among the tropical forage crops expressing the highest BNI activity (Subbarao et al. 2007). *B. humidicolas* was also characterized by an important genotypic variation in the amount of BNIs released by the root systems (Subbarao et al. 2009). For these reasons, this species may be considered a good candidate for BNI traits transfer into other cultivated grass through breeding approaches.

Intensive use of BNI technology, however, can have potential side effects that need to be considered. For instance, the increase in BNIs production and exudation can have a metabolic cost for the plant (Coskun et al. 2017) that needs to be quantified in order to maintain plant growth and carbon storage by the ecosystem. A meta-analysis also revealed that the use of nitrification inhibitors promoted the increase in NH_3 emission in agricultural soil by 20% (Qiao et al. 2015). NH_3 can later deposit and be oxidized into N_2O, resulting in indirect emission (Lam et al. 2017). This might not be the

case, however, in pasture soils where increased NH_3 emissions were not highlighted by the meta-analysis (Qiao et al. 2015). Further studies are needed to improve our understanding of mechanisms involved in the short and long-term response of pasture ecosystems to nitrification inhibitors.

3 CONCLUSIONS

In this study, we investigated the relationship between the photochemical capacity of an ecosystem and variations in CO_2 fluxes. To this end, three specific objectives were defined and consisted in (1) evaluating the photochemical capacity of primary grasslands species, (2) evaluating the impact of combined environmental constraints on processes involved in the light reaction of photosynthesis and (3) linking alterations in the ecosystem photochemical capacity to ecosystem CO_2 fluxes. We learned from this study that the investigated species were characterized by different acclimatization strategies. We also showed that the efficiency of electron transport at the different steps of the light reactions was impacted differently by environmental constraints. Finally, we showed that variations in GPP were not explained by changes in the ecosystem photochemical capacity. Our study provides a better understanding of the photosynthetic response to combined environmental constraints and their relationship with CO_2 fluxes. We also offer a new insight in the diversity of acclimatization mechanisms in a grassland ecosystem.

There are still some questions remaining to be answered, such as how alterations in photochemical capacity affected carbon assimilation at leaf-scale and to which extent. We also wonder whether plants exhibiting varied acclimatization mechanisms of photosynthesis actually benefit the ecosystem resilience or not. The contribution of soil to measured CO_2 fluxes also remains unknown.

Many perspectives arises from these results, in various fields of study. The definition of stress periods by ChlF can be exploited to associate stressful events to changes in BVOC emission, which was a major goal of the CROSTVOC project. The diversity of acclimatization mechanisms observed in response to environmental constraints also offers perspectives for physiological, ecological and evolutionary studies in order to identify the mechanisms underlying of these differences. These results may also provide potential targets for the development of varieties with improved abiotic stress resistance as the different process involved in the light reactions were differently affected.

Measurements of photochemical capacity performed at leaf-scale were associated with measurements of CO_2 fluxes by eddy covariance in a tentative approach to explain variations in CO_2 fluxes at the ecosystem level by phenomenon occurring at the leaf level. However, this technique showed spatial and temporal limitations, empha-

sizing the need of new tools with higher resolution for a better characterization of the spatial and temporal variation in the field. The development of such tools would offer new perspectives in ecological studies but also in any field of study willing to upscale phenomenons from the molecular level to a higher scale.

VI

Scientific communications

Publications

- Mozaffar A, Schoon N, Digrado A, Bachy A, Delaplace P, du Jardin P, Fauconnier M-L, Aubinet M, Heinesch B, and Amelynck C. 2017. Methanol emissions from maize: Ontogenetic dependence to varying light conditions and guttation as an additional factor constraining the flux. Atmospheric Environment 152: 405-417. doi: 10.1016/j.atmosenv.2016.12.041.

- Digrado A, Bachy A, Mozaffar A, Schoon N, Dalcq A-C, Amelynck C, Bussotti F, Fauconnier M-L, Aubinet M, Heinesch B, du Jardin P, and Delaplace P. 2017. Long-term measurements of chlorophyll a fluorescence using the JIP-test show that combined abiotic stresses influence the photosynthetic performance of the perennial ryegrass (*Lolium perenne* L.) in a managed temperate grassland. *Physiologia Plantarum*, 161(3): 355-371. doi: 10.1111/ppl.12594

- Mozaffar A, Schoon N, Bachy A, Digrado A, Heinesch B, Aubinet M, Fauconnier M-L, Delaplace P, du Jardin P, and Amelynck C. 2018. Biogenic volatile organic compound emissions from senescent maize leaves and a comparison with other leaf developmental stages. Atmospheric Environment 176: 71-81. doi: 10.1016/j.atmosenv.2017.12.020.

- Digrado A, Gourlez de la Motte L, Bachy A, Mozaffar A, Schoon N, Bussotti F, Amelynck C, Dalcq A-C, Fauconnier M-L, Aubinet M, Heinesch B, du Jardin P, and Delaplace P. 2017. Decrease in the photosynthetic performance of temperate grassland species does not lead to a decline in the gross primary production of the ecosystem. *Frontiers in Plants Science*: Accepted. doi: 10.3389/fpls.2018.00067.

Oral presentations

- Digrado A, Bachy A, Mozaffar A, Schoon N, Dalcq A-C, Amelynck C, Bussotti F, Fauconnier M-L, Aubinet M, Heinesch B, du Jardin P, and Delaplace P. 2017. Photosynthetic apparatus response of the *Lolium perenne* L. to environmental stresses in a temperate grassland by chlorophyll fluorescence. *EDT annual plant science meeting 2017*, Liège, Belgium.

Posters

- Digrado A, Mozaffar A, Bachy A, Schoon N, Amelynck C, Fauconnier M-L, Aubinet M, Heinesch B, du Jardin P, and Delaplace P. 2014. Impact of abiotic stresses on volatile organic compound production of field crops and grasslands. *19th National Symposium on Applied Biological Sciences*, Gembloux, Belgium.

- Heinesch B, Amelynck C, Aubinet M, Bachy A, Digrado A, Delaplace P, du Jardin P, Fauconnier M-L., Mozaffar A, and Schoon N 2014. CROSTVOC: an integrated project for studying the impact of abiotic stresses on BVOC production of field crops and grasslands. *Gordon Research Conference Biogenic Hydrocarbons & the Atmosphere, Interactions in a Changing World*, Girona, Spain.

- Michel C, Heinesch B, Bachy A, Aubinet M, Digrado A, Delaplace P, du jardin P, Fauconnier M-L, Amelynck C, Schoon N, and Mozaffar A. 2015. Environmental controls of biogenic volatile organic compound emissions from a grazed grassland in Dorinne, Belgium. *New Perspectives in Modeling and Measurement of Biogenic Volatile Organic Compounds Emissions by Remote Sensing*, Anvers, Belgium.

- Mozaffar A, Amelynck C, Bachy A, Digrado A, Delaplace P, du Jardin P, Fauconnier M-L, Schoon N, Aubinet M, and Heinesch B. 2015. Biogenic Volatile Organic Compound (BVOC) emissions from agricultural crop species: is guttation a possible source for methanol emissions following light/dark transition? *European Geosciences Union General Assembly 2015*, Vienna, Austria.

- Amelynck C, Heinesch B, Aubinet M, Bachy A, Delaplace P, Digrado A, du Jardin P, Fauconnier M-L, Mozaffar A, and Schoon N. 2015. The CROSTVOC project - an integrated approach to study the effect of stress on BVOC exchange between agricultural crops and grassland ecosystems and the atmosphere. *European Geosciences Union general Assembly 2015*, Vienna, Austria.

- Digrado A, Bachy A, Mozaffar A, Schoon N, Amelynck C, Fauconnier M-L, Aubinet M, Heinesch B, du Jardin P, and Delaplace P. 2016. Chlorophyll *a* fluorescence: a tool to assess the photosynthetic apparatus behavior. Terra inovation Fair, Gembloux, Belgique.

- Bachy A, Mozaffar A, Aubinet M, Amelynck C, Schoon N, Bodson B, Moureaux C, Digrado A, Delaplace P, du Jardin P, Fauconnier M-L, and Heinesch B. 2016. Disentangling soil from plant methanol exchanges in a maize field: a first step. *Gordon Research Conference Biogenic Hydrocarbons & the Atmosphere*, Girona, Spain.

- Mozaffara A, Schoon N, Digrado A, Bachy A, Delaplace P, du Jardin P, Fauconnier M-L, Aubinet M, Heinesch B, and Amelynck C. 2016. BVOC fluxes from maize: flux intensity, pattern, and composition changes from leaf emergence to senescence. *Gordon Research Conference Biogenic Hydrocarbons & the Atmosphere, Interactions in a Changing World*, Girona, Spain.

- Digrado A,, Bachy A, Mozaffar A, Schoon N, Dalcq A-C, Amelynck C, Bussotti F, Fauconnier M-L, Aubinet M, Heinesch B, du Jardin P, and Delaplace P. 2017. Long-term field study of the photosynthetic performance and acclimation potential of *Lolium perenne* L. facing combined environmental constraints in a temperate managed grassland. *2nd Agriculture and Climate Change Conference*, Sitges, Spain.

- Digrado A, Gourlez de la Motte L, Bachy A, Mozaffar A, Schoon N, Dalcq A-C, Amelynck C, Bussotti F, Fauconnier M-L, Aubinet M, Heinesch B, du Jardin P, and Delaplace P. 2017. Long-term field study of the influence of the photosynthetic performance of temperate grassland species on ecosystem CO_2 exchange fluxes at the ecosystem-scale. *Gordon Research Conference CO_2 Assimilation in Plants from Genome to Biome*, Lucca, Italy.

- Mozaffara A, Schoon N, Bachy A, Digrado A, Heinesch B, Aubinet M, Fauconnier M-L, Delaplace P, du Jardin P, and Amelynck C. 2017. Grazing-induced BVOC fluxes from a managed grassland. *European Geosciences Union General Assembly 2017*, Vienna, Austria.

BIBLIOGRAPHY

Aalto, J., Porcar-Castell, A., Atherton, J., Kolari, P., Pohja, T., Hari, P., Nikinmaa, E., PetÄJÄ, T., and Bäck, J. (2015). Onset of photosynthesis in spring speeds up monoterpene synthesis and leads to emission bursts. *Plant, Cell & Environment*, 38(11):2299–2312.

Abberton, M., Batley, J., Bentley, A., Bryant, J., Cai, H., Cockram, J., Costa de Oliveira, A., Cseke, L. J., Dempewolf, H., De Pace, C., Edwards, D., Gepts, P., Greenland, A., Hall, A. E., Henry, R., Hori, K., Howe, G. T., Hughes, S., Humphreys, M., Lightfoot, D., Marshall, A., Mayes, S., Nguyen, H. T., Ogbonnaya, F. C., Ortiz, R., Paterson, A. H., Tuberosa, R., Valliyodan, B., Varshney, R. K., and Yano, M. (2016). Global agricultural intensification during climate change: a role for genomics. *Plant Biotechnology Journal*, 14(4):1095–1098.

Adams, W. W. and Demmig-Adams, B. (2004). Chlorophyll Fluorescence as a Tool to Monitor Plant Response to the Environment. In *Papageorgiou, G.C. and Govindjee (Eds.) Chlorophyll a Fluorescence: A Signature of Photosynthesis*, chapter Chlorophyl, pages 583–604. Springer Netherlands, Dordrecht.

Adams, W. W., Muller, O., Cohu, C. M., and Demmig-Adams, B. (2013). May photoinhibition be a consequence, rather than a cause, of limited plant productivity? *Photosynthesis Research*, 117(1):31–44.

Adams III, W. W., Zarter, C. R., Mueh, K. E., Amiard, V., and Demmig-Adams, B. (2006). Energy Dissipation and Photoinhibition: A Continuum of Photoprotection. In *Demmig-Adams, B and Adams, William W and Mattoo, Autar K (Eds.) Photoprotection, Photoinhibition, Gene Regulation, and Environment*, pages 49–64. Springer, Dordrecht, The Netherlands.

Adir, N., Zer, H., Shochat, S., and Ohad, I. (2003). Photoinhibition - a historical perspective. *Photosynthesis Research*, 76(1):343.

Aigner, H., Wilson, R. H., Bracher, A., Calisse, L., Bhat, J. Y., Hartl, F. U., and Hayer-Hartl, M. (2017). Plant RuBisCo assembly in *E. coli* with five chloroplast chaperones including BSD2. *Science*, 358(6368):1272–1278.

Ajigboye, O. O., Bousquet, L., Murchie, E. H., and Ray, R. V. (2016). Chlorophyll fluorescence parameters allow the rapid detection and differentiation of plant responses in three different wheat pathosystems. *Functional Plant Biology*, 43(4):356–369.

Al-Khatib, K. and Paulsen, G. M. (1989). Enhancement of thermal injury to photosynthesis in wheat plants and thylakoids by high light intensity. *Plant Physiology*, 90(3):1041–1048.

Allen, V. G., Batello, C., Berretta, E. J., Hodgson, J., Kothmann, M., Li, X., McIvor, J., Milne, J., Morris, C., Peeters, A., Sanderson, M., Committee, T. F., and Terminology, G. (2011). An international terminology for grazing lands and grazing animals. *Grass and Forage Science*, 66(1):2–28.

Andralojc, P. J., Bencze, S., Madgwick, P. J., Philippe, H., Powers, S. J., Shield, I., Karp, A., and Parry, M. A. J. (2014). Photosynthesis and growth in diverse willow genotypes. *Food and Energy Security*, 3(2):69–85.

Andriuzzi, W. S. and Wall, D. H. (2017). Responses of belowground communities to large aboveground herbivores: Meta-analysis reveals biome-dependent patterns and critical research gaps. *Global Change Biology*, 23(9):3857–3868.

Aprile, A., Havlickova, L., Panna, R., Marè, C., Borrelli, G. M., Marone, D., Perrotta, C., Rampino, P., De Bellis, L., Curn, V., Mastrangelo, A. M., Rizza, F., and Cattivelli, L. (2013). Different stress responsive strategies to drought and heat in two durum wheat cultivars with contrasting water use efficiency. *BMC Genomics*, 14(1):821.

Arbona, V., López-Climent, M. F., Pérez-Clemente, R. M., and Gómez-Cadenas, A. (2009). Maintenance of a high photosynthetic performance is linked to flooding tolerance in citrus. *Environmental and Experimental Botany*, 66(1):135–142.

Arend, M., Brem, A., Kuster, T. M., and Günthardt-Goerg, M. S. (2013). Seasonal photosynthetic responses of European oaks to drought and elevated daytime temperature. *Plant Biology*, 15(s1):169–176.

Arimura, G.-I., Kost, C., and Boland, W. (2005). Herbivore-induced, indirect plant defences. *Biochimica et Biophysica Acta*, 1734:91–111.

Aro, E. M., McCaffery, S., and Anderson, J. M. (1994). Recovery from photoinhibition in peas (*Pisum sativum* L.) acclimated to varying growth irradiances (role of D1 protein turnover). *Plant Physiology*, 104(3):1033–1041.

Asada, K. (2006). Production and scavenging of reactive oxygen species in chloroplasts and their functions. *Plant Physiology*, 141(2):391–396.

Ashraf, M. and Harris, P. J. C. (2013). Photosynthesis under stressful environments: An overview. *Photosynthetica*, 51(2):163–190.

Atkin, O. K. and Tjoelker, M. G. (2003). Thermal acclimation and the dynamic response of plant respiration to temperature. *Trends in Plant Science*, 8(7):343–351.

Atkin, O. K., Westbeek, M. H. M., Cambridge, M. L., Lambers, H., and Pons, T. L. (1997). Leaf respiration in light and darkness. A comparison of slow- and fast-growing *Poa* species). *Plant Physiology*, 113(3):961 LP – 965.

Atkinson, R. and Arey, J. (2003). Atmospheric Degradation of Volatile Organic Compounds. *Chemical Reviews*, 103(12):4605–4638.

Aubinet, M. (2008). Eddy Covariance CO_2; Flux Measurements in Nocturnal Conditions: An Analysis of the Problem. *Ecological Applications*, 18(6):1368–1378.

Aubinet, M., Feigenwinter, C., Heinesch, B., Bernhofer, C., Canepa, E., Lindroth, A., Montagnani, L., Rebmann, C., Sedlak, P., and Van Gorsel, E. (2010). Direct advection measurements do not help to solve the night-time CO_2 closure problem: Evidence from three different forests. *Agricultural and Forest Meteorology*, 150(5):655–664.

Aubinet, M., Grelle, A., Ibrom, A., Rannik, Ü., Moncrieff, J., Foken, T., Kowalski, A. S., Martin, P. H., Berbigier, P., Bernhofer, C., Clement, R., Elbers, J., Granier, A., Grünwald, T., Morgenstern, K., Pilegaard, K., Rebmann, C., Snijders, W., Valentini, R., and Vesala, T. (1999). Estimates of the Annual Net Carbon and Water

Exchange of Forests: The EUROFLUX Methodology. *Advances in Ecological Research*, 30:113–175.

Bai, J., Xu, D. H., Kang, H. M., Chen, K., and Wang, G. (2008). Photoprotective function of photorespiration in *Reaumuria soongorica* during different levels of drought stress in natural high irradiance. *Photosynthetica*, 46(2):232–237.

Baker, N. R. (2008). Chlorophyll Fluorescence: A Probe of Photosynthesis In Vivo. *Annual Review of Plant Biology*, 59(1):89–113.

Baldocchi, D., Chu, H., and Reichstein, M. (2018). Inter-annual variability of net and gross ecosystem carbon fluxes: A review. *Agricultural and Forest Meteorology*, 249(Supplement C):520–533.

Baldocchi, D. D. (2003). Assessing the eddy covariance technique for evaluating carbon dioxide exchange rates of ecosystems: past, present and future. *Global Change Biology*, 9(4):479–492.

Baldocchi, D. D. (2008). Turner review No. 15. 'Breathing' of the terrestrial biosphere: lessons learned from a global network of carbon dioxide flux measurement systems. *Australian Journal of Botany*, 56(15):1–26.

Balla, K., Bencze, S., Bónis, P., Árendás, T., and Veisz, O. (2014). Changes in the photosynthetic efficiency of winter wheat in response to abiotic stress. *Open Life Sciences*, 9(5):519–530.

Balouchi, H. R. (2010). Screening Wheat Parents of Mapping Population for Heat and Drought Tolerance, Detection of Wheat Genetic Variation. *International Journal of Biological and Life Sciences*, 6(1):56–66.

Bamberger, I., Hörtnagl, L., Ruuskanen, T. M., Schnitzhofer, R., Müller, M., Graus, M., Karl, T., Wohlfahrt, G., and Hansel, A. (2011). Deposition Fluxes of Terpenes over Grassland. *Journal of geophysical research. Atmospheres : JGR*, 116(D14).

Bamberger, I., Hörtnagl, L., Schnitzhofer, R., Graus, M., Ruuskanen, T. M., Müller, M., Dunkl, J., Wohlfahrt, G., and Hansel, A. (2010). BVOC fluxes above mountain grassland. *Biogeosciences*, 7(5):1413–1424.

Baroli, I., Price, G. D., Badger, M. R., and von Caemmerer, S. (2008). The Contribution of Photosynthesis to the Red Light Response of Stomatal Conductance. *Plant Physiology*, 146(2):737–747.

Barton, L., Kiese, R., Gatter, D., Butterbach-bahl, K., Buck, R., Hinz, C., and Murphy, D. V. (2008). Nitrous oxide emissions from a cropped soil in a semi-arid climate. *Global Change Biology*, 14(1):177–192.

Barua, D. and Heckathorn, S. A. (2006). The interactive effects of light and temperature on heat-shock protein accumulation in *Solidago altissima* (Asteraceae) in the field and laboratory. *American Journal of Botany*, 93(1):102–109.

Beckett, M., Loreto, F., Velikova, V., Brunetti, C., Di Ferdinando, M., Tattini, M., Calfapietra, C., and Farrant, J. M. (2012). Photosynthetic limitations and volatile and non-volatile isoprenoids in the poikilochlorophyllous resurrection plant (*Xerophyta humilis* during dehydration and rehydration. *Plant, Cell & Environment*, 35(12):2061–2074.

Benckiser, G., Schartel, T., and Weiske, A. (2015). Control of NO_3^- and N_2O emissions in agroecosystems: a review. *Agronomy for Sustainable Development*, 35(3):1059–1074.

Bertolde, F. Z., Almeida, A.-A., Pirovani, C. P., Gomes, F. P., Ahnert, D., Baligar, V. C., and Valle, R. R. (2012). Physiological and biochemical responses of *Theobroma cacao* L. genotypes to flooding. *Photosynthetica*, 50(3):447–457.

Bielczynski, L. W., Schansker, G., and Croce, R. (2016). Effect of Light Acclimation on the Organization of Photosystem II Super- and Sub-Complexes in Arabidopsis thaliana.

Bijlsma, R. and Loeschcke, V. (2005). Environmental stress, adaptation and evolution: an overview. *Journal of Evolutionary Biology*, 18(4):744–749.

Björkman, O. and Demmig, B. (1987). Photon yield of O_2 evolution and chlorophyll fluorescence characteristics at 77 K among vascular plants of diverse origins. *Planta*, 170(4):489–504.

Blair, M. W., González, L. F., Kimani, P. M., and Butare, L. (2010). Genetic diversity, inter-gene pool introgression and nutritional quality of common beans (*Phaseolus*

vulgaris L.) from Central Africa. *TAG. Theoretical and Applied Genetics. Theoretische Und Angewandte Genetik*, 121(2):237–248.

Bodelier, P. L. E. and Laanbroek, H. J. (2004). Nitrogen as a regulatory factor of methane oxidation in soils and sediments. *FEMS Microbiology Ecology*, 47(3):265–277.

Bollig, C. and Feller, U. (2014). Impacts of drought stress on water relations and carbon assimilation in grassland species at different altitudes. *Agriculture, Ecosystems & Environment*, 188:212–220.

Borchard, N., Schirrmann, M., von Hebel, C., Schmidt, M., Baatz, R., Firbank, L., Vereecken, H., and Herbst, M. (2015). Spatio-temporal drivers of soil and ecosystem carbon fluxes at field scale in an upland grassland in Germany. *Agriculture, Ecosystems & Environment*, 211:84–93.

Bouchemal, K., Bouldjadj, R., Belbekri, M. N., Ykhlef, N., and Djekoun, A. (2017). Differences in antioxidant enzyme activities and oxidative markers in ten wheat (*Triticum durum* Desf.) genotypes in response to drought, heat and paraquat stress. *Archives of Agronomy and Soil Science*, 63(5):710–722.

Boughalleb, F., Denden, M., and Ben Tiba, B. (2009). Photosystem II photochemistry and physiological parameters of three fodder shrubs, *Nitraria retusa*, *Atriplex halimus* and *Medicago arborea* under salt stress. *Acta Physiologiae Plantarum*, 31(3):463–476.

Boureima, S., Oukarroum, A., Diouf, M., Cisse, N., and Van Damme, P. (2012). Screening for drought tolerance in mutant germplasm of sesame (Sesamum indicum) probing by chlorophyll a fluorescence. *Environmental and Experimental Botany*, 81:37–43.

Boval, M., Cruz, P., Ledet, J. E., Coppry, O., and Archimede, H. (2002). Effect of nitrogen on intake and digestibility of a tropical grass grazed by Creole heifers. *Journal of Agricultural Science*, 138(1):73–84.

Boval, M. and Dixon, R. M. (2012). The importance of grasslands for animal production and other functions: a review on management and methodological progress in the tropics. *Animal : An International Journal of Animal Bioscience*, 6(5):748–62.

Bremner, J. M. (1997). Sources of nitrous oxide in soils. *Nutrient Cycling in Agroecosystems*, 49(1):7–16.

Brendley, B. W. and Pell, E. J. (1998). Ozone-induced changes in biosynthesis of Rubisco and associated compensation to stress in foliage of hybrid poplar. *Tree physiology*, 18(2):81–90.

Bressan, M., Dall'Osto, L., Bargigia, I., Alcocer, M. J. P., Viola, D., Cerullo, G., D'Andrea, C., Bassi, R., and Ballottari, M. (2016). LHCII can substitute for LHCI as an antenna for photosystem I but with reduced light-harvesting capacity. *Nature Plants*, 2:16131.

Bresson, J., Vasseur, F., Dauzat, M., Koch, G., Granier, C., and Vile, D. (2015). Quantifying spatial heterogeneity of chlorophyll fluorescence during plant growth and in response to water stress. *Plant methods*, 11:23.

Brestic, M., Zivcak, M., Kalaji, H. M., Carpentier, R., and Allakhverdiev, S. I. (2012). Photosystem II thermostability in situ: environmentally induced acclimation and genotype-specific reactions in *Triticum aestivum* L. *Plant physiology and biochemistry : PPB / Société française de physiologie végétale*, 57:93–105.

Brestic, M. and Zivcak, M. (2013). PSII fluorescence techniques for measurement of drought and high temperature stress signal in crop plants: protocols and applications. In *Rout, G.R., and Das, A.B. (Eds.) Molecular Stress Physiology of Plants*, pages 87–131. Springer, Dordrecht, India.

Brilli, F., Barta, C., Fortunati, A., Lerdau, M., Loreto, F., and Centritto, M. (2007). Response of isoprene emission and carbon metabolism to drought in white poplar (*Populus alba*) saplings. *New Phytologist*, 175(2):244–254.

Brunner, A., Ammann, C., Neftel, A., and Spirig, C. (2007). Methanol exchange between grassland and the atmosphere. *Biogeosciences*, 4(3):395–410.

Buchner, O., Stoll, M., Karadar, M., Kranner, I., and Neuner, G. (2015). Application of heat stress in situ demonstrates a protective role of irradiation on photosynthetic performance in alpine plants. *Plant, Cell & Environment*, 38(4):812–26.

Buonasera, K., Lambreva, M., Rea, G., Touloupakis, E., and Giardi, M. T. (2011). Technological applications of chlorophyll a fluorescence for the assessment of environmental pollutants. *Analytical and Bioanalytical Chemistry*, 401(4):1139.

Busch, F. A. (2014). Opinion: The red-light response of stomatal movement is sensed by the redox state of the photosynthetic electron transport chain. *Photosynthesis Research*, 119(1):131–140.

Bussotti, F. (2004). Assessment of stress conditions in *Quercus ilex* L. leaves by O-J-I-P chlorophyll a fluorescence analysis. *Plant Biosystems - An International Journal Dealing with all Aspects of Plant Biology*, 138(2):101–109.

Bussotti, F., Agati, G., Desotgiu, R., Matteini, P., and Tani, C. (2005). Ozone foliar symptoms in woody plant species assessed with ultrastructural and fluorescence analysis. *The New phytologist*, 166(3):941–55.

Bussotti, F., Desotgiu, R., Cascio, C., Strasser, R. J., Gerosa, G., and Marzuoli, R. (2007a). Photosynthesis responses to ozone in young trees of three species with different sensitivities, in a 2-year open-top chamber experiment (Curno, Italy). *Physiologia Plantarum*, 130(1):122–135.

Bussotti, F., Strasser, R. J., and Schaub, M. (2007b). Photosynthetic behavior of woody species under high ozone exposure probed with the JIP-test: a review. *Environmental Pollution*, 147(3):430–437.

Bussotti, F., Desotgiu, R., Pollastrini, M., and Cascio, C. (2010). The JIP test: a tool to screen the capacity of plant adaptation to climate change. *Scandinavian Journal of Forest Research*, 25(sup8):43–50.

Bussotti, F., Desotgiu, R., Cascio, C., Pollastrini, M., Gravano, E., Gerosa, G., Marzuoli, R., Nali, C., Lorenzini, G., Salvatori, E., Manes, F., Schaub, M., and Strasser, R. J. (2011). Ozone stress in woody plants assessed with chlorophyll a fluorescence. A critical reassessment of existing data. *Environmental and Experimental Botany*, 73(1):19–30.

Bussotti, F., Ferrini, F., Pollastrini, M., and Fini, A. (2014). The challenge of Mediterranean sclerophyllous vegetation under climate change: From acclimation to adaptation. *Environmental and Experimental Botany*, 103:80–98.

Bussotti, F., Pollastrini, M., Holland, V., and Brüggemann, W. (2015). Functional traits and adaptive capacity of European forests to climate change. *Environmental and Experimental Botany*, 111:91–113.

Byrnes, R. C., Nùñez, J., Arenas, L., Rao, I., Trujillo, C., Alvarez, C., Arango, J., Rasche, F., and Chirinda, N. (2017). Biological nitrification inhibition by *Brachiaria* grasses mitigates soil nitrous oxide emissions from bovine urine patches. *Soil Biology and Biochemistry*, 107:156–163.

Calatayud, A. and Barreno, E. (2004). Response to ozone in two lettuce varieties on chlorophyll a fluorescence, photosynthetic pigments and lipid peroxidation. *Plant Physiology and Biochemistry*, 42(6):549–555.

Calatayud, V., Cerveró, J., and Sanz, M. J. (2007). Foliar, physiologial and growth responses of gour maple species exposed to ozone. *Water, Air, and Soil Pollution*, 185(1):239–254.

Calfapietra, C., Fares, S., and Loreto, F. (2009). Volatile organic compounds from Italian vegetation and their interaction with ozone. *Environmental Pollution*, 157(5):1478–1486.

Campos, H., Trejo, C., Peña-Valdivia, C. B., García-Nava, R., Conde-Martínez, F. V., and Cruz-Ortega, M. D. R. (2014). Photosynthetic acclimation to drought stress in Agave salmiana Otto ex Salm-Dyck seedlings is largely dependent on thermal dissipation and enhanced electron flux to photosystem I. *Photosynthesis research*, 122(1):23–39.

Cao, G., Tang, Y., Mo, W., Wang, Y., Li, Y., and Zhao, X. (2004). Grazing intensity alters soil respiration in an alpine meadow on the Tibetan plateau. *Soil Biology and Biochemistry*, 36(2):237–243.

Carvalho, L. C., Vidigal, P., and Amâncio, S. (2015). Oxidative stress homeostasis in grapevine (*Vitis vinifera* L.). *Frontiers in Environmental Science*, 3:20.

Carvalho, L. C., Coito, J. L., Gonçalves, E. F., Chaves, M. M., and Amâncio, S. (2016). Differential physiological response of the grapevine varieties Touriga Nacional and Trincadeira to combined heat, drought and light stresses. *Plant Biology*, 18(S1):101–111.

Cascio, C., Schaub, M., Novak, K., Desotgiu, R., Bussotti, F., and Strasser, R. J. (2010). Foliar responses to ozone of *Fagus sylvatica* L. seedlings grown in shaded and in full sunlight conditions. *Environmental and Experimental Botany*, 68(2):188–197.

Cavanagh, A. P. and Kubien, D. S. (2014). Can phenotypic plasticity in Rubisco performance contribute to photosynthetic acclimation? *Photosynthesis Research*, 119(1-2):203–214.

Ceppi, M. G., Oukarroum, A., Çiçek, N., Strasser, R. J., and Schansker, G. (2012). The IP amplitude of the fluorescence rise OJIP is sensitive to changes in the photosystem I content of leaves: a study on plants exposed to magnesium and sulfate deficiencies, drought stress and salt stress. *Physiologia plantarum*, 144(3):277–88.

Chadwick, D., Sommer, S., Thorman, R., Fangueiro, D., Cardenas, L., Amon, B., and Misselbrook, T. (2011). Manure management: Implications for greenhouse gas emissions. *Animal Feed Science and Technology*, 166:514–531.

Chang, J., Ciais, P., Viovy, N., Vuichard, N., Sultan, B., and Soussana, J.-F. (2015). The greenhouse gas balance of European grasslands. *Global Change Biology*, 21(10):3748–3761.

Chang, J., Ciais, P., Viovy, N., Vuichard, N., Herrero, M., Havlík, P., Wang, X., Sultan, B., and Soussana, J.-F. (2016). Effect of climate change, CO_2 trends, nitrogen addition, and land-cover and management intensity changes on the carbon balance of European grasslands. *Global Change Biology*, 22(1):338–350.

Chapuis-lardy, L., Wrage, N., Metay, A., Chotte, J.-L., and Bernoux, M. (2007). Soils, a sink for N_2O? A review. *Global Change Biology*, 13(1):1–17.

Chastain, D. R., Snider, J. L., Choinski, J. S., Collins, G. D., Perry, C. D., Whitaker, J., Grey, T. L., Sorensen, R. B., van Iersel, M., Byrd, S. A., and Porter, W. (2016). Leaf ontogeny strongly influences photosynthetic tolerance to drought and high temperature in *Gossypium hirsutum*. *Journal of Plant Physiology*, 199:18–28.

Chen, J., Luo, Y., Xia, J., Wilcox, K. R., Cao, J., Zhou, X., Jiang, L., Niu, S., Estera, K. Y., Huang, R., Wu, F., Hu, T., Liang, J., Shi, Z., Guo, J., and Wang, R.-W. (2017). Warming effects on ecosystem carbon fluxes are modulated by plant functional types. *Ecosystems*, 20:515.

Chen, K., Sun, X., Amombo, E., Zhu, Q., Zhao, Z., Chen, L., Xu, Q., and Fu, J. (2014). High correlation between thermotolerance and photosystem II activity in tall fescue. *Photosynthesis research*, 122(3):305–14.

Chen, M. and Blankenship, R. E. (2011). Expanding the solar spectrum used by photosynthesis. *Trends in Plant Science*, 16(8):427–431.

Chen, M., Schliep, M., Willows, R. D., Cai, Z.-L., Neilan, B. A., and Scheer, H. (2010). A Red-Shifted Chlorophyll. *Science*, 329(5997):1318 LP – 1319.

Chen, S., Kang, Y., Zhang, M., Wang, X., Strasser, R. J., Zhou, B., and Qiang, S. (2015). Differential sensitivity to the potential bioherbicide tenuazonic acid probed by the JIP-test based on fast chlorophyll fluorescence kinetics. *Environmental and Experimental Botany*, 112:1–15.

Chen, Z., Ding, W., Xu, Y., Müller, C., Yu, H., and Fan, J. (2016). Increased N_2O emissions during soil drying after waterlogging and spring thaw in a record wet year. *Soil Biology and Biochemistry*, 101:152–164.

Chung, D. W., Pružinská, A., Hörtensteiner, S., and Ort, D. R. (2006). The Role of Pheophorbide *a* Oxygenase Expression and Activity in the Canola Green Seed Problem. *Plant Physiology*, 142(1):88 LP – 97.

Ciccarelli, D., Picciarelli, P., Bedini, G., and Sorce, C. (2016). Mediterranean sea cliff plants: morphological and physiological responses to environmental conditions. *Journal of Plant Ecology*, 9(2):153–164.

Conrad, R. (1996). Soil microorganisms as controllers of atmospheric trace gases (H_2, CO, CH_4, OCS, N_2O, and NO). *Microbiological Reviews*, 60(4):609–640.

Contin, D. R., Soriani, H. H., Hernández, I., Furriel, R. P. M., Munné-Bosch, S., and Martinez, C. A. (2014). Antioxidant and photoprotective defenses in response to gradual water stress under low and high irradiance in two Malvaceae tree species used for tropical forest restoration. *Trees*, 28(6):1705–1722.

Contran, N., Günthardt-Goerg, M. S., Kuster, T. M., Cerana, R., Crosti, P., and Paoletti, E. (2013). Physiological and biochemical responses of *Quercus pubescens* to air warming and drought on acidic and calcareous soils. *Plant Biology*, 15(s1):157–168.

Coskun, D., Britto, D. T., Shi, W., and Kronzucker, H. J. (2017). Nitrogen transformations in modern agriculture and the role of biological nitrification inhibition. *Nature Plants*, 3(6):17074.

Crafts-Brandner, S. J. and Salvucci, M. E. (2002). Sensitivity of Photosynthesis in a C4 Plant, Maize, to Heat Stress. *Plant physiology*, 129(4):1773–1780.

Croft, H., Chen, J. M., Luo, X., Bartlett, P., Chen, B., and Staebler, R. M. (2017). Leaf chlorophyll content as a proxy for leaf photosynthetic capacity. *Global Change Biology*, 23(9):3513–3524.

Cruz de Carvalho, R., Cunha, A., and Marques da Silva, J. (2010). Photosynthesis by six Portuguese maize cultivars during drought stress and recovery. *Acta Physiologiae Plantarum*, 33(2):359–374.

Czyczyło-Mysza, I., Tyrka, M., Marcińska, I., Skrzypek, E., Karbarz, M., Dziurka, M., Hura, T., Dziurka, K., and Quarrie, S. A. (2013). Quantitative trait loci for leaf chlorophyll fluorescence parameters, chlorophyll and carotenoid contents in relation to biomass and yield in bread wheat and their chromosome deletion bin assignments. *Molecular Breeding*, 32(1):189–210.

Dagnelie, P. (2013). *Statistique théorique et appliquée. Tome 1. Statistique descriptive et bases de l'inférence statistique*. de Boeck, Bruxelles, BE.

Davison, B., Brunner, A., Ammann, C., Spirig, C., Jocher, M., and Neftel, A. (2008). Cut-induced VOC emissions from agricultural grasslands. *Plant Biology*, 10(1):76–85.

de Bossoreille de Ribou, S., Douam, F., Hamant, O., Frohlich, M. W., and Negrutiu, I. (2013). Plant science and agricultural productivity: Why are we hitting the yield ceiling? *Plant Science*, 210:159–176.

De Ronde, J., Cress, W., Krüger, G., Strasser, R., and Van Staden, J. (2004). Photosynthetic response of transgenic soybean plants, containing an Arabidopsis P5CR gene, during heat and drought stress. *Journal of Plant Physiology*, 161(11):1211–1224.

Degola, L., Trupa, A., and Aplocina, E. (2016). Forage quality and digestibility for calculation of enteric methane emission from cattle. In *Engineering for Rural De-*

velopment, volume 2016-Janua, pages 456–461, Latvia University of Agriculture, Institute of Agrobiotechnology, Latvia.

Demmig-Adams, B. and Adams, W. W. (2006). Photoprotection in an ecological context: the remarkable complexity of thermal energy dissipation. *The New phytologist*, 172(1):11–21.

Derks, A., Schaven, K., and Bruce, D. (2015). Diverse mechanisms for photoprotection in photosynthesis. Dynamic regulation of photosystem II excitation in response to rapid environmental change. *Biochimica et Biophysica Acta (BBA) - Bioenergetics*, 1847(4):468–485.

Desotgiu, R., Bussotti, F., Faoro, F., Iriti, M., Agati, G., Marzuoli, R., Gerosa, G., and Tani, C. (2010). Early events in *Populus* hybrid and *Fagus sylvatica* leaves exposed to ozone. *TheScientificWorldJournal*, 10:512–27.

Desotgiu, R., Cascio, C., Pollastrini, M., Gerosa, G., Marzuoli, R., and Bussotti, F. (2012a). Short and long term photosynthetic adjustments in sun and shade leaves of *Fagus sylvatica* L., investigated by fluorescence transient (FT) analysis. *Plant Biosystems*, 146(SUPPL. 1):206–216.

Desotgiu, R., Pollastrini, M., Cascio, C., Gerosa, G., Marzuoli, R., and Bussotti, F. (2012b). Chlorophyll alpha fluorescence analysis along a vertical gradient of the crown in a poplar (Oxford clone) subjected to ozone and water stress. *Tree physiology*, 32(8):976–86.

Dettmer, K. and Engewald, W. (2003). Ambient air analysis of volatile organic compounds using adsorptive enrichment. *Chromatographia*, 57(1):S339–S347.

Dickinson, P. J., Kumar, M., Martinho, C., Yoo, S. J., Lan, H., Artavanis, G., Charoensawan, V., Schöttler, M. A., Bock, R., Jaeger, K. E., and Wigge, P. A. (2018). Chloroplast Signaling Gates Thermotolerance in Arabidopsis. *Cell Reports*, 22(7):1657–1665.

Digrado, A., Bachy, A., Mozaffar, A., Schoon, N., Dalcq, A.-C., Amelynck, C., Bussotti, F., Fauconnier, M.-L., Aubinet, M., Heinesch, B., du Jardin, P., and Delaplace, P. (2017). Long-term measurements of chlorophyll a fluorescence using the JIP-test show that combined abiotic stresses influence the photosynthetic performance

of the perennial ryegrass (*Lolium perenne* L.) in a managed temperate grassland. *Physiologia Plantarum*, 161(3):355–371.

Ding, W., Cai, Z., and Tsuruta, H. (2004). Cultivation, nitrogen fertilization, and set-aside effects on methane uptake in a drained marsh soil in Northeast China. *Global Change Biology*, 10(10):1801–1809.

D'Ippoliti, D., Michelozzi, P., Marino, C., De'Donato, F., Menne, B., Katsouyanni, K., Kirchmayer, U., Analitis, A., Medina-Ramón, M., Paldy, A., Atkinson, R., Kovats, S., Bisanti, L., Schneider, A., Lefranc, A., Iñiguez, C., Perucci, C. A., Basu, R., Samet, J., Meehl, G., Tebaldi, C., Hajat, S., Kovats, S., Atkinson, R., Haines, A., Diaz, J., Jordán, A., Garcia, R., Kyselý, J., Michelozzi, P., De, F., Sardon, J., Robine, J., Cheung, S., Roy, S. L., Oyen, H. V., Griffiths, C., Michel, J., Herrmann, F., Weissekopf, M., Anderson, H., Foldy, S., Michelozzi, P., De, F., Schwartz, J., Michelozzi, P., Kirchmayer, U., Katsouyanni, K., Kalkstein, L., Valimont, K., O'Neill, M., Zanobetti, A., Schwartz, J., Liang, K., Zeger, S., Baccini, M., Biggeri, A., Accetta, G., Schwartz, J., Dockery, D., Hajat, S., Armstrong, B., Baccini, M., Fouillet, A., Rey, G., Wagner, V., Diggle, P., Liang, K., Zeger, S., Chiogna, M., Gaetan, C., Chiogna, M., Gaetan, C., Samoli, E., Aga, E., Touloumi, G., Egger, M., Smith, G. D., Altman, D., Bouchama, A., Tertre, A. L., Lefranc, A., Eilstein, D., Huynen, M., Martens, P., Schram, D., Sprung, C., El-Kassimi, F., Al-Mashhadani, S., Akhtar, J., Michelozzi, P., Accetta, G., Sario, M. D., Braga, A., Zanobetti, A., Schwartz, J., Hajat, S., Armstrong, B., Gouveia, N., and Wilkinson, P. (2010). The impact of heat waves on mortality in 9 European cities: results from the EuroHEAT project. *Environmental Health*, 9(1):37.

Drewer, J., Anderson, M., Levy, P. E., Scholtes, B., Helfter, C., Parker, J., Rees, R. M., and Skiba, U. M. (2017). The impact of ploughing intensively managed temperate grasslands on N_2O, CH_4 and CO_2 fluxes. *Plant and Soil*, 411(1):193–208.

Duan, W., Fan, P. G., Wang, L. J., Li, W. D., Yan, S. T., and Li, S. H. (2008). Photosynthetic response to low sink demand after fruit removal in relation to photoinhibition and photoprotection in peach trees. *Tree physiology*, 28(1):123–132.

Dudareva, N., Negre, F., Nagegowda, D. a., and Orlova, I. (2006). Plant volatiles: recent advances and future perspectives. *Critical Reviews in Plant Sciences*, 25(5):417–440.

Dudareva, N., Pichersky, E., and Gershenzon, J. (2004). Biochemistry of plant volatiles. *Plant Physiology*, 135(4):1893–1902.

Dutta, S., Mohanty, S., and Tripathy, B. C. (2009). Role of Temperature Stress on Chloroplast Biogenesis and Protein Import in Pea. *Plant Physiology*, 150(2):1050–1061.

Dwivedi, S. L., Scheben, A., Edwards, D., Spillane, C., and Ortiz, R. (2017). Assessing and Exploiting Functional Diversity in Germplasm Pools to Enhance Abiotic Stress Adaptation and Yield in Cereals and Food Legumes. *Frontiers in Plant Science*, 8(August):1–30.

Efeoğlu, B., Ekmekçi, Y., and Çiçek, N. (2009). Physiological responses of three maize cultivars to drought stress and recovery. *South African Journal of Botany*, 75(1):34–42.

Estrada, F., Escobar, A., Romero-Bravo, S., González-Talice, J., Poblete-Echeverría, C., Caligari, P. D., and Lobos, G. A. (2015). Fluorescence phenotyping in blueberry breeding for genotype selection under drought conditions, with or without heat stress. *Scientia Horticulturae*, 181:147–161.

Eurostat (2016). *Agriculture, forestry and fishery statistics*. Publications Office of the European Union, Luxembourg.

Evans, S. M., Sinclair, E. A., Poore, A. G. B., Steinberg, P. D., Kendrick, G. A., and Vergés, A. (2014). Genetic diversity in threatened *Posidonia australis* seagrass meadows. *Conservation Genetics*, 15(3):717–728.

Evans, S. M., Vergés, A., and Poore, A. G. B. (2017). Genotypic Diversity and Short-term Response to Shading Stress in a Threatened Seagrass: Does Low Diversity Mean Low Resilience? *Frontiers in Plant Science*, 8:1417.

Faria, T., Silvério, D., Breia, E., Cabral, R., Abadia, A., Abadia, J., Pereira, J. S., and Chaves, M. M. (1998). Differences in the response of carbon assimilation to summer stress (water deficits, high light and temperature) in four Mediterranean tree species. *Physiologia Plantarum*, 102(3):419–428.

Farquhar, G. D. and Sharkey, T. D. (1982). Stomatal Conductance and Photosynthesis. *Annual Review of Plant Physiology*, 33(1):317–345.

Feller, U. (2016). Drought stress and carbon assimilation in a warming climate: reversible and irreversible impacts. *Journal of Plant Physiology*, 203:84–94.

Feng, S., Leung, A. K., Ng, C. W. W., and Liu, H. W. (2017). Theoretical analysis of coupled effects of microbe and root architecture on methane oxidation in vegetated landfill covers. *Science of The Total Environment*, 599:1954–1964.

Fernández-Baco, L., Figueroa, M. E., Luque, T., and Davy, A. J. (1998). Diurnal and seasonal variations in chlorophyll a fluorescence in two mediterranean-grassland species under field conditions. *Photosynthetica*, 35(4):535–544.

Ferrieri, R. A., Gray, D. W., Babst, B. A., Schueller, M. J., Schlyer, D. J., Thorpe, M. R., Orians, C. M., and LERDAU, M. (2005). Use of carbon-11 in Populus shows that exogenous jasmonic acid increases biosynthesis of isoprene from recently fixed carbon. *Plant, Cell & Environment*, 28(5):591–602.

Feussner, I. and Wasternack, C. (2002). The lipoxygenase pathway. *Annual Review of Plant Biology*, 53:275–297.

Flexas, J., Bota, J., Galmés, J., Medrano, H., and Ribas-Carbó, M. (2006). Keeping a positive carbon balance under adverse conditions: responses of photosynthesis and respiration to water stress. *Physiologia Plantarum*, 127(3):343–352.

Flügge, U. I., Westhoff, P., and Leister, D. (2016). Recent advances in understanding photosynthesis. *F1000Research*, 5(2890):2234.

Foken, T., Aubinet, M., and Leuning, R. (2012). Eddy Covariance. In *Aubinet, M., Vesala, T., and Papale, D. (Eds.) Eddy Covariance. A Practical Guide to Measurement and Data Analysis*, pages 1–19. Springer, Dordrecht, Netherlands.

Foley, J. A., Ramankutty, N., Brauman, K. A., Cassidy, E. S., Gerber, J. S., Johnston, M., Mueller, N. D., O'Connell, C., Ray, D. K., West, P. C., Balzer, C., Bennett, E. M., Carpenter, S. R., Hill, J., Monfreda, C., Polasky, S., Rockstrom, J., Sheehan, J., Siebert, S., Tilman, D., and Zaks, D. P. M. (2011). Solutions for a cultivated planet. *Nature*, 478(7369):337–342.

Formighieri, C. (2015). Light Saturation of Photosynthesis. In Formighieri, C., editor, *Formighieri, C. (Eds.) Solar-to-fuel conversion in algae and cyanobacteria*, pages 55–58. Springer International Publishing, Cham, Switzerland.

Fox, J., Weisberg, S., Adler, D., Bates, D., Baud-Bovy, G., Ellison, S., Firth, D., Friendly, M., Gorjanc, G., Graves, S., Heiberger, R., Laboissiere, R., Monette, G., Duncan, M., Nilsson, H., Ogle, D., Ripley, B., Venables, W., Winsemius, D., Zeileis, A., and R-Core (2016). Car: Companion to applied regression.

Fukui, Y. and Doskey, P. V. (2000). Identification of nonmethane organic compound emissions from grassland vegetation. *Atmospheric Environment*, 34(18):2947–2956.

Furbank, R. T., Quick, W. P., and Sirault, X. R. R. (2015). Improving photosynthesis and yield potential in cereal crops by targeted genetic manipulation: Prospects, progress and challenges. *Field Crops Research*, 182:19–29.

Gago, J., Douthe, C., Coopman, R., Gallego, P., Ribas-Carbo, M., Flexas, J., Escalona, J., and Medrano, H. (2015). UAVs challenge to assess water stress for sustainable agriculture. *Agricultural Water Management*, 153:9–19.

Galbally, I. E. and Kirstine, W. (2002). The Production of Methanol by Flowering Plants and the Global Cycle of Methanol. *Journal of Atmospheric Chemistry*, 43(3):195–229.

Ganjurjav, H., Gao, Q., Borjigidai, A., Guo, Y., Wan, Y., Li, Y., Jiangcun, W., and Danjiu, L. (2014). Alpine grassland ecosystem respiration variation under irrigation in Northern Tibet. *Acta Ecologica Sinica*, 34(5):271–276.

García-Plazaola, J. I., Esteban, R., Fernández-Marín, B., Kranner, I., and Porcar-Castell, A. (2012). Thermal energy dissipation and xanthophyll cycles beyond the Arabidopsis model. *Photosynthesis Research*, 113(1):89–103.

Gargallo-Garriga, A., Sardans, J., Pérez-Trujillo, M., Oravec, M., Urban, O., Jentsch, A., Kreyling, J., Beierkuhnlein, C., Parella, T., and Peñuelas, J. (2015). Warming differentially influences the effects of drought on stoichiometry and metabolomics in shoots and roots. *New Phytologist*, 207(3):591–603.

Gawryś, M., Fastyn, P., Gawłowski, J., Gierczak, T., and Niedzielski, J. (2001). Prevention of water vapour adsorption by carbon molecular sieves in sampling humid gases. *Journal of Chromatography A*, 933(1):107–116.

Genty, B., Briantais, J.-M., and Baker, N. R. (1989). The relationship between the quantum yield of photosynthetic electron transport and quenching of chlorophyll fluorescence. *Biochimica et Biophysica Acta (BBA) - General Subjects*, 990(1):87–92.

Georgieva, K., Fedina, I., Maslenkova, L., and Peeva, V. (2003). Response of *chlorina* barley mutants to heat stress under low and high light. *Functional Plant Biology*, 30(5):515–524.

Georgieva, K., Sárvári, E., and Keresztes, A. (2010). Protection of thylakoids against combined light and drought by a lumenal substance in the resurrection plant *Haberlea rhodopensis*. *Annals of botany*, 105(1):117–26.

Georgieva, K., Tsonev, T., Velikova, V., and Yordanov, I. (2000). Photosynthetic activity during high temperature treatment of pea plants. *Journal of Plant Physiology*, 157(2):169–176.

Gerber, P., Steinfeld, H., Henderson, B., Mottet, A., Opio, C., Dijkman, J., Falcucci, A., and Tempio, G. (2013). Tackling Climate Change Through Livestock - A Global Assessment of Emissions and Mitigation Opportunities. Technical report, Food and Agriculture Organization of the United Nations (FAO), Rome, Italy.

Ghirardo, A., Koch, K., Taipale, R., na Zimmer, I., Schnitzler, J.-P., and Rinne, J. (2010). Determination of *de novo* and pool emissions of terpenes from four common boreal/alpine trees by $13CO_2$ labelling and PTR-MS analysis. *Plant, Cell & Environment*, 33(5):781–792.

Ghotbi-Ravandi, A. A., Shahbazi, M., Shariati, M., and Mulo, P. (2014). Effects of mild and severe drought stress on photosynthetic efficiency in tolerant and susceptible barley (*Hordeum vulgare* L.) genotypes. *Journal of Agronomy and Crop Science*, 200(6):403–415.

Gielen, B., Naudts, K., D'Haese, D., Lemmens, C., De Boeck, H. J., Biebaut, E., Serneels, R., Valcke, R., Nijs, I., and Ceulemans, R. (2007). Effects of climate warming and species richness on photochemistry of grasslands. *Physiologia Plantarum*, 131(2):251–262.

Gigot, C., Ongena, M., Fauconnier, M.-L., Wathelet, J.-P., du Jardin, P., and Thonart, P. (2010). The lipoxygenase metabolic pathway in plants: Potential for industrial

production of natural green leaf volatiles. *Biotechnology, Agronomy and Society and Environment*, 14(3):451–460.

Gilmanov, T. G., Verma, S. B., Sims, P. L., Meyers, T. P., Bradford, J. A., Burba, G. G., and Suyker, A. E. (2003). Gross primary production and light response parameters of four Southern Plains ecosystems estimated using long-term CO_2-flux tower measurements. *Global Biogeochemical Cycles*, 17(2):10.1029/2002GB002023.

Głowacka, K., Kromdijk, J., Kucera, K., Xie, J., Cavanagh, A. P., Leonelli, L., Leakey, A. D. B., Ort, D. R., Niyogi, K. K., and Long, S. P. (2018). Photosystem II Subunit S overexpression increases the efficiency of water use in a field-grown crop. *Nature Communications*, 9(1):868.

Goh, C.-H., Ko, S.-M., Koh, S., Kim, Y.-J., and Bae, H.-J. (2012). Photosynthesis and environments: photoinhibition and repair mechanisms in plants. *Journal of Plant Biology*, 55(2):93–101.

Goltsev, V., Zaharieva, I., Chernev, P., Kouzmanova, M., Kalaji, H. M., Yordanov, I., Krasteva, V., Alexandrov, V., Stefanov, D., Allakhverdiev, S. I., and Strasser, R. J. (2012). Drought-induced modifications of photosynthetic electron transport in intact leaves: analysis and use of neural networks as a tool for a rapid non-invasive estimation. *Biochimica et biophysica acta*, 1817(8):1490–8.

Gomez-Casanovas, N., DeLucia, N. J., Bernacchi, C. J., Boughton, E. H., Sparks, J. P., Chamberlain, S. D., and DeLucia, E. H. (2017). Grazing alters net ecosystem C fluxes and the global warming potential of a subtropical pasture. *Ecological Applications*, pages n/a–n/a.

Gomez-Casanovas, N., Hudiburg, T. W., Bernacchi, C. J., Parton, W. J., and DeLucia, E. H. (2016). Nitrogen deposition and greenhouse gas emissions from grasslands: uncertainties and future directions. *Global Change Biology*, 22(4):1348–1360.

Gould, K. S. (2004). Nature's Swiss Army Knife: The Diverse Protective Roles of Anthocyanins in Leaves. *Journal of Biomedicine and Biotechnology*, 2004(5):314–320.

Gourlez de la Motte, L., Jérôme, E., Mamadou, O., Beckers, Y., Bodson, B., Heinesch, B., and Aubinet, M. (2016). Carbon balance of an intensively grazed permanent grassland in southern Belgium. *Agricultural and Forest Meteorology*, 228:370–383.

Govindjee, Shevela, D., and Björn, L. O. (2017). Evolution of the Z-scheme of photosynthesis: a perspective. *Photosynthesis Research*, pages 1–11.

Grassi, G. and Magnani, F. (2005). Stomatal, mesophyll conductance and biochemical limitations to photosynthesis as affected by drought and leaf ontogeny in ash and oak trees. *Plant, Cell & Environment*, 28(7):834–849.

Gravano, E., Bussotti, F., Strasser, R. J., Schaub, M., Novak, K., Skelly, J., and Tani, C. (2004). Ozone symptoms in leaves of woody plants in open-top chambers: ultrastructural and physiological characteristics. *Physiologia Plantarum*, 121(4):620–633.

Groemping, U. and Matthias, L. (2013). Relaimpo: relative importance of regressors in linear models.

Grulke, N., Preisler, H., Rose, C., Kirsch, J., and Balduman, L. (2002). O_3 uptake and drought stress effects on carbon acquisition of ponderosa pine in natural stands. *New Phytologist*, 154(3):621–631.

Guidi, L., Degl'Innocenti, E., Remorini, D., Massai, R., and Tattini, M. (2008). Interactions of water stress and solar irradiance on the physiology and biochemistry of *Ligustrum vulgare*. *Tree Physiology*, 28(6):873–83.

Guidi, L. and Degl'Innocenti, E. (2011). Imaging of Chlorophyll a Fluorescence: A Tool to Study Abiotic Stress in Plants. In *Schanker, A., and Venkateswarlu, B. (Eds.) Abiotic Stress in Plants - Mechanisms and Adaptations*, chapter 1, pages 3–20. InTech.

Guidi, L. and Calatayud, A. (2014). Non-invasive tools to estimate stress-induced changes in photosynthetic performance in plants inhabiting Mediterranean areas. *Environmental and Experimental Botany*, 103:42–52.

Gunasekera, D. and Berkowitz, G. A. (1993). Use of Transgenic Plants with Ribulose-1,5-Bisphosphate Carboxylase/Oxygenase Antisense DNA to Evaluate the Rate Limitation of Photosynthesis under Water Stress. *Plant Physiology*, 103(2):629–635.

Gururani, M. A., Venkatesh, J., and Tran, L. S. P. (2015). Regulation of Photosynthesis during Abiotic Stress-Induced Photoinhibition. *Molecular Plant*, 8(9):1304–1320.

Hagemann, M. and Bauwe, H. (2016). Photorespiration and the potential to improve photosynthesis. *Current Opinion in Chemical Biology*, 35:109–116.

Hamdani, S., Qu, M., Xin, C.-P., Li, M., Chu, C., Govindjee, and Zhu, X.-G. (2015). Variations between the photosynthetic properties of elite and landrace Chinese rice cultivars revealed by simultaneous measurements of 820nm transmission signal and chlorophyll a fluorescence induction. *Journal of Plant Physiology*, 177C:128–138.

Hantson, S., Knorr, W., Schurgers, G., Pugh, T. A. M., and Arneth, A. (2017). Global isoprene and monoterpene emissions under changing climate, vegetation, CO_2 and land use. *Atmospheric Environment*, 155(Supplement C):35–45.

Haque, M. S., Kjaer, K. H., Rosenqvist, E., Sharma, D. K., and Ottosen, C.-O. (2014). Heat stress and recovery of photosystem II efficiency in wheat (*Triticum aestivum* L.) cultivars acclimated to different growth temperatures. *Environmental and Experimental Botany*, 99:1–8.

Harbinson, J. and Woodward, F. I. (1987). The use of light-induced absorbance changes at 820 nm to monitor the oxidation state of P-700 in leaves. *Plant, Cell & Environment*, 10(2):131–140.

Harley, P. C., Loreto, F., Di Marco, G., and Sharkey, T. D. (1992). Theoretical Considerations when Estimating the Mesophyll Conductance to CO_2 Flux by Analysis of the Response of Photosynthesis to CO_2. *Plant Physiology*, 98(4):1429–1436.

Hassan, I. A. (2006). Effects of water stress and high temperature on gas exchange and chlorophyll fluorescence in *Triticum aestivum* L. *Photosynthetica*, 44(2):312–315.

Hautot, M. (2011). *Contribution à l'élaboration du bilan carbone d'une prairie paturée en région wallone: étude de la productivité et de l'ingestion par le bétail. Master thesis*. Gembloux Agro Bio Tech.

Havaux, M. (1992). Stress tolerance of photosystem II in vivo: antagonistic effects of water, heat, and photoinhibition stresses. *Plant Physiology*, 100(1):424–432.

Havaux, M., Dall'Osto, L., and Bassi, R. (2007). Zeaxanthin Has Enhanced Antioxidant Capacity with Respect to All Other Xanthophylls in Arabidopsis Leaves and Functions Independent of Binding to PSII Antennae. *Plant Physiology*, 145(4):1506 LP – 1520.

Havaux, M., Tardy, F., Ravenel, J., Chanu, D., and Parot, P. (1996). Thylakoid membrane stability to heat stress studied by flash spectroscopic measurements of the electrochromic shift in intact potato leaves: influence of the xanthophyll content. *Plant, Cell & Environment*, 19(12):1359–1368.

Hayek, M. N., Wehr, R., Longo, M., Hutyra, L. R., Wiedemann, K., Munger, J. W., Bonal, D., Saleska, S. R., Fitzjarrald, D. R., and Wofsy, S. C. (2018). A novel correction for biases in forest eddy covariance carbon balance. *Agricultural and Forest Meteorology*, 250-251:90–101.

He, L., Hatier, J.-H., and Matthew, C. (2017a). Drought tolerance of two perennial ryegrass cultivars with and without AR37 endophyte. *New Zealand Journal of Agricultural Research*, 60(2):173–188.

He, N.-P., Han, X.-G., and Pan, Q.-M. (2005). Variations in the Volatile Organic Compound Emission Potential of Plant Functional Groups in the Temperate Grassland Vegetation of Inner Mongolia, China. *Journal of Integrative Plant Biology*, 47(1):13–19.

He, Y., Xu, M., Qi, Y., Dong, Y., He, X., Li, J., Liu, X., and Sun, L. (2017b). Differential Responses of Soil Microbial Community to Four-Decade Long Grazing and Cultivation in a Semi-Arid Grassland. *Sustainability*, 9:128.

Hector, A., Schmid, B., Beierkuhnlein, C., Caldeira, M. C., Diemer, M., Dimitrakopoulos, P. G., Finn, J. A., Freitas, H., Giller, P. S., Good, J., Harris, R., Högberg, P., Huss-Danell, K., Joshi, J., Jumpponen, A., Körner, C., Leadley, P. W., Loreau, M., Minns, A., Mulder, C. P. H., O'Donovan, G., Otway, S. J., Pereira, J. S., Prinz, A., Read, D. J., Scherer-Lorenzen, M., Schulze, E.-D., Siamantziouras, A.-S. D., Spehn, E. M., Terry, A. C., Troumbis, A. Y., Woodward, F. I., Yachi, S., and Lawton, J. H. (1999). Plant Diversity and Productivity Experiments in European Grasslands. *Science*, 286(5442):1123 LP – 1127.

Heil, M. (2008). Indirect defence via tritrophic interactions. *New Phytologist*, 178(1):41–61.

Hejcman, M., Hejcmanová, P., Pavlů, V., and Beneš, J. (2013). Origin and history of grasslands in Central Europe - a review. *Grass and Forage Science*, 68(3):345–363.

Heskel, M. A., Atkin, O. K., Turnbull, M. H., and Griffin, K. L. (2013). Bringing the Kok effect to light: A review on the integration of daytime respiration and net ecosystem exchange. *Ecosphere*, 4(8):1–14.

Hill, P. W., Garnett, M. H., Farrar, J., Iqbal, Z., Khalid, M., Soleman, N., and Jones, D. L. (2015). Living roots magnify the response of soil organic carbon decomposition to temperature in temperate grassland. *Global Change Biology*, 21(3):1368–1375.

Hirata, R., Hirano, T., Saigusa, N., Fujinuma, Y., Inukai, K., Kitamori, Y., Takahashi, Y., and Yamamoto, S. (2007). Seasonal and interannual variations in carbon dioxide exchange of a temperate larch forest. *Agricultural and Forest Meteorology*, 147(3):110–124.

Hitz, W. D. and Hanson, A. D. (1980). Determination of glycine betaine by pyrolysis-gas chromatography in cereals and grasses. *Phytochemistry*, 19(11):2371–2374.

Hoekstra, F. A., Golovina, E. A., and Buitink, J. (2001). Mechanisms of plant desiccation tolerance. *Trends in Plant Science*, 6(9):431–438.

Holopainen, J. K. and Gershenzon, J. (2010). Multiple stress factors and the emission of plant VOCs. *Trends in Plant Science*, 15(3):176–184.

Hoover, D. L., Knapp, A. K., and Smith, M. D. (2014). Contrasting sensitivities of two dominant C4 grasses to heat waves and drought. *Plant Ecology*, 215(7):721–731.

Hoover, D. L., Knapp, A. K., and Smith, M. D. (2016). The immediate and prolonged effects of climate extremes on soil respiration in a mesic grassland. *Journal of Geophysical Research: Biogeosciences*, 121(4):1034–1044.

Hopkins, W. G. and Hüner, N. P. A. (2008). *Introduction to Plant Physiology*. Wiley, New York, USA, 4th ed. edition.

Hubbart, S., Ajigboye, O. O., Horton, P., and Murchie, E. H. (2012). The photoprotective protein PsbS exerts control over CO_2 assimilation rate in fluctuating light in rice. *The Plant Journal*, 71(3):402–412.

Hüner, N. P., Dahal, K., Bode, R., Kurepin, L. V., and Ivanov, A. G. (2016). Photosynthetic acclimation, vernalization, crop productivity and 'the grand design of photosynthesis'. *Journal of Plant Physiology*, 203:29–43.

Husson, F., Josse, J., Le, S., and Mazet, J. (2016). FactoMineR: multivariate exploratory data analysis and data mining.

Hütsch, B. W. (2001). Methane oxidation in non-flooded soils as affected by crop production - invited paper. *European Journal of Agronomy*, 14(4):237–260.

Inyang, U., Vendramini, J. M. B., Sollenberger, L. E., Sellers, B., Adesogan, A., Paiva, L., and Lunpha, A. (2010). Forage species and stocking rate effects on animal performance and herbage responses of 'Mulato' and bahiagrass pastures. *Crop Science*, 50(3):1079–1085.

IPCC (2014). Climate Change 2014: Synthesis Report. Contribution of Working Groups I, II and III to the Fifth Assessment Report of the Intergovernmental Panel on Climate Change [Core Writing Team, R.K. Pachauri and L.A. Meyer (Eds.)]. Technical report, Intergovernmental Panel on Climate Change (IPCC), IPCC, Geneva, Switzerland.

Isbell, F., Craven, D., Connolly, J., Loreau, M., Schmid, B., Beierkuhnlein, C., Bezemer, T. M., Bonin, C., Bruelheide, H., DeLuca, E., Ebeling, A., Griffin, J. N., Guo, Q., Hautier, Y., Hector, A., Jentsch, A., Kreyling, J., Lanta, V., Manning, P., Meyer, S. T., Mori, A. S., Naeem, S., Niklaus, P. A., Polley, H. W., Reich, P. B., Roscher, C., Seabloom, E. W., Smith, M. D., Thakur, M. P., Tilman, D., Tracy, B. F., van der Putten, W. H., van Ruijven, J., Weigelt, A., Weisser, W. W., Wilsey, B., and Eisenhauer, N. (2015). Biodiversity increases the resistance of ecosystem productivity to climate extremes. *Nature*, 526(7574):574–577L.

Iyer, N. J., Tang, Y., and Mahalingam, R. (2013). Physiological, biochemical and molecular responses to a combination of drought and ozone in *Medicago truncatula*. *Plant, Cell and Environment*, 36(3):706–720.

Jahns, P. and Holzwarth, A. R. (2012). The role of the xanthophyll cycle and of lutein in photoprotection of photosystem II. *Biochimica et Biophysica Acta (BBA) - Bioenergetics*, 1817(1):182–193.

Jaksic, V., Kiely, G., Albertson, J., Oren, R., Katul, G., Leahy, P., and Byrne, K. A. (2006). Net ecosystem exchange of grassland in contrasting wet and dry years. *Agricultural and Forest Meteorology*, 139(3):323–334.

Jaleel, C. A., Manivannan, P., Wahid, A., Farooq, M., Al-Juburi, H. J., Somasundaram, R., and Panneerselvam, R. (2009). Drought stress in plants: A review on morphological characteristics and pigments composition. *International Journal of Agriculture and Biology*, 11(1):100–105.

Janka, E., Körner, O., Rosenqvist, E., and Ottosen, C.-O. (2013). High temperature stress monitoring and detection using chlorophyll a fluorescence and infrared thermography in chrysanthemum (*Dendranthema grandiflora*). *Plant Physiology and Biochemistry*, 67:87–94.

Janka, E., Körner, O., Rosenqvist, E., and Ottosen, C.-O. (2015). Using the quantum yields of photosystem II and the rate of net photosynthesis to monitor high irradiance and temperature stress in chrysanthemum (*Dendranthema grandiflora*). *Plant Physiology and Biochemistry*, 90:14–22.

Jarecki, M. K., Parkin, T. B., Chan, A. S. K., Hatfield, J. L., and Jones, R. (2008). Greenhouse Gas Emissions from Two Soils Receiving Nitrogen Fertilizer and Swine Manure Slurry. *Journal of Environmental Quality*, 37(4):1432–1438.

Järvi, S., Suorsa, M., and Aro, E.-M. (2015). Photosystem II repair in plant chloroplasts - Regulation, assisting proteins and shared components with photosystem II biogenesis. *Biochimica et Biophysica Acta (BBA) - Bioenergetics*, 1847(9):900–909.

Jedmowski, C., Bayramov, S., and Brüggemann, W. (2014). Comparative analysis of drought stress effects on photosynthesis of Eurasian and North African genotypes of wild barley. *Photosynthetica*, 52(4):564–573.

Jedmowski, C., Ashoub, A., Momtaz, O., and Brüggemann, W. (2015). Impact of Drought, Heat, and Their Combination on Chlorophyll Fluorescence and Yield of Wild Barley (*Hordeum spontaneum*). *Journal of Botany*, 2015:1–9.

Jiang, Y. and Huang, B. (2000). Effects of drought or heat stress alone and in combination on Kentucky bluegrass. *Crop Science*, 40(5):1358–1362.

Jiang, Y. and Huang, B. (2001). Physiological responses to heat stress alone or in combination with drought: A comparison between tall fescue and perennial ryegrass. *HortScience*, 36(4):682–686.

Jin, H., Li, M., Duan, S., Fu, M., Dong, X., Liu, B., Feng, D., Wang, J., and Wang, H.-B. (2016). Optimization of Light-Harvesting Pigment Improves Photosynthetic Efficiency. *Plant Physiology*, 172(3):1720–1731.

Johnson, G. N., Lawson, T., Murchie, E. H., and Raines, C. (2015). Photosynthesis in variable environments. *Journal of Experimental Botany*, 66(9):2371–2372.

Johnson, S. M., Lim, F.-L., Finkler, A., Fromm, H., Slabas, A. R., and Knight, M. R. (2014). Transcriptomic analysis of Sorghum bicolor responding to combined heat and drought stress. *BMC Genomics*, 15(1):456.

Jones, S. K., Helfter, C., Anderson, M., Coyle, M., Campbell, C., Famulari, D., Di Marco, C., Van Dijk, N., Sim Tang, Y., Topp, C. F. E., Kiese, R., Kindler, R., Siemens, J., Schrumpf, M., Kaiser, K., Nemitz, E., Levy, P. E., Rees, R. M., Sutton, M. A., and Skiba, U. M. (2017). The nitrogen, carbon and greenhouse gas budget of a grazed, cut and fertilised temperate grassland. *Biogeosciences*, 14(8):2069–2088.

Jones, S. K., Rees, R. M., Skiba, U. M., and Ball, B. C. (2005). Greenhouse gas emissions from a managed grassland. *Global and Planetary Change*, 47(2-4 SPEC. ISS.):201–211.

Kalaji, H. M., Bosa, K., Kościelniak, J., and Żuk-Gołaszewska, K. (2011). Effects of salt stress on photosystem II efficiency and CO_2 assimilation of two Syrian barley landraces. *Environmental and Experimental Botany*, 73:64–72.

Kalaji, H. M., Carpentier, R., Allakhverdiev, S. I., and Bosa, K. (2012). Fluorescence parameters as early indicators of light stress in barley. *Journal of Photochemistry and Photobiology. B: Biology*, 112:1–6.

Kalaji, H. M., Jajoo, A., Oukarroum, A., Brestic, M., Zivcak, M., Samborska, I. A., Cetner, M. D., Łukasik, I., Goltsev, V., and Ladle, R. J. (2016). Chlorophyll a fluorescence as a tool to monitor physiological status of plants under abiotic stress conditions. *Acta Physiologiae Plantarum*, 38(4):102.

Kalaji, H. M., Schansker, G., Brestic, M., Bussotti, F., Calatayud, A., Ferroni, L., Goltsev, V., Guidi, L., Jajoo, A., Li, P., Losciale, P., Mishra, V. K., Misra, A. N., Nebauer, S. G., Pancaldi, S., Penella, C., Pollastrini, M., Suresh, K., Tambussi, E., Yanniccari, M., Zivcak, M., Cetner, M. D., Samborska, I. A., Stirbet, A., Olsovska,

K., Kunderlikova, K., Shelonzek, H., Rusinowski, S., and Bąba, W. (2017). Frequently asked questions about chlorophyll fluorescence, the sequel. *Photosynthesis Research*, 132(13):13–66.

Kalaji, H. M., Schansker, G., Ladle, R. J., Goltsev, V., Bosa, K., Allakhverdiev, S. I., Brestic, M., Bussotti, F., Calatayud, A., Dąbrowski, P., Elsheery, N. I., Ferroni, L., Guidi, L., Hogewoning, S. W., Jajoo, A., Misra, A. N., Nebauer, S. G., Pancaldi, S., Penella, C., Poli, D., Pollastrini, M., Romanowska-Duda, Z. B., Rutkowska, B., Serôdio, J., Suresh, K., Szulc, W., Tambussi, E., Yanniccari, M., and Zivcak, M. (2014). Frequently asked questions about in vivo chlorophyll fluorescence: practical issues. *Photosynthesis Research*, 122(2):121–58.

Kasajima, I., Kawai-Yamada, M., and Uchimiya, H. (2011). Theories in PAM chlorophyll fluorescence measurement of plant leaves. In *Maes, K. J., and Willems, J. M. (Eds) Photochemistry: UV/VIS Spectroscopy, Photochemical Reactions and Photosynthesis*, pages 351–371. Nova Science Publishers, Inc., New York, USA.

Kataria, S. and Guruprasad, K. N. (2015). Exclusion of solar UV radiation improves photosynthetic performance and yield of wheat varieties. *Plant physiology and biochemistry : PPB / Socieété francÌ§aise de physiologie végétale*, 97:400–11.

Kautsky, H. and Hirsch, A. (1931). Neue Versuche zur Kohlensaureassimilation. *Die Naturwissenschaften*, 19(48):964–964.

Kesselmeier, J., Ciccioli, P., Kuhn, U., Stefani, P., Biesenthal, T., Rottenberger, S., Wolf, A., Vitullo, M., Valentini, R., Nobre, A., Kabat, P., and Andreae, M. O. (2002). Volatile organic compound emissions in relation to plant carbon fixation and the terrestrial carbon budget. *Global Biogeochemical Cycles*, 16(4):71–73.

Kollist, T., Moldau, H., Rasulov, B., Oja, V., Rämma, H., Hüve, K., Jaspers, P., Kangasjärvi, J., and Kollist, H. (2007). A novel device detects a rapid ozone-induced transient stomatal closure in intact Arabidopsis and its absence in abi2 mutant. *Physiologia Plantarum*, 129(4):796–803.

Kornyeyev, D., Logan, B. A., Tissue, D. T., Allen, R. D., and Holaday, A. S. (2006). Compensation for PSII Photoinactivation by Regulated Non-photochemical Dissipation Influences the Impact of Photoinactivation on Electron Transport and CO_2 Assimilation. *Plant and Cell Physiology*, 47(4):437–446.

Kos, M., van Loon, J. J. A., Dicke, M., and Vet, L. E. M. (2009). Transgenic plants as vital components of integrated pest management. *Trends in Biotechnology*, 27(11):621–627.

Krall, J. P. and Edwards, G. E. (1992). Relationship between photosystem II activity and CO_2 fixation in leaves. *Physiologia Plantarum*, 86(1):180–187.

Krause, G. H. and Jahns, P. (2004). Non-photochemical Energy Dissipation Determined by Chlorophyll Fluorescence Quenching: Characterization and Function. In *Papageorgiou, G.C., and Govindjee (Eds.) Chlorophyll a Fluorescence: A Signature of Photosynthesis*, pages 463–495. Springer, Dordrecht, The Netherlands.

Kromdijk, J., Głowacka, K., Leonelli, L., Gabilly, S. T., Iwai, M., Niyogi, K. K., and Long, S. P. (2016). Improving photosynthesis and crop productivity by accelerating recovery from photoprotection. *Science*, 354(6314):857–861.

Kugler, S., Horváth, L., and Machon, A. (2008). Estimation of nitrogen balance between the atmosphere and Lake Balaton and a semi natural grassland in Hungary. *Environmental Pollution*, 154(3):498–503.

Ladjal, M., Epron, D., and Ducrey, M. (2000). Effects of drought preconditioning on thermotolerance of photosystem II and susceptibility of photosynthesis to heat stress in cedar seedlings. *Tree Physiology*, 20(18):1235–1241.

Lam, S. K., Suter, H., Mosier, A. R., and Chen, D. (2017). Using nitrification inhibitors to mitigate agricultural N_2O emission: a double-edged sword? *Global Change Biology*, 23(2):485–489.

Laothawornkitkul, J., Taylor, J. E., Paul, N. D., and Hewitt, C. N. (2009). Biogenic volatile organic compounds in the Earth system: Tansley review. *New Phytologist*, 183(1):27–51.

Lata, J.-C., Degrange, V., Raynaud, X., Maron, P.-A., Lensi, R., and Abbadie, L. (2004). Grass populations control nitrification in savanna soils. *Functional Ecology*, 18(4):605–611.

Lauriano, J., Ramalho, J., Lidon, F., and Do Céu matos, M. (2006). Mechanisms of energy dissipation in peanut under water stress. *Photosynthetica*, 44(3):404–410.

Lavinsky, A. O., De Souza Sant'Ana, C., Mielke, M. S., De Almeida, A.-A., Gomes, F. P., França, S., and Da Costa Silva, D. (2007). Effects of light availability and soil flooding on growth and photosynthetic characteristics of *Genipa americana* L. seedlings. *New Forests*, 34(1):41–50.

Lawson, T. and Blatt, M. R. (2014). Stomatal Size, Speed, and Responsiveness Impact on Photosynthesis and Water Use Efficiency. *Plant Physiology*, 164(4):1556–1570.

Lawson, T., Simkin, A. J., Kelly, G., and Granot, D. (2014). Mesophyll photosynthesis and guard cell metabolism impacts on stomatal behaviour. *New Phytologist*, 203(4):1064–1081.

Lee, H.-Y., Chow, W. S., and Hong, Y.-N. (1999). Photoinactivation of photosystem II in leaves of *Capsicum annuum*. *Physiologia Plantarum*, 105(2):376–383.

Lemaire, G., Da Silva, S. C., Agnusdei, M., Wade, M., and Hodgson, J. (2009). Interactions between leaf lifespan and defoliation frequency in temperate and tropical pastures: a review. *Grass and Forage Science*, 64(4):341–353.

Leuning, R., Denmead, O. T., Lang, A. R. G., and Ohtaki, E. (1982). Effects of heat and water vapor transport on eddy covariance measurement of CO_2 fluxes. *Boundary-Layer Meteorology*, 23(2):209–222.

Li, M., Shimizu, M., and Hatano, R. (2015). Evaluation of N_2O and CO_2 hot moments in managed grassland and cornfield, southern Hokkaido, Japan. *CATENA*, 133:1–13.

Li, P. and Ma, F. (2012). Different effects of light irradiation on the photosynthetic electron transport chain during apple tree leaf dehydration. *Plant Physiology and Biochemistry*, 55:16–22.

Li, X., Yang, Y., Sun, X., Lin, H., Chen, J., Ren, J., Hu, X., and Yang, Y. (2014). Comparative Physiological and Proteomic Analyses of Poplar (*Populus yunnanensis*) Plantlets Exposed to High Temperature and Drought. *PLOS ONE*, 9(9):e107605.

Liska, A. J., Shevchenko, A., Pick, U., and Katz, A. (2004). Enhanced photosynthesis and redox energy production contribute to salinity tolerance in *Dunaliella* as revealed by homology-based proteomics. *Plant physiology*, 136(1):2806–17.

Liu, L., Guan, L., and Liu, X. (2017). Directly estimating diurnal changes in GPP for C3 and C4 crops using far-red sun-induced chlorophyll fluorescence. *Agricultural and Forest Meteorology*, 232:1–9.

Lloyd, J. and Taylor, J. A. (1994). On the temperature dependence of soil respiration. *Functional Ecology*, 8(3):315–323.

Loescher, H. W., Law, B. E., Mahrt, L., Hollinger, D. Y., Campbell, J., and Wofsy, S. C. (2006). Uncertainties in, and interpretation of, carbon flux estimates using the eddy covariance technique. *Journal of Geophysical Research: Atmospheres*, 111:D21.

Lognoul, M., Theodorakopoulos, N., Hiel, M.-P., Regaert, D., Broux, F., Heinesch, B., Bodson, B., Vandenbol, M., and Aubinet, M. (2017). Impact of tillage on greenhouse gas emissions by an agricultural crop and dynamics of N_2O fluxes: Insights from automated closed chamber measurements. *Soil and Tillage Research*, 167:80–89.

Long, S. P. and Bernacchi, C. J. (2003). Gas exchange measurements, what can they tell us about the underlying limitations to photosynthesis? Procedures and sources of error. *Journal of Experimental Botany*, 54(392):2393–2401.

Long, S. P., Humphries, S., and Falkowski, P. G. (1994). Photoinhibition of Photosynthesis in Nature. *Annual Review of Plant Physiology and Plant Molecular Biology*, 45(1):633–662.

Loreau, M., Naeem, S., Inchausti, P., Bengtsson, J., Grime, J. P., Hector, A., Hooper, D. U., Huston, M. A., Raffaelli, D., Schmid, B., Tilman, D., and Wardle, D. A. (2001). Biodiversity and Ecosystem Functioning: Current Knowledge and Future Challenges. *Science*, 294(5543):804 LP – 808.

Loreto, F., Ciccioli, P., Brancaleoni, E., Cecinato, A., Frattoni, M., Cicciolit, P., Brancaleonit, E., Cecinatot, A., Frarronit, M., and Sharkey, T. D. (1996). Different sources of reduced carbon contribute to form three classes of terpenoid emitted by *Quercus ilex* L. leaves. *Proc. Natl. Acad. Sci. USA*, 93(93):9966–9969.

Loreto, F., Förster, A., Dürr, M., Csiky, O., and Seufert, G. (1998). On the monoterpene emission under heat stress and on the increased thermotolerance of leaves of

Quercus ilex L. fumigated with selected monoterpenes. *Plant, Cell & Environment*, 21(1):101–107.

Loreto, F. and Schnitzler, J. P. (2010). Abiotic stresses and induced BVOCs. *Trends in Plant Science*, 15(3):154–166.

Loreto, F. and Velikova, V. (2001). Isoprene produced by leaves protects the photosynthetic apparatus against ozone damage, quenches ozone products, and reduces lipid peroxidation of cellular membranes. *Plant Physiology*, 127(4):1781–1787.

Lu, C. and Zhang, J. (1999). Effects of water stress on photosystem II photochemistry and its thermostability in wheat plants. *Journal of Experimental Botany*, 50(336):1199–1206.

Lu, T., Meng, Z., Zhang, G., Qi, M., Sun, Z., Liu, Y., and Li, T. (2017). Sub-high Temperature and High Light Intensity Induced Irreversible Inhibition on Photosynthesis System of Tomato Plant (*Solanum lycopersicum* L.).

Lugato, E., Panagos, P., Bampa, F., Jones, A., and Montanarella, L. (2014). A new baseline of organic carbon stock in European agricultural soils using a modelling approach. *Global Change Biology*, 20(1):313–326.

Luo, H.-B., Ma, L., Xi, H.-F., Duan, W., Li, S.-H., Loescher, W., Wang, J.-F., and Wang, L.-J. (2011). Photosynthetic responses to heat treatments at different temperatures and following recovery in grapevine (*Vitis amurensis* L.) leaves. *PloS one*, 6(8):e23033.

Ma, S., Baldocchi, D., Wolf, S., and Verfaillie, J. (2016). Slow ecosystem responses conditionally regulate annual carbon balance over 15 years in Californian oak-grass savanna. *Agricultural and Forest Meteorology*, 228-229(Supplement C):252–264.

Ma, S., Baldocchi, D. D., Xu, L., and Hehn, T. (2007). Inter-annual variability in carbon dioxide exchange of an oak/grass savanna and open grassland in California. *Agricultural and Forest Meteorology*, 147(3):157–171.

Machado, F., Dias, M. C., de Pinho, P. G., Araújo, A. M., Pinto, D., Silva, A., Correia, C., Moutinho-Pereira, J., and Santos, C. (2017). Photosynthetic performance and volatile organic compounds profile in *Eucalyptus globulus* after UVB radiation. *Environmental and Experimental Botany*, 140(Supplement C):141–149.

Machon, A., Horváth, L., Weidinger, T., Grosz, B., Pintér, K., Tuba, Z., and Führer, E. (2010). Estimation of net nitrogen flux between the atmosphere and a semi-natural grassland ecosystem in Hungary. *European Journal of Soil Science*, 61(5):631–639.

Maffei, M. E. (2010). Sites of synthesis, biochemistry and functional role of plant volatiles. *South African Journal of Botany*, 76(4, Sp. Iss. SI):612–631.

Magney, T. S., Frankenberg, C., Fisher, J. B., Sun, Y., North, G. B., Davis, T. S., Kornfeld, A., and Siebke, K. (2017). Connecting active to passive fluorescence with photosynthesis: a method for evaluating remote sensing measurements of Chl fluorescence. *New Phytologist*, page in press.

Mamadou, O., Gourlez de la Motte, L., De Ligne, A., Heinesch, B., and Aubinet, M. (2016). Sensitivity of the annual net ecosystem exchange to the cospectral model used for high frequency loss corrections at a grazed grassland site. *Agricultural and Forest Meteorology*, 228–229:360–369.

Manes, F., Donato, E., and Vitale, M. (2001). Physiological response of *Pinus halepensis* needles under ozone and water stress conditions. *Physiologia Plantarum*, 113(2):249–257.

Marosvölgyi, M. A. and van Gorkom, H. J. (2010). Cost and color of photosynthesis. *Photosynthesis Research*, 103(2):105–109.

Masojidek, J., Trivedi, S., Halshaw, L., Alexiou, A., and Hall, D. O. (1991). The synergistic effect of drought and light stresses in sorghum and pearl millet. *Plant Physiology*, 96(1):198–207.

Massacci, A., Nabiev, S., Pietrosanti, L., Nematov, S., Chernikova, T., Thor, K., and Leipner, J. (2008). Response of the photosynthetic apparatus of cotton (*Gossypium hirsutum*) to the onset of drought stress under field conditions studied by gas-exchange analysis and chlorophyll fluorescence imaging. *Plant Physiology and Biochemistry*, 46(2):189–195.

Mathur, S., Allakhverdiev, S. I., and Jajoo, A. (2011a). Analysis of high temperature stress on the dynamics of antenna size and reducing side heterogeneity of Photosystem II in wheat leaves (*Triticum aestivum*). *Biochimica et biophysica acta*, 1807(1):22–9.

Mathur, S., Jajoo, A., Mehta, P., and Bharti, S. (2011b). Analysis of elevated temperature-induced inhibition of photosystem II using chlorophyll a fluorescence induction kinetics in wheat leaves (*Triticum aestivum*). *Plant Biology*, 13(1):1–6.

Mathur, S. and Jajoo, A. (2015). Investigating deleterious effects of ultraviolet (UV) radiations on wheat by a quick method. *Acta Physiologiae Plantarum*, 37(6):121.

Matyssek, R., Le Thiec, D., Löw, M., Dizengremel, P., Nunn, A. J., and Häberle, K.-H. (2006). Interactions between drought and O_3 stress in forest trees. *Plant biology (Stuttgart, Germany)*, 8(1):11–17.

Maurenza, D., Marenco, R. A., Parolin, P., and Piedade, M. T. F. (2012). Physiological responses to flooding and light in two tree species native to the Amazonian floodplains. *Aquatic Botany*, 96(1):7–13.

Mauromicale, G., Ierna, A., and Marchese, M. (2006). Chlorophyll fluorescence and chlorophyll content in field-grown potato as affected by nitrogen supply, genotype, and plant age. *Photosynthetica*, 44(1):76–82.

Maxwell, K. and Johnson, G. N. (2000). Chlorophyll fluorescence - A practical guide. *Journal of Experimental Botany*, 51(345):659–668.

McAinsh, M. R., Evans, N. H., Montgomery, L. T., and North, K. A. (2002). Calcium signalling in stomatal responses to pollutants. *New Phytologist*, 153(3):441–447.

McAusland, L., Vialet-Chabrand, S., Davey, P., Baker, N. R., Brendel, O., and Lawson, T. (2016). Effects of kinetics of light-induced stomatal responses on photosynthesis and water-use efficiency. *New Phytologist*, 211(4):1209–1220.

McGinn, S. M., Beauchemin, K. A., Coates, T., and McGeough, E. J. (2014). Cattle Methane Emission and Pasture Carbon Dioxide Balance of a Grazed Grassland. *Journal of Environmental Quality*, 43(3):820–828.

Menzel, U. (2015). CCP: significance tests for canonical correlation analysis (CCA).

Mielke, M. S. and Schaffer, B. (2010). Leaf gas exchange, chlorophyll fluorescence and pigment indexes of *Eugenia uniflora* L. in response to changes in light intensity and soil flooding. *Tree Physiology*, 30(1):45–55.

Mielke, M. S. and Schaffer, B. (2011). Effects of soil flooding and changes in light intensity on photosynthesis of *Eugenia uniflora* L. seedlings. *Acta Physiologiae Plantarum*, 33(5):1661–1668.

Mishra, D., Shekhar, S., Agrawal, L., Chakraborty, S., and Chakraborty, N. (2017). Cultivar-specific high temperature stress responses in bread wheat (*Triticum aestivum* L.) associated with physicochemical traits and defense pathways. *Food Chemistry*, 221:1077–1087.

Mittler, R. (2006). Abiotic stress, the field environment and stress combination. *Trends in Plant Science*, 11(1):15–19.

Miyashita, H., Ikemoto, H., Kurano, N., Adachi, K., Chihara, M., and Miyachi, S. (1996). Chlorophyll d as a major pigment. *Nature*, 383(6599):402–402.

Mohanty, S., Grimm, B., and Tripathy, B. C. (2006). Light and dark modulation of chlorophyll biosynthetic genes in response to temperature. *Planta*, 224(3):692–699.

Mori, A. (2016). Greenhouse gas sink-source functions of grassland ecosystems. *Japan Agricultural Research Quarterly*, 50(3):187–190.

Morison, J. I. L., Baker, N. R., Mullineaux, P. M., and Davies, W. J. (2008). Improving water use in crop production. *Philosophical Transactions of the Royal Society B: Biological Sciences*, 363(1491):639 LP – 658.

Mosier, A., Schimel, D., Valentine, D., Bronson, K., and Parton, W. (1991). Methane and nitrous oxide fluxes in native, fertilized and cultivated grasslands. *Nature*, 350(6316):330–332.

Murata, N., Takahashi, S., Nishiyama, Y., and Allakhverdiev, S. I. (2007). Photoinhibition of photosystem II under environmental stress. *Biochimica et Biophysica Acta (BBA) - Bioenergetics*, 1767(6):414–421.

Murchie, E. H. and Lawson, T. (2013). Chlorophyll fluorescence analysis: a guide to good practice and understanding some new applications. *Journal of Experimental Botany*, 64(13):3983–98.

Murchie, E. H., Pinto, M., and Horton, P. (2009). Agriculture and the new challenges for photosynthesis research. *New Phytologist*, 181(3):532–552.

Nash, D., Miyao, M., and Murata, N. (1985). Heat inactivation of oxygen evolution in photosystem II particles and its acceleration by chloride depletion and exogenous manganese. *Biochimica et Biophysica Acta (BBA) - Bioenergetics*, 807(2):127–133.

Nellaepalli, S., Mekala, N. R., Zsiros, O., Mohanty, P., and Subramanyam, R. (2011). Moderate heat stress induces state transitions in *Arabidopsis thaliana*. *Biochimica et Biophysica Acta (BBA) - Bioenergetics*, 1807(9):1177–1184.

Niinemets, Ü. and Reichstein, M. (2003). Controls on the emission of plant volatiles through stomata: Differential sensitivity of emission rates to stomatal closure explained. *Journal of Geophysical Research D: Atmospheres*, 108(7):ACH 2–1 ACH 2–17.

Niinemets, Ü., Kuhn, U., Harley, P. C., Staudt, M., Arneth, A., Cescatti, A., Ciccioli, P., Copolovici, L., Geron, C., Guenther, A., Kesselmeier, J., Lerdau, M. T., Monson, R. K., and Peñuelas, J. (2011). Estimations of isoprenoid emission capacity from enclosure studies: Measurements, data processing, quality and standardized measurement protocols. *Biogeosciences*, 8(8):2209–2246.

Novak, S. M. and Fiorelli, J. L. (2010). Greenhouse gases and ammonia emissions from organic mixed crop-dairy systems: a critical review of mitigation options. *Agronomy for Sustainable Development*, 30(2):215–236.

Nussbaum, S., Geissmann, M., Eggenberg, P., Strasser, R. J., and Fuhrer, J. (2001). Ozone sensitivity in herbaceous species as assessed by direct and modulated chlorophyll fluorescence techniques. *Journal of Plant Physiology*, 158(6):757–766.

Ogaya, R., Peñuelas, J., Asensio, D., and Llusià, J. (2011). Chlorophyll fluorescence responses to temperature and water availability in two co-dominant Mediterranean shrub and tree species in a long-term field experiment simulating climate change. *Environmental and Experimental Botany*, 73:89–93.

Ohtaki, E. (1980). Turbulent transport of carbon dioxide over a paddy field. *Boundary-Layer Meteorology*, 19(3):315–336.

Oksanen, J., Blanchet, F. G., Friendly, M., Kindt, R., Legendre, P., McGlinn, D., Minchin, P. R., O'Hara, R. B., Simpson, G. L., Solymos, P., Stevens, M. H. H., Szoecs, E., and Wagner, H. (2012). Vegan : community ecology package.

Orr, D., Alcântara, A., Kapralov, M. V., Andralojc, J., Carmo-Silva, E., and Parry, M. A. J. (2016). Surveying Rubisco diversity and temperature response to improve crop photosynthetic efficiency. *Plant Physiology*.

Osório, M. L., Osório, J., and Romano, A. (2013). Photosynthesis, energy partitioning, and metabolic adjustments of the endangered Cistaceae species *Tuberaria major* under high temperature and drought. *Photosynthetica*, 51(1):75–84.

Osório, M. L., Osório, J., Vieira, A. C., Gonçalves, S., and Romano, A. (2011). Influence of enhanced temperature on photosynthesis, photooxidative damage, and antioxidant strategies in *Ceratonia siliqua* L. seedlings subjected to water deficit and rewatering. *Photosynthetica*, 49(1):3–12.

Oukarroum, A., Madidi, S. E., Schansker, G., and Strasser, R. J. (2007). Probing the responses of barley cultivars (*Hordeum vulgare* L.) by chlorophyll a fluorescence OLKJIP under drought stress and re-watering. *Environmental and Experimental Botany*, 60(3):438–446.

Oukarroum, A., Schansker, G., and Strasser, R. J. (2009). Drought stress effects on photosystem I content and photosystem II thermotolerance analyzed using Chl a fluorescence kinetics in barley varieties differing in their drought tolerance. *Physiologia Plantarum*, 137(2):188–99.

Oukarroum, A., El Madidi, S., and Strasser, R. J. (2012). Exogenous glycine betaine and proline play a protective role in heat-stressed barley leaves (*Hordeum vulgare* L.): A chlorophyll a fluorescence study. *Plant Biosystems - An International Journal Dealing with all Aspects of Plant Biology*, 146(4):1037–1043.

Oukarroum, A., El Madidi, S., and Strasser, R. J. (2016). Differential heat sensitivity index in barley cultivars (*Hordeum vulgare* L.) monitored by chlorophyll a fluorescence OKJIP. *Plant physiology and biochemistry : PPB / Societe francaise de physiologie vegetale*, 105:102–108.

Pallozzi, E., Fortunati, A., Marino, G., Loreto, F., Agati, G., and Centritto, M. (2013). BVOC emission from (*Populus* x (*canadensis* saplings in response to acute UV-A radiation. *Physiologia Plantarum*, 148(1):51–61.

Pan, X., Liu, Z., Li, M., and Chang, W. (2013). Architecture and function of plant light-harvesting complexes II. *Current Opinion in Structural Biology*, 23(4):515–525.

Pandey, P., Ramegowda, V., and Senthil-Kumar, M. (2015). Shared and unique responses of plants to multiple individual stresses and stress combinations: physiological and molecular mechanisms. *Frontiers in Plant Science*, 6(723):14.

Papageorgiou, G. and Govindjee (Eds.) (2004). *Chlorophyll a fluorescence: a signature of photosynthesis, vol 19., Advances in photosynthesis and respiration*, volume 19. Springer, Dordrecht, The Netherlands.

Parry, M. A. J., Reynolds, M., Salvucci, M. E., Raines, C., Andralojc, P. J., Zhu, X.-G., Price, G. D., Condon, A. G., and Furbank, R. T. (2011). Raising yield potential of wheat. II. Increasing photosynthetic capacity and efficiency. *Journal of Experimental Botany*, 62(2):453–467.

Peñuelas, J. and Llusià, J. (2003). BVOCs: plant defense against climate warming? *Trends in Plant Science*, 8(3):105–109.

Peñuelas, J. and Staudt, M. (2010). BVOCs and global change. *Trends in Plant Science*, 15(3):133–144.

Petrouleas, V. and Crofts, A. R. (2005). The Iron-Quinone Acceptor Complex BT. In *Wydrzynski, T.J., Satoh, K., and Freeman, J.A. (Eds.) Photosystem II; The light-driven water:plastoquinone oxidoreductase. Advances in photosynthesis and respiration vol 22*, pages 177–206. Springer, Dordrecht, The Netherlands.

Pettigrew, W. T. (2016). Cultivar variation in cotton photosynthetic performance under different temperature regimes. *Photosynthetica*, 54(4):502–507.

Pirzad, A. L., Shakiba, M. R., Zehtab-Salmasi, S., Mohammadi, S. A., Darvishzadeh, R., and Samadi, A. (2011). Effect of water stress on leaf relative water content, chlorophyll, proline and soluble carbohydrates in *Matricaria chamomilla* L. *Journal of Medicinal Plants Research*, 5(12):2483–2488.

Pollastri, S., Tsonev, T., and Loreto, F. (2014). Isoprene improves photochemical efficiency and enhances heat dissipation in plants at physiological temperatures. *Journal of Experimental Botany*, 65(6):1565–1570.

Pollastrini, M., Di Stefano, V., Ferretti, M., Agati, G., Grifoni, D., Zipoli, G., Orlandini, S., and Bussotti, F. (2011). Influence of different light intensity regimes on leaf features of *Vitis vinifera* L. in ultraviolet radiation filtered condition. *Environmental and Experimental Botany*, 73:108–115.

Pollastrini, M., Desotgiu, R., Camin, F., Ziller, L., Gerosa, G., Marzuoli, R., and Bussotti, F. (2014). Severe drought events increase the sensitivity to ozone on poplar clones. *Environmental and Experimental Botany*, 100:94–104.

Pollastrini, M., Holland, V., Brüggemann, W., Bruelheide, H., Dănilă, I., Jaroszewicz, B., Valladares, F., and Bussotti, F. (2016a). Taxonomic and ecological relevance of the chlorophyll a fluorescence signature of tree species in mixed European forests. *New Phytologist*, 212:51–65.

Pollastrini, M., Holland, V., Brüggemann, W., and Bussotti, F. (2016b). Chlorophyll a fluorescence analysis in forests. *Annali di Botanica*, 6(0):23–37.

Popp, A., Lotze-Campen, H., and Bodirsky, B. (2010). Food consumption, diet shifts and associated non-CO_2 greenhouse gases from agricultural production. *Global Environmental Change*, 20(3):451–462.

Porcar-Castell, A., Pfündel, E., Korhonen, J. F. J., and Juurola, E. (2008). A new monitoring PAM fluorometer (MONI-PAM) to study the short- and long-term acclimation of photosystem II in field conditions. *Photosynthesis research*, 96(2):173–9.

Pouresmael, M., Khavari-Nejad, R. A., Mozafari, J., Najafi, F., and Moradi, F. (2015). Diverse responses of tolerant and sensitive lines of Chickpea to drought stress. *Archives of Agronomy and Soil Science*, 61(11):1561–1580.

Prasad, C. S. and Gowda, N. K. S. (2005). Importance of trace minerals and relevance of their supplementation in tropical animal feeding system: A review. *Indian Journal of Animal Sciences*, 75(1):92–100.

Prasad, P. V. V., Pisipati, S. R., Momčilović, I., and Ristic, Z. (2011). Independent and Combined Effects of High Temperature and Drought Stress During Grain Filling on Plant Yield and Chloroplast EF-Tu Expression in Spring Wheat. *Journal of Agronomy and Crop Science*, 197(6):430–441.

Price, G. D., Pengelly, J. J. L., Forster, B., Du, J., Whitney, S. M., von Caemmerer, S., Badger, M. R., Howitt, S. M., and Evans, J. R. (2013). The cyanobacterial CCM as a source of genes for improving photosynthetic CO_2 fixation in crop species. *Journal of Experimental Botany*, 64(3):753–768.

Pulles, T. (2017). Engineering photosynthesis: a necessary tool to protect the world's climate? *Carbon Management*, 8(2):167–173.

Qiao, C., Liu, L., Hu, S., Compton, J. E., Greaver, T. L., and Li, Q. (2015). How inhibiting nitrification affects nitrogen cycle and reduces environmental impacts of anthropogenic nitrogen input. *Global Change Biology*, 21(3):1249–1257.

Rahbarian, R., Khavari-Nejad, R., Ganjeali, A., Bagheri, A., and Najafi, F. (2011). Drought Stress Effects on Photosynthesis, Chlorophyll Fluorescence and Water Relations in Tolerant and Susceptible Chickpea (*Cicer Arietinum* L.) Genotypes. *Acta Biologica Cracoviensia Series Botanica*, 53(1):47–56.

Rebmann, C., Göckede, M., Foken, T., Aubinet, M., Aurela, M., Berbigier, P., Bernhofer, C., Buchmann, N., Carrara, A., Cescatti, A., Ceulemans, R., Clement, R., Elbers, J. A., Granier, A., Grünwald, T., Guyon, D., Havránková, K., Heinesch, B., Knohl, A., Laurila, T., Longdoz, B., Marcolla, B., Markkanen, T., Miglietta, F., Moncrieff, J., Montagnani, L., Moors, E., Nardino, M., Ourcival, J.-M., Rambal, S., Rannik, Ü., Rotenberg, E., Sedlak, P., Unterhuber, G., Vesala, T., and Yakir, D. (2005). Quality analysis applied on eddy covariance measurements at complex forest sites using footprint modelling. *Theoretical and Applied Climatology*, 80(2):121–141.

Redillas, M. C. F. R., Strasser, R. J., Jeong, J. S., Kim, Y. S., and Kim, J.-K. (2011). The use of JIP test to evaluate drought-tolerance of transgenic rice overexpressing OsNAC10. *Plant Biotechnology Reports*, 5(2):169–175.

Rees, R. M., Bingham, I. J., Baddeley, J. A., and Watson, C. A. (2005). The role of plants and land management in sequestering soil carbon in temperate arable and grassland ecosystems. *Geoderma*, 128(1):130–154.

Reichstein, M., Falge, E., Baldocchi, D., Papale, D., Aubinet, M., Berbigier, P., Bernhofer, C., Buchmann, N., Gilmanov, T., Granier, A., Grunwald, T., Havrankova, K.,

Ilvesniemi, H., Janous, D., Knohl, A., Laurila, T., Lohila, A., Loustau, D., Matteucci, G., Meyers, T., Miglietta, F., Ourcival, J.-M., Pumpanen, J., Rambal, S., Rotenberg, E., Sanz, M., Tenhunen, J., Seufert, G., Vaccari, F., Vesala, T., Yakir, D., and Valentini, R. (2005). On the separation of net ecosystem exchange into assimilation and ecosystem respiration: review and improved algorithm. *Global Change Biology*, 11(9):1424–1439.

Retuerto, R., Fernandez-lema, B., Rodriguez-Roiloa, J. R., and Obeso, J. R. (2004). Increased photosynthetic performance in holly trees infested by scale insects. *Functional Ecology*, 18(5):664–669.

Retzlaff, W. A., Arthur, M. A., Grulke, N. E., Weinstein, D. A., and Gollands, B. (2000). Use of a single-tree simulation model to predict effects of ozone and drought on growth of a white fir tree. *Tree physiology*, 20(3):195–202.

Reynolds, M., Foulkes, M. J., Slafer, G. A., Berry, P., Parry, M. A. J., Snape, J. W., and Angus, W. J. (2009). Raising yield potential in wheat. *Journal of Experimental Botany*, 60(7):1899–1918.

Rho, H., Yu, D. J., Kim, S. J., and Lee, H. J. (2012). Limitation factors for photosynthesis in 'Bluecrop' highbush blueberry (*Vaccinium corymbosum*) leaves in response to moderate water stress. *Journal of Plant Biology*, 55(6):450–457.

Richmond, A. S., Wylie, A. R. G., Laidlaw, A. S., and Lively, F. O. (2015). Methane emissions from beef cattle grazing on semi-natural upland and improved lowland grasslands. *Animal*, 9(1):130–137.

Rios, J. A., Rios, V. S., Aucique-Pérez, C. E., Cruz, M. F. A., Morais, L. E., DaMatta, F. M., and Rodrigues, F. A. (2017). Alteration of photosynthetic performance and source-sink relationships in wheat plants infected by *Pyricularia oryzae*. *Plant Pathology*, 66(9):1496–1507.

Rios, V. S., Rios, J. A., Aucique-Pérez, C. E., Silveira, P. R., Barros, A. V., and Rodrigues, F. Á. (2018). Leaf gas exchange and chlorophyll a fluorescence in soybean leaves infected by *Phakopsora pachyrhizi*. *Journal of Phytopathology*, 166(2):75–85.

Ripoll, J., Bertin, N., Bidel, L. P. R., and Urban, L. (2016). A User's View of the Parameters Derived from the Induction Curves of Maximal Chlorophyll a Fluorescence: Perspectives for Analyzing Stress. *Frontiers in Plant Science*, 7:1679.

Rizhsky, L., Liang, H., and Mittler, R. (2002). The combined effect of drought stress and heat shock on gene expression in tobacco. *Plant Physiology*, 130(3):1143–51.

Rizhsky, L., Liang, H., Shuman, J., Shulaev, V., Davletova, S., and Mittler, R. (2004). When Defense Pathways Collide. The Response of Arabidopsis to a Combination of Drought and Heat Stress. *Plant physiology*, 134(4):1683–1696.

Roháček, K., Soukupová, J., and Barták, M. (2008). Chlorophyll fluorescence: a wonderful tool to study plant physiology and plant stress. In *Schoefs, B. (Eds.) Plant Cell Compartments - Selected Topics*, pages 41–104. Research Signpost, Kerala, India.

Roscher, C., Schumacher, J., Lipowsky, A., Gubsch, M., Weigelt, A., Pompe, S., Kolle, O., Buchmann, N., Schmid, B., and Schulze, E.-D. (2013). A functional trait-based approach to understand community assembly and diversity-productivity relationships over 7 years in experimental grasslands. *Perspectives in Plant Ecology, Evolution and Systematics*, 15(3):139–149.

Rosenstiel, T. N., Potosnak, M. J., Griffin, K. L., Fall, R., and Monson, R. K. (2003). Increased CO_2 uncouples growth from isoprene emission in an agriforest ecosystem. *Nature*, 421:256.

Ruban, A. V., Johnson, M. P., and Duffy, C. D. P. (2012). The photoprotective molecular switch in the photosystem II antenna. *Biochimica et Biophysica Acta (BBA) - Bioenergetics*, 1817(1):167–181.

Sage, R. F. (2013). Photorespiratory compensation: a driver for biological diversity. *Plant Biology*, 15(4):624–638.

Salvucci, M. E. and Ogren, W. L. (1996). The mechanism of Rubisco activase: Insights from studies of the properties and structure of the enzyme. *Photosynthesis Research*, 47(1):1–11.

Salvucci, M. E., Osteryoung, K. W., Crafts-Brandner, S. J., and Vierling, E. (2001). Exceptional Sensitivity of Rubisco Activase to Thermal Denaturation in Vitro and in Vivo. *Plant Physiology*, 127(3):1053 LP – 1064.

Savage, K., Phillips, R., and Davidson, E. (2014). High temporal frequency measurements of greenhouse gas emissions from soils. *Biogeosciences*, 11(10):2709–2720.

Schansker, G., Tóth, S. Z., and Strasser, R. J. (2005). Methylviologen and dibromothymoquinone treatments of pea leaves reveal the role of photosystem I in the Chl a fluorescence rise OJIP. *Biochimica et biophysica acta*, 1706(3):250–61.

Schansker, G., Yuan, Y., and Strasser, R. J. (2008). Chl a Fluorescence and 820 nm Transmission Changes Occurring During a Dark-to-Light Transition in Pine Needles and Pea Leaves: A Comparison. In Allen, J. F., Gantt, E., Golbeck, J. H., and Osmond, B., editors, *Allen, J.F., Gantt, E., Golbeck, J.H., and Osmond, B. (Eds.), Photosynthesis. Energy from the Sun: 14th International Congress on Photosynthesis*, pages 945–949. Springer Netherlands, Dordrecht.

Scheller, H. V. and Haldrup, A. (2005). Photoinhibition of photosystem I. *Planta*, 221(1):5–8.

Schneider, D., Volkmer, T., and Rögner, M. (2007). PetG and PetN, but not PetL, are essential subunits of the cytochrome b6f complex from *Synechocystis PCC* 6803. *Research in Microbiology*, 158(1):45–50.

Scholefield, P. A., Doick, K. J., Herbert, B. M. J., Hewitt, C. N. S., Schnitzler, J.-P., Pinelli, P., and Loreto, F. (2004). Impact of rising CO_2 on emissions of volatile organic compounds: isoprene emission from *Phragmites australis* growing at elevated CO_2 in a natural carbon dioxide spring. *Plant, Cell & Environment*, 27(4):393–401.

Schöttler, M. A., Tóth, S. Z., Boulouis, A., and Kahlau, S. (2015). Photosynthetic complex stoichiometry dynamics in higher plants: biogenesis, function, and turnover of ATP synthase and the cytochrome b6f complex. *Journal of Experimental Botany*, 66(9):2373–2400.

Schuler, M. L., Mantegazza, O., and Weber, A. P. M. (2016). Engineering C4 photosynthesis into C3 chassis in the synthetic biology age. *The Plant Journal*, 87(1):51–65.

Sengupta, D., Guha, A., and Reddy, A. R. (2013). Interdependence of plant water status with photosynthetic performance and root defense responses in *Vigna radiata* (L.) Wilczek under progressive drought stress and recovery. *Journal of photochemistry and photobiology. B, Biology*, 127:170–81.

Sharkey, T. D. (2005). Effects of moderate heat stress on photosynthesis: importance of thylakoid reactions, rubisco deactivation, reactive oxygen species, and thermotolerance provided by isoprene. *Plant, Cell and Environment*, 28(3):269–277.

Sharkey, T. D. and Loreto, F. (1993). Water stress, temperature, and light effects on the capacity for isoprene emission and photosynthesis of kudzu leaves. *Oecologia*, 95(3):328–333.

Sharkey, T. D. and Zhang, R. (2010). High Temperature Effects on Electron and Proton Circuits of Photosynthesis. *Journal of Integrative Plant Biology*, 52(8):712–722.

Shimizu, M., Hatano, R., Arita, T., Kouda, Y., Mori, A., Matsuura, S., Niimi, M., Jin, T., Desyatkin, A. R., Kawamura, O., Hojito, M., and Miyata, A. (2013). The effect of fertilizer and manure application on CH_4 and N_2O emissions from managed grasslands in Japan. *Soil Science and Plant Nutrition*, 59(1):69–86.

Signor, D. and Cerri, C. E. P. (2013). Nitrous oxide emissions in agricultural soils: a review .

Silvestre, S., de Sousa Araújo, S., Vaz Patto, M. C., and Marques da Silva, J. (2014). Performance index: An expeditious tool to screen for improved drought resistance in the *Lathyrus genus*. *Journal of Integrative Plant Biology*, 56(7):610–621.

Šimić, D., Lepeduš, H., Jurković, V., Antunović, J., and Cesar, V. (2014). Quantitative genetic analysis of chlorophyll a fluorescence parameters in maize in the field environments. *Journal of integrative plant biology*, 56(7):695–708.

Smit, M. F., Kruger, G. H. J., van Heerden, P. D. R., Pienaar, J. J., Weissflog, L., and Strasser, R. J. (2009). Effect of trifluoroacetate, a persistent degradation product of fluorinated hydrocarbons, on C3 and C4 crop plants. In *Allen, J.F., Gantt, E., Golbeck, J.H., and Osmond, B. (Eds.), Photosynthesis. Energy from the sun. 14th International Congress of Photosynthesis Glasgow 2007*, volume 47, pages 623–634. Springer, Dordrecht.

Smith, K. A., Ball, T., Conen, F., Dobbie, K. E., Massheder, J., and Rey, A. (2003). Exchange of greenhouse gases between soil and atmosphere: interactions of soil physical factors and biological processes. *European Journal of Soil Science*, 54(4):779–791.

Smith, P., Bustamante, M., Ahammad, H., Clark, H., Dong, H., Elsiddig, E., Haberl, H., Harper, R., House, J., Jafari, M., Masera, O., Mbow, C., Ravindranath, N., Rice, C., Abad, C. R., Romanovskaya, A., Sperling, F., and Tubiello, F. (2014). Agriculture, forestry and other land use (AFOLU). In *Edenhofer et al. (Eds.) Climate change 2014: mitigation of climate change. Contribution of working group III to the fifth assessment report of the IPCC*. Cambridge University Press,, Cambridge, United Kingdom and New York, United States of America.

Snider, J. L., Oosterhuis, D. M., Collins, G. D., Pilon, C., and Fitzsimons, T. R. (2013). Field-acclimated *Gossypium hirsutum* cultivars exhibit genotypic and seasonal differences in photosystem II thermostability. *Journal of Plant Physiology*, 170(5):489–96.

Sofo, A., Dichio, B., Montanaro, G., and Xiloyannis, C. (2009). Photosynthetic performance and light response of two olive cultivars under different water and light regimes. *Photosynthetica*, 47(4):602–608.

Soja, G., Pfeifer, U., and Soja, A.-M. (1998). Photosynthetic parameters as early indicators of ozone injury in apple leaves. *Physiologia Plantarum*, 104(4):639–645.

Soussana, J.-F. and Duru, M. (2007). Grassland science in Europe facing new challenges: biodiversity and global environmental change. *CAB Reviews Perspectives in Agriculture Veterinary Science Nutrition and Natural Resources*, 2(2):1–11.

Souza, R., Machado, E., Silva, J., Lagôa, A., and Silveira, J. (2004). Photosynthetic gas exchange, chlorophyll fluorescence and some associated metabolic changes in cowpea (*Vigna unguiculata*) during water stress and recovery. *Environmental and Experimental Botany*, 51(1):45–56.

Spielmann, F. M., Langebner, S., Ghirardo, A., Hansel, A., Schnitzler, J.-P., and Wohlfahrt, G. (2017). Isoprene and α-pinene deposition to grassland mesocosms. *Plant and Soil*, 410(1):313–322.

Spoustová, P., Synková, H., Valcke, R., and Čeřovská, N. (2013). Chlorophyll a fluorescence as a tool for a study of the *Potato virus Y* effects on photosynthesis of nontransgenic and transgenic *Pssu-ipt* tobacco. *Photosynthetica*, 51(2):191–201.

Staudt, M. and Bertin, N. (1998). Light and temperature dependence of the emission of cyclic and acyclic monoterpenes from holm oak (*Quercus ilex* L.) leaves. *Plant, Cell & Environment*, 21(4):385–395.

Staudt, M., Lhoutellier, L., and Wang, X. (2011). Monoterpene and sesquiterpene emissions from *Quercus coccifera* exhibit interacting responses to light and temperature. *Biogeosciences*, 8(9):2757–2771.

Steinfeld, H., Gerber, P., Wassenaar, T., Castel, V., Rosales, M., and de Haan, C. (2006). Livestock's long shadow - environmental issues and options. Technical report, The Food and Agriculture Organization of the United Nation (FAO), Rome, Italy.

Stirbet, A. and Govindjee (2011). On the relation between the Kautsky effect (chlorophyll a fluorescence induction) and Photosystem II: Basics and applications of the OJIP fluorescence transient. *Journal of Photochemistry and Photobiology B: Biology*, 104(1-2):236–257.

Stirbet, A. and Govindjee (2012). Chlorophyll a fluorescence induction: a personal perspective of the thermal phase, the J-I-P rise. *Photosynthesis research*, 113(1-3):15–61.

Stirbet, A., Lazár, D., Kromdijk, J., and Govindjee (2018). Chlorophyll a fluorescence induction: Can just a one-second measurement be used to quantify abiotic stress responses? *Photosynthetica*.

Strasser, B. J. (1997). Donor side capacity of Photosystem II probed by chlorophyll a fluorescence transients. *Photosynthesis Research*, 52(2):147–155.

Strasser, R. J., Srivastava, A., and Govindjee (1995). Polyphasic chlorophyll alpha fluorescence transient in plants and cyanobacteria. *Photochemistry and Photobiology*, 61(1):32–42.

Strasser, R. J. and Stirbet, A. D. (1998). Heterogeneity of photosystem II probed by the numerically simulated chlorophyll a fluorescence rise (O-J-I-P). *Mathematics and Computers in Simulation*, 48(1):3–9.

Strasser, R. J., Srivastava, A., and Tsimilli-Michael, M. (2000). The fluorescence transient as a tool to characterize and screen photosynthetic samples. In *Yunnus M, Pathre U and Mohanty P (Eds.) Probing photosynthesis: mechanism, regulation and adaptation*, chapter 25, pages 443–480. Taylor and Francis, London, UK.

Strasser, R. J. and Stirbet, A. D. (2001). Estimation of the energetic connectivity of PS II centres in plants using the fluorescence rise O-J-I-P. *Mathematics and Computers in Simulation*, 56(4-5):451–462.

Strasser, R. J., Tsimilli Michael, M., and Srivastava, A. (2004). Analysis of the chlorophyll a transient. In *Papageorgiou, G.C. and Govindjee (Eds.) Chlorophyll Fluorescence: A Signature of Photosynthesis*, pages 321–362. Kluwer Academic Publishers.

Strauss, A., Krüger, G., Strasser, R., and Heerden, P. V. (2006). Ranking of dark chilling tolerance in soybean genotypes probed by the chlorophyll a fluorescence transient O-J-I-P. *Environmental and Experimental Botany*, 56(2):147–157.

Štroch, M., Vrábl, D., Podolinská, J., Kalina, J., Urban, O., and Špunda, V. (2010). Acclimation of Norway spruce photosynthetic apparatus to the combined effect of high irradiance and temperature. *Journal of Plant Physiology*, 167(8):597–605.

Su, X., Ma, J., Wei, X., Cao, P., Zhu, D., Chang, W., Liu, Z., Zhang, X., and Li, M. (2017). Structure and assembly mechanism of plant $C_2S_2M_2$-type PSII-LHCII supercomplex. *Science*, 357(6353):815 LP – 820.

Subbarao, G. V., Rondon, M., Ito, O., Ishikawa, T., Rao, I. M., Nakahara, K., Lascano, C., and Berry, W. L. (2007). Biological nitrification inhibition (BNI)-is it a widespread phenomenon? *Plant and Soil*, 294(1):5–18.

Subbarao, G. V., Kishii, M., Nakahara, K., Ishikawa, T., Ban, T., Tsujimoto, H., George, T. S., Berry, W. L., Hash, C. T., and Ito, O. (2009). Biological nitrification inhibition (BNI)-Is there potential for genetic interventions in the Triticeae? *Breeding Science*, 59(5):529–545.

Subbarao, G. V., Sahrawat, K. L., Nakahara, K., Ishikawa, T., Kishii, M., Rao, I. M., Hash, C. T., George, T. S., Srinivasa Rao, P., Nardi, P., Bonnett, D., Berry, W., Suenaga, K., and Lata, J. C. (2012). *Biological nitrification inhibition-a novel strategy to regulate nitrification in agricultural systems*, volume 114. Elsevier Inc., 1 edition.

Subbarao, G. V., Rao, I. M., Nakahara, K., Sahrawat, K. L., Ando, Y., and Kawashima, T. (2013). Potential for biological nitrification inhibition to reduce nitrification and N_2O emissions in pasture crop-livestock systems. *animal*, 7(s2):322–332.

Subbarao, G. V., Yoshihashi, T., Worthington, M., Nakahara, K., Ando, Y., Sahrawat, K. L., Rao, I. M., Lata, J.-C., Kishii, M., and Braun, H.-J. (2015). Suppression of soil nitrification by plants. *Plant Science*, 233:155–164.

Subbarao, G. V., Arango, J., Masahiro, K., Hooper, A. M., Yoshihashi, T., Ando, Y., Nakahara, K., Deshpande, S., Ortiz-Monasterio, I., Ishitani, M., Peters, M., Chirinda, N., Wollenberg, L., Lata, J. C., Gerard, B., Tobita, S., Rao, I. M., Braun, H. J., Kommerell, V., Tohme, J., and Iwanaga, M. (2017). Genetic mitigation strategies to tackle agricultural GHG emissions: The case for biological nitrification inhibition technology. *Plant Science*, 262:165–168.

Takagi, K., Hirata, R., Ide, R., Ueyama, M., Ichii, K., Saigusa, N., Hirano, T., Asanuma, J., Li, S.-G., Machimura, T., Nakai, Y., Ohta, T., and Takahashi, Y. (2015). Spatial and seasonal variations of CO_2 flux and photosynthetic and respiratory parameters of larch forests in East Asia. *Soil Science and Plant Nutrition*, 61(1):61–75.

Takahashi, S., Milward, S. E., Fan, D.-Y., Chow, W. S., and Badger, M. R. (2009). How does cyclic electron flow alleviate photoinhibition in Arabidopsis? *Plant Physiology*, 149(3):1560–1567.

Tang, J. Y., Zielinski, R. E., Zangerl, A. R., Crofts, A. R., Berenbaum, M. R., and Delucia, E. H. (2006). The differential effects of herbivory by first and fourth instars of Trichoplusia ni (Lepidoptera: Noctuidae) on photosynthesis in Arabidopsis thaliana. *Journal of experimental botany*, 57(3):527–36.

Tezara, W., Mitchell, V. J., Driscoll, S. D., and Lawlor, D. W. (1999). Water stress

inhibits plant photosynthesis by decreasing coupling factor and ATP. *Nature*, 401(6756):914–917.

Thiry, A. A., Chavez Dulanto, P. N., Reynolds, M. P., and Davies, W. J. (2016). How can we improve crop genotypes to increase stress resilience and productivity in a future climate? A new crop screening method based on productivity and resistance to abiotic stress. *Journal of Experimental Botany*, 67(19):5593–5603.

Tiiva, P., Tang, J., Michelsen, A., and Rinnan, R. (2017). Monoterpene emissions in response to long-term night-time warming, elevated CO_2 and extended summer drought in a temperate heath ecosystem. *Science of The Total Environment*, 580(Supplement C):1056–1067.

Tikhonov, A. N. (2014). The cytochrome b6f complex at the crossroad of photosynthetic electron transport pathways. *Plant Physiology and Biochemistry*, 81:163–183.

Tikkanen, M., Mekala, N. R., and Aro, E.-M. (2014). Photosystem II photoinhibition-repair cycle protects Photosystem I from irreversible damage. *Biochimica et Biophysica Acta (BBA) - Bioenergetics*, 1837(1):210–215.

Tiwari, A., Mamedov, F., Grieco, M., Suorsa, M., Jajoo, A., Styring, S., Tikkanen, M., and Aro, E.-M. (2016). Photodamage of iron-sulphur clusters in photosystem I induces non-photochemical energy dissipation. *Nature Plants*, 2:16035.

Tóth, S. Z., Schansker, G., Garab, G., and Strasser, R. J. (2007a). Photosynthetic electron transport activity in heat-treated barley leaves: the role of internal alternative electron donors to photosystem II. *Biochimica et Biophysica Acta*, 1767(4):295–305.

Tóth, S. Z., Schansker, G., and Strasser, R. J. (2007b). A non-invasive assay of the plastoquinone pool redox state based on the OJIP-transient. *Photosynthesis Research*, 93(1-3):193–203.

Tozzi, E. S., Easlon, H. M., and Richards, J. H. (2013). Interactive effects of water, light and heat stress on photosynthesis in Fremont cottonwood. *Plant, Cell and Environment*, 36(8):1423–34.

Tsimilli-Michael, M., Eggenberg, P., Biro, B., Köves-Pechy, K., Vörös, I., and Strasser, R. (2000). Synergistic and antagonistic effects of arbuscular mycorrhizal fungi and Azospirillum and Rhizobium nitrogen-fixers on the photosynthetic activity of alfalfa, probed by the polyphasic chlorophyll a fluorescence transient O-J-I-P. *Applied Soil Ecology*, 15(2):169–182.

Tsimilli-Michael, M. and Strasser, R. J. (2008). In vivo assessment of stress impact on plant's vitality: applications in detecting and evaluating the beneficial role of mycorrhization on host plants. In *Varma, A. (Eds.) Mycorrhiza: State of the Art, Genetics and Molecular Biology, Eco-Function, Biotechnology, Eco-Physiology, Structure and Systematics (3rd edition)*, chapter In vivo As, pages 679–703. Springer, Berlin, Germany, Dordrecht, The Netherlands.

Tyystjärvi, E. (2008). Photoinhibition of Photosystem II and photodamage of the oxygen evolving manganese cluster. *Coordination Chemistry Reviews*, 252(3):361–376.

United Nations (UN) (2017). Department of Economic and Social Affairs. Population Division. World Population Prospects: The 2017 Revision, Key Findings and Advance Tables. Technical report, Working Paper No. ESA/P/WP/248.

van Heerden, P., Swanepoel, J., and Krüger, G. (2007). Modulation of photosynthesis by drought in two desert scrub species exhibiting C3-mode CO_2 assimilation. *Environmental and Experimental Botany*, 61(2):124–136.

van Heerden, P. D. R., Tsimilli Michael, M., Krüger, G. H. J., Strasser, R. J., and Kruger, G. H. J. (2003). Dark chilling effects on soybean genotypes during vegetative development: parallel studies of CO_2 assimilation, chlorophyll a fluorescence kinetics O-J-I-P and nitrogen fixation. *Physiologia plantarum*, 117(4):476–491.

van Meeningen, Y., Schurgers, G., Rinnan, R., and Holst, T. (2017). Isoprenoid emission response to changing light conditions of English oak, European beech and Norway spruce. *Biogeosciences Discussions*, pages 1–25.

Velikova, V., Tsonev, T., Barta, C., Centritto, M., Koleva, D., Stefanova, M., Busheva, M., and Loreto, F. (2009). BVOC emissions, photosynthetic characteristics and changes in chloroplast ultrastructure of (*Platanus orientalis* L. exposed to elevated CO_2 and high temperature. *Environmental Pollution*, 157(10):2629–2637.

Vellinga, T., van den Pol-van Dasselaar, A., and Kuikman, P. J. (2004). The impact of grassland ploughing on CO_2 and N_2O emissions in the Netherlands. *Nutrient Cycling in Agroecosystems*, 70(1):33–45.

Verma, K. K., Singh, M., Gupta, R. K., and Verma, C. L. (2014). Photosynthetic gas exchange, chlorophyll fluorescence, antioxidant enzymes, and growth responses of *Jatropha Curcas* during soil flooding. *Turkish Journal of Botany*, 38(1):130–140.

Vile, D., Pervent, M., Belluau, M., Vasseur, F., Bresson, J., Muller, B., Granier, C., and Simonneau, T. (2012). Arabidopsis growth under prolonged high temperature and water deficit: independent or interactive effects? *Plant, Cell and Environment*, 35(4):702–718.

Villányi, V., Ürmös, Z., Turk, B., Batič, F., and Csintalan, Z. (2014). Photosynthesis of ozone-sensitive and -resistant *Phaseolus vulgaris* genotypes under ambient ozone and moderate heat stress. *Photosynthetica*, 52(4):604–613.

von Caemmerer, S., Lawson, T., Oxborough, K., Baker, N. R., Andrews, T. J., and Raines, C. A. (2004). Stomatal conductance does not correlate with photosynthetic capacity in transgenic tobacco with reduced amounts of Rubisco. *Journal of Experimental Botany*, 55(400):1157–1166.

von Caemmerer, S., Quick, W. P., and Furbank, R. T. (2012). The Development of C_4 Rice: Current Progress and Future Challenges. *Science*, 336(6089):1671 LP – 1672.

Voss, I., Sunil, B., Scheibe, R., and Raghavendra, A. S. (2013). Emerging concept for the role of photorespiration as an important part of abiotic stress response. *Plant Biology*, 15(4):713–722.

Walther, S., Voigt, M., Thum, T., Gonsamo, A., Zhang, Y., Koehler, P., Jung, M., Varlagin, A., and Guanter, L. (2015). Satellite chlorophyll fluorescence measurements reveal large-scale decoupling of photosynthesis and greenness dynamics in boreal evergreen forests. *Global Change Biology*, 22(9):2979–2996.

Wang, P., Hendron, R.-W., and Kelly, S. (2017). Transcriptional control of photosynthetic capacity: conservation and divergence from Arabidopsis to rice. *New Phytologist*, page in press.

Wehr, R., Munger, J. W., McManus, J. B., Nelson, D. D., Zahniser, M. S., Davidson, E. A., Wofsy, S. C., and Saleska, S. R. (2016). Seasonality of temperate forest photosynthesis and daytime respiration. *Nature*, 534:680–683.

Werner, C., Correia, O., and Beyschlag, W. (2002). Characteristic patterns of chronic and dynamic photoinhibition of different functional groups in a Mediterranean ecosystem. *Functional Plant Biology*, 29(8):999–1011.

Werner, C., Ryel, R. J., Correia, O., and Beyschlag, W. (2001). Effects of photoinhibition on whole-plant carbon gain assessed with a photosynthesis model. *Plant, Cell & Environment*, 24(1):27–40.

Whitmarsh, J. and Govindjee (2001). Photosystem II. In *eLS*. John Wiley & Sons, Ltd. DOI: 10.1038/npg.els.0000669.

Whitney, S. M., Houtz, R. L., and Alonso, H. (2011). Advancing Our Understanding and Capacity to Engineer Nature's CO_2-Sequestering Enzyme, Rubisco. *Plant Physiology*, 155(1):27 LP – 35.

Wilson, R. S. and Franklin, C. E. (2002). Testing the beneficial acclimation hypothesis. *Trends in Ecology & Evolution*, 17(2):66–70.

Wohlfahrt, G. and Gu, L. (2015). The many meanings of gross photosynthesis and their implication for photosynthesis research from leaf to globe. *Plant, Cell & Environment*, 38(12):2500–2507.

Wrage, N., Velthof, G. L., Laanbroek, H. J., and Oenema, O. (2004). Nitrous oxide production in grassland soils: assessing the contribution of nitrifier denitrification. *Soil Biology and Biochemistry*, 36(2):229–236.

Xu, Z. Z. and Zhou, G. S. (2006). Combined effects of water stress and high temperature on photosynthesis, nitrogen metabolism and lipid peroxidation of a perennial grass *Leymus chinensis*. *Planta*, 224(5):1080–1090.

Xu, Z. Z., Zhou, G. S., Wang, Y. L., Han, G. X., and Li, Y. J. (2008). Changes in chlorophyll fluorescence in maize plants with imposed rapid dehydration at different leaf ages. *Journal of Plant Growth Regulation*, 27(1):83–92.

Yamamoto, Y., Aminaka, R., Yoshioka, M., Khatoon, M., Komayama, K., Takenaka, D., Yamashita, A., Nijo, N., Inagawa, K., Morita, N., Sasaki, T., and Yamamoto, Y. (2008). Quality control of photosystem II: impact of light and heat stresses. *Photosynthesis Research*, 98(1):589–608.

Yamamoto, Y., Kai, S., Ohnishi, A., Tsumura, N., Ishikawa, T., Hori, H., Morita, N., and Ishikawa, Y. (2014). Quality control of PSII: behavior of PSII in the highly crowded grana thylakoids under excessive light. *Plant & cell physiology*, 55(7):1206–15.

Yan, K., Chen, P., Shao, H., Zhang, L., and Xu, G. (2011). Effects of Short-Term High Temperature on Photosynthesis and Photosystem II Performance in Sorghum. *Journal of Agronomy and Crop Science*, 197(5):400–408.

Yan, K., Chen, P., Shao, H., Zhao, S., Zhang, L., Xu, G., and Sun, J. (2012). Responses of photosynthesis and photosystem II to higher temperature and salt stress in sorghum. *Journal of Agronomy and Crop Science*, 198(3):218–225.

Yan, K., Chen, P., Shao, H., Shao, C., Zhao, S., and Brestic, M. (2013). Dissection of photosynthetic electron transport process in sweet sorghum under heat stress. *PloS one*, 8(5):e62100.

Yi, X.-P., Zhang, Y.-L., Yao, H.-S., Luo, H.-H., Gou, L., Chow, W. S., and Zhang, W.-F. (2016). Different strategies of acclimation of photosynthesis, electron transport and antioxidative activity in leaves of two cotton species to water deficit. *Functional Plant Biology*, 43(5):448–460.

Yin, Z., Meng, F., Song, H., He, X., Xu, X., and Yu, D. (2010). Mapping quantitative trait loci associated with chlorophyll a fluorescence parameters in soybean (*Glycine max* (L.) Merr.). *Planta*, 231(4):875–885.

Yin, Z., Meng, F., Song, H., Wang, X., Chao, M., Zhang, G., Xu, X., Deng, D., and Yu, D. (2011). GmFtsH9 expression correlates with in vivo photosystem II function: chlorophyll a fluorescence transient analysis and eQTL mapping in soybean. *Planta*, 234(4):815–827.

Yin, Z., Qin, Q., Wu, F., Zhang, J., Chen, T., Sun, Q., Zhang, Y., Wang, H., and Deng, D. (2015). Quantitative trait locus mapping of chlorophyll a fluorescence parameters using a recombinant inbred line population in maize. *Euphytica*, 205(1):25–35.

Yoo, C. Y., Pence, H. E., Jin, J. B., Miura, K., Gosney, M. J., Hasegawa, P. M., and Mickelbart, M. V. (2011). The *Arabidopsis* GTL1 Transcription Factor Regulates Water Use Efficiency and Drought Tolerance by Modulating Stomatal Density via Transrepression of *SDD1*. *The Plant Cell*, 22(12):4128 LP – 4141.

Yuan, X. K., Yang, Z. Q., Li, Y. X., Liu, Q., and Han, W. (2016). Effects of different levels of water stress on leaf photosynthetic characteristics and antioxidant enzyme activities of greenhouse tomato. *Photosynthetica*, 54(1):28–39.

Zavalloni, C., Gielen, B., De Boeck, H. J., Lemmens, C., Ceulemans, R., and Nijs, I. (2009). Greater impact of extreme drought on photosynthesis of grasslands exposed to a warmer climate in spite of acclimation. *Physiologia Plantarum*, 136(1):57–72.

Zhang, X., Wang, L., Ma, F., and Shan, D. (2015). Effects of Arbuscular Mycorrhizal Fungi on N_2O Emissions from Rice Paddies. *Water, Air, & Soil Pollution*, 226(7):222.

Zhao, H. F., Zhao, Y., Zhang, C., Tao, X., and Xu, X. N. (2014). Growth, leaf gas exchange, and chlorophyll fluorescence responses of two cultivars of *Salix integra* Thunb. to waterlogging stress. *Journal of Agricultural Science and Technology*, 16(1):137–149.

Zheng, Y., Unger, N., Tadić, J. M., Seco, R., Guenther, A. B., Barkley, M. P., Potosnak, M. J., Murray, L. T., Michalak, A. M., Qiu, X., Kim, S., Karl, T., Gu, L., and Pallardy, S. G. (2017). Drought impacts on photosynthesis, isoprene emission and atmospheric formaldehyde in a mid-latitude forest. *Atmospheric Environment*, 167(Supplement C):190–201.

Zhu, L., Johnson, D. A., Wang, W., Ma, L., and Rong, Y. (2015). Grazing effects on carbon fluxes in a Northern China grassland. *Journal of Arid Environments*, 114:41–48.

Zhu, X.-G., Long, S. P., and Ort, D. R. (2008). What is the maximum efficiency with which photosynthesis can convert solar energy into biomass? *Current Opinion in Biotechnology*, 19(2):153–159.

Zivcak, M., Brestic, M., Balatova, Z., Drevenakova, P., Olsovska, K., Kalaji, H. M., Yang, X., and Allakhverdiev, S. I. (2013). Photosynthetic electron transport and spe-

cific photoprotective responses in wheat leaves under drought stress. *Photosynthesis Research*, 117(1):529–546.

Zivcak, M., Brestic, M., Kalaji, H. M., and Govindjee (2014). Photosynthetic responses of sun- and shade-grown barley leaves to high light: is the lower PSII connectivity in shade leaves associated with protection against excess of light? *Photosynthesis research*, 119(3):339–54.

Zivcak, M., Brestic, M., Kunderlikova, K., Olsovska, K., and Allakhverdiev, S. I. (2015). Effect of photosystem I inactivation on chlorophyll a fluorescence induction in wheat leaves: Does activity of photosystem I play any role in OJIP rise? *Journal of Photochemistry and Photobiology B: Biology*, 152(Pt B):18–21.

Živčák, M., Brestič, M., Olšovská, K., and Slámka, P. (2008). Performance index as a sensitive indicator of water stress in Triticum aestivum L. *Plant, Soil and Environment*, 54(4):133–139.

GLOSSARY

Acclimation/acclimatization: according to Wilson and Franklin (2002), refers to the adjustment of a physiological trait in response to changes in an environmental variable. Acclimation is used for changes of a single variable in a lab environment whereas acclimatization is used for changes of one or more variables under field condition. Whereas the physiological response can either be positive, negative or have a neutral effect for the stress tolerance of the considered organism, the terms acclimatization/acclimation will be used here to refer to positive effect.

Adaptation: in a population, refers to an evolution process leading to the selection of genotypes better fitted to the local environmental conditions (Bussotti et al. 2015).

Apparent photosynthesis: also referred as 'net photosynthesis', represents the true photosynthesis minus (dark- and photo-)respiration.

Gross primary production: is derived from the flux partitioning of the net ecosystem (CO_2) exchange measured by eddy covariance and is intended as an integration of the apparent photosynthesis.

Net ecosystem (CO_2) exchange: net balance between CO_2 uptake and release by the ecosystem.

Net primary productivity: net balance between CO_2 uptake and release by plants.

Photochemical capacity: ability and efficiency of the photosynthetic machinery to absorb and use a photon to produce chemical energy. Also referred as 'photosynthetic performance' in the Results section.

Photosynthetic capacity: according to the definition given by Hopkins and Hüner (2008), is determined by the balance between the carboxylation capacity and the electron transport capacity.

Photoinhibition: inactivation or a decrease in the efficiency of the PSII in response

to an excess of light absorption or a prolonged exposition, resulting in the reduction of the photosynthetic rate.

Photosynthetic performance: see *Photochemical capacity*.

Stress: from a physiological perspective, stress is defined as environmental changes leading to physiological responses of the individuals and affecting their performance.

True photosynthesis: also referred as 'gross photosynthesis', represents the total CO_2 fixed through carboxylation activity.

Water-use efficiency: defines the amount of assimilated CO_2 per unit of water used and can be expressed by the ratio A_{CO_2}/g_s in the case of the 'intrinsic' water-use efficiency and by the ratio A_{CO_2}/E in the case of the 'instantaneous' water-use efficiency (Morison et al. 2008).

SUPPLEMENTARY MATERIALS

Table S1 – Botanical diversity evaluated on 24 quadrats (0.5 x 0.5 m) during September 2010 and June 2011 at the Dorinne Terrestrial Observatory. The number of quadrats where the species was found (Presence), the frequency or probability of finding the species in a quadrat (F, [%]), the frequency relative to the total presence of all species (P, [%]) and the relative abundance (B, [%]). The relative abundance was calculated as the sum of the abundance index of the considered species for the 24 quadrats divided by the total abundance index for all species. The abundance index was based on the surface occupation of the considered species inside the quadrat and was evaluated on a scale from 0 to 3 the first year and on a scale from 0 to 10 the second year. The floristic inventory was realized by Hautot (2011) during his master thesis.

	September 2010				**June 2011**			
Species	**Presence**	**F**	**P**	**B**	**Presence**	**F**	**P**	**B**
Grass	70		62.5	75.2	100		68.0	88.6
Agrostis stolonifera L.	13	54.2	11.6	6.3	12	48.0	8.2	4.2
Alopecurus geniculatus L.	0	0.0	0.0	0.0	9	36.0	6.1	2.4
Bromus hordeaceus L.	0	0.0	0.0	0.0	1	4.0	0.7	0.2
Cynosurus cristatus L.	5	20.8	4.5	4.0	5	20.0	3.4	1.2
Dactylis glomerata L.	6	25.0	5.4	3.6	7	28.0	4.8	5.0
Elymus repens (L.) Gould	0	0.0	0.0	0.0	3	12.0	2.0	0.8
Festuca pratensis (Huds.) P. Beauv.	2	8.3	1.8	2.3	0	0.0	0.0	0.0
Holcus lanatus L.	11	45.8	9.8	9.9	11	44.0	7.5	4.6
Lolium multiflorum Lam.	0	0.0	0.0	0.0	1	4.0	0.7	0.2
Lolium perenne L.	24	100.0	21.4	43.7	25	100.0	17.0	61.0
Poa annua L.	0	0.0	0.0	0.0	1	4.0	0.7	0.2

Continued on next page

Table S1 – continued from previous page

	September 2010				June 2011			
Species	**Presence**	**F**	**P**	**B**	**Presence**	**F**	**P**	**B**
Poa pratensis L.	1	4.2	0.9	0.7	0	0.0	0.0	0.0
Poa trivialis L.	8	33.3	7.1	4.6	25	100.0	17.0	8.8
N-fixing dicots	22		19.6	15.9	20		13.6	5.6
Trifolium repens L.	22	91.7	19.6	15.9	20	80.0	13.6	5.6
Non-N-fixing dicots	20		17.9	8.9	27		13.6	5.8
Capsella bursa-pastoris (L.) Medik.	0	0.0	0.0	0.0	2	8.0	1.4	0.4
Carduus L.	1	4.2	0.9	0.3	2	8.0	1.4	0.6
Matricaria discoidea DC.	0	0.0	0.0	0.0	2	8.0	1.4	0.4
Plantago major L.	3	12.5	2.7	2.0	2	8.0	1.4	0.6
Ranunculus repens L.	1	4.2	0.9	0.3	6	24.0	4.1	1.4
Stellaria media (L.) Vill.	2	8.3	1.8	0.7	2	8.0	1.4	0.2
Taraxacum sp.	13	54.2	11.6	5.6	11	44.0	7.5	2.2
Total	**112**			**100**	**147**			**100**

Table S2 – Results of the General Linear Model analysis type (GLM) III. The assigned cluster number identified for each time period of measurement resulting from the principal component analysis-clustering based on meteorological data were used as a meteorological factor (Meteo.) in the GLM analysis to take account of the different meteorological conditions. The monitored plots were used as a block factor and was considered a random factor. Chlorophyll fluorescence data were square root-transformed previous to analysis to improve normality and homogeneity of variances, with the exception of PI_{ABS} due to the presence of negative values. DF, degree of freedom; SS, sum of squared; MS, mean squares.

Source	DF	SS	MS	F-Value	P-Value
Analysis of Variance for Transformed F_V/F_M					
pecies	2	7.102	3.551	165.51	0
Block	2	0.026	0.0129	0.26	0.78
Meteorological	2	59.515	29.7575	734.78	0
Species*Block	4	0.086	0.0215	1.72	0.237
Species*Meteo.	4	4.333	1.0833	86.49	0
Block*Meteo.	4	0.162	0.0405	3.23	0.074
Species*Block*Meteo.	8	0.1	0.0125	1.21	0.287
Error	15625	161.523	0.0103		
Total	15651	231.096			
Analysis of Variance for PI_{ABS}					
Species	2	208.5	104.27	14.56	0.015
Block	2	2.6	1.28	0.18	0.84
Meteorological	2	2556.6	1278.32	837.3	0
Species*Block	4	28.7	7.16	4.2	0.04
Species*Meteo.	4	37.6	9.4	5.46	0.02
Block*Meteo.	4	6.1	1.53	0.89	0.514
Species*Block*Meteo.	8	13.8	1.72	2.35	0.016
Error	15625	11462.5	0.73		
Total	15651	14295.1			
Analysis of Variance for Transformed Ψ_{E0}					
Species	2	11.399	5.69949	107.93	0
Block	2	0.089	0.04471	1.61	0.505

Continued on next page

Source	DF	SS	MS	F-Value	P-Value
Meteorological	2	0.756	0.378	41.23	0.002
Species*Block	4	0.211	0.05281	1.55	0.277
Species*Meteo.	4	1.946	0.48643	14.09	0.001
Block*Meteo.	4	0.037	0.00917	0.27	0.892
Species*Block*Meteo.	8	0.276	0.03453	3.12	0.002
Error	15625	173.108	0.01108		
Total	15651	188.116			
Analysis of Variance for Transformed ΔV_{IP}					
Species	2	9.49	4.7452	274.89	0
Block	2	0.168	0.0841	1.94	0.366
Meteorological	2	63.092	31.5461	518.05	0
Species*Block	4	0.069	0.0173	0.5	0.734
Species*Meteo.	4	7.789	1.9472	56.42	0
Block*Meteo.	4	0.244	0.0609	1.76	0.229
Species*Block*Meteo.	8	0.276	0.0345	2.59	0.008
Error	15625	208.039	0.0133		
Total	15651	286.885			

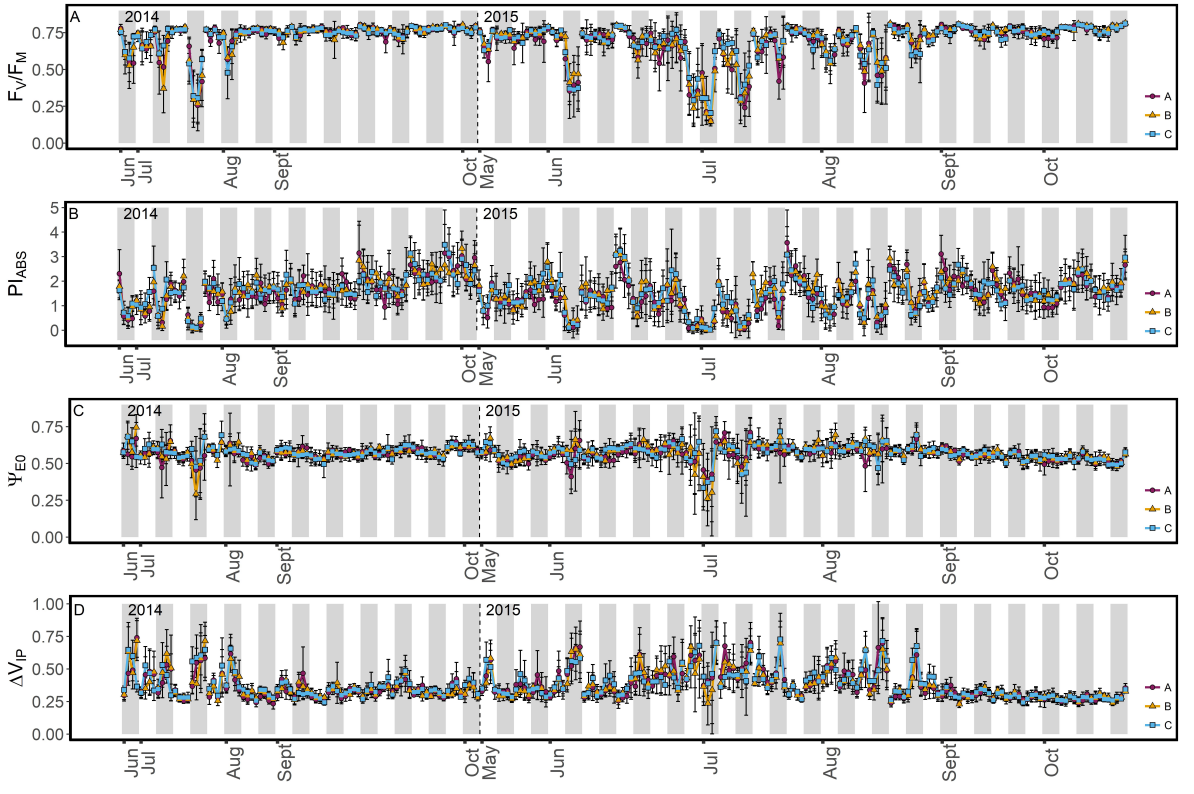

Figure S1 – Time course of ChlF parameters (F_V/F_M, PI_{ABS}, Ψ_{E0} and ΔV_{IP}) measured for *Lolium perenne* L., on the last fully developed leaf, in the three monitored plots in the grassland. For each measured day, the ChlF parameter average value (n = 7 or 8) $\pm$ SD for each of the four measurement time periods (11:00, 13:00, 15:00, and 17:00 h) is represented for the three monitored plots (A, purple; B, orange; C, blue).

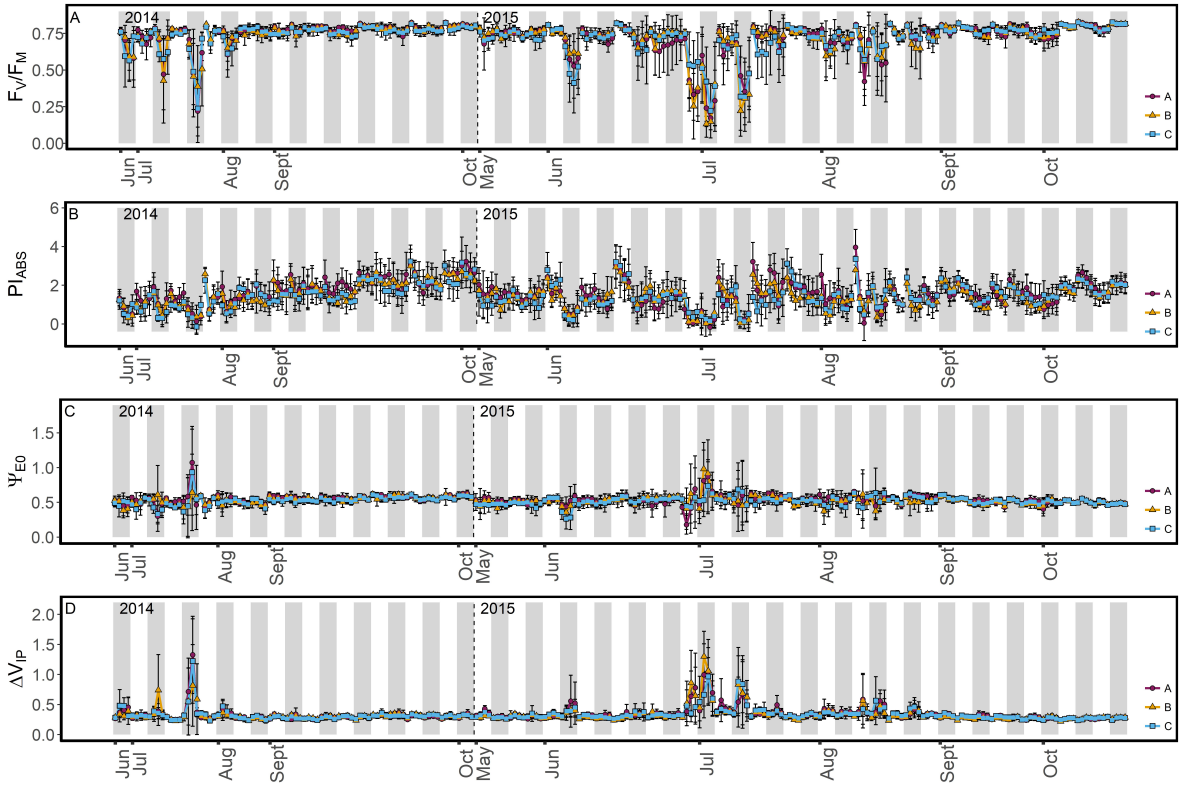

Figure S2 – Time course of ChlF parameters (F_V/F_M, PI_{ABS}, Ψ_{E0} and ΔV_{IP}) measured for *Taraxacum* sp. in the three monitored plots in the grassland. For each measured day, the ChlF parameter average value (n = 7 or 8) $\pm$ SD for each of the four measurement time periods (11:00, 13:00, 15:00, and 17:00 h) is represented for the three monitored plots (A, purple; B, orange; C, blue).

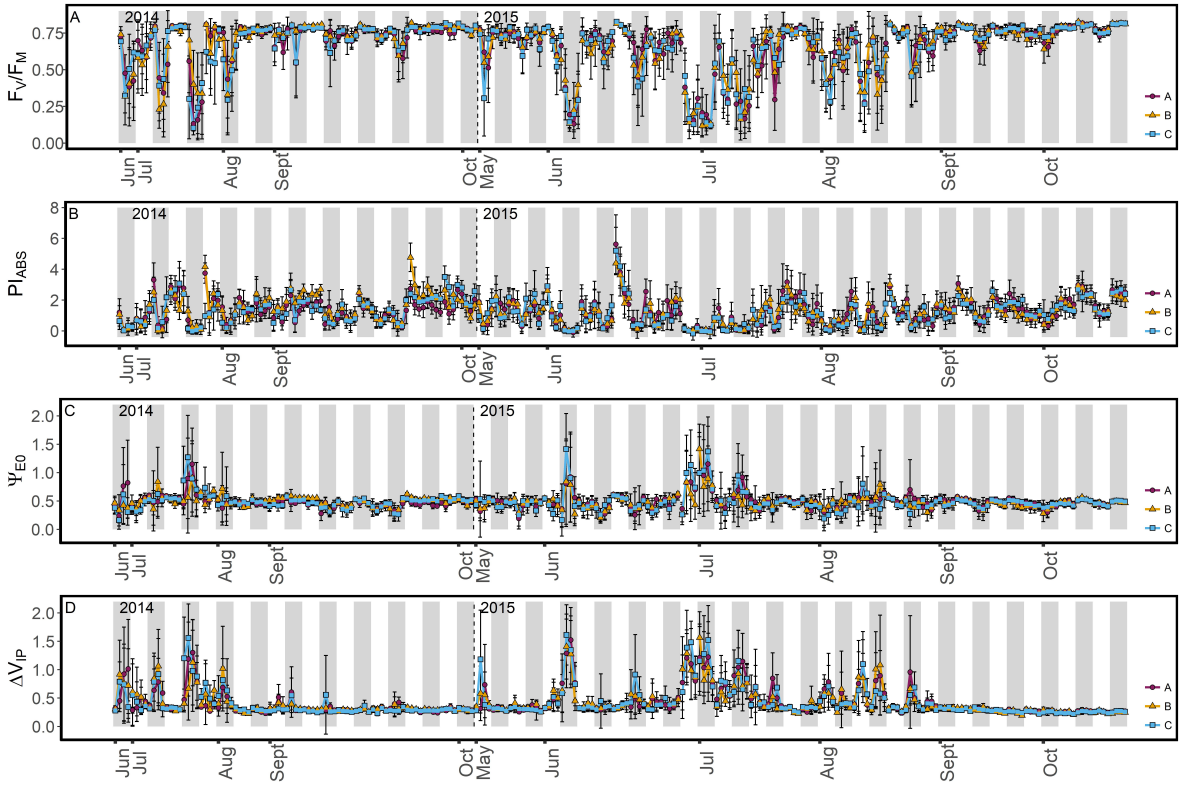

Figure S3 – Time course of ChlF parameters (F_V/F_M, PI_{ABS}, Ψ_{E0} and ΔV_{IP}) measured for *Trifolium repens* L. in the three monitored plots in the grassland. For each measured day, the ChlF parameter average value (n = 7 or 8) ± SD for each of the four measurement time periods (11:00, 13:00, 15:00, and 17:00 h) is represented for the three monitored plots (A, purple; B, orange; C, blue).

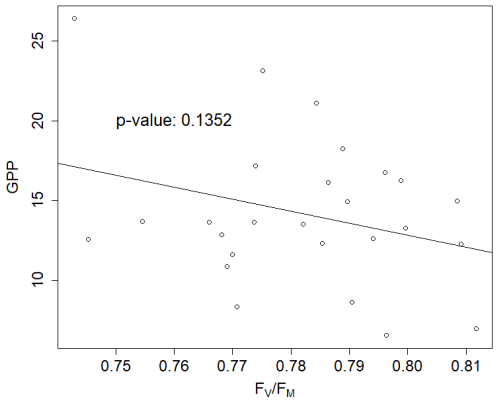

Figure S4 – Linear relationship between gross primary production (GPP, μmol CO_2 m^{-2} s^{-1}) and F_V/F_M under low light condition (PPFD values from 67.36 to 498.5 μmol m^{-2} s^{-1}). The selection of observations performed for PPFD values from 67.36 to 199.2 μmol m^{-2} s^{-1} leads to the same conclusion.

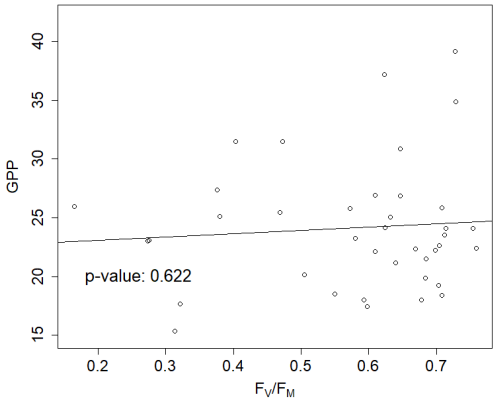

Figure S5 – Linear relationship between gross primary production (GPP, μmol CO_2 m^{-2} s^{-1}) and F_V/F_M under high light condition (PPFD values from 1511 to 1926 μmol m^{-2} s^{-1}).

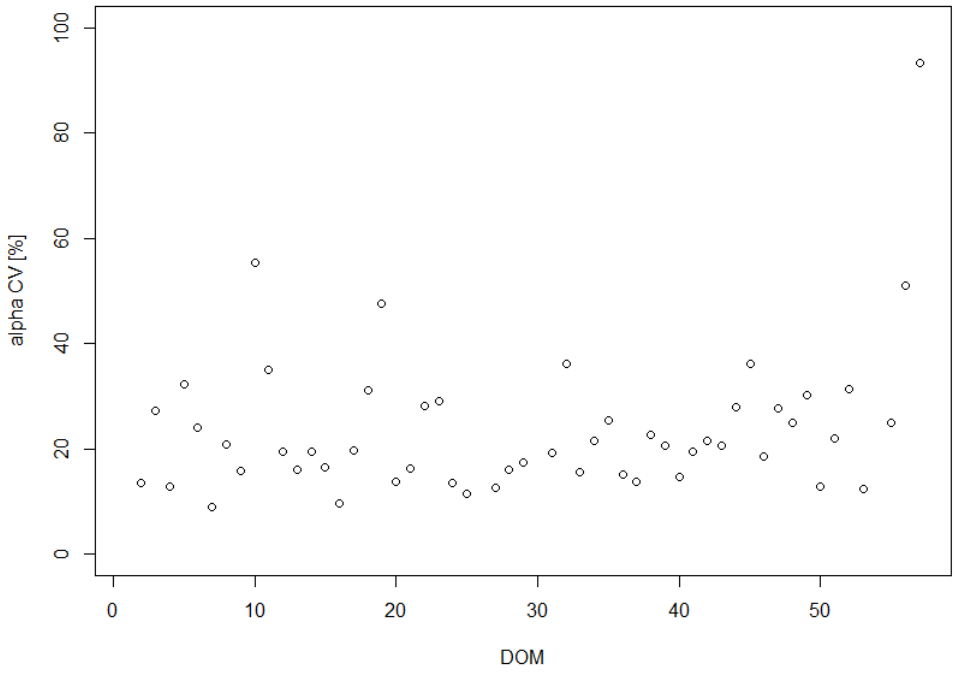

Figure S6 – Coefficient of variation (standard error/estimated value) for the quantum light efficient estimated for the Mitscherlich equation for each day of measurement (DOM). Two values with a coefficient of variation exceeding 100% (208% and 552%) are not represented in the figure.

"The important thing is not to stop questioning. Curiosity has its own reason for existence. One cannot help but be in awe when he contemplates the mysteries of eternity, of life, of the marvelous structure of reality. It is enough if one tries merely to comprehend a little of this mystery each day."

Albert Einstein (1879-1955)